

Interactions of microplastic, soil and
plant with a particular emphasis on
phosphorus

Tazeen Fatima Khan

Doctor of Philosophy

University of York

Environment and Geography

June 2022

Abstract

Relatively little is known about the impacts of microplastics in the soil, particularly the interactions between the microplastics and soil components (such as nutrients, enzymes and aggregates). Many of these interactions impact on the biochemical processes by changing the soil properties, that may directly/ indirectly influence the growth of plants. Although microplastic appeared to impact plants in previous studies, the effects varied, and possible reasons behind these impacts are largely unknown. The present thesis examines microplastic adsorbed phosphate, and how this could affect soil properties and plant growth, through laboratory and greenhouse experiments. The data showed that the microplastic had the potentiality to adsorb phosphate and UV weathering increased the adsorption. Adsorption on the microplastics was far lower compared to the soils. Experiments measuring the phosphate adsorption observed increased adsorption with the increasing concentration of the background electrolyte above and below the point of zero charge (PZC). According to the literature, phosphate adsorption was not expected to increase with the concentration of the background electrolyte below the PZC. Experiments investigating the soil properties and estimating plant parameters found that the microplastic did not show any negative effect on soil and plant when applied at a 0.05 % rate. Nevertheless, an application rate of 0.50 % and 5.00 % did cause negative responses to the soil and plant. We used a range of environmentally relevant to higher than environmentally relevant concentrations of microplastic in both incubation and greenhouse experiments. Our data indicated reductions in available phosphate which were consistent with the reduced plant growth. However, we could not confirm whether reduced phosphate availability was driving reduced plant growth since other factors also changed in response to the microplastics that might also be responsible for the reductions in plant growth.

The present thesis on the soil and plant responses *vis-à-vis* microplastic additions indicates that the interaction between the microplastic and soil leads to reduced growth of plants, and pervasive microplastic impacts may have consequences for terrestrial environments.

Table of contents

Abstract.....	2
Table of contents.....	3
List of tables (short titles).....	7
List of figures (short titles).....	8
Author’s Declaration.....	11
Abbreviations/ Glossary	12
Chapter 1	14
General introduction	14
1.1. Introduction.....	14
1.2. Aims and objectives of the thesis.....	16
1.3. Outlines of the thesis.....	17
1.4. References	20
Chapter 2	24
Review of literature	24
2.1. Introduction.....	24
2.2. Historical development of plastics	24
2.3. Environmental presence of microplastics	29
2.4. Sources of microplastics	32
2.4.1. <i>Primary microplastics</i>	32
2.4.2. <i>Secondary microplastics</i>	32
2.5. Properties of microplastics.....	33
2.5.1. Physical properties.....	33
2.5.2. Chemical properties.....	33
2.6. Fate of microplastics in the terrestrial environment	34
2.7. Impacts of microplastics in the soil	37
2.7.1. Impacts on soil nutrients, properties and processes.....	37
2.7.2. Impacts on soil organisms.....	39
2.8. Impacts of microplastics on plants	41
2.9. Role of phosphorus in soil and plant	43
2.10. Sources of phosphorus in the soil.....	44
2.11. Phosphorus loss pathways	45

2.12. Fate and behaviour of phosphorus in the soil.....	45
2.13. Adsorption to the microplastic.....	47
2.13.1. Adsorption mechanisms	47
2.13.2. Adsorption isotherms	51
2.13.3. Factors affecting adsorption to microplastic	52
2.14. Knowledge gaps identified	58
2.15. Identified experiments for the thesis	59
2.16. References	60
Chapter 3	84
Impacts of microplastics on phosphate adsorption	84
3.1. Introduction	84
3.2. Materials and methodology	86
3.2.1. Materials	86
3.2.2. Methods.....	86
3.2.3. Experiment with UV radiation	87
3.2.4. Kinetic experiments	89
3.2.5. Adsorption isotherms	90
3.2.6. Desorption experiments	92
3.2.7. Quality control and statistical analysis	93
3.3. Results.....	94
3.3.1. HDPE characterisation	94
3.3.2. Kinetics experiments.....	96
3.3.3. Adsorption isotherms	97
3.3.4. Desorption experiments	104
3.4. Discussion	106
3.4.1. Pristine and weathered microplastics characterisation	106
3.4.2. Kinetics experiments.....	106
3.4.3. Adsorption experiments	107
3.4.4. Desorption experiments	116
3.5. Conclusion	118
3.6. References	119
Chapter 4	134
Effects of pH and concentration of background electrolyte	134

4.1. Introduction	134
4.2. Materials and methodology	136
4.2.1. Materials	136
4.2.2. Determination of point of zero charge (PZC).....	136
4.2.3. Effects of pH and concentration of background electrolyte on phosphate adsorption	137
4.2.4. Quality control and statistical analysis	138
4.3. Results.....	139
4.3.1. Determination of point of zero charge (PZC).....	139
4.3.2. Effects of pH and concentration of background electrolyte on partition coefficient	140
4.3.3. Effects of pH and concentration of background electrolyte on Langmuir parameters.....	143
4.3.4. Effects of pH and concentration of background electrolyte on Freundlich parameters.....	148
4.4. Discussion	154
4.4.1. Phosphate adsorption at point of zero charge (PZC).....	154
4.4.2. Effects of pH on phosphate adsorption	155
4.4.3. Effects of concentration of background electrolyte on phosphate adsorption	158
4.4.4. Effects of interaction between pH and concentration of background electrolyte on phosphate adsorption.....	160
4.5. Conclusion	163
4.6. References	164
Chapter 5	171
Impacts of microplastic on soil properties and plant growth	171
5.1. Introduction.....	171
5.2. Materials and methodology	173
5.2.1. Materials	173
5.2.2. Incubation experiment.....	174
5.2.3. Greenhouse experiment	176
5.2.4. Measurements of plant growth parameters	177
5.2.5. Determination of soil parameters	178
5.2.6. Quality control and statistical analysis	181

5.3. Results.....	183
5.3.1. Soil parameters	183
5.3.2. Plant parameters.....	203
5.4. Discussion	206
5.4.1. Microplastics impact on soil properties and plant growth	206
5.5. Conclusion	218
5.6. References	220
Chapter 6	236
General discussion and future research.....	236
6.1. Introduction	236
6.2. Main findings	237
6.3. Research limitations	241
6.4. Future researches	243
6.5. References	246
Appendix A.....	249
Appendix B.....	256
Appendix C.....	278

List of tables (short titles)

Table 2.1. Characteristics and uses of major plastic types in Europe.	26
Table 2.2. Summary of selected studies detailing type, concentration, experiment type and impacts of microplastics on soil nutrients, properties and processes.....	38
Table 2.3. Summary of the selected studies detailing type, concentration, size and effects of microplastics on plant parameters..	42
Table 3.1. Properties of HDPE (mean \pm standard deviation).....	94
Table 3.2. Functional groups and appearances for the FTIR spectra of microplastic used in the study before and after exposure to UV radiation..	96
Table 3.3 Partition coefficient (K_d) values for phosphorus adsorption to different solids..	99
Table 3.4. Langmuir and Freundlich adsorption isotherm parameters for phosphorus to different solid types..	102
Table 3.5. Hysteresis index (HI) for different solid types.	104
Table 3.6. Studies detailing phosphate adsorption on different types of iron oxides and soil organic matter.	114
Table 4.1. Point of zero charge (PZC) of the different solids.....	139
Table 4.2. Binding constants (L/ mg) for phosphorus adsorption at different values of pH (2 to 12) and different concentrations of background electrolyte (0 to 0.10 M NaNO ₃)..	146
Table 4.3. Heterogeneity factors (1/ n) for phosphorus adsorption at different values of pH (2 to 12) and different concentrations of background electrolyte (0 to 0.10 M NaNO ₃)..	152
Table 5.1. Effects of different factors on exchangeable cations for incubated soils.	188
Table 5.2. Effects of different factors on exchangeable cations for greenhouse soils..	188
Table 5.3. Correlations of respiration rate, pH and water extractable carbon for (a) incubation and (b) greenhouse experiments.....	202
Table 5.4. Plant height (cm), leaf chlorophyll content (g/ m ²), fresh and dry weight of shoot biomass (g), fresh and dry weight of root biomass (g), fresh and dry root: shoot ratio and plant P (%).	204

List of figures (short titles)

Figure 1.1. A conceptual diagram of the different thesis chapters, their relationship to the research questions posed at the end of the literature review, and their relationships to each other.	19
Figure 2.1. Annual production of plastics worldwide.	25
Figure 2.2. Fate and transport of microplastics in the environment.	35
Figure 2.3. Phosphorus pools in the soil.	46
Figure 2.4. Adsorption of organic compound to the microplastic through several mechanisms.	47
Figure 2.5. Factors affecting the adsorption of hydrophobic organic pollutant on the microplastic.	53
Figure 3.1. Exposure of HDPE to UV radiation using UV lamp.	89
Figure 3.2. Changes in FTIR spectra of HDPE after exposure to UV radiation with 185 nm and 365 nm wavelength.	95
Figure 3.3. Changes in phosphorus concentration over time for different solid types	97
Figure 3.4. Adsorption of phosphorus for different solids types	100
Figure 3.5. Langmuir adsorption isotherms of phosphorus for different solid types	101
Figure 3.6. Percentage (%) of P desorption from different solids	105
Figure 4.1. Partition coefficient, K_d for different solids	141
Figure 4.2. Maximum adsorption capacity, C_{SM} for different solids	144
Figure 4.3. Freundlich constant, $\log K_f$ for different solids	150
Figure 5.1. Incubation experiment conducted in a controlled temperature room for a period of 30 days.	174
Figure 5.2. Experimental design for both incubation and greenhouse experiments.	175
Figure 5.3. Greenhouse experiment with ryegrass (<i>Lolium perenne</i>) conducted for a total period of seven weeks	176
Figure 5.4. Respiration rate for (a) incubated and (b) greenhouse soil following HDPE treatments.	183
Figure 5.5. Phosphatase enzyme activity for (a) incubated and (b) greenhouse soil following HDPE treatments.	184
Figure 5.6. Soil pH for (a) incubated and (b) greenhouse soil following HDPE treatments.	186

Figure 5.7. Concentration of exchangeable cations	189
Figure 5.8. ECEC for (a) incubated and (b) greenhouse soil following HDPE treatments. .	191
Figure 5.9. TCEC for (a) incubated and (b) greenhouse soil following HDPE treatments ..	192
Figure 5.10. CWEC for (a) incubated and (b) greenhouse soil following HDPE treatments.	194
Figure 5.11. HWEC for (a) incubated and (b) greenhouse soil following HDPE treatments.	194
Figure 5.12. Olsen P for (a) incubated and (b) greenhouse soil following HDPE treatments.	196
Figure 5.13. NH_4^+ for (a) incubated and (b) greenhouse soil following HDPE treatments.	197
Figure 5.14. NO_3^- for (a) incubated and (b) greenhouse soil following HDPE treatments.	198
Figure 5.15. Phosphorus in soil pore water for (a) incubated and (b) greenhouse soil following HDPE treatments.....	199
Figure 5.16. Soil water holding capacity for (a) incubated and (b) greenhouse soil following HDPE treatments.....	200
Figure 5.17. Water stable aggregates for (a) incubated and (b) greenhouse soil following HDPE treatments.....	201

Acknowledgements

First and foremost, I would like to thank my supervisor, Prof. Mark E. Hodson, for his exemplary guidance, excellent monitoring and constant encouragement throughout the course of this thesis. His input has been invaluable in developing my skills as a researcher which will carry me a long way in the journey of life. He has always been very approachable and encouraging. Without his guidance and persistent help this dissertation would not have been possible.

I take this opportunity to express my profound gratitude and thanks to the Commonwealth Scholarship Commission in the United Kingdom for funding my PhD project. I am highly indebted to them.

I wish to express my earnest thankfulness to Alistair Boxall for his help with the experimental design. My thanks to J. Brett Sallach in accessing and using his equipment and his scientific guidance. My thanks to Slyvia Toet for her constructive suggestions and valuable feedback over the past three years. My thanks to numerous people who aided with my sample collection and experimental chapters. I would like to express a deep sense of gratitude to Mark Hodson for assisting me with soil sampling. I want to thank Rebecca Sutton, Matt Pickering and Deborah Sharpe for their help in accessing and using analytical instruments and their scientific guidance over the past three years. My thanks and appreciations also go to Tamsyn Kiss, Katey Valentine, Golam Rabbani and Tanvir Ahmed Chowdhury who have willingly helped me out throughout my PhD. Thank you for your understanding and constant encouragement. I want to extend my thanks to Jason Daff for providing the necessary facilities for my experimental setup in the greenhouse. My thanks to Martyn Godwin at the Department of Biology for accessing the XRF and assisting me with the measurements of plant phosphorus.

My thanks to my family and friends. Near and far, scientists and non-scientists, your support, confidence and interest have kept me going through the difficult stages of my PhD.

Finally saving the best until last, my thanks to my parents, Parvez Ali Anwar Khan and Fahima Rokhsana, for their unwavering support and endless patience. Thank you for understanding as I complained about experiments going wrong, and for cheering as I described experiments going right. With all my heart: thank you.

Author's Declaration

This work was funded by the Commonwealth Scholarship Commission in the UK. I declare that this thesis is a presentation of original work and I am the sole author although I did it under the direct supervision of Professor Mark. E. Hodson.

This work has not previously been presented for an award at this, or any other, University. All sources are acknowledged as references. No papers have yet been published from this work at the time of writing. The data in Chapter 3 were presented at the British Society of Soil Science Early Careers Researcher Conference in UK, Sheffield University, April 16 - 17th, 2019 (Talk), and the Geological Society Plastics in the Environment Virtual Conference, March 15th, 2021 (Poster). A part of the results from the Chapter 5 were presented at the SETAC Europe Virtual Annual Meeting, 3 - 6th May, 2021 (Poster). Results from the Chapters 3, 4 and 5 have been presented internally in the Department of Environment and Geography, University of York, UK (Talk and Poster).

Abbreviations/ Glossary

AMX	Amoxicillin
ATR	Attenuated Total Reflectance
BDE 47	2,2',4,4'-tetrabromodiphenyl ether
CEC	Cation Exchange Capacity
CIP	Ciprofloxacin
CWEC	Cold Water Extractable Carbon
CRM	Certified Reference Material
CV	Coefficient of Variation
DCP	2,4-dichlorophenol
DOC	Dissolved Organic Carbon
DOM	Dissolved Organic Matter
ECEC	Effective Cation Exchange Capacity
FOSA	Perfluorooctane Sulfonamide
FTIR	Fourier Transform Infrared Spectroscopy
HDPE	High Density Polyethylene
HI	Hysteresis Index
HOC	Hydrophobic Organic Compound
HWEC	Hot Water Extractable Carbon
ICP-OES	Inductively Coupled Plasma Optical Emission Spectrometry
ISO	International Organization for Standardization
LDPE	Low Density Polyethylene
MCP	4-chlorophenol
MP	Microplastic
MUB	Modified Universal Buffer
NOM	Natural Organic Matter
OTC	Oxytetracycline
PA	Polyamide
PAC	Polyacrylic
PBS	Polybutylene Succinate
PBT	Polyhydroxy Butyrate
PCB 47	3,3',4,4'-Tetrachlorobiphenyl

Abbreviations/ Glossary

PES	Polyester
PLB	Biodegradable Plastic
PS	Polystyrene
PP	Polypropylene
PET	Polyethylene Terephthalate
PFOS	Perfluorooctane Sulfonate
PMP	Pristine Microplastic
PU	Polyurethane
PVC	Polyvinylchloride
P-XRF	Portable X-Ray Fluorescence Spectrometry
PZC	Point of Zero Charge
SSA	Specific Surface Area
SZD	Sulfadiazine
TC	Tetracycline
TCP	2, 4,6-Trichlorophenol
TCS	Triclosan
TCEC	Total Cation Exchange Capacity
T _g	Glass Transition Temperature
TMP	Trimethoprim
TOC Analyser	Total Organic Carbon Analyser
UNEP	United Nations Environment Programme
USDA	United States Department of Agriculture
WEC	Water Extractable Carbon
WHC	Water Holding Capacity
WMP	Weathered Microplastic
WSA	Water Stable Aggregate
WoSCC	Web of Science Core Collection

Chapter 1

General introduction

1.1. Introduction

Though there was a longer period of time when plastics were viewed as a super material that were very beneficial to society, now it is widely acknowledged that the plastics degrade to microplastics in the natural environment (Horton *et al.*, 2017; Nizzetto *et al.*, 2016). Oceans and aquatic environments have been the focus of microplastic research for the last decade. The awareness that terrestrial environments may also be afflicted with microplastics was developed comparatively recently although terrestrial microplastic pollution is higher than the marine pollution (Horton *et al.*, 2017). In the European Union between 4,73,000 and 9,10,000 metric tonnes of microplastic is released annually within the terrestrial environment, between 4 and 23 times the amount estimated to be released to the oceans (Horton *et al.*, 2017).

Using microplastic research citation data from the Web of Science Core Collection (WoSCC) during the period of 2004 to 2019, Horton and Barnes (2020) reported that the number of records relating to microplastic research (peer-reviewed journal articles) increased from less than 100 to more than 1000 yearly outputs during the 15-year study. On May 8, 2020, Qin *et al.* (2020) collected data using the same WoSCC database, for the time period spanning January 1, 2020 to April 30, 2020, and identified 442 publications on microplastics. This value was less than the expected value for one-third of the year 2020 (567), which might be a result of the significant disruption caused by the COVID-19 pandemic. He *et al.* (2020) used scientometric analysis to understand the current status of microplastic research in the terrestrial environment and summarised the impacts of microplastics on the two major components of the terrestrial environment, soil and plants. The bibliometric analysis conducted by Qin *et al.* (2020) illustrated the potential sources and spatial distributions of microplastics, the impacts of microplastics on soil organisms, and the interactions of microplastics with metals and pesticides present in the soil. Using the cluster-based VOSviewer software, He *et al.* (2020) demonstrated that the number of publications on microplastics in the terrestrial environment increased rapidly since 2009. A total of 3529

authors contributed to the 877 publications related to microplastics in the terrestrial environment. Avio *et al.* (2015a, 2015b) observed that the rise in the number of scientific publications on the microplastic impacts in the terrestrial environment occurred when the first United Nations Environment Assembly of the United Nations Environment Programme (UNEP) issued the resolution UNEP/ EA.1/ L.8, which emphasised critical activities to address terrestrial microplastics. The studies on the microplastic in the terrestrial environment concentrated on the source, distribution and occurrence (Wu *et al.*, 2019; Yang *et al.*, 2019; Zhang *et al.*, 2019a), the transport and fate in the soils (Yu *et al.*, 2019; Yang *et al.*, 2019), soil–plant interaction (Wang *et al.*, 2020; Liu *et al.*, 2020), risk and toxicity (Zarfl *et al.*, 2019; Zhang *et al.*, 2019b).

The majority of all plastics ever produced (approximately 60 % equivalent to 4900 million tons) have been discarded and are now present in terrestrial environment (Geyer *et al.*, 2017). The terrestrial environment particularly agricultural soils are prone to being exposed to the microplastic, as several pathways for plastic addition and incorporation exist in agroecosystems. Sources of microplastic in the terrestrial environment include landfills (Nizzetto *et al.*, 2016), plastic mulch (Bläsing and Amelung, 2018; Kasirajan and Ngouajio, 2012; Steinmetz *et al.*, 2016), virgin plastic flakes, pre-production plastic pellets (Foitzik *et al.*, 2018), sewage sludge and laundry dust (Carr *et al.*, 2016; Mahon *et al.*, 2017). Because of their large surface area and hydrophobic nature, microplastics easily adsorb contaminants including metals (Hodson *et al.*, 2017; Decho, 2000) and persistent organic pollutants (POPs) (Bakir *et al.*, 2014a; 2014b; Velzeboer *et al.*, 2014) which are well documented in the marine environment. The adsorption - desorption of contaminant on/ from the microplastic is complicated in the soil since the soil is a heterogeneous system comprising much biodiversity (Hector and Hooper, 2002; Zavaleta *et al.*, 2010), and a mixture of dynamic factors such as microplastic characteristics (e.g. composition, structure, binding energy and surface properties), release medium (e.g. pH, temperature, salinity, ionic strength and concentration of background electrolyte), and contamination factors (e.g. solubility, redox state, charges and stability) are involved (Yu *et al.*, 2020; Wang *et al.*, 2020; Li *et al.*, 2018). Not only the contaminant, adsorption of soil nutrients (particularly essential nutrient) on the microplastic can change the form of nutrient (converting inorganic form to organic) within the soil where the availability of the nutrient often dominates soil properties and ultimately plant growth. Soils are effectively a temporary reservoir of nutrients for the plants. Phosphate, as an essential soil nutrient, undergoes several biochemical transformations, including conversion from the mineral phosphate to the organic phosphate that are not accessible to the

plants leading to the decreased growth of plants (Liu and Chen, 2008; Doolette and Smernic, 2010). The phosphate is considered as the *energy currency* of the plant that drives most biochemical reactions (Weil and Brady, 2016).

1.2. Aims and objectives of the thesis

The overarching aim of this thesis was to investigate the impacts of microplastics on the soil and plant. This was achieved through a series of laboratory experiments and a greenhouse experiment involving HDPE microplastic typically used in industry and ryegrass commonly grown on the UK soil. The experiments were carried out with and without microplastics in the soils of differing organic matter content (low and high organic matter soil; these soils were used in the incubation and greenhouse experiments). The hypotheses of this thesis were:

- Microplastic has the potentiality to adsorb the phosphate and weathered microplastic adsorbs more phosphate than the pristine one.
- Soil pH and concentration of the background electrolyte impact the adsorption of phosphate to the microplastic surface.
- Plant growth is limited due to the reduced amount of available forms of phosphate in the soil.

A set of objectives to test the above-mentioned hypotheses were outlined below:

- To determine the potential of microplastic to adsorb phosphate and to determine whether the adsorption is reversible;
- To determine whether the adsorption of phosphate on the microplastic is impacted by the pH and concentration of the background electrolyte;
- To determine the potential of microplastic treatments to impact the soil;
- To observe plant growth in response to the microplastic treatments.

1.3. Outlines of the thesis

This PhD thesis comprises six chapters including laboratory experiments (Chapters 3, 4 and 5) and a greenhouse experiment (Chapter 5). The contents of each chapter are described briefly below:

- Chapter 1 presents a general introduction on the presence of microplastic in the terrestrial environment, sources of microplastic and historical development of the microplastic research. The chapter introduces the adsorption of metals and organic molecules to the microplastic present in the soil. Finally, the chapter summarizes the hypotheses, aims, objectives and different outlines of the thesis.
- Chapter 2 reviews production of plastics worldwide, characteristics and uses of major plastics in Europe. The chapter reviews our understanding of how microplastic is generated in the terrestrial environment, and the abundance and distribution of microplastic. The chapter briefly presents factors, processes and mechanisms that influence fate and transport of the microplastic in the terrestrial environment. It provides a comprehensive knowledge on the impacts of microplastic through modification of soil properties and how this affect the plants. It introduces the potentiality of microplastic to adsorb different elements, adsorption mechanisms and how various factors influence the adsorption process. The chapter briefly discusses the role of phosphate in soil fertility and subsequent benefits in term of plant growth, and also the importance of studying the adsorption of phosphate to the microplastic surface. Finally, this chapter identifies relevant knowledge gaps based on the current state of knowledge on the impacts of microplastics in the soil, and outlines the three key questions that this thesis aimed to answer.
- Chapter 3 investigates the potential of HDPE microplastic used extensively in industry to adsorb one of the essential plant nutrients, phosphate. The experiment was done on two types of soil differing in organic matter content, low and high organic matter soil. The chapter determines the comparative adsorption of phosphate on the pristine and UV weathered microplastics. The experiment compares the phosphate adsorption between the microplastics and soils, and examines whether the adsorption is reversible.

- Chapter 4 investigates the changes in phosphate adsorption with the different ranges of pH and different concentrations of the background electrolyte. The chapter compares and contrasts the pristine microplastics, UV weathered microplastics, low organic matter soils and high organic matter soils indicating the trends in the adsorptions of phosphate with the changes in pH and concentration of the background electrolyte.
- Chapter 5 aims to bring together the elements of Chapter 3 and 4, and investigates how microplastics interact with soil and plants. The experiment was conducted to clarify contradicting literature findings about the interactions between the microplastic, soil and plant. The incubation experiment described in this chapter was conducted with different combinations of microplastic and soil. The chapter measures the respiration rate, enzyme activity, pH, exchangeable cations, cation exchange capacity, cold and hot water extractable carbon, Olsen phosphorus, ammonium, nitrate, soil water holding capacity, water stable aggregates and pore water phosphorus in responses to the different microplastic treatments (including controls) collected from the incubation experiment. The incubation experiment was followed by a greenhouse experiment by transferring the incubated soils to the greenhouse to investigate how the microplastic interact with the soil in presence of plant roots. The chapter estimates the growth of plant in response to the microplastic treatments.

The detailed aims of each experiment are given within the relevant chapters. A conceptual diagram (Figure 1.1) demonstrates the interrelation of the different chapters, and their relation to the research questions posed at the end of the literature review.

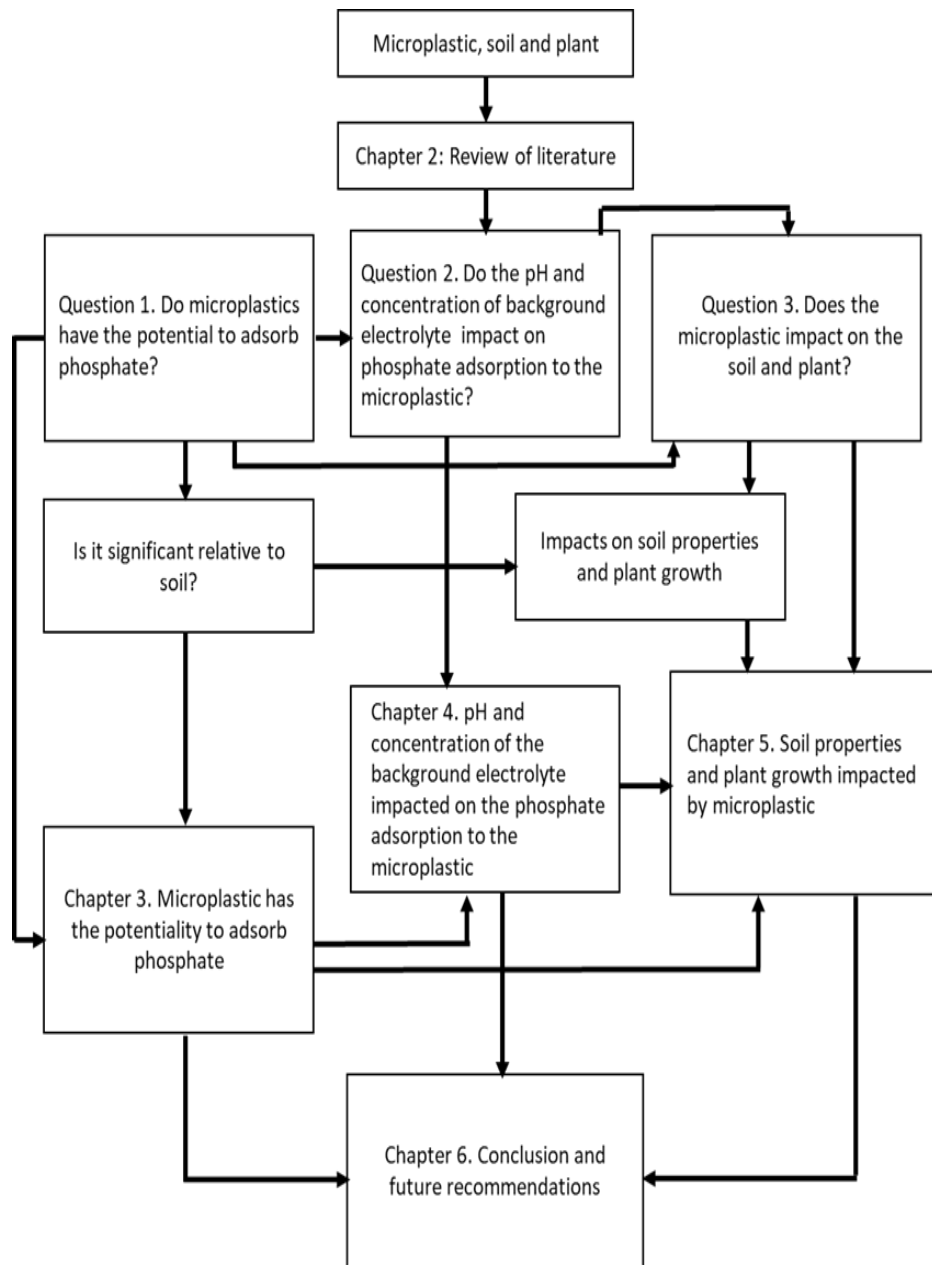


Figure 1.1. A conceptual diagram of the different thesis chapters, their relationship to the research questions posed at the end of the literature review, and their relationships to each other.

1.4. References

- Avio, C. G., Gorbi, S., and Regoli, F. (2015a). Experimental development of a new protocol for extraction and characterization of microplastics in fish tissues: first observations in commercial species from Adriatic Sea. *Marine Pollution Bulletin*, 111, 18–26.
- Avio, C. G., Gorbi, S., Milan, M., Benedetti, M., Fattorini, D.; d’Errico, G., Pauletto, M., Bargelloni, L., and Ragoli, F. (2015b). Pollutants bioavailability and toxicological risk from microplastics to marine mussels. *Environmental Pollution*, 198, 211–222.
- Bakir, A., Rowland, S. J., and Thompson, R. C. (2014a). Enhanced desorption of persistent organic pollutants from microplastics under simulated physiological conditions. *Environmental Pollution*, 185, 16-23.
- Bakir, A., Rowland, S. J., and Thompson, R. C. (2014b). Transport of persistent organic pollutants by microplastics in estuarine conditions. *Estuarine, Coastal and Shelf Science*, 140, 14-21.
- Bläsing, M. and Amelung, W. (2018). Plastics in soil: analytical methods and possible sources. *Science of the Total Environment*, 612, 422–435.
- Carr, S.A., Liu, J., and Tesoro, A.G. (2016). Transport and fate of microplastic particles in wastewater treatment plants. *Water Res.* 91, 174-182.
- Decho, A. W. (2000). Microbial biofilms in intertidal systems: an overview. *Continental Shelf Research*, 20, 1257–1273.
- Doolette, A. L. and Smernik, R. J. (2010). Soil organic phosphorus speciation using spectroscopic techniques. In: Bunemann, E. K., Oberson, A., and Frossard, E. (eds). *Phosphorus in action: biological processes in soil phosphorus cycling*. Berlin: Springer.
- Foitzik, M.-J., Unrau, H.-J., Gauterin, F., Dörnhöfer, J., and Koch, T. (2018). Investigation of ultra fine particulate matter emission of rubber tires. *Wear*, 394–395, 87-95.

Geyer, R., Jambeck, J. R., and Law, K. L. (2017). Production, use, and fate of all plastics ever made. *Science Advances*, 3, 1-19.

He, D., Bristow, K., Filipovic, V., Lv, J., and He, H. (2020). Microplastics in terrestrial ecosystems: a scientometric analysis. *Sustainability*, 12, 1-15.

Hector, A. and Hooper, A. (2002). Darwin and the first ecological experiment. *Science*, 295, 639-640.

Hodson, M. E., Duffus-Hodson, C. A., Clark, A., Prendergast-Miller, M. T., and Thorpe, K. L. (2017). Plastic bag derived-microplastics as a vector for metal exposure in terrestrial invertebrates. *Environmental Science and Technology*, 51, 4714-4721.

Horton, A. A., Walton, A., Spurgeon, D. J., Lahive, E., and Svendsen, C. (2017). Microplastics in freshwater and terrestrial environments: evaluating the current understanding to identify the knowledge gaps and future research priorities. *Science of the Total Environment*, 586, 127–141.

Horton, A. A. and Barnes, D. K. A. (2020). Microplastic pollution in a rapidly changing world: Implications for remote and vulnerable marine ecosystems. *Science of the Total Environment*, 738, 1-9.

Kasirajan, S. and Ngouajio, M. (2012). Polyethylene and biodegradable mulches for agricultural applications: a review. *Agronomy for Sustainable Development*, 32, 501-529.

Li, J., Zhang, K., and Zhang, H. (2018). Adsorption of antibiotics on microplastics. *Environmental Pollution*, 237, 460–467.

Liu, Y. and Chen, J. (2008). Phosphorus Cycle. In: Jorgensen, S. E. and Fath, B. D. (eds). *Encyclopedia of Ecology*, Amsterdam: Elsevier Science.

Liu, K., Wang, X., Song, Z., Nian, W., and Li, D. (2020). Terrestrial plants as a potential temporary sink of atmospheric microplastics during transport. *Science of the Total Environment*, 742, 1-15.

Mahon, A. M., O'Connell, B., Healy, M. G., O'Connor, I., Officer, R., Nash, R., and Morrison, L. (2017). Microplastics in sewage sludge: effects of treatment. *Environmental Science and Technology*, 51, 810–818.

Nizzetto, L., Bussi, G., Futter, M. N., Butterfield, D., and Whitehead, P. G. (2016). A theoretical assessment of microplastic transport in river catchments and their retention by soils and river sediments. *Environmental Science: Processes and Impacts*, 18, 1050-1059.

Qin, F., Du, J., Gao, J., Liu, G., Song, Y., Yang, A., Wang, H., Ding, Y., and Wang, Q. (2020). Bibliometric Profile of Global Microplastics Research from 2004 to 2019. *International Journal of Environmental Research and Public Health*, 17, 1-15.

Steinmetz, Z., Wollmann, C., Schaefer, M., Buchmann, C., David, J., and Tröger, J. (2016). Plastic mulching in agriculture: trading short-term agronomic benefits for long-term soil degradation? *Science of the Total Environment*, 550, 690–705.

Velzeboer, I., Kwadijk, C. J. A. F., and Koelmans, A. A. (2014). Strong sorption of PCBs to nanoplastics, microplastics, carbon nanotubes, and fullerenes. *Environmental Science and Technology*, 48, 4869-4876.

Wang, F., Zhang, X., Zhang, S., Zhang, S., and Sun, Y. (2020). Interactions of microplastics and cadmium on plant growth and arbuscular mycorrhizal fungal communities in an agricultural soil. *Chemosphere*, 254, 1-14.

Weil, R., and Brady, N. C. (2016). *Nature and properties of soils*. London: Pearson New International Edition.

Wu, P. F., Huang, J. S., Zheng, Y. L., Yang, Y. C., Zhang, Y., He, F., Chen, H., Quan, G. X., Yan, J. L., and Li, T. T. (2019). Environmental occurrences, fate, and impacts of microplastics. *Ecotoxicology and Environmental Safety*, 184, 1-16.

Yang, X. M., Lwanga, E. H., Bemani, A., Gertsen, R., Salanki, T., Guo, X. T., Fu, H. M., Xue, S., Ritsema, C., and Geissen, V. (2019). Biogenic transport of glyphosate in the presence of LDPE microplastics: a mesocosm experiment. *Environmental Pollution*, 245, 829–835.

Yu, M., van der Ploeg, M., Lwanga, E. H., Yang, X. M., Zhang, S. L., Ma, X. Y., Ritsema, C. J., and Geissen, V. (2019). Leaching of microplastics by preferential flow in earthworm (*Lumbricus terrestris*) burrows. *Environmental Chemistry*, 16, 31–40.

Yu, F., Li, Y., Huang, G., Yang, C., Chen, C., Zhou, T., Zhao, Y. and Ma, J. (2020). Adsorption behavior of the antibiotic levofloxacin on microplastics in the presence of different heavy metals in an aqueous solution. *Chemosphere*, 260, 1-11.

Zarfl, C. Promising techniques and open challenges for microplastic identification and quantification in environmental matrices. *Analytical and Bioanalytical Chemistry*, 411, 3743–3756.

Zavaleta, E. S., Pasari, J. R., Hulvey, K. B., and Tilman, G. D. (2010). Sustaining multiple ecosystem functions in grassland communities requires higher biodiversity. *Proceedings of the National Academy of Sciences*, 107, 1443-1446.

Zhang, S. L., Wang, J. Q., Liu, X., Qu, F. J., Wang, X. S., Wang, X. R., Li, Y., and Sun, Y. K. (2019a). Microplastics in the environment: A review of analytical methods, distribution, and biological effects. *Trends in Analytical Chemistry*, 111, 62–72.

Zhang, G. S., Zhang, F. X., and Li, X. T. (2019b). Effects of polyester microfibers on soil physical properties: perception from a field and a pot experiment. *Science of the Total Environment*, 670, 1–7.

Chapter 2

Review of literature

2.1. Introduction

Microplastics are tiny fragments of any type of plastic less than 5 mm in diameter (GESAMP, 2015). The properties of microplastics include a higher surface area per unit mass and greater reactivity compared to the macroplastics (Nizzetto *et al.*, 2016a; 2016b). Research into the impacts of microplastics on terrestrial ecosystems is in its infancy. Therefore, most research is still in its initial development phase and hence experiments are being conducted on a small scale. Understanding the long-term fate and behaviour of the microplastics is pivotal for understanding their potential impacts on the environment. This literature review will start by providing an overview of microplastics, their environmental fate and then go on to their impacts particularly in the terrestrial ecosystems. The report will also examine how different elements adsorb to microplastics and discuss the mechanisms and factors associated with these adsorptions. At the end of this review, knowledge gaps are identified regarding the impacts of microplastics on terrestrial ecosystems.

2.2. Historical development of plastics

Thompson *et al.* (2009a) defined plastics as organic polymers of high molecular mass containing other substances such as additives, dyes, fillers. The plastics can be used in a wide range of types and forms, including natural polymers, modified polymers, thermosetting plastics and, more recently, biodegradable plastics, mainly because of their versatility (PlasticsEurope, 2008, Cai *et al.*, 2017). Due to the flexible nature, plastics can be transformed into any shape in order to increase their functionality, making them compatible for use in domestic, industrial and developmental purposes (Thompson *et al.*, 2009a; Brach *et al.*, 2018).

Different types of plastics have benefited human society since 1600 BC when the ancient Mesoamericans processed natural rubber into figurines and bands. The first synthetic plastic, Bakelite, was made from phenol and formaldehyde. The surge in chemical technology led to

an explosion in production of different forms of synthetic plastics around the 1920s, with mass production beginning in the 1940s and 1950s with optimization of inexpensive manufacturing techniques. Development of the modern plastics expanded in the first fifty years of the 20th century, with fifteen new classes of polymers being synthesized (Anthony and Mike, 2009; Cole *et al.*, 2014). There are currently some twenty different groups of plastics, each with numerous grades and varieties. Production of plastics has increased substantially over the last sixty years from around 1.5 million metric tons in 1950 to approximately 367 million metric tons in 2020 (Figure 2.1). A recent study by Andrady and Neal (2009) and Dehaut *et al.* (2016) has predicted that the net plastic production by 2050 will be around 34 billion tons.

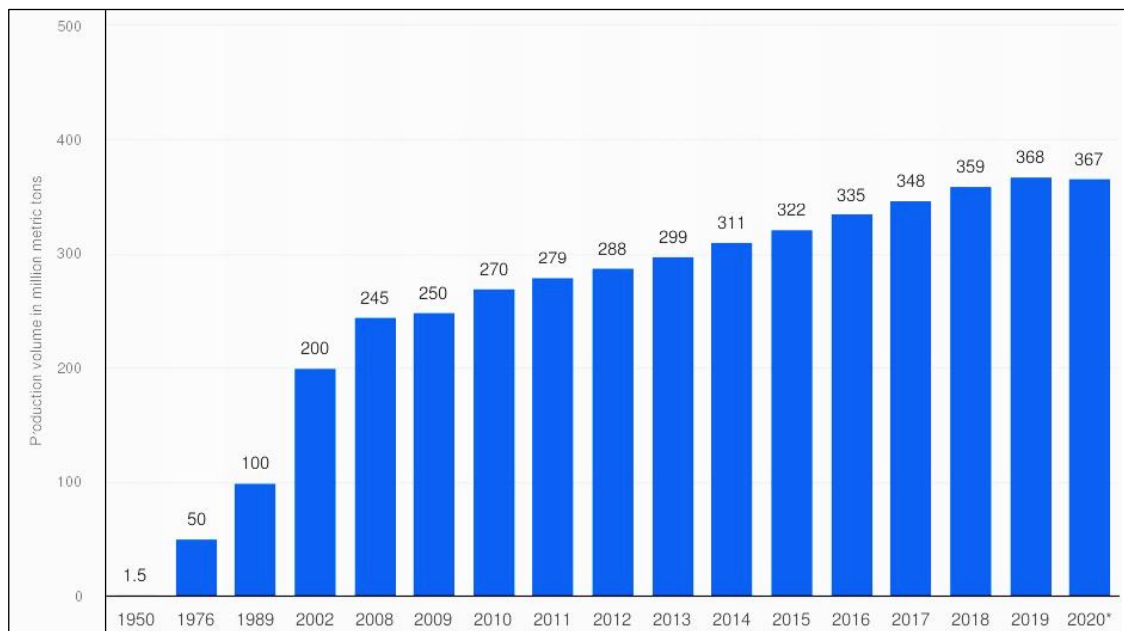


Figure 2.1. Annual production of plastics worldwide. Production of plastic increased by nearly 245 fold from 1950 to 2019. Production in 2020 decreased by approximately 0.3 % compared to 2019 due to the impacts of Covid pandemic on the plastic industries. Data collected from PlasticsEurope, 2013, 2021.

In Europe, packaging applications are the largest application sector representing 39.6 % of the total plastics demand. Construction sector is the second largest application with 20.3 % following the automotive sector with a share of 8.5 % of the total demand. According to PlasticsEurope (2017), polyethylene comprised 28 %, polypropylene 19 %, polyvinyl chloride 10 % and polystyrene 7 % of the total plastic productions in Europe. The characteristics and uses of different types of plastics in Europe are shown in Table 2.1.

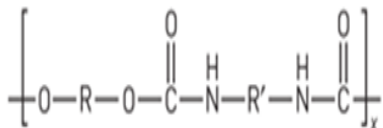
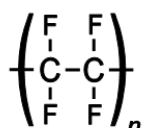
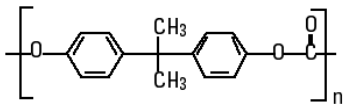
Table 2.1. Characteristics and uses of major plastic types in Europe.

Plastic type	Global plastic usage (%)	Characteristics	Uses	References
<p>Polyvinylchloride</p> $\left[\begin{array}{cc} \text{H} & \text{Cl} \\ & \\ -\text{C} & -\text{C}- \\ & \\ \text{H} & \text{H} \end{array} \right]_n$	10.3	Rigid; can be blended with other materials; readily available; cheap; good tensile strength.	Construction materials, non-food packaging, plumbing products, electrical cable insulation, clothing, vacuum foaming, medical tubing, etc.	Kurkcu <i>et al.</i> , 2012; Alzeer and MacKenzie, 2013.
<p>Low density polyethylene</p> $\left(\begin{array}{cc} \text{H} & \text{H} \\ & \\ -\text{C} & -\text{C}- \\ & \\ \text{H} & \text{H} \end{array} \right)_n$	17.2	Can be elongated under stress; higher tensile strength; high impact and puncture resistant; good electrical properties.	Shopping bags, film for food containers, disposable packaging, reusable bags, etc.	Kurkcu <i>et al.</i> , 2012.
<p>High density polyethylene</p> $\left(\begin{array}{cc} \text{H} & \text{H} \\ & \\ -\text{C} & -\text{C}- \\ & \\ \text{H} & \text{H} \end{array} \right)_n$	12.1	Large strength to density ratio; strong intermolecular force and tensile strength; can tolerate higher temperatures.	Piping for water and sewer, snowboards, boats, folding chairs, carrier bags, screw closures, hydraulic seals, biomaterial for hip, knee and spine implants, etc.	Gaurav <i>et al.</i> , 2014; Thompson <i>et al.</i> , 2009a; 2009b.

Table 2.1 (continued). Characteristics and uses of major plastic types in Europe.

Plastic type	Global plastic usage (%)	Characteristics	Uses	References
<p>Polystyrene</p> $\left[\text{CH}_2 - \underset{\text{C}_6\text{H}_5}{\text{CH}} \right]_n$	7.0	Thermoplastic; brittle; poor barrier to oxygen and water vapour; low melting point; slow biodegradation.	Protective packaging, spectacles frames, plastic cups, clamshells; tumblers, disposable cutlery, etc.	Andrady, 2011; Barnes <i>et al.</i> , 2009.
<p>Polypropylene</p> $\left(\underset{\text{CH}_3}{\text{CH}} - \text{CH}_2 \right)_n$	19.2	Low density; high stiffness; heat resistance; chemical inertness; steam barrier properties; good transparency; good hinge property; easy to weld; can be recycled.	Textile, carpet backings, food packaging, crates, pails, corrugated boards, folders, car bumpers, dashboards, sewerage pipes, furniture, etc.	Kurkcu <i>et al.</i> , 2012.
<p>Polyethylene terephthalate</p> $\left(\text{O} - \text{C}(=\text{O}) - \text{C}_6\text{H}_4 - \text{C}(=\text{O}) - \text{O} - \text{CH}_2 - \text{CH}_2 \right)_n$	7.0	Absorbs little water; gas barrier properties; chemical resistant, transparency.	Capacitors, graphics, film base, recording tapes, pressure-sensitive adhesive tapes, industrial uses, blister packs, etc.	Xingyou <i>et al.</i> , 2006.

Table 2.1 (continued). Characteristics and uses of major plastic types in Europe.

Plastic type	Global plastic usage (%)	Characteristics	Uses	References
<p>Polyurethane</p> 	7.5	Thermoplastic; high reactivity; good tensile strength; good compression strength; abrasion resistant.	Coating and adhesive industries, mattresses, insulation panels, conveyor belt systems, etc.	Wessel <i>et al.</i> , 2016.
<p>Others: polytetrafluoroethylene, polycarbonate etc.</p>  	19.7	Highly flexible; resistant to acid, alkali, alcohols; high melting point; highly insoluble in most solvents; high electrical resistance; high water resistant; 250 times stronger than glass; high elasticity; absorbs little moisture; high voltage insulating characteristics.	Injection, teflon coated pans, enclosures for electronic assemblies, kitchen appliances, keyboard keycaps, roofing sheets, electrical connectors, insulators, dialysis equipment parts, gamma sterilisable instrument covers, etc.	Conte and Igartua, 2012; Desale and Pawar, 2018; Gaylor <i>et al.</i> , 2013.

2.3. Environmental presence of microplastics

Despite having a number of benefits, several properties of plastics such as low cost, low density and longevity result in high usage that are causing serious ecological as well as environmental problems (Thompson *et al.*, 2009a; 2009b). Many authors observed that these environmental problems are mostly due to the resistant characteristics of plastics (Walker and Xanthos, 2018). Plastics find their way to terrestrial environments through different sources and as a result of certain natural processes as well as anthropogenic activities. Plastics in the environment continue to degrade and over time become steadily smaller, eventually forming 'microplastics'. Different types of microplastics are found in the terrestrial environments - whether as intentionally manufactured microplastics leaking to the environment, fragments of macroplastics already present in the environment and plastics disintegrating into the microplastics prior to reaching the environment (Horton *et al.*, 2017; Moore, 2008).

One third of the marine plastic waste ends up in soils each year through the actions of various factors including activities of soil biota, agricultural practices, soil properties, and physico-chemical properties of microplastics (Rillig *et al.*, 2017). Other hotspots of microplastics in terrestrial environment have been reported in the proximity of cities, freshwater beaches and dams (Ballent *et al.*, 2016; Horton *et al.*, 2017). Microplastic concentrations could be as high as 7 % of the weight of soil in the case of a highly contaminated soil (Fuller and Gautam, 2016). Microplastic originates from the scraps of plastics or plastic dust during production and handling of plastics in the industries, which by far is the most common source of microplastics in terrestrial environments. Microfibres from textile laundering are believed to form a significant component of microplastics entering soil, mainly through sewage sludge and compost applications (Hartline *et al.*, 2016). Microfibres have been reported to still have their original properties in agricultural soil up to 15 years after the sludge additions (Zubris and Richards, 2005). Application of sewage sludge from the wastewater treatment plants as an organic fertiliser is a popular practice in many countries which adds microplastics to the terrestrial environments (Nizzetto *et al.*, 2016b). Between 80 % and 90 % of the microplastics are retained in sludge varying according to the plastic type and sewage treatment used (Mahon *et al.*, 2017; Talvitie *et al.*, 2017). The application rate of sludge in European agricultural lands ranges from 0 % to 91 % of the dry weight of the soil (w/ w) that equates to average and maximum areal per capita loadings of 0.2 and 8 mg microplastics/ ha/ yr. It was estimated that 1,270 to 2,130 tons of microplastics per million inhabitants are annually released in European cities, which is equivalent to a yearly addition of 63,000 – 4,30,000 tons of

microplastics to croplands (Nizzetto *et al.*, 2016a; 2016b). These figures far exceed the total accumulated burden of microplastics currently estimated to be present in surface water of global oceans. Microplastics can be released to the terrestrial environments during municipal waste collection, processing, transportation and landfilling. Uses of polytunnel, plastic greenhouse, horticultural foil, silage bailing and plastic mulch in agriculture do not degrade well in the soil and therefore is associated with the discharge of microplastic residues into the soil (Steinmetz *et al.*, 2016) (see section 2.4.2). In some cases, plastic mulches are made with oxo-plastics which are sold to farmers as products not to be collected after use. Oxo-plastic contains a pro-degradant catalyst (salts of manganese or iron) that enhances the biodegradation of the oxo-plastic in presence of oxygen in the open environment. The biodegradability potential of the oxo-plastic is limited by climatic factors and thus its use adds microplastics in soil (Steinmetz *et al.*, 2016). Studies showed that the microplastics can accumulate in terrestrial environments through the increasing use of organic fertiliser since the organic fertiliser contains significant quantities of microplastics (Weithmann *et al.*, 2018). The number of microplastic particles the researchers found in the organic fertiliser ranged widely from 14 to 895 particles per kilogram of the organic fertiliser produced (Weithmann *et al.*, 2018). Besides, microplastic can be emitted to the terrestrial environments through maintenance and construction activities, building of artificial turfs used in sport fields, abrasion of tyres, road dust, littering, irrigation with wastewater, flooding, plastic recycling, indoor dust (present in carpets, furniture, kitchen ware), laundry (detergent, fibres from garments), use of pharmaceutical products (vaccines, drugs) and personal care products (facewash, toothpaste, shower gel, hair care products, makeup products) as well as atmospheric deposition (Duis and Coors, 2016; Browne *et al.*, 2007). Terrestrial microplastic contamination is estimated as being 4 to 23 times higher than the marine contamination, depending on the type and condition of the environment (Mahon *et al.*, 2017; Talvitie *et al.*, 2017). It was hypothesised that fragmentation and weathering of plastics on land is facilitated through sunlight that exerts greater impact on the formation of microplastics compared to that in water (Horton *et al.*, 2017).

Currently there are approximately 165 million tons of plastics in the world's oceans which have the potential to become microplastics in due course (Walker, 2018). Distribution and concentration of the microplastics in the marine environment are influenced by environmental (Imhof *et al.*, 2017; Kim *et al.*, 2015) and anthropogenic factors (Sarafraz *et al.*, 2016). Key environmental factors include wave currents (Kim *et al.*, 2015), tides, cyclones, wind directions (Liubartseva *et al.*, 2016; Thiel *et al.*, 2013), wind velocity, river hydrodynamics

(Besseling *et al.*, 2017), mixing and vertical redistribution in the water column (Collignon *et al.*, 2012). Marine microplastic contamination originates mainly from the marine activities, such as accidental loss or illegal disposal during fishing or offshore drilling (Horton *et al.*, 2017; Moore, 2008), that can be deposited on urban beaches and pristine sediments (Andrady, 2011; Barnes *et al.*, 2009; Moore, 2008). Researchers speculated that nurdles, spilled into the oceans from shipping vessels, can add microplastics to the marine environment (Jambeck *et al.*, 2015). Microplastics showed intestinal uptake in the blue mussels (Ward and Kach, 2009; Wegner *et al.*, 2012), adsorption onto green algae and subsequent movement through the aquatic food chain via zooplankton to fish (Bhattacharya *et al.*, 2010; Cedervall *et al.*, 2012). Studies reported that the ubiquity of microplastics in the oceans affected organisms through entanglement (Clukey *et al.*, 2017; Duncan *et al.*, 2017), ingestion (Au *et al.*, 2017; Gramentz, 1988) and vector of transport for invasive species (Thiel *et al.*, 2013; Clark, 1997). Microplastics can be used as oviposition sites by ocean insects that affect their abundance and dispersion (Goldstein *et al.*, 2012). Bacteria and algae can be attached to the microplastic debris that serves as a vector for spreading harmful algal blooms and faecal indicator organisms (Keswani *et al.*, 2016).

Majority of research conducted to date on microplastics were focused on the marine ecosystems while there were a few studies regarding microplastics in the freshwater ecosystems. Microplastics have been reported in 34 freshwater species throughout the world. Ingestion of microplastics has been reported by Pinheiro *et al.* (2017) for over 600 taxa (Pinheiro *et al.* (2017; Silva-Cavalcanti *et al.*, 2017), being fish among the most affected taxa (Silva-Cavalcanti *et al.*, 2017). 83 % of the freshwater fish ingested microplastics which were found in their gut (Silva-Cavalcanti *et al.*, 2017).

2.4. Sources of microplastics

Microplastics found in the environment differ in size, shape and chemical composition that originate from a variety of different sources. Microplastics can be categorized as primary and secondary based on their origin.

2.4.1. Primary microplastics

Primary microplastics, marketed as micro-beads or micro-exfoliates, are microscopic in size and are used in facial-cleansers, cosmetics (Allen *et al.*, 2022; Derraik, 2002), or as vectors for drugs (Patel *et al.*, 2009). Other sources include medical tools, drilling fluids for oil and gas exploration, industrial abrasives, production scraps, pre-production plastics, plastic regranulates, etc. Microplastics in the skin cleaners were found to be polyethylene (PE), polypropylene (PP) and polystyrene (PS) having size of 74 – 420 μm . It was estimated that in 2012, around 6 % of the liquid skin cleaning products marketed in the Europe contain microplastics (Patel *et al.*, 2009; Derraik, 2002). Most cleaning and beauty products typically contain 0.05 % to 12 % of the microplastic particles, of which PE and PS are the dominant types (Fendall and Sewell, 2009). Primary microplastics used in air-blasting technology (stream of air under pressure used for various technical purposes) involve blasting acrylic, melamine, engines and boat hulls to remove rust and paint. Raw materials used for the fabrication of plastic products, namely plastic resin pellets or flakes and plastic powder, are another important source of primary microplastics. Virgin plastic pellets typically 2 – 5 mm can also be considered as primary microplastics (Costa *et al.*, 2010).

2.4.2. Secondary microplastics

Secondary microplastics refer to tiny plastic fragments derived from the breakdown of larger plastic debris due to the physical, biological and chemical processes (Thompson *et al.*, 2004; Barnes *et al.*, 2009) leading to a reduction in the structural integrity of the larger plastic debris (Browne *et al.*, 2007). UV radiation in sunlight causes oxidation and photo-degradation of the polymer matrix that result in the bond cleavage and consequently renders the plastic to weather and fragment (Andrady, 2011). Secondary microplastic sources include littering, illegal plastic waste dumping, losses of plastics from the landfill site, sewage sludge, wastewater treatment plant, agricultural plastic, synthetic polymer additive used to improve soil quality, biowaste, plastic laminated paper, materials discarded from the merchant ships, fishing vessels, recreational boats and aquaculture facilities (Duis and Coors, 2016). Several

processes generate secondary microplastics such as abrasion from car tyres, abrasion of fibres from the textiles, release of fibres from hygiene products, abrasion from household plastics, abrasion during paint use and removal, spills, painting of ships, cars and roads (Browne *et al.*, 2007).

2.5. Properties of microplastics

Physical properties of the microplastic include particle size, shape and surface area whereas chemical properties include polymer type, additives, surface chemistry and crystallinity. Potential risks posed by the microplastics largely depend on their physical and chemical properties (Lambert *et al.*, 2017).

2.5.1. Physical properties

Particle size is important for interacting with biota as described by Montes-Burgos *et al.* (2010). Ingestion and accumulation of microplastics by biota typically increases exponentially with the decreasing particle size (Lambert and Wagner, 2016; Gray and Weinstein, 2017). Shape determines the interaction of the polymer particles with the biological systems. Particles with irregular or needle-like shape may attach more readily to internal and external surfaces and exert a greater effect than cubic or spherical shape. For instance, a significant decrease in the growth of *Hyalella Azteca* was observed during the exposure to polypropylene fibres while the polyethylene beads did not show any change in the growth (Au *et al.*, 2015). Surface area per unit mass increases with the decreasing particle size. Surface area of microplastics can be calculated by spherical equivalent diameter for primary microplastics whereas it can cause underestimation for irregularly shaped secondary microplastics (Lambert and Wagner, 2016).

2.5.2. Chemical properties

The plastics tend to release chemicals which include residual monomers, starting substances, solvents, catalysts, biocides and additives incorporated during the production, processing and handling of the plastics. All these chemicals released from the plastics can cause toxicity (Andrady, 2017). Polyvinyl chloride (PVC) contains chloride and dioxins (Mersiowsky *et al.*, 2001). Polycarbonate (PC) disrupts the endocrine function and polystyrene has carcinogenic properties (Lithner *et al.*, 2011). Likewise, Polyethylene terephthalate (PET)

leaches endocrine-disrupting chemicals called phthalates (Wagner and Oehlmann, 2009). The rate of leaching depends on the pore diameter of the polymer, molecular size of the monomer, concentration in the parent plastic and degree of degradation. The plastic surface can be changed by the formation of the OH, O, N oxides and other photo-generated radicals that causes the surface to crack and open up new surfaces leading to the formation of distinctly shaped microplastics that are different from the primary microbeads. Changes in the surface chemistry influence interaction between the microplastic particles and microbes (Stabnikova *et al.*, 2021), cell uptake, retention, etc. (Ke and Lamm, 2011). Crystallinity affects the hydration and swelling behaviour by influencing the density and permeability. Preferential degradation in the amorphous region of the polymer increases overall crystallinity as size of the microplastic decreases (Chen *et al.*, 2000; Gopferich, 1996).

2.6. Fate of microplastics in the terrestrial environment

A recent study showed that the global emissions of plastics will be around 53 million tons per year by 2030 (Borrelle *et al.*, 2020), of which around 79 % would be landfilled or abandoned in the terrestrial ecosystems (Geyer *et al.*, 2017). Soil is subjected to both primary (see section 2.4.1) and secondary (see section 2.4.2) inputs of microplastics and thus broader research efforts are pivotal to understand the source, exposure, transport and fate of microplastics in the terrestrial environment. Microplastic is cycled through the different components of the environment and transported from the land to sea by surface runoff and erosion. Microplastic can be returned to the land from the sea during high tides and flooding (Figure 2.2). The extent of overall deposition, retention and transport of microplastics depends on human behaviour, particle characteristics, weather, topography, hydrology and environmental conditions (Horton *et al.*, 2017). Low flows and changes in river depth or velocity lead to deposition of particulate matter, whereas high velocity and erosion could lead to mobilisation of previously sedimented particles. Microplastic transport within a river system can be influenced by surrounding land use which might affect erosion, irrigation and runoff. Transportation of microplastics through biopores has been identified as a possible source of microplastics in groundwater (Huerta Lwanga *et al.*, 2016; Rillig *et al.*, 2017), although leaching of microplastics to groundwater is largely affected by soil texture, particle size, density, shape, pH and ionic strength (Pachapur *et al.*, 2016). Rapid leaching of microplastics takes place where there is high groundwater table and coarse soils; although the mechanism was not explained by Scheurer and Bigalke (2018).

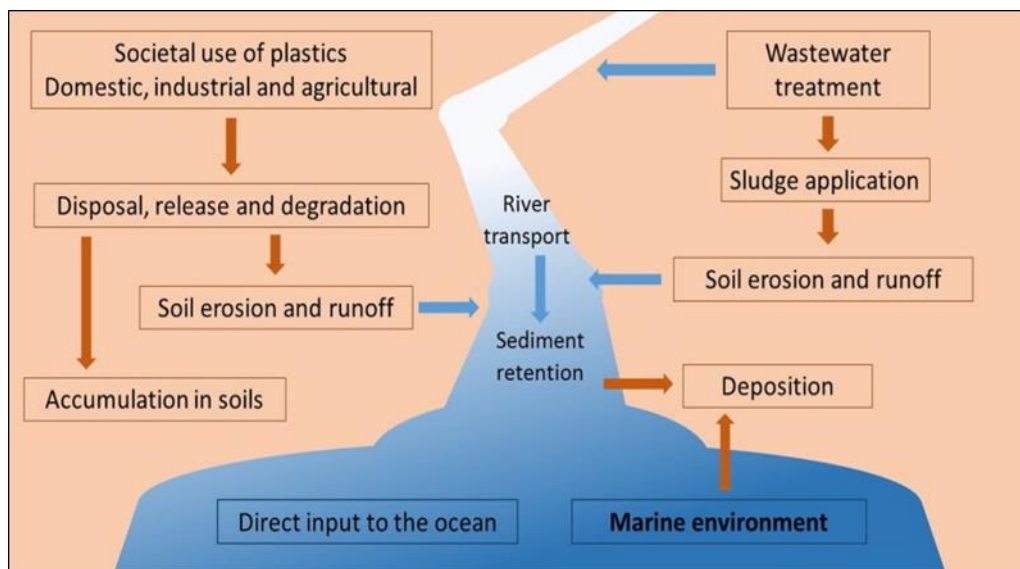


Figure 2.2. Fate and transport of microplastics in the environment. Microplastics are released from different sources into the soil which are transported from the land to sea by runoff and erosion. Microplastics are returned to the land from the sea during through sediment retention and deposition. The figure was adapted from Horton *et al.* (2017).

Microplastics might be subject to in-situ degradation, either by photodegradation or mechanical fragmentation (Naden *et al.*, 2016) resulting in changes in chemical structures and physical properties. For example, sheets of LDPE that had been immersed for six months in sea water lost 1.5 – 2.5 % of their weight (Moore, 2008). Microplastics in topsoil tend to degrade rapidly due to direct exposure to UV radiation, increased oxygen availability, freeze–thaw cycle, physical abrasion, higher temperature and agricultural practices (Shah *et al.*, 2008). Disintegration is decreased by low temperature, low oxygen levels and by fouling or coverage with water or sediment reducing exposure to UV radiation. Hence, photo-oxidative disintegration is relatively effective on a beach surface, but extremely slow in the deep ocean and for plastics buried in sediment or soil (Lambert *et al.*, 2014; Hammer *et al.*, 2012). Soil microbial communities and terrestrial organisms enhance biodegradation of plastics that leads to the progressive fragmentation from macro to microscale. For example, boring activity of isopods substantially contributes to the fragmentation of expanded polystyrene (EPS) used in aquaculture facilities (Rillig, 2012). Similarly, soil organisms, such as earthworms, that ingest plastic debris together with soil could contribute to the fragmentation (Yu *et al.*, 2022; Lahive *et al.*, 2022).

Long term storage of microplastics in the soil is promoted by incorporation of microplastics into the soil aggregates and consequently the soil acts as a sink of microplastics. Accumulations of the microplastics occur through burial where successive floods bury contaminated layers followed by remobilization of stored microplastics that result from the disturbance of the buried layers (Steinmetz *et al.*, 2016). Particle burial reduces degradation potential and increases the rate of preservation in marine and lacustrine sediment profiles (Corcoran *et al.*, 2015) indicating that there is the probability of a similar effect in the soil systems. Erosion by both water and wind transports microplastic particles across soil systems and eventually towards streams and rivers. Detailed mechanisms of these processes have not yet been investigated, however, inferences can be drawn from the wider domain of microplastic research (Nizzetto *et al.*, 2016a). Nizzetto *et al.* (2016a) assessed the transport and retention of microplastics mediated by size and density, and they found that the microplastics having densities higher than the water ($> 1 \text{ g/ cm}^3$) can be retained in sediment as well as soil. Small microplastics (0.001–0.005 mm) are transported effectively, regardless of their densities (Nizzetto *et al.*, 2016a). Interactions with the biota, once in the environment, can influence the fate and transport of microplastics in the environment. For example, biofouling (accumulation of microorganisms), adherence to the appendages of organisms, ingestion and egestion have the potential to alter the dispersal of microplastics in the environment leading to the trophic transfer of the microplastics (Maaß *et al.*, 2017).

2.7. Impacts of microplastics in the soil

Currently researchers are focusing on the impacts of microplastics in the environment particularly terrestrial ecosystems. Most studies to date focused on the impacts of microplastics in the aquatic ecosystems and there are some studies regarding the impacts of microplastics in the terrestrial ecosystems derived mainly from the sewage sludge and agricultural plastic mulch (Yu *et al.*, 2022; Kasirajan and Ngouajio, 2012; Dubaish and Liebezeit, 2013).

2.7.1. Impacts on soil nutrients, properties and processes

Nutrients, physico-chemical properties and processes of soil are affected by the presence of microplastics. Researchers demonstrated the effects of microplastics on soil carbon, nitrogen (Liu *et al.*, 2017), organic matter (Boots *et al.*, 2019), pH, bulk density, water holding capacity, hydraulic conductivity (Anderson *et al.*, 2018b; Boots *et al.*, 2019; Qi *et al.*, 2018), aggregate stability (Qi *et al.*, 2018), soil structure (Anderson *et al.*, 2018a; Anderson *et al.*, 2018b), enzyme and microbial activities (Liu *et al.*, 2017; Yang *et al.*, 2018; Lee *et al.*, 2014) as well as the nitrification process (Liu *et al.*, 2017; Jones *et al.*, 2004). Impacts of microplastics on the soil vary depending on the type, size, shape, concentration of microplastic, soil texture and soil intrinsic properties (pH, moisture content, etc.). For instance, Zhao *et al.* (2021) observed that the polyethylene foams and films increased the soil pH whereas soil pH was decreased with the addition of polyethylene fragments as discussed by Qi *et al.* (2018). Table 2.2 summarises major studies detailing the type of microplastic, concentration/ size, experiment type and impacts on the soil.

Table 2.2. Summary of selected studies detailing type, concentration, experiment type and impacts of microplastics on soil nutrients, properties and processes. Concentration of the microplastic is expressed as the percentage of dry weight of the soil (w/ w).

Type of microplastic	Concentration of microplastic	Type of experiment	Impacts of microplastics on soil	References
PVC	7 - 28 %	Incubation	Increase in activities of fluorescein diacetate hydrolase and phenol oxidase; increase in the contents of C, N and P in dissolved organic matter; inhibition in nitrification.	Liu <i>et al.</i> , 2017
PP	7 – 28 %	Incubation	Increase in soil microbial respiration; increase in urease, β -glucosidase and phosphatase enzymes.	Yang <i>et al.</i> , 2018
PAC, PA, PES, PEHD	2 %	In situ	Decrease in water stable aggregates; decrease in soil forming dry aggregates larger than 1 mm; decrease in bulk density; decrease in water holding capacity of soil; decrease in microbial activities.	Anderson <i>et al.</i> , 2018b
PLA, PEHD, CF	0.001 - 0.100 %	Laboratory	Decrease in soil pH; decrease in macro and micro aggregates	Boots <i>et al.</i> , 2019; Liang <i>et al.</i> , 2021
PA, PC, PES, PET, PP, PS, PU	0.4 %	Incubation	Increase/ decrease in soil pH; increase/ decrease in activities of acid phosphatase, β -D-glucosidase, cellobiosidase, N- β -glucosaminidase; decrease in microbial respiration.	Zhao <i>et al.</i> , 2021
HDPE, PP, PS, PET	0.2 – 2.0 %	Greenhouse	Increase/ decrease in bulk density, increase/ decrease in water stable aggregates, change in soil structure, increase in evapotranspiration.	Machado <i>et al.</i> , 2019

*PVC = polyvinyl chloride, PP = polypropylene, PAC = polyacrylic, PA = polyamide, PES = polyester, HDPE = high-density polyethylene, PLA = biodegradable polylactic acid, CF = clothing fibres, PC = polycarbonate, PET = polyethylene terephthalate, PS = polystyrene, polyurethane = PU.

2.7.2. Impacts on soil organisms

Based on the literature, it was reported that approximately 265 species have been affected by the microplastic debris, of which more than 180 were soil species (Laist, 1997). Most of the studies regarding the impacts of microplastics on the soil organisms can be summarized as (a) accumulation of microplastics or additives released from the microplastics in soil organisms that may exert adverse effects (Rodriguez-Seijo *et al.*, 2017; Huerta Lwanga *et al.*, 2017a; Gaylor *et al.*, 2013; Rillig *et al.*, 2017), (b) horizontal and vertical movement of microplastics affecting the organisms living above and below the soil (Huerta Lwanga *et al.*, 2017a; Maaß *et al.*, 2017), (c) direct ingestion and transfer of microplastics from one organism to another resulting in unwanted effects on their bodies (Costa *et al.*, 2016). Soil species *viz.*, earthworms (Huerta Lwanga *et al.*, 2016; Huerta Lwanga *et al.*, 2017a; Hodson *et al.*, 2017; Rillig *et al.*, 2017; Rillig, 2012; Rodriguez-Seijo *et al.*, 2017; Gaylor *et al.*, 2013), nematodes (Kiyama *et al.*, 2012), microarthropods (Zhu *et al.*, 2018a), collembolans (Maaß *et al.*, 2017; Zhu *et al.*, 2018b), isopods (Kokalj *et al.*, 2018), protists (Rillig and Bonkowski, 2018; Geisen and Bonkowski, 2017) and digging mammals (Rillig, 2012) have been studied to date in both field and laboratory conditions. These studies were conducted for investigating the potential of microplastics on the physiology of species across many ecological niches, although the effects varied between the species and plastic types (Moore, 2008; von Moos *et al.*, 2012). For example, less than 150 µm light-density polyethylene showed significant reductions in body weight and growth rate as well as increase in the mortality of *Lumbricus terrestris* (Huerta Lwanga *et al.*, 2017a). High-density polyethylene with an average area of 0.92 mm² acted as a vector to increase bioavailability of metal but there was no effect of metal on the body weight and mortality of *Lumbricus terrestris* (Hodson *et al.*, 2017). Researches were also conducted on fitness, reproduction, ingestion, egestion (Huerta Lwanga *et al.*, 2017a; 2017b; Huerta Lwanga *et al.*, 2016; Rillig *et al.*, 2017), histopathological damage and immune system (Rodriguez-Seijo *et al.*, 2017) of earthworms in response to the microplastic additions. Studies showed how the activities of earthworms impacted on the transport, redistribution and accumulation of microplastics in the deeper soil layers (Huerta Lwanga *et al.*, 2017a; 2017b; Rillig *et al.*, 2017; Gaylor *et al.*, 2013), and transfer of the microplastics from the earthworms to other organisms in the soil food web (Chen *et al.*, 2013; Hong *et al.*, 2017).

Nematode, *Caenorhabditis elegans*, were reported to ingest and accumulate microplastics (0.5 to 1 µm) in their gut (Kiyama *et al.*, 2012). Previous studies reported the significant

impacts of microplastics on the growth, reproduction (Maaß *et al.*, 2017; Rillig, 2012) and absorption of carbon, nitrogen in the collembolan (*Folsomia candida* and *Proisotoma minuta*) tissues (Zhu *et al.*, 2018b).

Trophic transfer of commercial polyvinyl chloride (PVC) having 80-250 µm diameter was demonstrated from the prey species, *Folsomia candida*, to the predator, *Hypoaspis aculeifer*, ultimately influencing the transfer of PVC to other soil biota in the soil food chain (Zhu *et al.*, 2018a). Microplastics from the plastic bags and facial cleansers did not affect the ingestion, defecation, food assimilation, mortality and body mass of the isopod, *Porcellio scaber* (Kokalj *et al.*, 2018).

Various soil-borne taxa, including ciliates, flagellates, amoebae and protists uptake microplastic beads depending on the size, shape and composition of the microplastic, cell size, degree of starvation, culture age and physiological state of the species (Rillig and Bonkowski, 2018). Fenchel (1980) suggested the uptake of latex microparticles (0.09 to 5.7 mm size) in 14 species of ciliates, of which two were soil ciliates (*Colpoda spp.*). When considering flagellates, uptake and incorporation rates of microplastics are species specific and rely on the nutritional status of flagellates. However, amoebae can engulf whole bacterial colonies with their pseudopodia and thus may not be as specific in food uptake as flagellates (Rillig, 2012). Transfer of microplastics into the soil food chain and uptake of microplastics by soil protists were studied by Rillig and Bonkowski (2018), Geisen and Bonkowski (2017).

2.8. Impacts of microplastics on plants

Studies showed that the microplastics can cause significant responses in plants at the individual, cellular and molecular levels mainly due to the changes in soil physico-chemical properties. However, contrary findings were found in some studies, where impacts of microplastics on plants vary depending on the plant species, soil characteristics, type, size, shape and concentration of the microplastic (Table 2.3). Qi *et al.* (2018) observed decrease in wheat growth while Zhang *et al.* (2015) observed improved corn quality in microplastic contaminated soils. Machado *et al.* (2019) mentioned that polyester and polyamide triggered significant increases in plant metabolic functions, while weaker effects were observed in plants exposed to high-density polyethylene, polyethylene terephthalate and polypropylene.

It was well documented that the microplastics interact with the metals and organic compounds (Holmes *et al.*, 2012; Rochman *et al.*, 2014; Hodson *et al.*, 2017; Massos and Turner, 2017) leading to the changes in soil properties that in turn impact on plants. This interaction between the microplastic and metal/ organic compound include two aspects: (a) adsorption/ desorption of metals and organic compounds by the microplastic particles (Abdurahman *et al.*, 2020; Goedecke *et al.*, 2017; Gregory, 1996), and (b) release of chemicals from the microplastics added during the manufacture of plastics (Bradney *et al.*, 2019; Hermsen *et al.*, 2017; Herrera *et al.*, 2017). Although exact mechanisms remain unclear, decreased plant growth (Qi *et al.*, 2018; Lozano and Rillig, 2020; Boots *et al.*, 2019) in microplastic contaminated soils was possibly due to potential stress caused by the degradation of byproducts of microplastics (Boots *et al.*, 2019), nutrient immobilization (Qi *et al.*, 2018; Rillig, 2018), reductions in water and/or nutrient availability (Boots *et al.*, 2019; Machado *et al.*, 2019), changes in soil pH (Lozano and Rillig, 2020; Zhao *et al.*, 2021), interferences with the stability and formation of soil aggregates (Machado *et al.*, 2019; Zhang *et al.*, 2018). Increase in plant growth (Zhang *et al.*, 2015; Tao *et al.*, 2012) due to the presence of microplastics could be attributable to high carbon content of microplastics that could feed the soil microbes leading to increased microbial activities (Huang *et al.*, 2019; Fei *et al.*, 2020; Liu *et al.*, 2017). Due to their high sorption capacity, microplastics play an important role in accumulating metals/ organic compounds leading to a significant impact on the biogeochemical cycling of these metals/ organic compounds (Yu *et al.*, 2022; Akhbarizadeh *et al.*, 2017; Bradney *et al.*, 2019; Hosler *et al.*, 1999). It is worth to be noted that no study was conducted till today regarding the impacts of microplastics on soil phosphorus although phosphorus is reported to be one of the macronutrients.

Table 2.3. Summary of the selected studies detailing type, concentration, size and effects of microplastics on plant parameters. Concentration of microplastic is expressed as the percentage of dry weight of the soil (w/ w) unless otherwise stated.

Plant species	Type of microplastic	Concentration of microplastic	Size of microplastic	Effects on plants	References
Wheat (<i>Triticum aestivum</i>)	PELD, PLA	1.0 %	50.0 µm – 1.0 mm	Decreases in number of fruits, root biomass, shoot biomass, stem diameter, area of leaf, plant height; increases in chlorophyll content, number of tillers.	Qi <i>et al.</i> , 2018
Grasses (<i>Festuca brevipila</i> , <i>Holcus Lanatus</i> , <i>Lolium perenne</i>)	PES, PLB	0.4 %	0.5 – 363.0 µm	Increases/ decreases in root biomass, shoot biomass; increase in chlorophyll-a/ chlorophyll-b ratio; decrease in shoot height; inhibition in seed germination.	Lozano and Rillig, 2020; Boots <i>et al.</i> , 2019
Spring onion (<i>Allium fistulosum</i>)	HDPE, PET, PES, PS, PA, PP	2.0 %	8.0 – 754 µm	Increases in root length, root area, root biomass, root: shoot ratio; decreases in leaf diameter, shoot biomass, leaf water content, leaf nitrogen content; decreases in root diameter, root tissue density.	Machado <i>et al.</i> , 2019
Maize (<i>Zea mays</i>)	HDPE, PLB	0.1 – 10.0 %	100.0 – 154.0 µm	Decrease in leaf chlorophyll content	Wang <i>et al.</i> , 2020a
Rice (<i>Oryza sativa</i>)	PES	50.0 – 500.0 mg/ L	8.5 – 30.7 µm	Decreases in shoot biomass, shoot length, root length.	Wu <i>et al.</i> , 2020
Carrot (<i>Daucus carota</i>)	PP, PS, PA, PET, PU, PC	0.1 – 4.0 %	4 mm	Increases in root biomass, shoot biomass.	Lozano <i>et al.</i> , 2020

*PELD = low-density polyethylene, PLA = polylactic acid, PES = polyester, PLB = biodegradable plastic, HDPE = high-density polyethylene, PET = polyethylene terephthalate, PES = polyester, PS = polystyrene, PA = polyamide, PP = polypropylene, PU = polyurethane, PC = polycarbonate.

2.9. Role of phosphorus in soil and plant

Being a macronutrient, phosphorus has garnered increasing attention due to its importance in maintaining soil fertility and crop production. Although most plants contain only about 0.2 to 0.4 % P by weight (Weil and Brady, 2002), P plays a critical role in cell division leading to the development of new plant tissue. Phosphorus is an essential nutrient both as a part of the plant structural compounds (such as ATP, NADPH, nucleic acids, phospholipids, plasma membranes and sugar-phosphates) and as a catalyst in the conversion of numerous biochemical reactions in plants (Stigter and Plaxton, 2015). Phosphorus is noted especially for its role in capturing and converting the sun's energy into the useful plant compounds during the photosynthesis (Carstensen *et al.*, 2018). Phosphorus is a vital component of DNA and also RNA, which determine the genetic code to build proteins and other compounds essential for plant structure and genetic transfer. The structures of both DNA and RNA are linked together by phosphorus bonds. Phosphorus acts as a vital substrate for a host of physiological processes, such as respiration, signal transduction, energy metabolism (Burman *et al.*, 2009), metabolism of carbon and nitrogen compounds and carbohydrate transportation (Béne *et al.*, 2015).

Available literature suggested that the phosphorus deficiency disturbs the physiological processes of the plant which in turn leads to the stunted growth of plant. The stunted plant growth induced by phosphorus deficiency was correlated with smaller leaf sizes and a lessened number of leaves. The most common phosphorus deficiency symptoms (visual symptoms) include: (1) affects older and lower leaves first, (2) bright red stems, (3) leaves become dark in colour particularly blue/ dark green/ purple, (4) leaves become shiny, thick and stiff with yellow patches (Zambrosi *et al.*, 2014). Insufficient soil P can result in delayed crop maturity, reduced flower development and decreased crop yield (Béne *et al.*, 2015; Sun *et al.*, 2016). Phosphorus deficiency can alter the metabolism and translocation of the carbohydrates, such as soluble sugars and organic acids. Increased accumulation of carbohydrates, especially sucrose, was observed in the leaves of many plant species under P deficiency which caused darkening of the leaves (Dong *et al.*, 2004). Secretion of organic acids is one of the most important low-P responses in plants, which dissolves soil P via acidification and complexation, and confers differing levels of low-P tolerance in crops (Dong *et al.*, 2004).

2.10. Sources of phosphorus in the soil

Phosphorus is usually considered a limiting nutrient because plants require large amounts of P on a daily basis, but the quantities of P in the soil solution is low, typically ranging from 0.3 to 3.0 kg/ ha (Mengel *et al.*, 2001). Phosphorus concentration is in the range of 500 to 10,000 kg/ ha in the upper 50 cm of the soil (Weil and Brady, 2002). Low P concentration in the soil is typically due to the high rate of chemical fixation and slow diffusion property of the P (Meng *et al.*, 2021). Thus, humans often apply phosphate fertilisers for the better development of the plants. Common sources of organic phosphorus fertiliser include phosphate rock, colloidal phosphate, bat guano (bird feces), steamed bone meal, fish bone meal, poultry manure and compost. Naturally occurring phosphate rock is a slowly soluble P source containing 4 to 20 % of total P expressed on the basis of nominal phosphorus pentoxide (P₂O₅) concentration (Meng *et al.*, 2021). Limestones and mudstones are common phosphate bearing rocks. The phosphate rock is washed and then dried in a lagoon. The dried by-product is known as colloidal rock phosphate. Clay is added to the colloidal rock phosphate and hence this is called soft rock phosphate, although it is no softer than the regular rock phosphate (Barker, 2019). Bat guano and bone meal are among the less commonly cited P sources but can have high P contents. Bat guano contains P ranging from 7 to 12 % and bone meal has a P content between 1 and 9 % (Nelson and Janke, 2007). Bone sources of P are more readily absorbed by plants (Nelson and Janke, 2007). Although the manures and composts are organically based P sources, the majority of the P present in soil is inorganic and readily available to the plants. Inorganic P accounts for about 75 to 90 % of the total P present in the manure and compost (Eghball *et al.*, 2002). Previous study (Leytem and Westermann, 2005) showed that the P uptake from the manure and compost was equal to or greater than the P uptake from commercial P fertilisers. The most common phosphate fertilisers that are chemically produced (manufactured in the industry) include superphosphate (9.0 % P), double superphosphate (17.5 % P), triple superphosphate (20.0 % P), monoammonium phosphate (21.0 % P), diammonium phosphate (20.0 % P) and ammonium polyphosphate (P concentration not found) (Green, 2015).

2.11. Phosphorus loss pathways

According to Jarvie *et al.* (2013) and Kerr *et al.* (2016), phosphorus is lost from the soil by (1) erosion, (2) surface runoff, (3) crop harvesting and (4) leaching. Panagos *et al.* (2022) and Orgiazzi *et al.* (2018) estimated that approximately 25 % of the P applied annually to the agricultural soil is uptaken by the growing crops, the remaining 75 % becomes bound in the soil profile or is lost to the water. As the major part of the soil P is tightly adsorbed to the mineral particles, bound within the soil organic matter, P is typically lost from the soils to water bodies via erosion by water. Alewell *et al.* (2020) predicted that the agricultural soils worldwide will be depleted by 4 to 19 kg ha⁻¹ yr⁻¹, with average losses of P due to the erosion by water contributing over 50 % of the total P losses. Surface runoff carries away both the dissolved P and particulate (eroded soil particles) P from the soil surface. Surface runoff typically occurs when the precipitation rate exceeds the infiltration capacity of the soil, or when the soil is already saturated and cannot absorb any more water. The amount of P loss in the runoff, is governed by the amount and intensity of the precipitation, climate and soils. Phosphorus is uptaken by the plants and is removed from the soil when the agricultural crop is harvested or the grass is grazed. Leaching is the loss of soluble P from the sub-surface soil as water percolates vertically down the soil profile. Since P is a limiting nutrient, P fertilization is typically required to meet the crop demand leading to the build-up of P in the soil. Excess P (soluble form of the P) is leached from the sub-surface soil as water percolates vertically down the soil profile (Orgiazzi *et al.*, 2018).

2.12. Fate and behaviour of phosphorus in the soil

Phosphorus exists in four different pools of the soil on the basis of its availability to the plants. Once the phosphorus enters the soil through various sources, P cycles between several P pools via different processes *viz.*, weathering, precipitation, mineralization, immobilization, adsorption and desorption (Figure 2.3). Weathering, mineralization and desorption increase the plant available P whilst immobilization, precipitation and adsorption decrease the plant available P. Phosphorus exists in different pools (soil solution P, mineral P, adsorbed P and organic P) of the soil on the basis of its availability to the plants. Different forms of P present in the soil are governed by the soil and fertiliser characteristics, soil organic matter content, clay content, cation exchange capacity, soil pH, initial P status, soil sorption strength, soil exchangeable Ca, Fe, Al and soil moisture content (Liu and Chen, 2008).

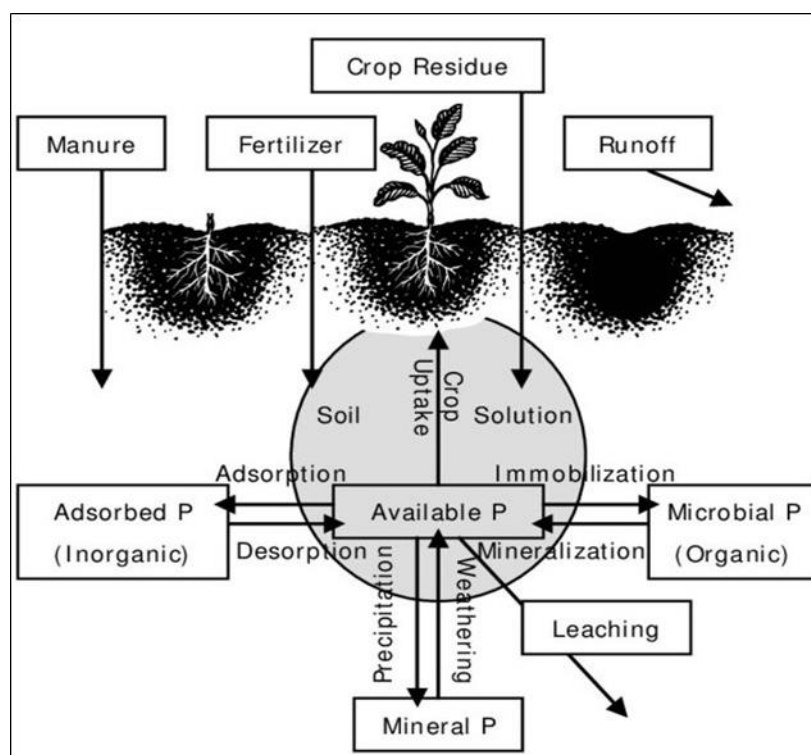


Figure 2.3. Phosphorus pools in the soil. The phosphorus transformation processes are weathering-precipitation, mineralization-immobilization, and adsorption-desorption. Weathering, mineralization and desorption increase plant available phosphorus. Immobilization, precipitation and adsorption decrease plant available phosphorus. The figure was adapted from Lal (2017).

Phosphorus in the soil solution is completely accessible but this makes up only a minute fraction of the total soil P. Plants uptake P from the soil solution as orthophosphate ion (either HPO_4^{2-} or H_2PO_4^-). The proportion in which these two forms are absorbed is determined by soil pH. For example, more HPO_4^{2-} is taken up at higher soil pH whilst $\text{H}_2\text{PO}_4^{2-}$ is predominately uptaken by the plants at lower soil pH (Parham *et al.*, 2002). High concentrations of H^+ shift the equilibrium to the more protonated form according to the equation: $\text{HPO}_4^{2-} + \text{H}^+ \leftrightarrow \text{H}_2\text{PO}_4^-$ (Meng *et al.*, 2001). The bulk of the soil P is virtually inaccessible. More than 90 % of the total P present in soil is present as insoluble (non labile) which includes primary phosphate minerals (e.g. phosphate rock), adsorbed P (adsorption of P onto Ca, Fe, Al compounds, clays, and silicate minerals) and organic P (occurs in plant residues and soil organic matter). Non labile fraction is a source of slowly available P (Meng *et al.*, 2001). A proportion of the insoluble P is more accessible than that of the bulk reserves which is the labile fraction of P. In this labile fraction, P is in rapid equilibrium with the soil

solution P. Removal of P from the soil solution by plant roots disturbs the equilibrium between the soil solution, P concentration and the labile pool at the solid soil phase which leads to a release of P into the soil solution (Meng *et al.*, 2001).

2.13. Adsorption to the microplastic

2.13.1. Adsorption mechanisms

Microplastics adsorb metal and organic compounds because of their large surface area and hydrophobicity. Previous studies reported that the primary mechanisms by which microplastics adsorb organic molecules in the aquatic environment include hydrogen bonding, π - π interaction, electrostatic interaction, Van der Waals force and pore filling mechanism (Martinho *et al.*, 2022; Lee *et al.*, 2013; Liboiron *et al.*, 2016; Liebezeit and Dubaish, 2012) as shown in the Figure 2.4.

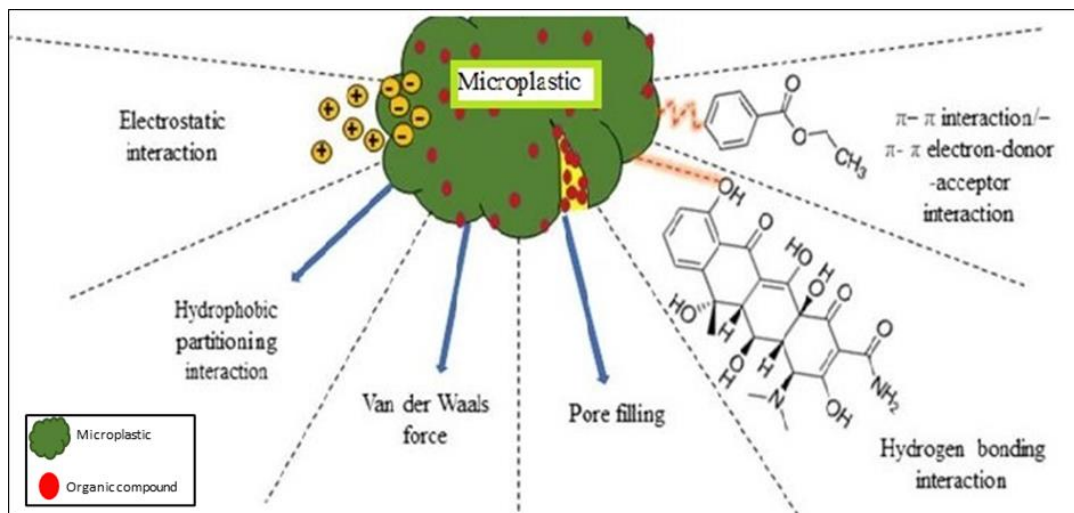


Figure 2.4. Adsorption of organic compound to the microplastic through several mechanisms. The mechanisms are hydrogen bonding, π - π interaction, electrostatic interaction, hydrophobic interaction, Van der Waals force and pore filling mechanism.

Hydrogen bonds are weak electrostatic interactions involving H^+ ions and can affect the adsorption on the microplastic when proton donor and proton acceptor groups are involved (Liu *et al.*, 2019). Zhang *et al.* (2018b) reported that the adsorption of oxytetracycline onto the polystyrene (PS) was due to the hydrogen bonding since the surface of the PS contained carboxyl and ester carbonyl groups. Li *et al.* (2018) demonstrated that the amide group

(proton donor group) of polyamide (PA) and the carbonyl group (proton donor group) of amoxicillin (AMX), tetracycline (TC), and ciprofloxacin (CIP) formed the hydrogen bonds enhancing the sorption affinities of the AMX, TC, CIP on the PA.

For the microplastics with benzene rings in their structure, π - π interaction is a key driving force that acts between the aromatic molecules (Bakir *et al.*, 2014). Huffer and Hofmann (2016) studied the sorption behaviour of seven aliphatic and aromatic organic compounds (n-hexane, cyclohexane, benzene, toluene, chlorobenzene, ethylbenzoate, naphthalene) to the polyamide (PA), polystyrene (PS), polyvinyl chloride (PVC) and polyethylene (PE) microplastics in the aqueous solution. Hüffer and Hofmann (2016) reported that the sorption capacity of the PS was the highest, which was likely because of the π - π interaction between the aromatic phenyl group of the PS and the aromatic organic compound. Liu *et al.* (2019) showed that the sorption capacity of the PS for ciprofloxacin (CIP) reached the highest earlier than the PVC, because the π - π bond enhanced the interaction between the microplastic and CIP. The sorption capacity of the PS for tetracycline (TC) was greater than that of the polyethylene and polypropylene which might be due to the presence of a benzene ring in both the PS microplastic and TC. The benzene ring enhanced the sorption of TC to the microplastic via polarity and π - π interaction (Xu *et al.*, 2018a). Furthermore, the π - π electron-donor-acceptor (EDA) interaction involves a special noncovalent attraction between the electron donor and the electron acceptor. For example, Wang *et al.* (2019) reported that the π - π EDA interaction influenced the sorption of nitrobenzene to the polystyrene (PS) microplastic. The PS acted as a π -electron donor and nitrobenzene acted as a stronger π -electron acceptor due to the strong electron-withdrawing nitro group and electron-depleted benzene ring (Wang *et al.*, 2019).

Electrostatic interaction occurs when both the microplastic and the organic compound have electric charges. Typically the electrostatic interaction occurs at a specific pH (Wang *et al.*, 2020a). If the pH of the adsorption environment exceeds the point of zero charge (PZC) of the microplastic, their surface becomes negatively charged and electrostatically attract positively charged compounds. However, when the pH of the adsorption environment is below the PZC of the microplastic, they are deprotonated and exist in an anionic form causing electrostatic repulsion and thus, inhibit the adsorption of the negatively charged compounds (Wu *et al.*, 2019; Wang *et al.*, 2020b). Li *et al.* (2018) studied the sorption behaviour of five antibiotics namely sulfadiazine (SZD), amoxicillin (AMX), tetracycline (TC), ciprofloxacin (CIP) and trimethoprim (TMP) to the microplastics and observed that the CIP had the highest

sorption capacity than the other antibiotics. In the freshwater system, the SZD, AMX, TC and TMP were in zwitterionic and anionic forms, while the CIP was in cationic form. The polyethylene (PE), polystyrene (PS), polyester (PES), polyamide (PA) and polyvinyl chloride (PVC) used in the study were negatively charged (pH was higher than the PZC) enhancing the sorption capacity of the cationic CIP by the electrostatic attraction (Li *et al.*, 2018). Li *et al.* (2019) reported that the sorption affinity of the triclosan (TCS) on the polystyrene (PS) microplastic decreased with the increasing pH from 6 to 11. At this pH range (6 to 11), the TCS was in the anionic form, and the negative charges of the TCS increased with the increases of the pH. Thus, electrostatic repulsion between the TCS and negatively charged PS increased which reduced the sorption affinity of the TCS.

The adsorption of the 9-nitroanthrene (9-NAnt) by the polyethylene (PE), polypropylene (PP) and polystyrene (PS) (Zhang *et al.*, 2020), adsorptions of the perfluorooctane sulfonate (PFOS) and perfluorooctane sulfonamide (FOSA) by the PE (Wang *et al.*, 2015), and adsorptions of the 4-chlorophenol (MCP), 2,4-dichlorophenol (DCP) and 2, 4,6-trichlorophenol (TCP) by the polyethylene terephthalate (PET) took place due to the hydrophobic interactions (Liu *et al.*, 2020). The octanol/water partition coefficient (K_{ow} /Log K_{ow}) represents the hydrophobicity of a substance (Zhang *et al.*, 2012). Organic compounds with high Log K_{ow} values are likely to be absorbed by the microplastics more easily. Fang *et al.* (2019) observed that the fungicides were adsorbed by the PS which were consistent with their respective Log K_{ow} values. While studying the behaviour of the bisphenol adsorption on the microplastic, Wu *et al.* (2019) observed a strong linear relationship between the equilibrium adsorption efficiency and the Log K_{ow} value, indicating that the hydrophobic interaction is the primary mechanism by which the microplastic adsorbs bisphenol.

According to Guo *et al.* (2012), PE microplastics are nonpolar without specific functional groups and could only interact with the organic compounds (phenanthrene, naphthalene, lindane, and 1-naphthol) by Van der Waals force. Xu *et al.* (2018b) found that both the sulfamethoxazole (SMX) and PE were negatively charged under experimental pH of 6.8. The hydrophobic interaction and electrostatic interaction could not explain the sorption of the SMX sorption on the PE, which might be attributed to the Van der Waals interaction. Furthermore, the partition effect refers to the distribution of the target organic molecule between the adjacent water layer on the surface of the microplastic and the host solution, and mainly relies on the Van der Waals forces as a form of linear adsorption (Liu *et al.*, 2016). The n value of the adsorption isotherm, corresponding to the adsorption of the aliphatic and

aromatic organic compounds by the polyethylene (PE) microplastic is approximately 1, indicating the strong linearity. Therefore, the aliphatic and aromatic organic compounds are adsorbed to the microplastics via the partition effect (Hüffer and Hofmann, 2016). Guo *et al.* (2019) applied the Freundlich model to confirm that the n value for the adsorption of antibiotics by the polyethylene (PE) and polystyrene (PS) is also around 1 suggesting that the isotherm is linear. Therefore, the partition effect is also an important mechanism by which the microplastics adsorb the organic compounds. Liu *et al.* (2019) revealed that the adsorptions of the diethyl phthalate (DEP) and dibutyl phthalate (DBP) by the PE and PS were due to the partition effects since the adsorption isotherms were strongly linear.

It was reported that there are many pores of different sizes in the microplastic particles (Guo *et al.*, 2018; Zhang *et al.*, 2018b) and thereby, the organic compounds can enter the pores and may be trapped in those pores. Zhang *et al.* (2018b) observed that the sorption of oxytetracycline (OTC) by beached and virgin polystyrene (PS) foam involved the pore-filling mechanism. The beached PS foam adsorbed more than the virgin PS foam, which was attributed to the higher micropore area of the beached foam. The micropore area of the virgin PS foam was $0.004 \pm 0.02 \text{ m}^2/\text{g}$, but the micropore area of the beached PS foam was $0.50 \pm 0.02 \text{ m}^2/\text{g}$. The average pore diameter of the virgin PS foam was five times more than the beached PS foam. Zhang *et al.* (2017) illustrated that the sorption capacity of the PS to the OTC was significantly higher than that of PE, which was mainly because the PS had more folds and pore structure than the PE particles.

A number of studies (Decho, 2000; Rochman *et al.*, 2014; Turner, 2016; Catrouillet *et al.*, 2021) have reported the adsorption of metals to the microplastics in the aquatic environment although as far as the author is aware no study until today has determined the mechanism by which the metal is adsorbed to the microplastic surface. It was hypothesised that this adsorption is caused by either the specific or the non-specific interactions between the metal and microplastic (Zhou *et al.*, 2020). Presumably, metal adsorption proceeds through the specific interactions between the metal cations (e.g. Cu^{2+})/ oxyanions (e.g. CrO_4^{2-}) with the polar regions of the plastic surfaces, or via the non-specific interactions between the metal-organic complexes adsorbed in the neutral regions and the hydrophobic surfaces of the microplastics (Holmes *et al.*, 2012). Ashton *et al.* (2010) hypothesised that the mechanisms of accumulating metals to the microplastics in the water body was related to the co-precipitation or adsorption on the hydrated oxides of Fe and Mn. Tang *et al.* (2021) assumed that the divalent metal cation (e.g. Ni^{2+} , Cu^{2+} , and Zn^{2+}) might interact with

the carboxylate anion present on the microplastic through the electrostatic attraction leading to the adsorption of the divalent metal to the microplastic. In a study by Guo and Wang (2019), it was hypothesised that the adsorption of metal onto the microplastic occurs due to (i) the surface diffusion of metal on the microplastic film; (ii) the pore volume diffusion of metal in the microplastic; (iii) the adsorption on the accessible active sites.

2.13.2. Adsorption isotherms

Adsorption isotherm is the relationship between the amount of adsorbate in the liquid phase and the adsorbate adsorbed on the surface of the microplastic at equilibrium at constant temperature (Zhang *et al.*, 2020).

2.13.2.1. Langmuir adsorption isotherm

The Langmuir adsorption isotherm makes several assumptions about the system in which the adsorption to the microplastic is occurring. These assumptions are: (i) the surface of the sorbent is homogeneous, (ii) each surface site on the adsorbent can accommodate only one adsorbate from solution (monolayer coverage), and (iii) there is no interaction between the adsorbate molecules once they are adsorbed (Jalali and Moharrami, 2007; Zhou *et al.*, 2018). Langmuir binding constant (b) in the Langmuir model is an important parameter for measuring the strength of the attraction between the surface and the adsorbing molecule (Liu *et al.*, 2019). A number of studies showed that the adsorptions on the microplastics were best described by the Langmuir isotherms indicating that the adsorptions involved the monolayer adsorption. For example, adsorption of levofloxacin (OFL) onto PVC microplastic (Yu *et al.*, 2020), adsorption of tri-*n*-butyl phosphate, tris-(2,3- dibromopropyl) isocyanurate and hexabromocyclododecanes on PP microplastic (Liu *et al.*, 2018) were best described by the Langmuir isotherms.

The equation for the Langmuir adsorption isotherm is:

$$\frac{C_s}{C_{aq}} = \frac{bC_{SM}}{1 + C_{aq}b}$$

Where C_s (mg/ kg) is the adsorption capacity; C_{aq} (mg/ L) represents the equilibrium solution concentration; C_{SM} (mg/ kg) is the theoretical monolayer capacity and b (L/ mg) is the binding constant (Sposito, 2004; Sparks, 2003).

2.13.2.2. Freundlich adsorption isotherm

In contrast to the Langmuir adsorption isotherm, the Freundlich adsorption isotherm assumes that the adsorbent has a heterogeneous surface (Jalali and Moharrami, 2007; Zhou *et al.*, 2018). Therefore, this isotherm can be used to model multi-layer adsorption (Jalali and Moharrami, 2007; Zhou *et al.*, 2018). Unlike the Langmuir isotherm, no maximum adsorption value can be calculated using the Freundlich adsorption isotherm (Stumm and Morgan, 1996). The Freundlich constant (K_f) of the Freundlich model largely depends on the interactions between the adsorbent and the microplastic. The parameter $1/n$ in the Freundlich model indicates the surface heterogeneity, suggesting that the adsorption decreases as the adsorbate concentration increases as there are no sites on the microplastic available for further sorption. Typically the value of $1/n$ is $0 \leq 1/n \leq 1$ (Sposito, 2004; Sparks, 2003). Researchers (Li *et al.*, 2021; Wang *et al.*, 2020a; Zhang *et al.*, 2018a; Liu *et al.*, 2019) used the Freundlich models to fit the adsorptions on the microplastics indicating that the processes involved multilayer adsorption. For example, adsorption of the pesticides on the polyethylene (PE) microplastic (Li *et al.*, 2021), adsorption of triclosan on the polyethylene (PE) and polyhydroxybutyrate (PBT) microplastics (Tong *et al.*, 2021) were best described by the Freundlich isotherms.

The equation for the Freundlich adsorption isotherm is:

$$C_s = K_f C_{aq}^{1/n}$$

Where C_s is the equilibrium solid phase concentration (mg/ kg), K_f is a Freundlich constant, C_{aq} is the equilibrium solution concentration (mg/ L) and $1/n$ is another Freundlich constant, the heterogeneity factor (Sposito, 2004; Sparks, 2003).

2.13.3. Factors affecting adsorption to microplastic

Previous studies observed that the adsorption of metals and organic molecules to the surfaces of microplastic in aquatic ecosystems is significantly affected by microplastic properties (particle size, specific surface area, crystallinity, functional groups, polarity) and a range of environmental factors (weathering, pH, temperature, ionic strength/ concentration of the background electrolyte) (Martinho *et al.*, 2022; Ateia *et al.*, 2022; Zhang *et al.*, 2020; Fastelli

et al., 2016). Figure 2.5 summarises how the factors influence the adsorption capacity of microplastics in aquatic ecosystems.

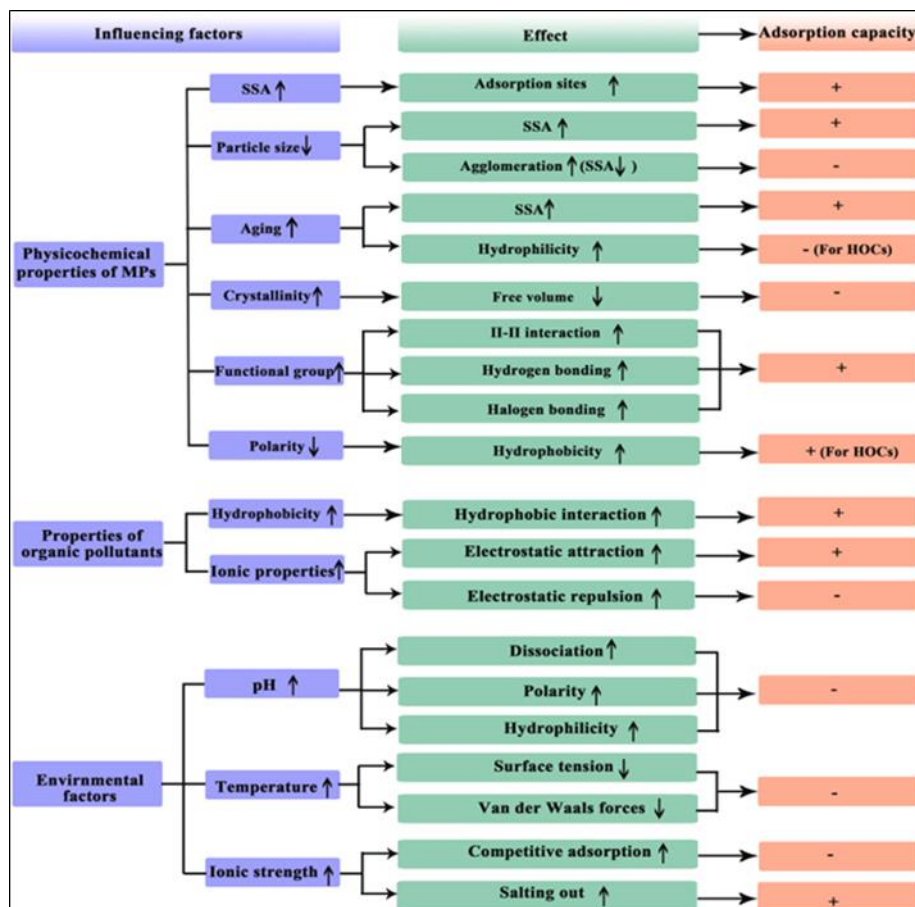


Figure 2.5. Factors affecting the adsorption of hydrophobic organic pollutant on the microplastic. MP = microplastic, SSA = specific surface area, HOC = hydrophobic organic compound. A combination of the physicochemical properties of the microplastic, properties of the organic pollutant and surrounding environmental factors influence the adsorption on the microplastic. Plus sign (+) indicates the positive effects and minus sign (-) indicates the negative effects. The figure was adapted from Wang *et al.* (2020a).

2.13.3.1. Microplastic particle size and specific surface area

Theoretically the smaller the particle size and the larger the specific surface area (SSA) of the microplastic, the greater their number of adsorption sites and the amount of organic compound they can adsorb (Figure 2.5). For example, the adsorption of 3,6 dibromocarbazole to the polypropylene (PP) was 28 % when the particle size of the PP was 2 mm whilst the adsorption was 12 % with the 5 mm PP (Zhang *et al.*, 2019). Wang *et al.* (2019) reported that the adsorption of the nitrobenzene increased when the specific surface area (SSA) of the polyester (PES) was increased from 0.4 m²/ g to 27.6 m²/ g. The particle size of the microplastic is not always inversely proportional to their SSA. The measured SSA (63.4 m²/ g) of 50 nm PS was lower than the theoretical value of 114.3 m²/ g, which may be due to the agglomeration of PS and subsequent decrease in SSA (Wang *et al.*, 2019). Thus, the log K_d values of 50 nm PS was lower than that of 235 nm PS. The adsorption capacity of 2 μm PS was lower than that of 10 μm PS, which may also due to the agglomeration of PS and consequent decrease in SSA (Enders *et al.*, 2015). Previous studies reported that microplastic of smaller size are less stable than larger particles. 70 nm polystyrene (PES) particles could aggregate into 361 nm aggregates in seawater within 6 weeks (Velzeboer *et al.*, 2014) whereas 30 nm PS could rapidly aggregate into 968 nm aggregates within 16 min (Wegner *et al.*, 2012). Therefore, the effect of particle size on the adsorption capability of microplastics is due to the combined effects of particle size and agglomeration. Particle size only affects the adsorption capacity of microplastics within a certain range and ultimately depends on the SSA.

2.13.3.2. Crystallinity

In the natural environment, microplastics usually contain crystalline and amorphous regions. For instance, polyethylene (PE) and polyamide (PA) have semi-crystalline structures whereas polyester (PS) and polyvinyl chloride (PVC) have amorphous structures (Guo *et al.*, 2019). The crystalline region, which has regularly arranged molecular segments, is held together strongly and can easily be condensed, while the amorphous region has irregular molecular segments and is loose (Teuten *et al.*, 2009). The amorphous region of the microplastic has a larger free volume and organic molecules show a greater affinity for this amorphous region than the crystalline region, indicating that, the higher the crystallinity of the microplastic, the weaker their adsorption capacities for the organic molecule (Figure 2.5). The complexity, chain configuration, and glass transition temperature (T_g) of the microplastic affect the crystallinity of the microplastic. The T_g represents the temperature at which the amorphous

region of the plastic changes from a rubber-like to a glass-like form. At the glass transition temperatures of the polybutylene succinate (PBS) and polylactic acid (PLA), PBS appears as a rubbery polymer, while PLA appears as a glassy polymer. Molecular links in the glassy polymer (PLA) are dense and cross-linked, which hinders the movement of the organic compounds. Therefore, PBS has a greater fipronil (insecticide) adsorption capacity than the PLA (Gong *et al.*, 2019).

2.13.3.3. Functional groups and polarity

The functional groups and polarity of the microplastics determine their sorption behaviours. Hüffer and Hofmann (2016) studied the adsorption properties of the PA, PE, PVC, PS, and found that the PS had the strongest adsorption capacity due to a strong π - π interaction between the PS and toluene, facilitating high levels of adsorption. The roles of the functional groups and polarity of the microplastic for influencing the adsorption process were discussed in detail in the section 2.13.1.

2.13.3.4. Weathering

Microplastics undergo changes in their surface structures and functional groups due to the external environmental factors, including the ultraviolet radiation, water (corrosion) and temperature (Zhang *et al.*, 2018a). As the microplastics age, some of their bonds including the C-H and C-C are oxidized (Lang *et al.*, 2020). The resultant oxygen-containing functional groups increase their hydrophilicity or strengthen the hydrogen bonds between the microplastics and organic molecules, thereby improving their adsorption capacity. The PVC exhibits characteristic peaks of carbonyl and vinyl esters following the photo-induced weathering (Liu *et al.*, 2018). The PS has characteristic peaks of the carbonyl and phenolic hydroxyl in their structure following the high-temperature weathering (Ding *et al.*, 2020). The tensile vibrations of peroxy-radicals (C-O), C-OH, and C=O present in the high-temperature weathered PS indicated an increase in the number of oxygen-containing functional groups (Mao *et al.*, 2020). The hydrogen bonds, formed between the weathered PS and organic compounds, are thus, increased the adsorption capacity of the PS particles for the organic compounds (Ding *et al.*, 2020; Liu *et al.*, 2018). In contrast, the weathering of the microplastics decreases their adsorption capacity for hydrophobic organic compounds. Juan *et al.* (2020) observed that the adsorption of 2,2',4,4'-tetrabromodiphenyl ether (BDE-47) by the weathered PS was lower than that of the pristine PS.

2.13.3.5. pH

Under different pH levels, microplastics and organic compounds contain different charges that affect the adsorption process. Increases in the pH promote the dissociation of the dissociable organic compounds resulting in the formation of negatively charged hydrophilic substances, which reduces the hydrophobic effect and triggers electrostatic repulsion between the microplastic and organic compound. Wang *et al.* (2015) reported that the perfluorooctane sulfonate (PFOS) adsorption capacity of the PS increases as the solution pH decreases. With a decrease in the pH from 7 to 3, the level of the PFOS adsorption onto the PS increases from 0 to 0.3 $\mu\text{g/g}$. At the pH 3.0 – 7.0, PFOS predominantly exists in its anionic form, and the surface of the PS becomes protonated when the pH decreases which increases the PFOS adsorption by the PS (Wang *et al.*, 2015). 9-nitroanthrene (9-NAnt) adsorption capacities of the PP and PS decrease as the pH increases. When the pH exceeds 7, the negative potential of the PP, PS and polarity of 9-Nant increase, resulting in strong electrostatic repulsion between the microplastics and 9-Nant (Zhang *et al.*, 2020).

2.13.3.6. Ionic strength/ concentration of the background electrolyte

When the organic compounds are adsorbed by the microplastics via an electrostatic mechanism, the salt ions in water and organic substances compete for the adsorption sites on the microplastics, thereby reducing the adsorption of organic compounds. When the mechanism is related to the hydrophobicity, the presence of salt ions induces the “salting out” effect, which lowers the solubility of the organic compounds and promotes their hydrophobic interaction with the microplastics. Zhang *et al.* (2018b) studied the influence of the ionic strengths of NaCl, CaCl₂, and Na₂SO₄ on the oxytetracycline (OTC) adsorption by the PE and the findings demonstrated that the adsorption of OTC by the PE decreased with the increasing ionic strength. The Ca²⁺ and Na⁺ compete with the OTC for cation exchange sites on the surface of microplastics. Zhang *et al.* (2018b) observed that the adsorption of the OTC by microplastics in presence of CaCl₂ was stronger than that in the presence of NaCl or Na₂SO₄, indicating that ternary complexes formed between OTC, Ca²⁺ and the functional groups on the surface of the microplastics thereby promoting the adsorption. The presence of Ca²⁺ and Na⁺ decreased the adsorption of 9-NAnt by PP and PS, as the ions occupy the adsorption sites on the surfaces of microplastics. High Na⁺ concentrations increase the density and viscosity of the solution and hinder the movement of 9-NAnt from the solution to the surface of microplastics (Zhang *et al.*, 2020). The triclosan (TCS) adsorption capacity increases with the increases in the NaCl concentration. When the NaCl content increased

from 8.75 % to 35 %, the adsorption capacity of the PVC for the TCS increased by 43.8 % (Ma *et al.*, 2019). This is primarily due to the “salting out” that occurred during the adsorption, which reduced the solubility of TCS in solution and promoted the adsorption of TCS onto the PVC as described by Fang *et al.* (2019).

2.13.3.7. Temperature

Temperature can significantly affect the adsorption capability of the microplastics. Under lower temperature conditions, organic compounds can be easily adsorbed onto the microplastics as the surface tension of adsorption increases and solubility of organic compounds in water decreases. Therefore, the distribution of the organic compounds on the surface of the microplastics increases, resulting in a greater level of adsorption (Zhan *et al.*, 2016). Zhan *et al.* (2016) reported that the adsorption of 3,3',4,4'-tetrachlorobiphenyl (PCB 77) to the PP decreased with the increasing temperature, which could primarily be attributed to the decrease in the surface tension of the solution and unfavourable contact between PCB77 and PP. Within a temperature range of 4 – 32 °C, the water solubility of the PCB77 increases as the temperature increases (Dickhut *et al.*, 1986) which hinders its adsorption onto the microplastics. Liu *et al.* (2018) found that the adsorption of tris-(2,3-dibromopropyl) isocyanurate and hexabromocyclododecane by microplastics decreasing with increasing temperature, which is due to the weakening of the Van der Waals forces (section 2.13.1) and surface tension.

2.14. Knowledge gaps identified

On the basis of the above review the knowledge gaps that I have identified in this thesis are environmental fate, potential impacts and ecological risks of microplastics in the terrestrial ecosystems have received much less attention whilst there are some evidences for microplastic contamination of the soils. Further research is required to determine the impacts of microplastics on soil and subsequent impacts on plants.

Being highly resistant to degradation, particulate microplastics are ubiquitous in the soil (Kumar *et al.*, 2020), and eventually would reach levels that could affect the soil properties particularly nutrient status crucial for the growth of plants. Thus, the soil tends to act as a long-term sink for the microplastics, and it is necessary to explore the fate and behaviour of microplastics on the soil properties, biogeochemical cycles as well as the growth of plants which are prerequisite to assess hazards and risks posed by the microplastic debris. The research should be used to determine whether legislation to control the microplastic pollution is necessary to protect the environment.

There are three key questions that therefore arise for this thesis:

- 1) Do microplastics have the potential to adsorb phosphate, an essential plant nutrient?
- 2) Do the effects of pH and concentration of background electrolyte impact on the adsorption of phosphate to the microplastic?
- 3) Does the microplastic impact on the soil properties and growth of plants?

2.15. Identified experiments for the thesis

On the basis of the knowledge gaps identified above, the following experiments were designed.

- (a) An initial laboratory experiment (Chapter 3) was carried out to determine the potential of two types of microplastics – pristine and weathered to adsorb plant nutrient, phosphorus, in two soil samples differing in organic matter content. The adsorption of P to the mixture of microplastic and soil were also investigated.
- (b) On the basis of the initial experiment results, laboratory experiments (Chapter 4) were carried out to determine the effects of different pH (ranging from 2 to 12) and various concentrations of the background electrolyte (ranging from 0 to 0.1 M NaNO₃) on the microplastic, soil as well as mixture of the microplastic and soil.
- (c) An incubation experiment (Chapter 5) was carried out to test the effects of different levels of microplastic treatments ranging from 0 % to 5.00 % which was considered environmentally relevant for the soils exposed to high human pressure and industrialization. This incubation experiment was carried out to know the effects of microplastic on soil physico-chemical properties and whether these effects are different in the presence of plants and in the soils of two different contents of organic matter. To observe the effects on plants, a greenhouse pot experiment (Chapter 5) with ryegrass (*Lolium perenne*) was carried out with the incubated soils. The detailed aims and measured parameters of each experiment are given within the relevant chapters.

2.16. References

Abdurahman, A., Cui, K., Wu, J., Li, S., Gao, R., Dai, J., Liang, W., and Zeng, F. (2020). Adsorption of dissolved organic matter (DOM) on polystyrene microplastics in aquatic environments: kinetic, isotherm and site energy distribution analysis. *Ecotoxicology and Environmental Safety*, 198, 1-12.

Akhbarizadeh, R., Moore, F., Keshavarzi, B., and Moeinpour, A. (2017). Microplastics and potentially toxic elements in coastal sediments of Iran's main oil terminal (Khark Island). *Environmental Pollution*, 220, 720–731.

Alewell, C., Ringeval, B., Ballabio, C., Robinson, D. A., Panagos, P., and Borrelli, P. (2020). Global phosphorus shortage will be aggravated by soil erosion. *Nature Communications*, 11, 1-12.

Allen, S., Allen, D., Karbalaei, S., Maselli, V. and Walker, T. R. (2022). Micro(nano)plastics sources, fate, and effects: What we know after ten years of research. *Journal of Hazardous Materials Advances*, 6, 1-12.

Alzeer, M. and MacKenzie, K. (2013). Synthesis and mechanical properties of novel composites of inorganic polymers (geopolymers) with unidirectional natural flax fibres (*Phormium tenax*), *Applied Clay Science*, 75, 148–152.

Anderson, A. S. M., Kloas, W., Zarfl, C., Hempel, S., and Rillig, M. C. (2018a). Microplastics as an emerging threat to terrestrial ecosystems. *Global Change Biology*, 24, 1405–1416.

Anderson, A. M., Chung, W. L., Jennifer, T., Werner, K., Anika, L., Roland, B., and Matthias, C. R. (2018b). Impacts of microplastics on the soil biophysical environment. *Environmental Science and Technology*, 52, 9656-9665.

Andrady, A. L. (2011). Microplastics in the marine environment. *Marine Pollution Bulletin*, 62, 1596-1605.

Andrady, A. L. and Neal, M. A. (2009). Applications and societal benefits of plastics. *Philosophical Transactions of the Royal Society of London: Biological Sciences*, 364, 1977–1984.

Anthony, L. A. and Mike, A. N. (2009). Applications and societal benefits of plastics. *Philosophical Transactions of the Royal Society of London: Biological Sciences*, 364, 1977–1984.

Ashton, K., Holmes, L., and Turner, A. (2010). Association of metals with plastic production pellets in the marine environment. *Marine Pollution Bulletin*, 60, 2050-2055.

Ateia, M., Ersan, G., Alalm, M. G., Boffito, D. C. and Karanfil, T. (2022). Emerging investigator series: microplastic sources, fate, toxicity, detection, and interactions with micropollutants in aquatic ecosystems – a review of reviews. *Environmental Science: Processes and Impacts*, 24, 172-195.

Au, S. Y., Bruce, T. F., Bridges, W. C., and Klaine, S. J. (2015). Responses of *Hyalella azteca* to acute and chronic microplastic exposures. *Environmental Toxicology and Chemistry*, 34, 2564–2572.

Au, S. Y., Lee, C. M., Weinstein, J. E., van den Hurk, P., and Klaine, S. J. (2017). Trophic transfer of microplastics in aquatic ecosystems: identifying critical research needs. *Integrated Environmental Assessment and Management*, 13, 505–509.

Bakir, A., Rowland, S. J., and Thompson, R. C. (2014). Transport of persistent organic pollutants by microplastics in estuarine conditions. *Estuarine, Coastal and Shelf Science*, 140, 14–21.

Ballent, A., Corcoran, P. L., Madden, O., Helm, P. A., and Longstaffe, F. J. (2016). Sources and sinks of microplastics in Canadian Lake Ontario nearshore, tributary and beach sediments. *Marine Pollution Bulletin*, 110, 383–395.

Barker, A. V. (2019). Fertilizers. In: Worsfold, P., Poole, C., Townshend, A., and Miro, M. (2019). *Encyclopedia of Analytical Science*. Netherlands: Elsevier.

Barnes, D. K. A., Galgani, F., Thompson, R. C., and Barlaz, M. (2009). Environmental accumulation and fragmentation of plastic debris in global. *Philosophical Transactions of the Royal Society of London: Biological Sciences*, 364, 1985-1998.

Béné, C., Barange, M., Subasinghe, R., Pinstруп-Andersen, P., Merino, G., Hemre, G. I., and Williams, M. (2015). Feeding 9 billion by 2050—putting fish back on the menu. *Food Security*, 7, 261–274.

Bhattacharya, P., Lin, S. J., Turner, J. P., and Ke, P. C. (2010). Physical adsorption of charged plastic nanoparticles affects algal photosynthesis. *Journal of Physical Chemistry*, 114, 16556–16561.

Besseling, E., Quik, J. T. K., Sun, M., and Koelmans, A. A. (2017). Fate of nano and microplastic in freshwater systems: a modeling study. *Environmental Pollution*, 220, 540–548.

Boots, B., Russell, C. W., and Green, D. S. (2019). Effects of microplastics in soil ecosystems: above and below ground. *Environmental Science and Technology*, 53, 496–506.

Borrelle, S. B., Ringma, J., Law, K. L., Monnahan, C. C., Lebreton, L., Mccivern, A., Murphy, E., Jambeck, J., Leonard, G. H., Hilleary, M. A., Eriksen, M., Possingham, H. P., Frond, H. D., Gerber, L. R., Polidoro, B., Tahir, A., Bernard, M., Mallos, N., Barnes, M., and Rochman, C.M. (2020). Predicted growth in plastic waste exceeds efforts to mitigate plastic pollution. *Science*, 369, 501-510.

Brach, L., Deixonne, P., Bernard, M. F., Durand, E., Desjean, M. C., Perez, E., van Sebille, E., and Ter Halle, A. (2018). Anticyclonic eddies increase accumulation of microplastic in the North Atlantic subtropical gyre. *Marine Pollution Bulletin*, 126, 191–196.

Bradney, L., Wijesekara, H., Palansooriya, K. N., Obadamudalige, N., Bolan, N. S., Ok, Y. S., and Kirkham, M. B. (2019). Particulate plastics as a vector for toxic trace-element uptake by aquatic and terrestrial organisms and human health risk. *Environment International*, 131, 932-937.

Browne, M. A., Galloway, T., and Thompson, R. (2007). Microplastic – an emerging contaminant of potential concern? *Integrated Environmental Assessment and Management*, 3, 559–561.

Burman, U., Garg, B. K., and Kathju, S. (2009). Effect of phosphorus application on clusterbean under different intensities of water stress. *Journal of Plant Nutrition*, 32, 668–680.

Cai, L., Wang, J., Peng, J., Tan, Z., Zhan, Z., Tan, X., and Chen, Q. (2017). Characteristic of microplastics in the atmospheric fallout from Dongguan city, China: preliminary research and first evidence. *Environmental Science and Pollution Research*, 24, 928-935.

Carstensen, A., Herdean, A., Schmidt, S. B., Sharma, A., Spetea, C., Pribil, M., and Husted, S. (2018). The impacts of phosphorus deficiency on the photosynthetic electron transport chain. *Plant Physiology*, 177, 271–284.

Catrouillet, C., Davranche, M., Khatib, I., Fauny, C., Wahl, A., and Gigault, J. (2021). Metals in microplastics: determining which are additive, adsorbed, and bioavailable. *Environmental Science: Processes and Impacts*, 23, 553-560.

Cedervall, T., Hansson, L. A., Lard, M., Frohm, B., and Linse, S. (2012). Food chain transport of nanoparticles affects behaviour and fat metabolism in fish. *PLOS One*, 7, 244-254.

Chen, D. R., Bei, J. Z., and Wang, S. G., (2000). Polycaprolactone microparticles and their biodegradation. *Polymer Degradation and Stability*, 67, 455–459.

Chen, Y., Wu, C., Zhang, H., Lin, Q., Hong, Y., and Luo, Y. (2013). Empirical estimation of pollution load and contamination levels of phthalate esters in agricultural soils from plastic film mulching in China. *Environmental Earth Sciences*, 70, 239.

Clark, R. B. (1997). *Marine Pollution*. Oxford: Clarendon Press.

Clukey, K. E., Lepczyk, C. A., Balazs, G. H., Work, T. M., and Lynch, J. M. (2017). Investigation of plastic debris ingestion by four species of sea turtles collected as bycatch in pelagic Pacific longline fisheries. *Marine Pollution Bulletin*, 120, 117–125.

Cole, M., Webb, H., Lindeque, P. K., Fileman, E. S., Halsband, C., and Galloway, T. S. (2014). Isolation of microplastics in biota-rich seawater samples and marine organisms. *Scientific Reports*, 4, 4528.

Collignon, A., Hecq, J. H., Glagani, F., Voisin, P., Collard, F., and Goffart, A. (2012). Neustonic microplastic and zooplankton in the North Western Mediterranean Sea. *Marine Pollution Bulletin*, 64, 861-864.

Conte, M. and Igartua, A. (2012). Study of PTFE composites tribological behaviour, *Wear*, 296, 568–574.

Corcoran, P. L., Norris, T., Ceccanese, T., Walzak, M. J., Helm, P. A., and Marvin, C. H. (2015). Hidden plastics of Lake Ontario, Canada and their potential preservation in the sediment record. *Environmental Pollution*, 204, 17–25.

Costa, M. F., Ivar do Sul, J. A., Silva-Cavalcanti, J. S., Araújo, M. C., Spengler, A., and Tourinho, P. S. (2010). On the importance of size of plastic fragments and pellets on the strandline: a snapshot of a Brazilian beach. *Environmental Monitoring and Assessment*, 168, 299–304.

Costa, J. P., Santos, P. S., Duarte, A. C., and Rocha-Santos, T. (2016). (Nano) plastics in the environment - sources, fates and effects. *Science of the Total Environment*, 566, 15-26.

Decho, A. W. (2000). Microbial biofilms in intertidal systems: an overview. *Continental Shelf Research*, 20, 1257–1273.

Dehaut A., Cassone, A. L., Frere, L., Hermabessiere, L., Himber, C., Rinnert, E., Riviere, G., Lambert, C., Soudant, P., Huvet, A., Duflos, G., and Paul-Pont, I. (2016). Microplastics in seafood: benchmark protocol for their extraction and characterization. *Environmental Pollution*, 215, 223–233.

Derraik, J. G. B. (2002). The pollution of the marine environment by plastic debris: a review. *Marine Pollution Bulletin*, 44, 842–852.

- Desale, D. D. and Pawar, H. B. (2018). Performance analysis of polytetrafluoroethylene as journal bearing material. *Procedia Manufacturing*, 20, 414-419.
- Dickhut, R. M., Andren, A. W., and Armstrong, D. E. (1986). Aqueous solubilities of six polychlorinated biphenyl congeners at four temperatures. *Environmental Science and Technology*, 20, 807–810.
- Ding, L., Mao, R., Ma, S., Guo, X., and Zhu, L. (2020). High temperature depended on the ageing mechanism of microplastics under different environmental conditions and its effect on the distribution of organic pollutants. *Water Research*, 174, 191–196.
- Dong, D., Peng, X., and Yan, X. (2004). Organic acid exudation induced by phosphorus deficiency and/or aluminium toxicity in two contrasting soybean genotypes. *Plant Physiology*, 122, 190–199.
- Dubaish, F. and Liebezeit, G. (2013). Suspended microplastics and black carbon particles in the Jade system, southern North Sea. *Water Air and Soil Pollution*, 224, 1352-1354.
- Duis, K. and Coors, A. (2016). Microplastics in the aquatic and terrestrial environment: sources (with a specific focus on personal care products), fate and effects. *Environmental Sciences Europe*, 28, 12-30.
- Duncan, E. M., Boterelli, L. R., Broderick, A. C., Galloway, T. S., Lindeque, P. K., Nuno, A., and Godley, B. J. (2017). A global review of marine turtle entanglement in anthropogenic debris: a baseline for further action. *Endangered Species Research*, 34, 431–448.
- Eghball, B., Wienhold, B. J., Gilley, J. E., and Eigenberg, R. A. (2002). Mineralization of manure nutrients. *Journal of Soil Water Conservation*, 57, 470–473.
- Enders, K., Lenz, R., Stedmon, C. A., and Nielsen, T. G. (2015). Abundance, size and polymer composition of marine microplastics $\geq 10\mu\text{m}$ in the Atlantic Ocean and their modelled vertical distribution. *Marine Pollution Bulletin*, 100, 70–81.

Fang, S., Yu, W., Li, C., Liu, Y., Qiu, J., and Kong, F. (2019). Adsorption behavior of three triazole fungicides on polystyrene microplastics. *Science of the Total Environment*, 691, 1119–1126.

Fastelli, P., Blašković, A., Bernardi, G., Romeo, T., Čížmek, H., Andaloro, F., Russo, G. F., Guerranti, C., and Renzi, M. (2016). Plastic litter in sediments from a marine area likely to become protected (Aeolian Archipelago's islands, Tyrrhenian sea). *Marine Pollution Bulletin*, 113, 526–529.

Fenchel, T. (1980). Suspension feeding in ciliated protozoa: functional response and particle size selection. *Microbial Ecology*, 6, 13-25.

Fendall, L. S. and Sewell, M. A. (2009). Contributing to marine pollution by washing your face: microplastics in facial cleansers. *Marine Pollution Bulletin*, 58, 1225–1228.

Fuller, S. and Gautam, A. (2016). A procedure for measuring microplastics using pressurized fluid extraction. *Environmental Science and Technology*, 50, 5774–80.

Gaurav, M., Haripada, B., Pramod, K. B., and Veena, C. (2014). Mechanical and morphological properties of high density polyethylene and polylactide blends. *Journal of Polymer Engineering*, 34, 813–821.

Gaylor, M. O., Harvey, E., and Hale, R. C. (2013). Polybrominated diphenyl ether (PBDE) accumulation by earthworms (*Eisenia fetida*) exposed to biosolids, poly-urethane foam microparticle, and Penta-BDE-amended soils. *Environmental Science and Technology*, 47, 831-839.

Geisen, S. and Bonkowski, M. (2017). Methodological advances to study the diversity of soil protists and their functioning in soil food webs. *Applied Soil Ecology*, 123, 328-333.

GESAMP (2015). Sources, fate and effects of microplastics in the marine environment: a global assessment. In: Kershaw, P. J. (ed.). *GESAMP report and studies no. 90*. London: Joint Group of Experts on Scientific Aspects of Marine Environmental Protection.

Goedecke, C., Mülow-Stollin, U., Hering, S., Richter, J., Piechotta, C., Paul, A., and Braun, U. (2017). A first pilot study on the sorption of environmental pollutants on various microplastic materials. *Journal of Environmental Analytical Chemistry*, 4, 100-109.

Geyer, R., Jambeck, J. R., and Law, K. L. (2017). Production, use, and fate of all plastics ever made. *Science Advances*, 3, 1-11.

Goldstein, M. C., Rosenberg, M., and Cheng, L. (2012). Increased oceanic microplastic debris enhances oviposition in an endemic pelagic insect. *Biology Letters*, 8, 817-820.

Gong, W., Jiang, M., Han, P., Liang, G., Zhang, T., and Liu, G. (2019). Comparative analysis on the sorption kinetics and isotherms of fipronil on nondegradable and biodegradable microplastics. *Environmental Pollution*, 254, 1-15.

Gopferich, A. (1996). Mechanisms of polymer degradation and erosion. *Biomaterials*, 17, 103–114.

Grammentz, D. (1988). Involvement of loggerhead turtle with the plastic, metal, and hydrocarbon pollution in the central Mediterranean. *Marine Pollution Bulletin*, 19, 11-13.

Gray, A. D. and Weinstein, J. E. (2017). Size and shape-dependent effects of microplastic particles on adult daggerblade grass shrimp (*Palaemonetes pugio*). *Environmental Toxicology and Chemistry*, 36, 3074–3080.

Green, B. W. (2015). Fertilizers in aquaculture. In: Davis, D. A. (ed). *Feed and Feeding Practices in Aquaculture*. Cambridge: Woodhead Publishing Limited.

Gregory, M. R. (1996). Plastic ‘scrubbers’ in hand cleansers: a further (and minor) source for marine pollution identified. *Marine Pollution Bulletin*, 32, 867–871.

Guo, X., Wang, X., Zhou, X., Kong, X., Tao, S., and Xing, B. (2012). Sorption of four hydrophobic organic compounds by three chemically distinct polymers: role of chemical and physical composition. *Environmental Science and Technology*, 46, 7252–7259.

Guo, X., Pang, J., Chen, S., and Jia, H. (2018). Sorption properties of tylosin on four different microplastics. *Chemosphere*, 209, 240–245.

Guo, X. and Wang, J. (2019). Sorption of antibiotics onto aged microplastics in freshwater and seawater. *Marine Pollution Bulletin*, 149, 1-14.

Guo, X., Chen, C., and Wang, J. (2019). Sorption of sulfamethoxazole onto six types of microplastics. *Chemosphere*, 228, 300–308.

Hammer, J., Kraak, M. H., and Parsons, J. R. (2012). Plastics in the marine environment: the dark side of a modern gift. *Reviews of Environmental Contamination and Toxicology*, 220, 1–44.

Hartline, N. L., Bruce, N. J., Karba, S. N., Ruff, E. O., Sonar, S. U., and Holden, P. A. (2016). Microfiber masses recovered from conventional machine washing of new or aged garments. *Environmental Science and Technology*, 50, 11532-11538.

Hermsen, E., Pompe, R., Besseling, E., and Koelmans, A. A. (2017). Detection of low numbers of microplastics in North Sea fish using strict quality assurance criteria. *Marine Pollution Bulletin*, 122, 253–258.

Herrera, A., Asensio, M., Martínez, I., Santana, A., Packard, T., and Gómez, M. (2017). Microplastic and tar pollution on three Canary Islands beaches: an annual study. *Marine Pollution Bulletin*, 129, 494–502.

Hodson, M.E., Duffus-Hodson, C.A., Clark, A., Prendergast-Miller, M.T., and Thorpe, K.L. (2017). Plastic bag derived-microplastics as a vector for metal exposure in terrestrial invertebrates. *Environmental Science and Technology*, 51, 4714-4721.

Holmes, L. A., Turner, A., and Thompson, R. C. (2012). Adsorption of trace metals to plastic resin pellets in the marine environment. *Environmental Pollution*, 160, 42–48.

Hong, S.H., Shim, W.J., and Hong, L. (2017). Methods of analysing chemicals associated with microplastics: a review. *Analytical Methods*, 9, 1361-1368.

Horton, A. A., Walton, A., Spurgeon, D. J., Lahive, E., and Svendsen, C. (2017). Microplastics in freshwater and terrestrial environments: evaluating the current understanding to identify the knowledge gaps and future research priorities. *Science of the Total Environment*, 586, 127–141.

Hosler, D., Burkett, S. L., and Tarkanian, M. J. (1999). Prehistoric polymers: rubber processing in ancient mesoamerica. *Science*, 284, 1988-1991.

Huerta Lwanga, E., Gertsen, H., Gooren, H., Peters, P., Salanki, T., van der Ploeg, M., Besseling, E., Koelmans, A. A., and Geissen, V. (2016). Microplastics in the terrestrial ecosystem: implications for *Lumbricus terrestris* (Oligochaeta, Lumbricidae). *Environmental Science and Technology*, 50, 2685-2691.

Huerta Lwanga, E., Gertsen, H., Gooren, H., Peters, P., Salanki, T., van der Ploeg, M., Besseling, E., Koelmans, A.A., and Geissen, V. (2017a). Incorporation of microplastics from litter into burrows of *Lumbricus terrestris*. *Environmental Pollution*, 220, 523-531.

Huerta Lwanga, E., Vega, J.M., Quej, V.K., Chi, J. A., Cid, L.S., Chi, C., Segura, G.E., Gertsen, H., Salanki, T., van der Ploeg, M., Koelmans, A. A., and Geissen, V. (2017b). Field evidence for transfer of plastic debris along a terrestrial food chain. *Scientific Reports*, 7, 14071.

Hüffer, T., and Hofmann, T., 2016. Sorption of non-polar organic compounds by micro-sized plastic particles in aqueous solution. *Environmental Pollution*, 214, 194–201.

Imhof, H. K., Sigl, R., Brauer, E., Feyl, S., Giesemann, P., Klink, S., Leupolz, K., Löder, M. G., Löschel, L. A., Missun, J., Muszynski, S., Ramsperger, A. F., Schrank, I., Speck, S., Steibl, S., Trotter, B., Winter, I., and Laforsch, C. (2017). Spatial and temporal variation of macro, meso and microplastic abundance on a remote coral island of the Maldives, Indian Ocean. *Marine Pollution Bulletin*, 116, 340–347.

Jalali, M. and Moharrami, S. (2007). Competitive adsorption of trace elements in calcareous soils of western Iran. *Geoderma*, 140, 156-163.

Jambeck, J. R., Geyer, R., and Wilcox, C. (2015). Plastic waste inputs from land into the ocean. *Science*, 347, 769-777.

Jarvie, H. P., Sharpley, A. N., Withers, P. J. A., Scott, J. T., Haggard, B. E., and Neal, C. (2013). Phosphorus mitigation to control river eutrophication: murky waters, inconvenient truths, and “Postnormal” science. *Journal of Environmental Quality*, 42, 295–304.

Jones, D. L., Shannon, D., Murphy, D. V., and Farrar, J. (2004). Role of dissolved organic nitrogen (DON) in soil N cycling in grassland soils. *Soil Biology and Biochemistry*, 36, 749-756.

Juan, W., Pengcheng, X., Qinghua, C., Dong, M., Wei, G., Tao, J., and Chao, C. (2020). Effects of polymer aging on sorption of 2, 2', 4, 4' tetrabromodiphenyl ether by polystyrene microplastics. *Chemosphere*, 253, 126706.

Kasirajan, S. and Ngouajio, M. (2012). Polyethylene and biodegradable mulches for agricultural applications: a review. *Agronomy for Sustainable Development*, 32, 501-529.

Ke, P. C. and Lamm, M. H. (2011). A biophysical perspective of understanding nanoparticles at large. *Physical Chemistry Chemical Physics*, 13, 273–283.

Kerr, J. M., DePinto, J. V., McGrath, D., Sowa, S. P., and Swinton, S. M. (2016). Sustainable management of great Lakes watersheds dominated by agricultural land use. *Journal of Great Lakes Research*, 42, 1252–1259.

Keswani, A., Oliver, D. M., Gutierrez, T., and Quilliam, R. S. (2016). Microbial hitchhikers on marine plastic debris: human exposure risks at bathing waters and beach environments. *Marine Environmental Research*, 118, 10–19.

Kim, I. S., Chae, D. H., Kim, S. K., Choi, S. B., and Woo, S. B. (2015). Factors influencing the spatial variation of microplastics on high-tidal coastal beaches in Korea. *Archives of Environmental Contamination and Toxicology*, 69, 299–309.

Kiyama, Y., Miyahara, K., and Ohshima, Y. (2012). Active uptake of artificial particles in the nematode *Caenorhabditis elegans*. *Journal of Experimental Biology*, 215, 1178–1183.

Kokalj, A. J., Horvat, P., Skalar, T., and Krzan, A. (2018). Plastic bag and facial cleanser derive microplastic do not affect feeding behavior and energy reserves of terrestrial isopods. *Science of the Total Environment*, 615, 761-766.

Kumar, M., Xiong, X., He, M., Tsang, D. C. W., and Bolan, N. S. (2020). Microplastics as pollutants in agricultural soils. *Environmental Pollution*, 265, 914–980.

Kurkcu, P., Andena, L., and Pavan, A. (2012). An experimental investigation of the scratch behaviour of polymers: influence of rate dependent bulk mechanical properties. *Wear*, 290, 86–93.

Lahive, E., Cross, R., Saarloos, A. I., Horton, A. A., Svendsen, C., Hufenus, R., and Mitrano, D. M. (2022). Earthworms ingest microplastic fibres and nanoplastics with effects on egestion rate and long-term retention. *Science of the total Environment*, 807, 1-10.

Laist, D. W. (1997). Impacts of marine debris: entanglement of marine life in marine debris including a comprehensive list of species with entanglement and ingestion records. In: Coe, J. M. and Rogers, D. B. (eds). *Marine debris - sources, impacts and solutions*. New York: Springer-Verlag.

Lal, R. (2017). Pathways and Fate of Phosphorus in Agroecosystems. In: Lal, R. and Stewart, B. A. (eds). *Soil Phosphorus*. Boca Raton: CRC Press.

Lambert, S., Sinclair, C. J., and Boxall, A. B. (2014). Occurrence, degradation and effect of polymer-based materials in the environment. *Reviews of Environmental Contamination and Toxicology*, 227, 1–53.

Lambert, S. and Wagner, M. (2016). Characterisation of nanoplastics during the degradation of polystyrene. *Chemosphere*, 145, 265–268.

Lambert, S., Scherer, C., and Wagner, M. (2017). Ecotoxicity testing of microplastics: considering the heterogeneity of physicochemical properties. *Integrated Environmental Assessment and Management*, 13, 470-475.

Lang, M., Yu, X., Liu, J., Xia, T., Wang, T., Jia, H., and Guo, X. (2020). Fenton aging significantly affects the heavy metal adsorption capacity of polystyrene microplastics. *Science of the total Environment*, 722, 762-769.

Lee, J., Hong, S., Song, Y. K., Hong, S. H., Jang, Y. C., Jang, M., Heo, N. W., Han, G. M., Lee, M. J., Kang, D., and Shim, W. J. (2013). Relationships among the abundances of plastic debris in different size classes on beaches in South Korea. *Marine Pollution Bulletin*, 77, 349–354.

Lee, H., Shim, W. J., and Kwon, J. H. (2014). Sorption capacity of plastic debris for hydrophobic organic chemicals. *Science of the Total Environment*, 470, 1545-1552.

Leytem, A. B. and Westermann, D. T. (2005). Phosphorus availability to barley from manures and fertilizers on a calcareous soil. *Soil Science*, 170, 401–412.

Li, J., Zhang, K., and Zhang, H. (2018). Adsorption of antibiotics on microplastics. *Environmental Pollution*, 237, 460–467.

Li, Y., Li, M., Li, Z., Yang, L., and Liu, X. (2019). Effects of particle size and solution chemistry on triclosan sorption on polystyrene microplastic. *Chemosphere*, 231, 308–314.

Li, H., Wang, F., Li, J., Deng, S., and Zhang, S. (2021). Adsorption of three pesticides on polyethylene microplastics in aqueous solutions: kinetics, isotherms, thermodynamics, and molecular dynamics simulation. *Chemosphere*, 264, 1-9.

Liang, Y., Lehmann, A., Yang, G., Leifheit, E. F., and Rillig, M. C. (2021). Effects of microplastic fibers on soil aggregation and enzyme activities are organic matter dependent. *Frontiers in Environmental Science*, 9, 1-11.

Liboiron, M., Liboiron, F., Wells, E., Richard, N., Zahara, A., Mather, C., Bradshaw, H., and Murichi, J. (2016). Low plastic ingestion rate in Atlantic cod (*Gadus morhua*) from Newfoundland destined for human consumption collected through citizen science methods. *Marine Pollution Bulletin*, 113, 428–437.

Liebezeit, G. and Dubaish, F. (2012). Microplastics in beaches of the East Frisian islands Spiekeroog and Kachelotplate. *Bulletin of Environmental Contamination and Toxicology*, 89, 213-217.

Lithner, D., Larsson, A., and Dave, G. (2011). Environmental and health hazard ranking and assessment of plastic polymers based on chemical composition. *Science of the Total Environment*, 409, 3309-3324.

Liu, Y. and Chen, J. (2008). Phosphorus Cycle. In: Jorgensen, S. E. and Fath, B. D. (eds). *Encyclopedia of Ecology*, Amsterdam: Elsevier Science.

Liu, L., Fokkink, R., and Koelmans, A. A. (2016). Sorption of polycyclic aromatic hydrocarbons to polystyrene nanoplastic. *Environmental Toxicology and Chemistry*, 35, 1650–1655

Liu, H., Yang, X., Liu, G., Liang, C., Xue, S., Chen, H., Ritsema, C.J., and Geissen, V. (2017). Response of soil dissolved organic matter to microplastic addition in Chinese loess soil. *Chemosphere*, 185, 907-917.

Liu, G., Zhu, Z., Yang, Y., Sun, Y., Yu, F., and Ma, J. (2018). Sorption behavior and mechanism of hydrophilic organic chemicals to virgin and aged microplastics in freshwater and seawater. *Environmental Pollution*, 246, 26–33.

Liu, F., Liu, G., Zhu, Z., Wang, S., and Zhao, F. (2019). Interactions between microplastics and phthalate esters as affected by microplastics characteristics and solution chemistry. *Chemosphere*, 214, 688–694.

Liu, P., Lu, K., Li, J., Wu, X., Qian, L., Wang, M., and Gao, S. (2020). Effect of aging on adsorption behavior of polystyrene microplastics for pharmaceuticals: adsorption mechanism and role of aging intermediates. *Journal of Hazardous Materials*, 384, 1-12.

Liubartseva, S., Coppini, G. Lecci, R., and Creti, S. (2016). Regional approach to modelling the transport of floating plastic debris in the Adriatic Sea. *Marine Pollution Bulletin*, 103, 115–127.

Lozano, Y. M. and Rillig, M.C. (2020). Effects of microplastic fibers and drought on plant communities. *Environmental Science and Technology*, 54, 6166–6173.

Lozano, Y. M., Lehnert, T., Linck, L. T., Lehmann, A., and Rillig, M. C. (2020). Microplastic shape, polymer type and concentration affect soil properties and plant biomass. *Frontiers in Plant Science*, 12, 1-14.

Ma, J., Zhao, J., Zhu, Z., Li, L., and Yu, F. (2019). Effect of microplastic size on the adsorption behavior and mechanism of triclosan on polyvinyl chloride. *Environmental Pollution*, 254, 1-14.

Maaß, S., Daphi, D., Lehmann, A., and Rillig, M. C. (2017). Transport of microplastics by two collembolan species. *Environmental Pollution*, 225, 456-459.

Machado, A. A. S., Lau, C. W., Kloas, W., Bergmann, J., Bachelier, J. B., Faltin, E., Becker, R., Görlich, A. S. and Rillig, M. C. (2019). Microplastics can change soil properties and affect plant performance. *Environmental Science and Technology*, 53, 6044 – 6052.

Mahon, A. M., O'Connell, B., Healy, M. G., O'Connor, I., Officer, R., Nash, R., and Morrison, L. (2017). Microplastics in sewage sludge: effects of treatment. *Environmental Science and Technology*, 51, 810–818.

Mao, R., Lang, M., Yu, X., Wu, R., Yang, X., and Guo, X. (2020). Aging mechanism of microplastics with UV irradiation and its effects on the adsorption of heavy metals. *Journal of Hazardous Materials*. 393, 501-515.

Martinho, S. D., Fernandes, V. C., Figueiredo, S. A., and Delerue-Matos, C. (2022). Microplastic pollution focused on sources, distribution, contaminant interactions, analytical methods, and wastewater removal strategies: a review. *International Journal of Environmental Research and Public Health*, 19, 1-24.

Massos, A. and Turner, A. (2017). Cadmium, lead and bromine in beached microplastics. *Environmental Pollution*, 227, 139–145.

Meng, X., Chen, W., Wang, Y., Huang, Z., Ye, X., Chen, L., and Yang, L. (2021). Effects of phosphorus deficiency on the absorption of mineral nutrients, photosynthetic system performance and antioxidant metabolism in *Citrus grandis*. *PLOS One*, 16, 1-20.

Mengel, K., Kirkby, E. A., Kosegarten, H., and Appel, T. (2001). Phosphorus. *In: Mengel, K., Kirkby, E. A., Kosegarten, H., and Appel, T. (eds). Principles of Plant Nutrition*. Dordrecht: Springer.

Mersiowsky, I., Brandsch, R., and Ejlertsson, J. (2001). Screening for organotin compounds in European landfill leachate. *Journal of Environmental Quality*, 30, 1604-1611.

Montes-Burgos, I., Walczyk, D., Hole, P., Smith, J., Lynch, I., and Dawson, K. (2010). Characterisation of nanoparticle size and state prior to nanotoxicological studies. *Journal of Nanoparticle Research*, 12, 47–53.

Moore, C. J. (2008). Synthetic polymers in the marine environment: a rapidly increasing, long-term threat. *Environmental Research*, 108, 131-139.

Naden, P. S., Murphy, J. F., Old, G. H., Newman, J., Scarlett, P., Harman, M., Duerdoth, C. P., Hawczak, A., Pretty, J. L., Arnold, A., Laizé, C., Hornby, D. D., Collins, A. L., Sear, D. A., and Jones, J. I. (2016). Understanding the controls on deposited fine sediment in the streams of agricultural catchments. *Science of the Total Environment*, 547, 366-381.

Nelson, N. O. and Janke, R. R. (2007). Phosphorus sources and management in organic production systems. *American Society for Horticultural Science*, 17, 442-454.

Nizzetto, L., Bussi, G., Futter, M. N., Butterfield, D., and Whitehead, P. G. (2016a). A theoretical assessment of microplastic transport in river catchments and their retention by soils and river sediments. *Environmental Science: Processes and Impacts*, 18, 1050-1059.

Nizzetto, L., Futter, M., and Langaas, S. (2016b). Are agricultural soils dumps for microplastics of urban origin? *Environmental Science and Technology*, 50, 10777–10779.

Orgiazzi, A., Ballabio, C., Panagos, P., Jones, A., and Fernández-Ugalde, O. (2018). LUCAS soil, the largest expandable soil dataset for Europe: a review. *European Journal of Soil Science*, 69, 140–153.

Pachapur, V. L., Dalila, L. A., Cledón, M., Brar, S. K., Verma, M., and Surampalli, R. Y. (2016). Behaviour and characterization of titanium dioxide and silver nanoparticles in soils. *Science of the Total Environment*, 563, 933–943.

Panagos, P., Muntwyler, A., Liakos, L., Borrelli, P., Biavetti, I., Bogonos, M., and Lugato, E. (2022). Phosphorus plant removal from European agricultural land. *Journal of Consumer Protection and Food Safety*, 17, 5–20.

Parham, J. A., Deng, S. P., Raun, W. R., and Johnson, G. V. (2002). Long-term cattle manure application in soil. I. Effect on soil phosphorus levels, microbial biomass C, and dehydrogenase and phosphatase activities. *Biology and Fertility of Soils*, 35, 328-337.

Patel, M. M., Goyal, B. R., Bhadada, S. V., Bhatt, J. S., and Amin, A. F. (2009). Getting into the brain: approaches to enhance brain drug delivery. *CNS Drugs*, 23, 35–58.

Pinheiro, C., Oliveira, U., and Vieira, M. (2017). Occurrence and impacts of microplastics in freshwater fish. *Journal of Aquaculture and Marine Biology*, 5, 00138.

PlasticsEurope (2021). *Plastics – the facts 2021: an analysis of European plastics production, demand and waste data*. Belgium: PlasticsEurope.

PlasticsEurope (2017). *Plastics – the facts 2017: an analysis of European plastics production, demand and waste data*. Belgium: PlasticsEurope.

PlasticsEurope (2013). *Plastics – the facts 2013: an analysis of European latest plastics production, demand and waste data*. Belgium: PlasticsEurope.

PlasticsEurope (2008). *The compelling facts about plastics, analysis of plastics production, demand and recovery for 2006 in Europe*. Belgium: PlasticsEurope.

Qi, Y. L., Yang, X. M., Pelaez, A. M., Lwanga, E. H., Beriot, N., Gertsen, H., Garbeva, P., and Geissen, V. (2018). Macro- and micro- plastics in soil-plant system: effects of plastic mulch film residues on wheat (*Triticum aestivum*) growth. *Science of the Total Environment*, 645, 1048–1056.

Rillig, M. C. (2012). Microplastic in terrestrial ecosystems and the soil? *Environmental Science and Technology*, 46, 6453-6454.

Rillig, M. C., Ziersch, L., and Hempel, S. (2017). Microplastic transport in soil by earthworms. *Scientific Reports*, 7, 1-6.

Rillig, M. C. and Bonkowski, M. (2018). Microplastic and soil protists: a call for research. *Environmental Pollution*, 241, 1128-1131.

Rochman, C. M., Hentschel, B. T., Teh, S. J., and The, S. J. (2014). Longterm sorption of metals is similar among plastic types: implications for plastic debris in aquatic environments. *PLOS One*, 9, 1-10.

Rodriguez-Seijo, A., Lourenço, J., Rocha-Santos, T.A.P., da Costa, J., Duarte, A.C., Vala, H., and Pereira, R. (2017). Histopathological and molecular effects of micro-plastics in *Eisenia andrei* Bouche. *Environmental Pollution*, 220, 495-503.

Sarafraz, J., Rajabizadeh, M., and Kamrani, E. (2016). The preliminary assessment of abundance and composition of marine beach debris in the northern Persian Gulf, Bandar Abbas City, Iran. *Journal of Marine Biological Association*, 96, 131–135.

Scheurer, M. And Bigalke, M. (2018). Microplastics in Swiss floodplain soils. *Environmental Science and Technology*, 52, 3591-3598.

Shah, A. A., Hasan, F., Hameed, A., and Ahmed, S. (2008) Biological degradation of plastics: a comprehensive review. *Biotechnology Advances*, 26, 246–265.

Silva-Cavalcanti, J. S., Silva, J. D. B., Franca, E. J., Araujo, M. C. B., and Gusmao, F. (2017). Microplastics ingestion by a common tropical freshwater fishing resource. *Environmental Pollution*, 221, 218-226.

- Sparks, D. L. (2003). *Environmental soil chemistry*. Michigan: Academic Press.
- Sposito G. (2004). *Surface chemistry of natural particles*. Oxford: Oxford University Press.
- Stabnikova, O., Stabnikov, V., Marinin, A., Klavins, M., Klavins, L., and Vaseashta, A. (2021). Microbial life on the surface of microplastics in natural waters. *Applied Sciences*, 11, 1-19.
- Steinmetz, Z., Wollmann, C., Schaefer, M., Buchmann, C., David, J., Tröger, J., Muñoz, K., Frör, O., and Schaumann, G. E. (2016). Plastic mulching in agriculture. Trading short-term agronomic benefits for long term soil degradation? *Science of the Total Environment*, 550, 690–705.
- Stigter, K. A. and Plaxton, W. C. (2015). Molecular mechanisms of phosphorus metabolism and transport during leaf senescence. *Plants*, 4, 773–798.
- Stumm W. and Morgan J. J. (1996). *Aquatic chemistry - chemical equilibria and rates in natural waters*. New York: Wiley.
- Sun, L., Song, L., Zhang, Y., Zheng, Z., and Liu, D. (2016). Arabidopsis PHL2 and PHR1 act redundantly as the key components of the central regulatory system controlling transcriptional responses to phosphate starvation. *Plant Physiology*, 170, 499–514.
- Talvitie, J., Mikola, A., Setälä, O., Heinonen, M., and Koistinen, A. (2017). How well is microliter purified from wastewater? A detailed study on the stepwise removal of microliter in a tertiary level wastewater treatment plant. *Water Research*, 109, 164–172.
- Tang, S., Lin, L., Wang, X., Yu, A., and Sun, X. (2021). Interfacial interactions between collected nylon microplastics and three divalent metal ions [Cu(II), Ni(II), Zn(II)] in aqueous solutions. *Journal of Hazardous Materials*, 403, 1-12.
- Teuten, E.L., Saquing, J.M., Knappe, D.R., Barlaz, M.A., Jonsson, S., Bjorn, A., Rowland, S.J., Thompson, R.C., Galloway, T.S., Yamashita, R., Ochi, D., Watanuki, Y., Moore, C., Viet, P.H., Tana, T.S., Prudente, M., Boonyatumanond, R., Zakaria, M.P., Akkhavong, K., Ogata, Y., Hirai, H., Iwasa, S., Mizukawa, K., Hagino, Y., Imamura, A., Saha, M., and

Takada, H. (2009). Transport and release of chemicals from plastics to the environment. *Philosophical Transactions of the Royal Society of London: Biological Sciences*, 364, 2027–2045.

Thiel, M., Hinojosa, I. A., Miranda, L., Pantoja, J. F., Rivadeneira, M. M. and Vásquez, N. (2013). Anthropogenic marine debris in the coastal environment: A multi-year comparison between coastal waters and local shores. *Marine Pollution Bulletin*, 71, 307–316.

Thompson, R. C., Olsen, Y., Mitchell, R. P., Davis, A., Rowland, S. J., John, A. W. G., McGonigle, D., and Russell, A. E. (2004). Lost at sea: where is all the plastic? *Science*, 304, 838.

Thompson, R. C., Swan, S. H., Moore, C. J., and vomSaal, F. S. (2009a). Our plastic age. *Philosophical Transactions of the Royal Society of London: Biological Sciences*, 364, 1973–1976.

Thompson, R. C., Charles, J. M., vomSaal, F. S., and Swan, S. H. (2009b). Plastics, the environment and human health: current consensus and future trends. *Philosophical Transactions of the Royal Society of London: Biological Sciences*, 364, 2153–2166.

Tong, H., Hu, X., Zhong, X., and Jiang, Q. (2021). Adsorption and desorption of triclosan on biodegradable polyhydroxybutyrate microplastics. *Environmental Toxicology and Chemistry*, 40, 72–78.

Turner, A. (2016). Heavy metals, metalloids and other hazardous elements in marine plastic litter. *Marine Pollution Bulletin*, 111, 136–142.

Velzeboer, I., A, F. K. C. J., A, A. K., 2014. Strong sorption of PCBs to nanoplastics, microplastics, carbon nanotubes, and fullerenes. *Environmental Science and Technology*, 48, 4869–4876.

von Moos, N., Burkhardt-Holm, P., and Kohler, A. (2012). Uptake and effects of microplastics on cells and tissue of the blue mussel *Mytilus edulis* L. after an experimental exposure. *Environmental Science and Technology*, 46, 11327–11335.

Wagner, M. and Oehlmann, J. (2009). Endocrine disruptors in bottled mineral water: total estrogenic burden and migration from plastic bottles. *Environmental Science and Pollution Research*, 16, 278–286.

Walker, T. R. (2018). Drowning in debris: solutions for a global pervasive marine pollution problem. *Marine Pollution Bulletin*, 126, 338.

Walker, T. R. and Xanthos, D. (2018). A call for Canada to move toward zero plastic waste by reducing and recycling single-use plastics. *Resources, Conservation and Recycling*, 133, 99–100.

Wang, F., Shih, K. M., and Li, X. Y. (2015). The partition behavior of perfluorooctanesulfonate (PFOS) and perfluorooctanesulfonamide (FOSA) on microplastics. *Chemosphere*, 119, 841–847.

Wang, J., Liu, X., Liu, G., Zhang, Z., Wu, H., Cui, B., Bai, J., and Zhang, W. (2019). Size effect of polystyrene microplastics on sorption of phenanthrene and nitrobenzene. *Ecotoxicology and Environmental Safety*, 173, 331–338.

Wang, Q., Bai, J., Ning, B., Fan, L., Sun, T., Fang, Y., Wu, J., Li, S., Duan, C., Zhang, Y., Liang, J., and Gao, Z. (2020a). Effects of bisphenol A and nanoscale and microscale polystyrene plastic exposure on particle uptake and toxicity in human Caco-2 cells. *Chemosphere*, 254, 1-9.

Wang, F., Zhang, M., Sha, W., Wang, Y., Hao, H., Dou, Y., and Li, Y. (2020b). Sorption behavior and mechanisms of organic contaminants to nano and microplastics. *Molecules*, 25, 1-17.

Ward, J. E. and Kach, D. J. (2009). Marine aggregates facilitate ingestion of nanoparticles by suspension-feeding bivalves. *Marine Environmental Research*, 68, 137–142.

Wegner, A., Besseling, E., Foekema, E. M., Kamermans, P., and Koelmans, A. A. (2012). Effects of nanopolystyrene on the feeding behaviour of the blue mussel (*Mytilus edulis* L.). *Environmental Toxicology and Chemistry*, 31, 2490–2497.

Weil, R., and Brady, N. C. (2002). *Nature and properties of soils*. London: Pearson New International Edition.

Weithmann, N., Möller, J. N., Löder, M. G. J., Piehl, S., Laforsch, C., and Freitag, R. (2018). Organic fertilizer as a vehicle for the entry of microplastic into the environment. *Science Advances*, 4, 8060-8064.

Wessel, C. C., Lockridge, G. R., Battiste, D., and Cebrian, J. (2016). Abundance and characteristics of microplastics in beach sediments: insights into microplastic accumulation in beach sediments: insights into microplastic accumulation in northern Gulf of Mexico estuaries. *Marine Pollution Bulletin*, 109, 178–183.

Wu, P., Cai, Z., Jin, H., and Tang, Y. (2019). Adsorption mechanisms of five bisphenol analogues on PVC microplastics. *Science of the Total Environment*, 650, 671–678.

Wu, X., Liu, Y., Yin, S., Xiao, K., and Yang, J. (2020). Metabolomics revealing the response of rice (*Oryza sativa* L.) exposed to polystyrene microplastics. *Environmental Pollution*, 266, 115–159.

Xingyou, T., Xian, Z., Wentao, L., Jin, Z., Changjiu, R., and Ping, C. (2006). Preparation and properties of poly (ethylene terephthalate)/ silica nanocomposites. *Journal of Molecular Science*, 45, 310-317.

Xu, B., Liu, F., Brookes, P. C., and Xu, J. (2018a). Microplastics play a minor role in tetracycline sorption in the presence of dissolved organic matter. *Environmental Pollution*, 240, 87–94.

Xu, B., Liu, F., Brookes, P. C., and Xu, J. (2018b). The sorption kinetics and isotherms of sulfamethoxazole with polyethylene microplastics. *Marine Pollution Bulletin*, 131, 191–196.

Yang, X., Bento, C. P. M., Chen, H., Zhang, H., Xue, S., Huerta Lwanga, E., Zomer, P., Ritsema, C. J., and Geissen, V. (2018). Influence of microplastic addition on glyphosate decay and soil microbial activities in Chinese loess soil. *Environmental Pollution*, 242, 338-347.

- Yu, F., Li, Y., Huang, G., Yang, C., Chen, C., Zhou, T., Zhao, Y. and Ma, J. (2020). Adsorption behavior of the antibiotic levofloxacin on microplastics in the presence of different heavy metals in an aqueous solution. *Chemosphere*, 260, 1-11.
- Yu, H., Ying, Z., Tan, W. and Zhang, Z. (2022). Microplastics as an emerging environmental pollutant in agricultural soils: effects on ecosystems and human health. *Frontiers in Environmental Science*, 6, 1-18.
- Zambrosi, F. C. B., Ribeiro, R. V., Marchiori, P. E. R., Cantarella, H., and Landell, M. G. A. (2014). Sugarcane performance under phosphorus deficiency: physiological responses and genotypic variation. *Plant and Soil*, 386, 273–283.
- Zhan, Z., Wang, J., Peng, J., Xie, Q., Huang, Y., and Gao, Y. (2016). Sorption of 3,3',4,4' -tetrachlorobiphenyl by microplastics: a case study of polypropylene. *Marine Pollution Bulletin*, 110, 559–563.
- Zhang, Q., Yang, C., Lin, S., Sun, H., Shen, Y., Tan, H., and Lin, C. (2012). Determination of n-octanol/ water partition coefficient of melamine. *Guizhou Science*, 30, 60–62.
- Zhang, K., Li, J., Li, X., and Zhang, H. (2017). Mechanisms and kinetics of oxytetracycline adsorption-desorption onto microplastics. *Environmental Chemistry*, 36, 2531–2540.
- Zhang, S., Xiaomei, Y., Hennie, G., Piet, P., Tamás, S., and Violette, G. (2018a). A simple method for the extraction and identification of light density microplastics from soil. *Science of the Total Environment*, 616, 1056–1065.
- Zhang, H., Wang, J., Zhou, B., Zhou, Y., Dai, Z., Zhou, Q., Christie, P., and Luo, Y. (2018b). Enhanced adsorption of oxytetracycline to weathered microplastic polystyrene: kinetics, isotherms and influencing factors. *Environmental Pollution*, 243, 1550–1557.
- Zhang, X., Zheng, M., Yin, X., Wang, L., Lou, Y., Qu, L., Liu, X., Zhu, H., and Qiu, Y. (2019). Sorption of 3,6-dibromocarbazole and 1,3,6,8-tetrabromocarbazole by microplastics. *Marine Pollution Bulletin*, 138, 458-463.

Zhang, Y., Kang, S., Allen, S., Allen, D., Gao, T., and Sillanpaa, M. (2020). Atmospheric microplastics: a review on current status and perspectives. *Earth Science Review*, 203, 1-10.

Zhao, T., Lozano, Y. M., and Rillig, M. C. (2021). Microplastics increase soil pH and decrease microbial activities as a function of microplastic shape, polymer type, and exposure time. *Frontiers in Environmental Science*, 9, 67-74.

Zhou, Q., Haibo, Z., Chuancheng, F., Yang, Z., Zhenfei, D., Yuan, L., Chen, T., and Yongming, L. (2018). The distribution and morphology of microplastics in coastal soils adjacent to the Bohai Sea and the Yellow Sea. *Geoderma*, 322, 201–208.

Zhou, Y., Yang, Y., Liu, G., and Liu, H. W. (2020). Adsorption mechanism of cadmium on microplastics and their desorption behavior in sediment and gut environments: the roles of water pH, lead ions, natural organic matter and phenanthrene. *Water Research*, 184, 1-14.

Zhu, D., Bi, Q.F., Xiang, Q., Chen, Q.L., Christie, P., Ke, X., Wu, L.H., and Zhu, Y.G. (2018a). Trophic predator-prey relationships promote transport of microplastics compared with the single *Hypoaspis aculeifer* and *Folsomia candida*. *Environmental Pollution*, 235, 150-154.

Zhu, D., Chen, Q.L., An, X.L., Yang, X.R., Christie, P., Ke, X., Wu, L.H., and Zhu, Y.G. (2018b). Exposure of soil collembolans to microplastics perturbs their gut microbiota and alters their isotopic composition. *Soil Biology and Biochemistry*, 116, 302-310.

Zubris, K. A. V. and Richards, B. K. (2005). Synthetic fibers as an indicator of land application of sludge. *Environmental Pollution*, 2, 201–211.

Chapter 3

Impacts of microplastics on phosphate adsorption

3.1. Introduction

Plastic production is reported to have increased from around two million tonnes per year in 1950 to 380 million tonnes in 2021, an increase in annual production of nearly 200-fold (Lebreton *et al.*, 2019; PlasticsEurope, 2013; PlasticsEurope, 2017). Around eight million metric tonnes of plastics end up in the oceans each year (Jambeck *et al.*, 2015); however, more than 80 % of these plastics have been produced, and disposed of in terrestrial environments (Talvitie *et al.*, 2017) from diverse sources (Li *et al.*, 2014). One thousand to more than four thousand plastic particles were found in per kg of sludge (dry mass) collected from the wastewater treatment plants in Europe (Zubris *et al.*, 2005; Browne *et al.*, 2011; Briassoulis *et al.*, 2010).

Commercial high-density polyethylene (HDPE) is a lightweight and chemical resistant plastic widely used in industrial sectors. It was estimated that the production of HDPE was 47.5 million tons in 2016 occupying a share of 46 % of total polyethylene production globally (PlasticsEurope, 2008). HDPE released from different sources can be turned into microplastics due to the weathering resulting from UV radiation, elevated temperature (Horton *et al.*, 2017), abrasive or mechanic force and microbial activities (Singh and Sharma, 2008; Nizzetto *et al.*, 2016a; 2016b).

It has been well documented that microplastics are capable of adsorbing metals (Hodson *et al.*, 2017; Decho, 2000; Rochman *et al.*, 2014) and organic compounds (Bakir *et al.*, 2014a; 2014b; Velzeboer *et al.*, 2014; Wang *et al.*, 2015; Hueffer and Hofmann, 2016). However, there has been virtually no research on the sorption of essential plant nutrients (essential plant nutrients are those that are required in large quantities for the plants and without these nutrients the plants are not able to complete their life cycle) on the microplastics. Essential nutrients can interact with microplastics in urban and rural soils, potentially altering the geochemical environment. It is well established that the essential nutrients play crucial role in developing plant cells, functioning of

the cell membranes and activating enzymes that lead to regulating vital biochemical processes. Microplastics appeared to reduce plant growth which was documented in previous studies (Qi *et al.*, 2018; Zhang *et al.*, 2015; Machado *et al.*, 2019). However, possible reasons behind the reductions in plant growth due to the presence of microplastics are still unknown. Some of these reasons include the adsorption of plant nutrients, impacts on soil properties and microbial activities as suggested in previous studies (Qi *et al.*, 2018; Zhang *et al.*, 2015; Machado *et al.*, 2019). Understanding the interactions between essential nutrient and microplastic is warranted for the evaluation of their fate and behaviour in terrestrial ecosystems. Thus, the current chapter investigates the adsorption of plant nutrient to the microplastics.

Typically phosphorus, one of the essential nutrients, occurs in the soil as phosphate (H_2PO_4^- , HPO_4^{2-} , PO_4^{3-}). Phosphate is essential for plant productivity and soil fertility, but excess phosphate can be detrimental to the plants (Spohn and Kuzyakov, 2013; Weil and Brady, 2016). Phosphate concentration in the soil typically ranges from 0.003 to 3.000 mg/ kg (Weil and Brady, 2016). Due to its low concentration, phosphate is often regarded as a limiting nutrient and its concentration can be enhanced by application of phosphate fertilizers. Once phosphate enters the soil, it cycles between several phosphate pools which determines its availability to plants. Deficiency in available phosphate in soil may exert negative impacts on plant growth (Weil and Brady, 2016).

Our hypothesis for the present study is that phosphate is adsorbed to the microplastic surfaces. Based on the hypothesis, the study aims to determine whether the microplastics can adsorb phosphate and whether any adsorbed phosphate can be desorbed. To address this aim, a set of objectives was outlined below.

- To determine the potential of microplastics generated from industrial HDPE to adsorb phosphate;
- To determine the differences in adsorption between pristine and weathered HDPE;
- To determine whether the adsorption is reversible.

3.2. Materials and methodology

3.2.1. Materials

Two types of soil were collected from York, UK with contrasting organic matter contents. Soil with low organic matter content (S1) was collected from an arable field at grid reference 53° 52' 25.2" N, 1° 19' 47.0" W, located in Big Substation East field at the University of Leeds experimental farm; soil with high organic matter content (S2) was collected from a flower bed which is located at grid reference 53° 56' 41.0" N, 1° 3' 04.9" W on the University of York campus.

3.2.2. Methods

The soils were air-dried, visible roots and plant debris were discarded and the soils were ground gently to break up larger soil aggregates. After that the soils were sieved at 2 mm, thoroughly homogenized and finally characterised. Soil texture was determined manually (USDA, 1951). A ball of soil was placed between thumb and forefinger, gently pushing the soil with the thumb and working it upward to make a ribbon. The ribbon was allowed to emerge and extend over the forefinger, breaking from its own weight, and finally the texture of the soil was determined from the length and strength of the ribbon. The pH of the soil was determined by mixing air-dried soil and deionised water at a ratio of 1:2.5 followed by shaking for 15 minutes. The suspension was allowed to settle and pH was measured using an Accumet AB150 pH meter calibrated with pH 4.0, 7.0 and 10.0 buffers (Rowell, 1994). Soil organic matter was determined by heating 20 g of air-dried soil overnight at 105 °C, reweighed and then combusted at 350 °C overnight. Mass loss on ignition (LOI) was determined and used as a proxy for organic matter content (Hoogsteen *et al.*, 2018; Rowell, 1994). S1 soil had a silty loam texture with a pH of 7.63 ± 0.13 and organic matter content of 3.58 ± 0.15 % ($n = 5$, \pm standard deviation); S2 soil had a loamy texture having a pH of 7.11 ± 0.09 and organic matter content of 4.62 ± 0.13 % ($n = 5$, \pm standard deviation).

Commercial grade high-density polyethylene (HDPE) microplastics powder (Model No. SMHD-3006H) was purchased from Qingdao Sunsoar Tech. Co., Ltd. located in Shandong, China. The HDPE was produced using rotational molding technique (Sunsoar Tech, n.d.). HDPE is popularly known worldwide for its massive strength-to-density ratio (PlasticsEurope, 2013). HDPE is

lightweight, cheap and weather resistant widely used in industries and packaging sectors. HDPE is suitable for a wide range of applications from heavy-duty damp proof membranes to light, flexible bags and films due to the unique characteristics of HDPE. HDPE is a durable, versatile plastic that offers fantastic impact resistance and tensile strength. The molecules in the HDPE are packed together so tightly that give rise to incredible toughness and rigidity. HDPE is easily processed, recycled and resistant to chemicals (acids, alkalis and alcohols), corrosion, absorption and abrasion (PlasticsEurope, 2013, 2017). Average area, perimeter, circularity, roundness, major axis, minor axis, aspect ratio and diameter were determined using ImageJ software (Java-based image processing program) (Schneider *et al.*, 2012). Circularity is a measure of how closely the particle has a circular geometry and is calculated as $4\pi \times \text{Area} / (\text{perimeter})^2$. Major and minor axes are the length of the major and minor axes of the smallest ellipse that encloses a particle; aspect ratio is the ratio of the major and minor axes. A histogram showing diameter distributions of HDPE is given in Figure A1. The plastic was confirmed to be HDPE by comparing its spectrum with other reported analyses of untreated HDPE (Lin *et al.*, 2015; Maheswari *et al.*, 2013; Figure A2) using Fourier Transform Infrared Spectroscopy (FTIR) equipped with an ATR platinum diamond attenuated total reflectance accessory and a potassium bromide beam splitter. The differences between the spectra will be due to the variation in analysis conditions and trace amounts of additional additives, such as plasticizers and dyes. Spectra were scanned in the range of 400 to 4000 cm^{-1} . Each spectrum comprised of 144 scans with a 4 cm^{-1} resolution. The ATR crystal of the instrument was cleaned with 70 % 2-propanol and a blank sample was analysed first to establish a background spectrum for background correction of subsequent spectra. Background spectrum showed a broad intense peak at 1575 and 1660 cm^{-1} representative of the H-O-H bond in water. Water was also represented by a peak at 3791 cm^{-1} corresponding to the O-H bond. No other peaks were observed in the background spectrum. When background measurement was completed, approximately 2 g of HDPE powder was placed onto the ATR crystal and spectra were obtained.

3.2.3. Experiment with UV radiation

An UV lamp (Analytikjena PN 90-0019-01, USA) with a wavelength of 365 nm and another UV lamp with a wavelength of 185 nm (ozone generating) was used to simulate weathering of HDPE. We selected 365 and 185 nm wavelengths since they are present in natural sunlight. 365 nm UV

radiation is reported to be UV-A which is a long-wave UV whereas 185 nm ozone generating UV radiation is UV-C which is a short-wave UV (ISO 21348). This approach mimicked the weathering of HDPE in natural environment and looked at the effect of weathering on adsorption. Approximately 10 g pristine microplastic (PMP) were placed in a 100 ml conical flask in a 1 mm deep layer that covered the bottom of the flask (Figure 3.1). There was a distance of 5 cm between the sample and the radiation source. The sample flask was wrapped in laboratory grade aluminium foil and the HDPE was exposed to the 185 nm UV radiation for four hours a day over a period of five months. Another conical flask (100 ml) comprising 10 g PMP was also treated in the same way with 365 nm UV radiation. FTIR spectra were observed every two weeks. The pristine microplastic (PMP) (Figure A3) exposed to the 185 nm ozone producing light was clumped together after treating with UV radiation (Figure A4) whereas no change (no clumping) was observed for the PMP exposed to the 365 nm UV radiation. A control treatment (not treated with UV radiation) comprising HDPE in a foil wrapped flask was also established which was kept inside a cupboard to ensure darkness (free from any kind of light). Ultrasonic probe (MSE Soniprep 150 Plus) was used to separate the weathered microplastics (WMP) for observing the variations in the properties (average area, perimeter, circularity, roundness, major axis, minor axis, aspect ratio and diameter) of PMP and WMP. Approximately 5 g WMP were placed in a 100 ml beaker followed by adding 20 ml deionized water in such a way that the WMP were fully submersed in water. The WMP were separated with the use of the ultrasonic probe. The WMP were then picked up using a tweezer and left for 24 hours at room temperature for drying. After that, the properties of the WMP were determined using ImageJ software (Schneider *et al.*, 2012).

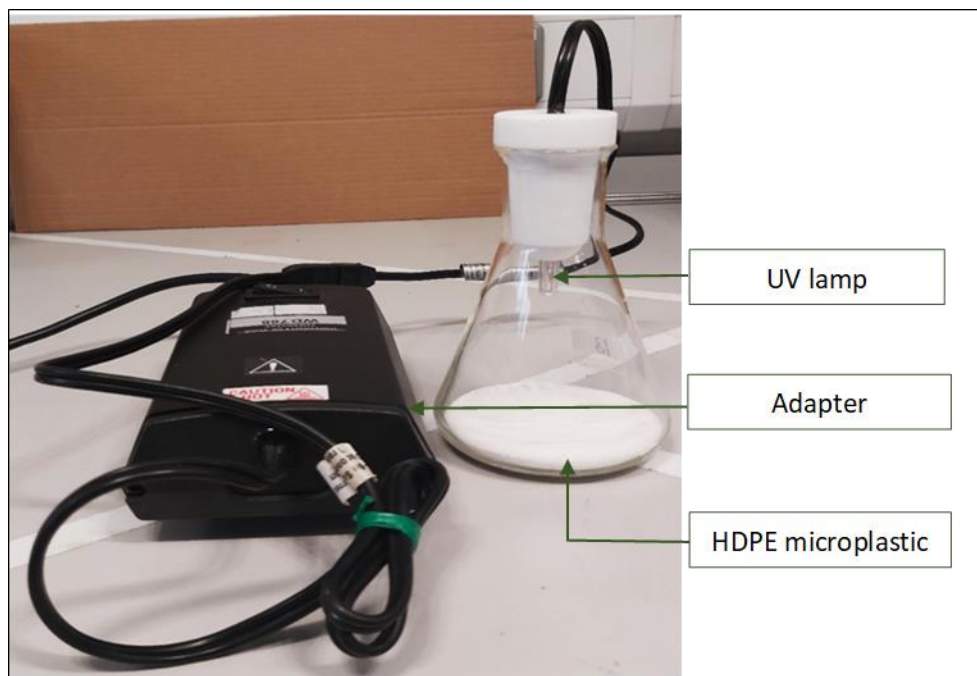


Figure 3.1. Exposure of HDPE to UV radiation using UV lamp. Exposure duration was four hours per day over a period of five months. The model no. for the UV lamp is Analytikjena PN 90-0019-01, USA and the power supply is PS-1.

3.2.4. Kinetic experiments

An adsorption experiment was carried out to determine whether the microplastic can adsorb phosphate and to establish time to equilibrium prior to running a full adsorption experiment. Both pristine (PMP) and weathered microplastics (WMP) were washed with analytical grade n-hexane (95 %) and methanol (99.85 %) for 24 hours each to remove any kind of impurities and then dried at room temperature. After that, 0.2 g HDPE (PMP, WMP) were placed into the screw-cap glass vials (50 ml) and 30 ml of 5 mg/ L phosphorus solution was added obtained by dissolving analytical grade potassium dihydrogen phosphate (KH_2PO_4) in a background electrolyte of 0.1 M NaNO_3 , to maintain a constant ionic strength in the solution. Aluminium foils were wrapped around the top of the vials before putting the lids on and then the vials were shaken on a flatbed shaker at 180 rpm at 20 °C (Moazed *et al.*, 2010). Control vials, containing P solution but without HDPE were also treated the same way. After 1, 3, 6, 14, 24 and 48 hours triplicate sacrificial

replicates were filtered through Whatman No. 42 filter paper and the supernatant was analyzed for P content using an Inductively Coupled Plasma Optical Emission Spectrometry (ICP-OES, Thermo Scientific ICAP 7000 Series, UK). Similar adsorption experiments were carried out using 0.2 g soil (S1, S2) and also a mixture of soil and microplastics (S1 + PMP, S1 + WMP, S2 + PMP, S2 + WMP) in 30 ml of P solution. Regarding the mixture of soil and microplastics, 0.1 g soil and 0.1 g HDPE were mixed in 30 ml of P solution so that the total weight of the solid became 0.2 g. The basic operational principles of the ICP-OES are provided in Appendix A (Section A1).

It is worth to be noted that in the present study, we determined the total phosphorus content in our samples using the ICP-OES. We did not measure the speciation of P. As we measured the content of total P and did not measure its speciation in the following we refer to the adsorption and desorption of phosphate assuming that the majority of the P was present as PO_4^{3-} or related, e.g. HPO_4^{2-} ion. Nonetheless, all concentrations reported are for total P. Data from the kinetic experiments indicated that adsorption had reached a steady state within 24/ 14 hours (Table S1). Although different solids reached steady state at different time (24/ 14 hours), we used 24 hours for further adsorption experiments for the convenience of our study.

3.2.5. Adsorption isotherms

Adsorption experiments were conducted using 0.2 to 200.0 mg/ L phosphorus solution with triplicate of all solids and solid-free control treatments (containing 0.1 M NaNO_3) at each concentration. Isotherms were constructed using data from the experiments in which 0.2 g solid were shaken at 180 rpm at 20 °C in glass vials for 24 hours in 30 ml P solution (from KH_2PO_4) in a background electrolyte of 0.1 M NaNO_3 . These suspensions were filtered and analyzed for phosphorus with ICP-OES (Thermo Scientific ICAP 7000 Series, UK). The amount of P adsorbed on solid was calculated from the difference between solid-free control and sample treatments at the end of the adsorption period (Sparks, 2003; Sposito, 1989). Data were fitted to the linear (Equation 1) and non-linear (Langmuir: Equation 2 and Freundlich: Equation 3) isotherms (Jalali and Peikam, 2013; Zhou *et al.*, 2005; Tian *et al.*, 2006). As the partition coefficient (K_d) is the ratio of phosphorus adsorbed to the solid (C_s) to the phosphorus concentration present in the solution (C_{aq}), K_d was calculated from the slope of linear regression

(independent variable: C_{aq} , dependent variable: C_s). Linear regression was forced through the origin (0, 0) for the calculation of K_d .

$$K_d = \frac{C_s}{C_{aq}} \quad (1)$$

$$\frac{C_s}{C_{aq}} = \frac{bC_{SM}}{1 + C_{aq}b} \quad (2)$$

$$C_s = K_f C_{aq}^{1/n} \quad (3)$$

where K_d is the partition coefficient (L/ kg); C_s is the concentration of phosphorus adsorbed on solid (mg/ kg); C_{aq} is the equilibrium P concentration in solution (mg/ L); b is the binding constant (L/ mg); C_{SM} is the maximum adsorption capacity (mg/ kg); K_f and n is the Freundlich constants related to adsorption.

3.2.6. Desorption experiments

Desorption experiments were undertaken to determine whether microplastic could release previously sorbed phosphate and to compare release rates with those from soils. Desorption experiment was performed after the supernatants obtained in the adsorption experiment were removed. Residual solids on Whatman No. 42 filter paper that had sorbed P were washed with 30 ml saturated NaCl (Han *et al.*, 2018) to remove free phosphorus. After the samples were washed, 30 ml of 0.1 M NaNO₃ was added with each sample. Samples were then shaken at 180 rpm for 24 hours followed by filtration. The supernatants were analyzed using the ICP-OES (Thermo Scientific ICAP 7000 Series, UK) to determine the P concentration in solution and the percentage of P desorption was calculated using Equation 4 (Bai *et al.*, 2017; Han *et al.*, 2018). The hysteresis index (HI) was calculated to determine the reversibility of the adsorption experiment using Equation 5 (Ding *et al.*, 2019).

$$P_{des}(\%) = (A-B) \times (100/A) \quad (4)$$

where A is the total mass of phosphorus available for desorption determined by multiplying adsorbed P on solid (mg/ kg) with the mass of solid (kg); B is the total mass of P that has desorbed determined by multiplying the P concentration in solution after desorption (mg/ L) with the volume of solution (mg/ L).

$$HI = \frac{C_s - C_{des}}{C_s} \quad (5)$$

where C_s is the initial concentration of phosphorus adsorbed on solid (mg/ kg) and C_{des} is the concentration of phosphorus desorbed from the solid (mg/ kg).

3.2.7. Quality control and statistical analysis

Detection limits for the analytical instruments used were calculated as the mean plus six times the standard deviation of ten repeated measurements of the blank standard (Walsh, 1997). For statistical analysis of solution data value below detection limit was given a value equal to the detection limit (Helsel, 2007). Accuracy of calibration was determined by analysis of an in-house certified reference material (CRM). Analytical precision was calculated from the coefficient of variation (CV) determined from duplicate analysis of 10 % of the samples that were at least 100 times higher than the detection limit and determining the median of the difference between the duplicate measurements expressed as a percentage of their mean value (Gill and Ramsey, 1997). Quality control data for chemical analysis associated with each set of experiments are provided in Table A1.

All data were analyzed using IBM SPSS Statistics (version 25) or SigmaPlot (version 14) software. Data were tested for normal distribution using the Shapiro-Wilk and Kolmogorov-Smirnov test and equal variance using Levene's mean test. Data were normally distributed for all analyses. In the kinetic experiments, a two-way analysis of variance (ANOVA) was used to test for significant difference in phosphorus concentration between solid type (factor 1) and time (factor 2). Post hoc analysis was used for pairwise comparisons within significant ($p \leq 0.05$) values of time using Tukey's method at 5 % level of significance, to determine the time point at which the concentration of P reached the steady state. Linear and non-linear models (Langmuir and Freundlich) were used to fit the adsorption isotherm of P (Liu *et al.*, 2019a; Zuo *et al.*, 2019). In case of desorption experiments, regression analysis was done on the percentage of desorption (dependent variable) to detect whether there were different regression results for the different solids.

3.3. Results

3.3.1. HDPE characterisation

Average area of the pristine microplastic (PMP) was $0.06 \pm 0.01 \text{ mm}^2$, circularity 0.96 ± 0.52 , aspect ratio 0.46 ± 0.15 and diameter $238.11 \pm 82.52 \text{ }\mu\text{m}$ ($n = 300$, \pm standard deviation) (Table 3.1). PMP had a white and powdery texture (Figure A3) which showed a tendency to clump together upon UV weathering by 185 nm wavelength UV radiation (Figure A4). No change in the texture, average area, perimeter, circularity, roundness, major axis, minor axis, aspect ratio and diameter were observed for the PMP treated with the 365 nm wavelength UV radiation.

Table 3.1. Properties of HDPE (mean \pm standard deviation). Value of n is 300. Subsamples of the particles were scattered on a slide, flattened by over-laying a piece of glass and images captured with a Zeiss PlanNeoFluar Microscope at 33.5 magnification. The particles analysed were not overlapping and not lying on the edges of the image. Images were analysed using ImageJ software.

Parameter	Value for PMP	Value for WMP
Average area (mm^2)	0.06 ± 0.01	0.09 ± 0.001
Perimeter (mm)	0.25 ± 0.50	0.28 ± 1.13
Circularity	0.96 ± 0.52	0.97 ± 0.71
Roundness	0.89 ± 0.33	0.91 ± 0.23
Major axis (mm)	0.24 ± 0.09	0.25 ± 0.09
Minor axis (mm)	0.14 ± 0.06	0.15 ± 0.05
Aspect ratio	0.46 ± 0.15	0.48 ± 0.14
Diameter (μm)	238.11 ± 82.52	249.86 ± 38.61

*PMP = pristine HDPE, WMP = weathered HDPE

FTIR spectra of the pristine microplastic (PMP) treated with ozone producing 185 nm wavelength UV radiation remained same in the first 60 days of exposure and after that changes in IR band happened more quickly. From day 75, a new peak was detectable in the form of the growth of a peak at 1743 cm^{-1} (Table 3.2), which became more visible on Day 105 (Figure 3.2,

Table 3.2). Thus, UV exposure with 185 nm wavelength has led to the development of a new functional group in the PMP which was used as a good proxy for weathered microplastics. However, there was no change in the FTIR spectra after exposure to the 365 nm radiation and was not used further in the adsorption experiments.

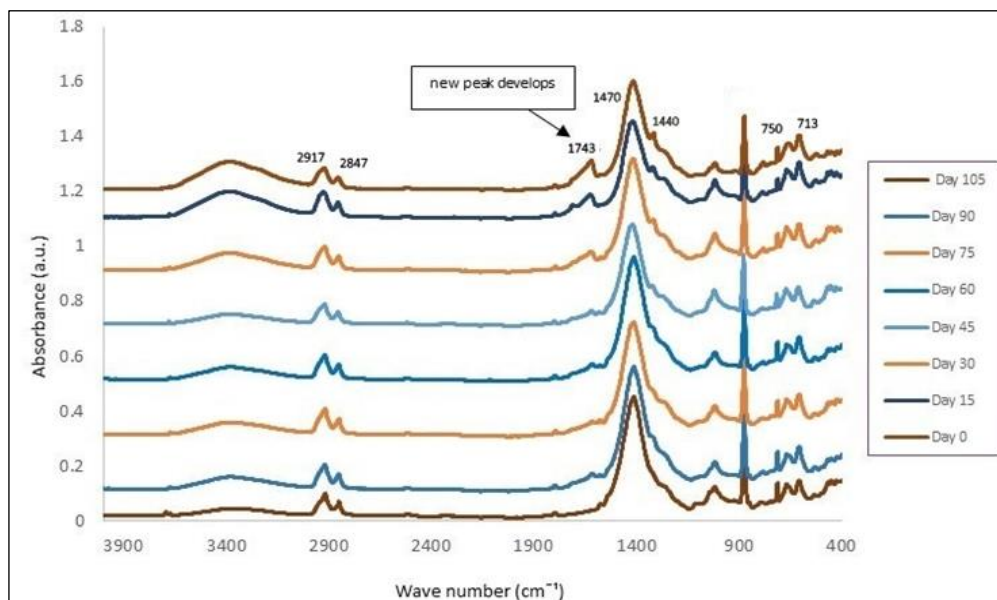


Figure 3.2. Changes in FTIR spectra of HDPE after exposure to UV radiation with 185 nm and 365 nm wavelength. Exposure duration was four hours per day over a period of five months. The bottom-most spectrum shows pristine microplastic which was not UV treated. Microplastic treated with 365 nm wavelength for five months looks like the bottom-most spectrum indicating the pristine microplastic.

Table 3.2. Functional groups and appearances for the FTIR spectra of microplastic used in the study before and after exposure to UV radiation. FTIR spectra were scanned in the range of 400 to 4000 cm^{-1} . Each spectrum comprised 144 scans with a 4 cm^{-1} resolution. Asterisk (*) sign indicated FTIR spectra of weathered microplastic.

Absorption bands (cm^{-1})	Functional group	Appearance	References
2917	C-H stretching	Strong	Asensio <i>et al.</i> , 2009; Noda <i>et al.</i> , 2007; Nishikida and Coates, 2003
2847	C-H stretching	Weak	Asensio <i>et al.</i> , 2009; Noda <i>et al.</i> , 2007; Nishikida and Coates, 2003
1743*	C=O stretching	Strong	Martínez-Romo <i>et al.</i> , 2015; Telmo <i>et al.</i> , 2011; Wypych, 2003
1470	CH ₂ bending	Medium	Asensio <i>et al.</i> , 2009; Coates, 2000; Nishikida and Coates, 2003
1440	CH ₂ bending	Medium	Asensio <i>et al.</i> , 2009; Verleye <i>et al.</i> , 2001; Nishikida and Coates, 2003
750	CH ₂ rocking	Strong	Verleye <i>et al.</i> , 2001; Noda <i>et al.</i> , 2007; Nishikida and Coates, 2003
713	CH ₂ rocking	Strong	Asensio <i>et al.</i> , 2009; Noda <i>et al.</i> , 2007; Nishikida and Coates, 2003

3.3.2. Kinetics experiments

Concentration of phosphate in solution was decreased over time for all solids bearing suspensions and then reached a steady state (Figure 3.3) which was confirmed by Tukey test. Different solids reached steady state at different times (Table A2). It is noteworthy that the weathered microplastic (WMP) reached the steady state sooner (14 hours; $p \leq 0.05$) than it did on the pristine microplastic (PMP) (24 hours; $p \leq 0.05$). When the soil was mixed with pristine microplastics, it reached the steady state later than the mixture of soil and weathered microplastics (Table A2).

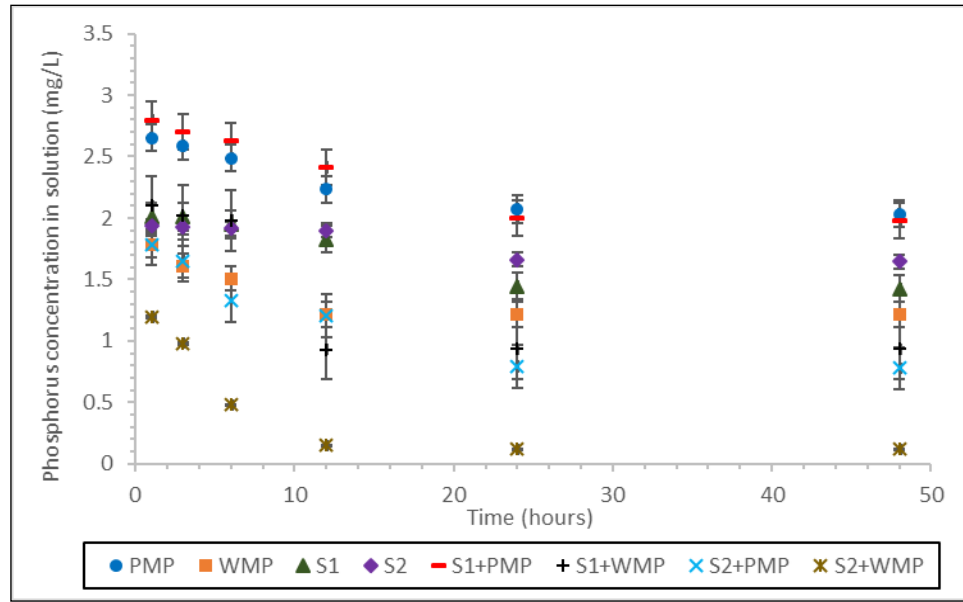


Figure 3.3. Changes in phosphorus concentration over time for different solid types: PMP = pristine HDPE, WMP = weathered HDPE, S1 = low organic matter soil, S2 = high organic matter soil, S1 + PMP = mixture of low organic matter soil and pristine HDPE, S1 + WMP = mixture of low organic matter soil and weathered HDPE, S2 + PMP = mixture of high organic matter soil and pristine HDPE, S2 + WMP = mixture of high organic matter soil and weathered HDPE. For each case, 0.2 g solid was added to 30 ml P solution and shaken for different time intervals. Error bars indicate standard deviations of means with three replicates ($n = 3$).

3.3.3. Adsorption isotherms

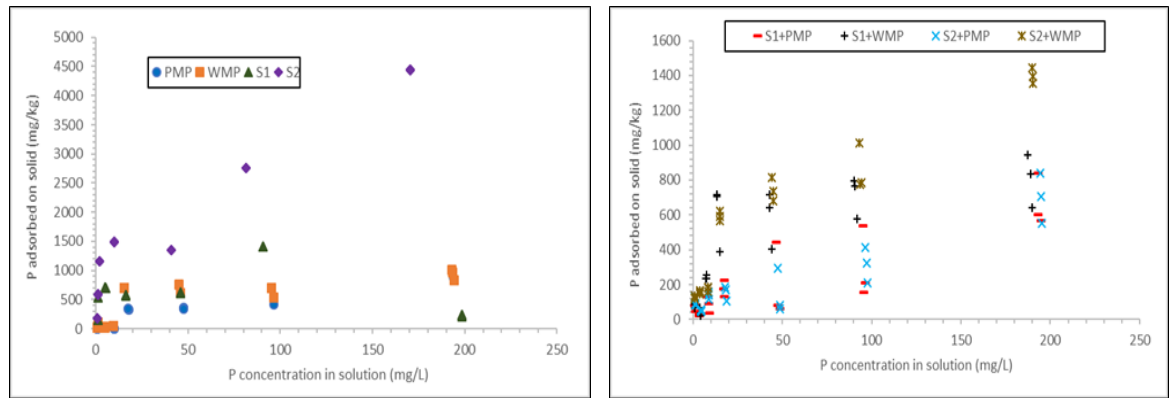
Adsorption isotherms were constructed for all solid types using the data from experiments in which 0.2 g solid was shaken for 24 hours in 30 ml phosphorus solution. Phosphate adsorption to different solid types was best described by different types of linear and non-linear (Langmuir and Freundlich) isotherms as shown in Table 3.3 and Table 3.4, indicating the relationship between the equilibrium concentration of phosphorus solution and the concentration adsorbed to the microplastic surface (Stumm and Morgan, 1996). Although Langmuir isotherm was not a good fit for either pristine microplastic (PMP) or weathered microplastic (WMP), the fit to the Langmuir isotherm was used to determine the maximum adsorption capacities, C_{SM} , and binding constants, b (Table 3.4). When microplastic was present as a single solid in the adsorption experiment, phosphate adsorbed on the WMP was greater than that of the PMP (Figure 3.4,

Figure 3.5, Table 3.3, Table 3.4) indicated by higher values of partition coefficient (K_d) and maximum adsorption capacity (C_{SM}). When the soil was present as a single solid in the adsorption experiment, adsorption was higher for the S2 than S1 (Table 3.3, Table 3.4). There were large differences in the values of K_d , C_{SM} and $\log K_f$ for the S1 and S2. However, no variation was found between the values of $1/n$ for the S1 and S2. For both soil types, when soil was mixed with pristine microplastics, adsorption was lower than the mixture of soil and weathered microplastics (Figure 3.4, Figure 3.5, Table 3.3, Table 3.4) indicated by relatively lower values of K_d for the mixture of soil and pristine microplastics. 95 % confidence intervals around the mean values of Langmuir and Freundlich parameters for the soil + pristine microplastics and soil + weathered microplastics were overlapped and thus they were unlikely to be significantly different. The same trend was followed by both soil types (Table 3.4).

Table 3.3 Partition coefficient (K_d) values for phosphorus adsorption to different solids. Mass of solid used is 0.2 g and volume of solution is 30 ml. Concentrations of P range from 0.2 – 200.0 mg/L. Equilibrium time for the adsorption experiment is 24 hours. Reported values are calculated from the linear regression of 30 values ($n = 30$ for each set of data). K_d is determined from the slope of linear regression (independent variable: phosphorus concentration present in the solution, C_{aq} ; dependent variable: phosphorus adsorbed to the solid, C_s). 95 % confidence interval is calculated which are shown in brackets. Upper and lower limit of confidence intervals are separated by comma (,). Unit of K_d is L/ kg for all solid types.

Solid type	Partition coefficient (K_d)	R^2 value	p value
PMP	10.74 (6.71, 14.77)	0.95	≤ 0.05
WMP	29.13 (17.68, 40.57)	0.65	≤ 0.05
S1	220.01 (170.54, 291.46)	0.61	≤ 0.05
S2	328.22 (315.06, 345.64)	0.91	≤ 0.05
S1 + PMP	20.87 (12.14, 29.60)	0.81	≤ 0.05
S1 + WMP	81.89 (43.48, 120.31)	0.61	≤ 0.05
S2 + PMP	22.09 (11.66, 32.51)	0.88	≤ 0.05
S2 + WMP	60.34 (41.27, 79.41)	0.86	≤ 0.05

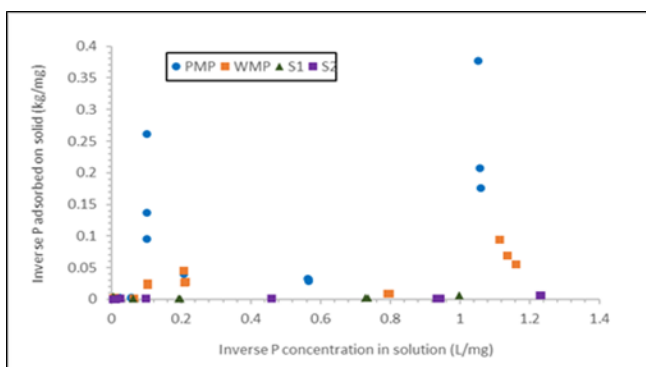
*PMP = pristine HDPE, WMP = weathered HDPE, S1 = low organic matter soil, S2 = high organic matter soil, S1 + PMP = mixture of low organic matter soil and pristine HDPE, S1 + WMP = mixture of low organic matter soil and weathered HDPE, S2 + PMP = mixture of high organic matter soil and pristine HDPE, S2 + WMP = mixture of high organic matter soil and weathered HDPE. Partition coefficient is calculated as the $K_d = \frac{C_s}{C_{aq}}$, where, C_s = amount of phosphorus adsorbed on solid (mg/ kg), C_{aq} = concentration of phosphorus in equilibrium solution (mg/ L).



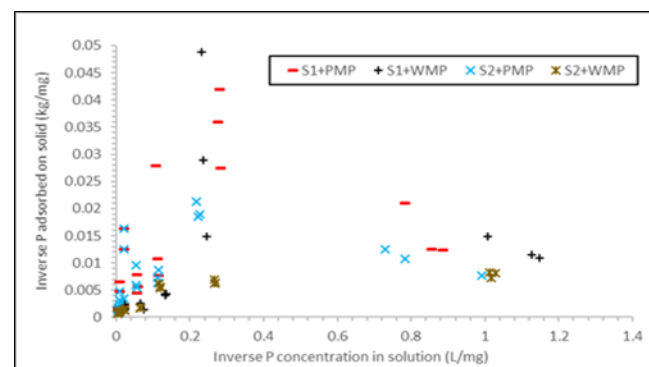
(a)

(b)

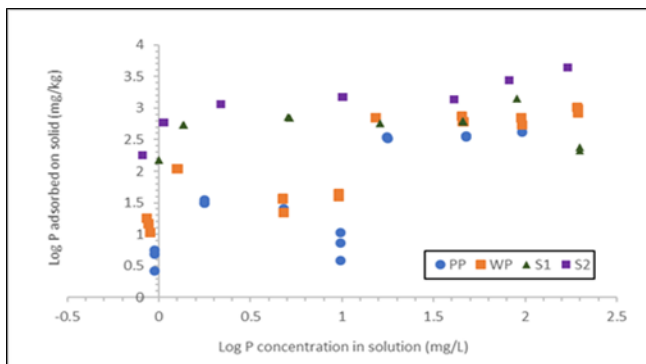
Figure 3.4. Adsorption of phosphorus for different solids types: (a) PMP = pristine HDPE, WMP = weathered HDPE, S1 = low organic matter soil, S2 = high organic matter soil; (b) S1 + PMP = mixture of low organic matter soil and pristine HDPE, S1 + WMP = mixture of low organic matter soil and weathered HDPE, S2 + PMP = mixture of high organic matter soil and pristine HDPE, S2 + WMP = mixture of high organic matter soil and weathered HDPE. 0.2 g solid was added to 30 ml P solution and shaken for 24 hours. For each set of solid samples, number of replicates is 3 and concentration is 10. Some data points are overlapping and thus all the replications are not visible.



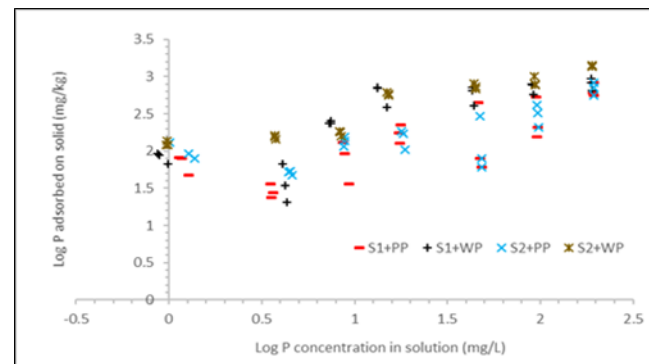
(a)



(b)



(c)



(d)

Figure 3.5. Langmuir adsorption isotherms of phosphorus for different solid types: (a) PMP = pristine HDPE, WMP = weathered HDPE, S1 = low organic matter soil, S2 = high organic matter soil; (b) S1 + PMP = mixture of low organic matter soil and pristine HDPE, S1 + WMP = mixture of low organic matter soil and weathered HDPE, S2 + PMP = mixture of high organic matter soil and pristine HDPE, S2 + WMP = mixture of high organic matter soil and weathered HDPE; Freundlich isotherms for (c) PMP, WMP, S1, S2; (d) S1 + PMP, S1 + WMP, S2 + PMP, S2 + WMP. 0.2 g solid was added to 30 ml P solution and shaken for 24 hours. For each set of data, number of replicates is 3 and concentration is 10. Some data points are overlapping and thus all the replications are not visible.

Table 3.4. Langmuir and Freundlich adsorption isotherm parameters for phosphorus to different solid types. Mass of solid used is 0.2 g. Volume of solution is 30 ml. Concentrations of P range from 0.2 – 200.0 mg/ L. Equilibrium time for the adsorption experiment is 24 hours. Reported values are calculated from the linear regression of 30 values (n = 30 for each set of data). For Langmuir isotherm, C_{SM} and b are determined from the intercept ($1/ C_{SM}$) and slope ($1/ bC_{SM}$) of linear regression (independent variable: inverse of phosphorus concentration present in the solution, $1/ C_{aq}$; dependent variable: inverse of phosphorus adsorbed to the solid, $1/ C_s$) respectively. For Freundlich isotherm, $\log K_f$ and $1/ n$ are determined from the intercept and slope of linear regression (independent variable: log value of phosphorus concentration present in the solution, $\log C_{aq}$; dependent variable: log value of phosphorus adsorbed to the solid, $\log C_s$) respectively. 95 % confidence interval is calculated which are shown in brackets. Upper and lower limit of confidence intervals are separated by comma (,).

Langmuir isotherms				Freundlich isotherms				
Solid type	C_{SM} (mg/ kg)	b (L/ mg)	R^2 value	p value	$\log K_f$	1/ n	R^2 value	p value
PMP	78.74 (54.69, 101.08)	0.07 (0.03, 0.09)	0.20	≤ 0.05	0.81 (0.07, 1.54)	0.95 (0.49, 1.45)	0.79	≤ 0.05
WMP	285.71 (220.02, 320.26)	0.09 (0.05, 1.12)	0.52	≤ 0.05	2.49 (2.04, 2.95)	1.73 (1.48, 1.99)	0.70	≤ 0.05
S1	322.58 (201.36, 396.28)	0.02 (-0.01, 0.04)	0.95	≤ 0.05	4.45 (4.11, 5.18)	0.59 (0.28, 0.67)	0.71	≤ 0.05
S2	507.56 (467.13, 563.49)	0.06 (0.05, 0.08)	0.94	≤ 0.05	5.64 (5.29, 5.98)	0.69 (0.17, 0.79)	0.94	≤ 0.05

*PMP = pristine HDPE, WMP = weathered HDPE, S1 = low organic matter soil, S2 = high organic matter soil. Langmuir equation is expressed as $\frac{C_s}{C_{aq}} =$

$\frac{bC_{SM}}{1 + C_{aq}b}$, where, C_s = amount of phosphorus adsorbed on solid (mg/ kg), C_{aq} = concentration of phosphorus in equilibrium solution (mg/ L), C_{SM} = maximum

adsorption capacity (mg/ kg), b = binding constant (L/ mg). Freundlich equation is expressed as $C_s = K_f C_{aq}^{1/n}$ where, C_s = amount of phosphorus adsorbed on solid (mg/ kg), C_{aq} = concentration of phosphorus in equilibrium solution (mg/ L), $\log K_f$ = Freundlich constant, $1/ n$ = heterogeneity factor.

Table 3.4 (continued). Langmuir and Freundlich adsorption isotherm parameters for phosphorus to different solid types.

Solid type	Langmuir isotherms				Freundlich isotherms			
	C _{SM} (mg/ kg)	b (L/ mg)	R ² value	p value	log K _f	1/ n	R ² value	p value
S1 + PMP	129.87 (95.98, 201.46)	0.47 (-0.23, 0.58)	0.45	≤0.05	5.52 (4.80, 5.94)	0.51 (0.41, 0.69)	0.81	≤0.05
S1 + WMP	227.27 (186.45, 296.13)	0.49 (-0.10, 0.57)	0.43	≤0.05	5.81 (4.95, 6.07)	0.53 (0.42, 0.78)	0.82	≤0.05
S2 + PMP	244.74 (203.04, 294.23)	0.81 (0.53, 1.23)	0.51	≤0.05	1.72 (1.29, 2.15)	0.39 (0.09, 0.68)	0.81	≤0.05
S2 + WMP	384.54 (274.65, 426.13)	0.84 (0.57, 1.26)	0.89	≤0.05	2.00 (1.73, 2.28)	0.49 (0.30, 0.69)	0.96	≤0.05

*S1 + PMP = mixture of low organic matter soil and pristine HDPE, S1 + WMP = mixture of low organic matter soil and weathered HDPE, S2 + PMP = mixture of high organic matter soil and pristine HDPE, S2 + WMP = mixture of high organic matter soil and weathered HDPE. Langmuir equation is expressed as $\frac{C_s}{C_{aq}} = \frac{bC_{SM}}{1 + C_{aq}b}$, where, C_s = amount of phosphorus adsorbed on solid (mg/ kg), C_{aq} = concentration of phosphorus in equilibrium solution (mg/ L), C_{SM} = maximum adsorption capacity (mg/ kg), b = binding constant (L/ mg). Freundlich equation is expressed as $C_s = K_f C_{aq}^{1/n}$ where, C_s = amount of phosphorus adsorbed on solid (mg/ kg), C_{aq} = concentration of phosphorus in equilibrium solution (mg/ L), log K_f = Freundlich constant, 1/ n = heterogeneity factor.

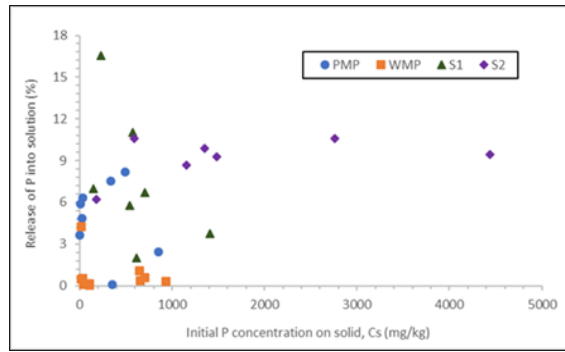
3.3.4. Desorption experiments

Desorption of phosphate was lower from the weathered microplastic (WMP) than the pristine microplastic (PMP) (Figure 3.6). Desorption of phosphate from both soils (S1, S2) was higher than the pristine microplastic (PMP). High organic matter soil (S2) did desorb more P compared to that of the low organic matter soil (S1) (Figure 3.6). When the soil was mixed with microplastics, we observed same trend for both soil types. Phosphate desorption was similar from the soil + pristine microplastics and soil + weathered microplastics (Figure 3.6). The hysteresis index (HI) of phosphorus was higher for the WMP compared to the PMP, S1 and S2. HI of phosphorus was higher for the S2 than the S1 (Table 3.5). HI was similar for the soil + pristine microplastics and soil + weathered microplastics which was true for both soil types. A higher value of HI indicates more hysteresis (Ding *et al.*, 2019).

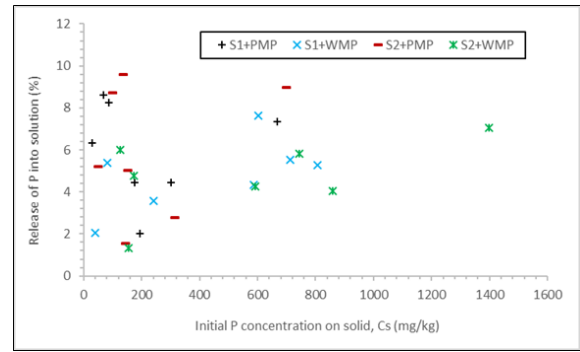
Table 3.5. Hysteresis index (HI) for different solid types. Mass of solid used is 0.2 g and volume of solution is 30 ml. Concentrations of P range from 0.2 – 200.0 mg/ L. Equilibrium time for the desorption experiment is 24 hours. HI is calculated from the mean of 30 values (n = 30 for each set of data). 95 % confidence interval is calculated which are shown in brackets. Upper and lower limit of confidence intervals are separated by comma (,).

Solid type	C _s (mg/ kg)	C _{des} (mg/ kg)	HI
PMP	263.53 (234.63, 293.33)	11.32 (1.03, 23.19)	0.95 (0.94, 0.96)
WMP	316.36 (302.63, 336.36)	3.72 (-2.08, 9.12)	0.99 (0.98, 1.00)
S1	404.01 (386.15, 424.56)	50.54 (20.41, 83.06)	0.87 (0.86, 0.88)
S2	1760.69 (1723.45, 1798.33)	175.27 (164.22, 189.14)	0.90 (0.89, 0.91)
S1 + PMP	217.86 (205.36, 234.36)	14.75 (3.23, 27.58)	0.93 (0.92, 0.94)
S1 + WMP	428.76 (411.48, 451.03)	23.88 (12.66, 36.57)	0.94 (0.93, 0.95)
S2 + PMP	211.78 (196.32, 228.61)	17.16 (10.53, 23.23)	0.92 (0.91, 0.93)
S2 + WMP	569.23 (544.18, 596.42)	31.39 (25.57, 38.26)	0.94 (0.93, 0.95)

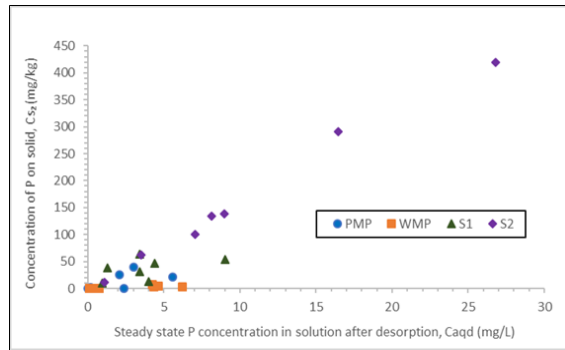
*PMP = pristine HDPE, WMP = weathered HDPE, S1 = low organic matter soil, S2 = high organic matter soil; S1 + PMP = mixture of low organic matter soil and pristine HDPE, S1 + WMP = mixture of low organic matter soil and weathered HDPE, S2 + PMP = mixture of high organic matter soil and pristine HDPE, S2 + WMP = mixture of high organic matter soil and weathered HDPE. Hysteresis Index (HI) is calculated using $(C_s - C_{des}) / C_s$, where C_s = amount of phosphorus adsorbed on solid (mg/ kg), C_{des} = amount of phosphorus desorbed from the solid (mg/ kg).



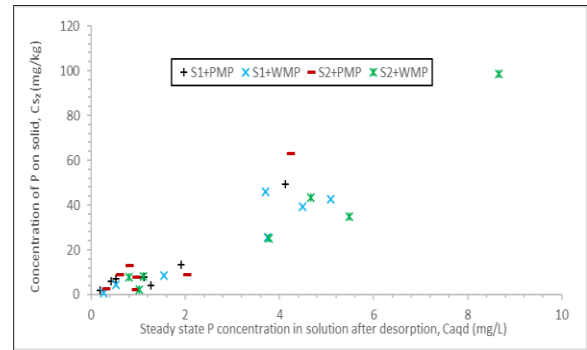
(a)



(b)



(c)



(d)

Figure 3.6. Percentage (%) of P desorption from different solids: (a) PMP = pristine HDPE, WMP = weathered HDPE, S1 = low organic matter soil, S2 = high organic matter soil; (b) S1 + PMP = mixture of low organic matter soil and pristine HDPE, S1 + WMP = mixture of low organic matter soil and weathered HDPE, S2 + PMP = mixture of high organic matter soil and pristine HDPE, S2 + WMP = mixture of high organic matter soil and weathered HDPE; Final concentration of desorbed P from (c) PMP, WMP, S1, S2; (d) S1 + PMP, S1 + WMP, S2 + PMP, S2 + WMP. 0.2 g solid was added to 30 ml of 0.1 M NaNO_3 solution and shaken for 24 hours. For each set of data, number of replicates is 3 and concentration is 10. Some data points are overlapping and thus all the replications are not visible.

3.4. Discussion

3.4.1. Pristine and weathered microplastics characterisation

FTIR spectrum of the pristine microplastic (PMP) showed distinct peaks at 2917, 2847, 1470, 1440, 750 and 713 cm^{-1} (Figure 3.2, Table 3.2). This was consistent with other studies (Martínez-Romo *et al.*, 2015; Asensio *et al.*, 2009; Noda *et al.*, 2007; Charles and Ramkumaar, 2009) where authors observed FTIR spectra at the same wave numbers present in the HDPE microplastics. Presence of C=O (carbonyl) stretching in the weathered microplastic (WMP) occurring at around 1743 cm^{-1} (Figure 3.2, Table 3.2) might be due to the photo-oxidation of microplastics as absorption of UV radiation results in the formation of free radicals (Gardette *et al.*, 2013; Carpentieri *et al.*, 2011). Hydrogen atoms would have abstracted from the macromolecular chain of the PMP and added to an unsaturated group (cross-linking reaction) or to oxygen; and consequently, hydroperoxides would form. Peroxy and hydroxide radicals generating from hydroperoxide would lead to the formation of carbonyl group (Gardette *et al.*, 2013; Carpentieri *et al.*, 2011).

3.4.2. Kinetics experiments

The extent of phosphate adsorption by all solids was found to increase and then gradually approach a more or less constant value (steady state) with the increase in time (Figure 3.3). Rate of increase in phosphate adsorption was higher within the first 14 hours of the experiment but there was a little increase in adsorption between 14 to 24 hours (Figure 3.3) as in other experiments (Wang *et al.*, 2013). Wang *et al.* (2013) reported relatively rapid adsorption of phosphate from 1 to 15 hours, followed by a slow adsorption after 15 hours, although the adsorption was likely to be highly dependent on pH and characteristics of adsorbate. As the time proceeds, some sites of the microplastic experience adsorption and there remain fewer charged adsorption sites that have yet to adsorb an oppositely charged ions (Arai and Sparks, 2001). There is less adsorption of phosphate, as there remain fewer adsorption sites (Wang *et al.*, 2013). The weathered microplastic (WMP) could have relatively more adsorption sites and it reached steady state sooner than the pristine microplastic (PMP) (Figure 3.3) possibly because of having stronger affinity for the phosphate ions than the PMP. Oxygen of the carbonyl group (C = O) present in the WMP was noticeable at the surface with a negative charge which would repel the negatively

charged phosphate ions and possibly there was cation bridging between the phosphate ions and the functional groups on the WMP. The presence of ions promotes cation bridging, particularly with the multivalent ions like phosphate (MacKay and Canterbury, 2005).

3.4.3. Adsorption experiments

Microplastics have the potential to adsorb hydrophilic molecules (negatively charged) which was observed in previous studies (Liu *et al.*, 2019a; Liu *et al.*, 2019b; Bakir *et al.*, 2014a; Bakir *et al.*, 2014b; Massos and Turner, 2017; Turner and Holmes, 2015). Since the phosphate (PO_4^{3-}) ion is hydrophilic in nature, it was expected that HDPE microplastics used in our study would adsorb PO_4^{3-} which was verified in our kinetic experiments. We would expect that most of the P in our study were present as PO_4^{3-} ions. Phosphate is charged and polar (Marc, 2005) whilst microplastics are nonpolar. Thus, electrostatic attraction is unlikely between PO_4^{3-} ions and microplastics, suggesting that adsorption of PO_4^{3-} (Figure 3.4, Figure 3.5) is either by specific adsorption (adsorbed ions are typically bound by chemical attraction through the formation of inner sphere complexes) or through hydrogen bonding / Van der Waals forces (Ma *et al.*, 2019). Adsorption of PO_4^{3-} to microplastics is highly dependent on pH and ionic strength of the solution (Fei *et al.*, 2015).

Values of partition coefficient (K_d), maximum adsorption capacity (C_{SM}), and heterogeneity factor ($1/n$) for the pristine microplastic (PMP) (Table 3.3, Table 3.4) were similar to those reported for the HDPE particles in previous studies for different adsorbates (Li *et al.*, 2018; Holmes *et al.*, 2012), but the values of binding constant (b) and Freundlich constant ($\log K_f$) were far lower, possibly reflecting the variations in the binding energy and surface chemistry of the microplastics or the ionic strength of seawater used in the experiments (Li *et al.*, 2018; Holmes *et al.*, 2012). Seawater has higher ionic strength (approximately 0.7 M) compared to that of the soil solution (approximately 0.1 M) (Edmeades *et al.*, 1985) which might be the reason for the higher values of b and $\log K_f$ in Li's and Holmes's studies. Effect of ionic strength on phosphate adsorption varies with the pH and occurs through its effect on the electrostatic potential in the plane of adsorption (Barrow, 1984). At pH values above the PZC (point of zero charge) adsorption of phosphate increases with increasing ionic strength whilst pH values below the PZC decreases adsorption with decreasing ionic strength (Bolan *et al.*, 1986). Both the pH and ionic

strength have been demonstrated to affect the adsorption of PO_4^{3-} ions in previous studies (Sposito, 1989; Jafvert, 1990). According to Westall *et al.* (1999), changes in the pH influence the protonation/ deprotonation of ions, and ionic strength impacts on the competition for the adsorption sites, thereby affecting the adsorption. The studies by Li *et al.* (2018) and Holmes *et al.* (2012) did not determine the pH or PZC of the microplastic. The pH value of seawater is approximately 8.1 which was reported by Millero (2001). The PZC of the microplastic was determined 6.31 in our study (Chapter 4). Therefore, we assumed that the microplastics used in Li's (2018) and Holmes's (2012) studies experienced higher values of pH than the PZC that would result in higher adsorptions (higher values of b and $\log K_f$) due to the higher ionic strength of seawater. Thus, it becomes imperative to determine the impacts of pH and ionic strength on the adsorption of phosphate and we will study that in Chapter 4.

When present as the only solid in the adsorption experiment, the WMP adsorbed significantly more phosphate than the PMP (Figure 3.4, Figure 3.5, Table 3.3, Table 3.4). Similar to our findings, Hüffer *et al.* (2018) and Holmes *et al.* (2012) observed increased adsorption of metals by the UV weathered microplastics. They suggested that that the increased adsorption was due to the increases in area and polarity (Hüffer *et al.*, 2018) as well as greater heterogeneity (Holmes *et al.*, 2012) of the WMP particles which was consistent with our study. The WMP used in our study had higher area ($0.09 \pm 0.001 \text{ mm}^2$, \pm standard deviation; Table 3.1) compared to the PMP ($0.06 \pm 0.01 \text{ mm}^2$; \pm standard deviation; Table 3.1) and increased polarity due to the introduction of oxygen containing functional groups (C=O) into the polymer structure (Figure 3.2). Our study observed higher values of $\log K_f$ and $1/n$ for the WMP than the PMP (Table 3.4) indicating greater surface heterogeneity of the WMP. The study by Holmes *et al.* (2012) had a meaningful hypothesis although we identified some limitations for the study. Holmes's (2012) hypothesis was that weathered microplastic adsorbs more than the pristine ones and the authors proved the hypothesis in their study. Sources of the virgin and weathered microplastics used were different in Holmes's study (2012). The virgin polyethylene was obtained from a local plastic processing industry whereas the weathered polyethylene was collected from three different coastal beaches. The weathered polyethylene may not have been like the pristine polyethylene. The pristine and weathered microplastics should be same material to draw a meaningful conclusion from Holmes's study (2012). In another study (Brennecke *et al.*, 2016), it was suggested that weathered polyvinyl chloride (PVC) adsorbed higher amounts of Cu and Zn compared to the pristine polystyrene (PS) which was presumably due to the increased polarity and higher area of the

weathered PVC. It is noteworthy that PS and PVC used in Brennecke's study (2016) are two different plastics and they vary in chemical composition and properties. For instance, PS contains a phenyl group in its structure and is non polar in nature. In contrast, PVC has chloride in its structure and is slightly polar than the PS. We would expect the PVC to be more adsorptive than the PS because of their molecular structure and polarity. In contrast to our findings, Hüffer *et al.* (2018) reported that the adsorption on the WMP in aqueous ecosystem was approximately one order of magnitude lower than on the PMP. Polystyrene microplastic develops cracks upon weathering and these cracks make the microplastic susceptible to water penetration (Muller *et al.*, 2018; Endo *et al.*, 2005). Oxygen containing functional groups (polar in nature) of the WMP could allow the formation of bonds with the penetrated water molecules. As a result, polarity and reactivity of the WMP could reduce leading to a lower adsorption of the adsorbate in Hüffer's study (2018) as suggested by Brant (2011) and Hüffer *et al.* (2013). For both the PMP and WMP, the poor fits to the Langmuir isotherm indicated that phosphate adsorption energy did not distribute homogeneously and thereby the assumption of site limitation for monolayer sorption was not valid (Banihashemi and Droste, 2014). The $1/n$ values of both the PMP and WMP samples deviated from 1, indicating that both the microplastics followed multilayer adsorption on the heterogeneous surface (Liu *et al.*, 2019a; 2019b).

When present as the single solid, adsorption of phosphate by the PMP and WMP was far lower compared to the values of both soil types (Figure 3.4, Figure 3.5, Table 3.3, Table 3.4). Values of partition coefficient (K_d), maximum adsorption capacity (C_{SM}), Freundlich constant ($\log K_f$) and heterogeneity factor ($1/n$) of the PMP and WMP were far lower compared to the values of S1 and S2 (Table 3.3, Table 3.4). Typically the soil is a porous solid with various sizes of pores on its surface (Pignatello, 1998). Phosphate could be adsorbed in the pore spaces within the soils (Schwarz *et al.*, 2012). Additionally, higher adsorption of PO_4^{3-} on the soils than microplastics could result from the stronger electrostatic attraction between charged surfaces of the soil (resulting from the charged functional groups) and negatively charged PO_4^{3-} ions. Adsorption on the soil is likely to be highly dependent on the size, shape, heterogeneity of soil particles and pH of the soil solution (Pignatello, 1998). Comparatively lower amounts of PO_4^{3-} could be adsorbed to the microplastics due to the non-polar nature of microplastics. In contrast to our findings, Chen *et al.* (2021) demonstrated that the sorption of triclosan on soil was lower than on the polystyrene (PS) microplastics. Lower electronegativity together with strong hydrophobicity of the PS (Rodrigues *et al.*, 2019) determined the higher adsorption of the triclosan on the PS compared to

the soil used in Chen's study (2021). Chen *et al.* (2021) observed higher adsorption on the microplastics compared to the soil which was possibly resulting from the π - π interaction (Li *et al.*, 2018) and the increased distance between the polymer chains in PS (Alimi *et al.*, 2018). The triclosan could be sorbed in between the polymer chains. The affinity of triclosan to the soil is likely to be determined by the physico-chemical properties of soil, particularly the type and volume of the soil pore (Pignatello, 1998; Wu *et al.*, 2009; Li *et al.*, 2019). Since the molecular size of triclosan is about 0.693 nm (Nghiem and Coleman, 2008), the triclosan may block the soil pores and inhibit triclosan from penetrating into the pores, resulting in the decrease in pore-filling fraction. This blockage mechanism could result in a lower sorption on the soil than the microplastics in Chen's study (2021).

Data of S1 were best described by Langmuir isotherm (Figure 3.5, Table 3.4) suggesting a strong covalent bond between the phosphate and soil, and the adsorption consisted entirely of a monolayer at the surface (Debicka *et al.*, 2016; Han *et al.*, 2018). Data of S2 (Figure 3.4, Figure 3.5, Table 3.3, Table 3.4) were best fitted to all three (linear, Langmuir and Freundlich) isotherms and thus any isotherm could be used to describe the phosphate adsorption characteristics of the S2. Both Langmuir and Freundlich isotherms indicated chemisorption which could imply that the reactions between adsorbate (phosphate) and adsorbent (soil) are highly specific as well as anions and cations compete for the adsorption sites (Sparks, 2003). Comparatively higher level of phosphate adsorption exhibited by S2 (Figure 3.4, Figure 3.5, Table 3.3, Table 3.4) was most likely due to its higher organic matter content relative to the S1. Similar findings were found by Yang *et al.* (2019) who observed that organic matter significantly increased maximum phosphate adsorption capacity in soil although this effect was governed by soil pH, soil texture and type of organic matter. Some authors suggested that organic matter increases phosphate adsorption by increasing the binding energy of the adsorbed phosphate (Kreller *et al.*, 2003; Guppy *et al.*, 2005) which was also observed in our study (Table 3.4). Humic acid is the main phosphate adsorption sites in soil organic matter containing various functional groups with different charges (Lin *et al.*, 2017). Humic acid interacts with iron oxides through complexation and/ or chelation increasing directly or indirectly the adsorption of phosphate in soil (Yan *et al.*, 2016; Wang *et al.*, 2015). Higher phosphate adsorption by the S2 was partly supported by our findings in Chapter 5 where we observed that high organic matter soil significantly reduced available P compared to the low organic matter soil. Values of C_{SM} , b , $\log K_f$ and $1/n$ of both the S1 and S2 were close to the values of soils for phosphate reported in the literatures (Table 3.6).

In addition, both the pristine microplastic (PMP) and weathered microplastic (WMP) samples had lower C_{SM} values compared to the values for iron oxides reported in literatures (Table 3.4, Table 3.6). However, values of b , $\log K_f$ and $1/n$ were close to the reported values for iron oxides (Table 3.4, Table 3.6). Iron oxides are strongly adsorptive for phosphate (Ramalho, 1977) and thus we would expect the soil (probably contains 1 % iron oxides) to be far less adsorptive than the iron oxides. Close correlations have been found between a soil's capacity to adsorb phosphate and the content of iron oxides in the soil (Borggard *et al.*, 1990). Several mechanisms are responsible for adsorbing phosphate to the iron oxides: (a) iron oxides can be readily hydrolysed (broken down by reaction with water) to form amorphous oxides which are reported as having high surface area which results in the adsorption of phosphate (Ramalho, 1977), (b) negatively charged functional groups (e.g. carboxyl, phenol) present in the soil can be adsorbed to the iron oxides by cationic bridging (Hinsinger, 2001), (c) phosphate can be adsorbed on to the surfaces of iron oxides through specific adsorption, where these iron oxides are negatively charged (Asomaning, 2020). Specific adsorption is characterised by formation of inner-sphere complexes, where no water molecules are interposed between the phosphate and the iron oxides suggesting that phosphate molecules/ ions are strongly bonded via covalent binding or ligand exchange (Essington, 2003; Sparks, 2003; Sposito, 2008), (d) phosphate is preferentially adsorbed by hydroxyl surface groups in iron oxides. Hydroxylation occurs when Fe ions on mineral surfaces are exposed to the water and complete its coordination with hydroxyl groups (Essington, 2003; Sparks, 2003; Sposito, 2008). It is noteworthy that the adsorption of phosphate on iron oxides is likely to be highly dependent on pH and ionic strength of the solution (Stabnikov *et al.*, 2004; Dzombak and Morel, 1990). In our study, phosphate in the solution could be adsorbed to the functional groups present in microplastics. Based on the values of C_{SM} reported in the literatures (Table 3.6), we would expect that approximately 400 times lower phosphate will be adsorbed to the PMP whereas 110 times lower phosphate for the WMP compared to the iron oxides.

We observed substantially lower adsorptions on the mixture of S1 and PMP than the averages of S1 and PMP samples (Figure 3.4, Figure 3.5, Table 3.3, Table 3.4). Similar phenomenon was happened with the S1 + WMP samples. In addition, our values of phosphate adsorption for the mixture of soil and microplastics (Table 3.4) were far lower than the reported adsorption by iron oxides (Table 3.6). Lower adsorption for the soil and microplastic mixture compared to the soil or iron oxides could be due to the effect of dilution. Since iron oxides are one of the components of soil, soil is less sorptive for phosphate than the iron oxides. Similarly given the relatively low

sorption of phosphate by the microplastics we would expect an equal mass mixture of soil and microplastic to be less sorptive than the soil by itself. Other reasons for the lower adsorption of soil and microplastic mixture than the soil or iron oxides could be due to the changes in pH of the solution and presence of lesser amounts of phosphate adsorbing compounds in soil. We have already demonstrated in our study (Chapter 5) and other studies (Zhang *et al.*, 2020; Zhao *et al.*, 2021; Lozano *et al.*, 2020) that microplastics tended to increase the pH of the soil solution which might impact on phosphate adsorption. Theoretically increasing pH is known to either increase or decrease or to have no effect on phosphate adsorption in soil (Lopez-Hernandez and Burnham, 1974; Cerozi and Fitzsimmon, 2016). Agbenin (1996) reported an increase in phosphate adsorption with increasing pH which was attributed to the retention of Ca^{2+} ions in the soil. At high soil pH, Ca^{2+} ion constitutes the dominant cation in the cation exchange sites that creates positive charges on soil surfaces (Huang and Stumm, 1973) for the adsorption of phosphate anions by electrostatic attraction. Nwoke *et al.* (2003) found that the adsorption of phosphate decreased with increasing soil pH and this was attributed to the increased negative charge on the soil surface causing electrostatic repulsion of the phosphate. We observed increases in phosphate adsorption with increases in pH for all solids (Chapter 4). When the pH of the solution was increased from 2.0 to 12.0, phosphate adsorption was less on the soil + microplastics than on the soil/ microplastic only (Chapter 4). However, it was tricky to differentiate between phosphate adsorption and phosphate precipitation and thus, phosphate removed from the solution might have precipitated rather than adsorbed. Effects of pH on the adsorption of phosphate to different solids used in our study will be discussed in details in the next chapter. Furthermore, since the soil was more adsorptive than the microplastic, adsorption on the mixture of soil and microplastic was expected to be dominated by the soil. Lower adsorption of phosphate on the mixture of soil and microplastic (compared to the average of adsorption of the soil and microplastic) was likely due to the impacts of microplastics on the adsorption sites in the soil. For example, microplastics could release additives, plasticisers, etc. which could compete for the phosphate adsorption sites in the soil. The additives, plasticisers, etc. could change the pH of the soil solution that might impact on the lowering of the adsorption on the soil + microplastic as demonstrated in Chapter 4.

Above data suggest that the microplastics have the tendency to adsorb phosphate and the weathered microplastic (WMP) has the potentiality to increase the adsorption of phosphate. Both the pristine (PMP) and weathered microplastics (WMP) are likely to adsorb less phosphate than

the soil and iron oxides. Competitive adsorption results in lower levels of phosphate adsorption in the mixture of soil and microplastic. Given the far higher adsorption of phosphate to soil than the microplastics, fate and behaviour of phosphate in the soil seems unlikely to be much impacted by the microplastics.

Table 3.6. Studies detailing phosphate adsorption on different types of iron oxides and soil organic matter. Source and concentration of phosphorus are different in each study. Concentration of phosphate is converted to phosphorus. Values of all parameters are converted to one single unit for the convenience of study.

Type of solid	Source of P	Initial concentration of P (mg/ L)	Solid: liquid (g/ L)	Equilibrium time (hours)	C _{SM} (mg/ kg)	b (L/ mg)	log K _f	1/ n	References
S1	KH ₂ PO ₄	0.2 – 200.0	0.006	24	322.58	0.02	4.45	0.59	Author's own data
S2	KH ₂ PO ₄	0.2 – 200.0	0.006	24	507.56	0.06	5.64	0.69	
Ferrihydrite	KH ₂ PO ₄	66.7 – 333.3	0.005	8	66600.00	0.005	3.31	1.12	Ajmal <i>et al.</i> , 2018
Ferrihydrite	KH ₂ PO ₄	1.0 – 250.0	0.002	24	22170.00	0.17	0.88	0.21	Yan <i>et al.</i> , 2016
Goethite	KH ₂ PO ₄	66.7 – 333.3	0.005	8	50500.00	0.007	3.31	1.10	Ajmal <i>et al.</i> , 2018
Goethite	KH ₂ PO ₄	1.0 – 250.0	0.002	24	4670.00	0.13	0.11	0.27	Yan <i>et al.</i> , 2016
Magnetite	KH ₂ PO ₄	66.7 – 333.3	0.005	8	57800	0.0058	3.316	1.29	Ajmal <i>et al.</i> , 2018
Hematite	KH ₂ PO ₄	2.0 - 20.0	0.02	24	---	---	0.21	1.35	Xiao <i>et al.</i> , 2009
Bayoxide	NaH ₂ PO ₄	0.0 – 45.6	0.05	504	37740.00	1.28	1.28	0.17	Lalley <i>et al.</i> , 2016
Iron oxide tailing	KH ₂ PO ₄	0.50 – 50.0	0.02	24	8210	0.44	0.56	0.19	Zeng <i>et al.</i> , 2004
Iron oxide nanoparticle	KH ₂ PO ₄	100 – 2000	0.60	24	5030	25.75	0.60	0.12	Yoon <i>et al.</i> , 2014
Black soil	KH ₂ PO ₄	0.0 – 240.0	0.05	24	847.74	0.03	2.72	0.32	Han <i>et al.</i> , 2018
Sandy soil	KH ₂ PO ₄	0.0 – 36.0	0.60	24	556.45	0.09	6.87	0.35	Debicka <i>et al.</i> , 2016
Silty loam soil	KH ₂ PO ₄	4 – 70	0.03	24	598	0.17	2.20	0.44	Moazed <i>et al.</i> , 2010

*C_{SM} = maximum adsorption capacity (mg/ kg), b = binding constant (L/ mg), log K_f = Freundlich constant, 1/ n = heterogeneity factor, S1 = low organic matter soil, S2 = high organic matter soil.

Table 3.6 (continued). Studies detailing phosphate adsorption on different types of iron oxides and soil organic matter.

Type of solid	Source of P	Initial concentration of P (mg/ L)	Solid: liquid (g/ L)	Equilibrium time (hours)	C _{SM} (mg/ kg)	b (L/ mg)	log K _f	1/ n	References
Weathered soil	KH ₂ PO ₄	0 – 200	0.04	24	1533.5	0.02	2.26	0.38	Guedes <i>et al.</i> , 2016
Peat soil (containing organic matter > 60 %)	KH ₂ PO ₄	0 – 100	0.2	24	2830	0.23	8.26	0.49	Yang <i>et al.</i> , 2022; Yusran, 2010
Organic soil (containing organic matter ~ 20 %)	KH ₂ PO ₄	0 – 70	0.08	24	2298	0.19	7.58	0.86	Litaor <i>et al.</i> , 2003

*C_{SM} = maximum adsorption capacity (mg/ kg), b = binding constant (L/ mg), log K_f = Freundlich constant, 1/ n = heterogeneity factor.

3.4.4. Desorption experiments

We could not find any study in the literature concerned with the desorption of phosphate from the microplastics following the adsorption. Our data indicated that the desorption of phosphate was quite low compared to the phosphate adsorption. Desorption isotherms did not coincide with the adsorption which is known as hysteresis. Low levels of desorption were consistent with the adsorption being more like the specific (adsorbed ions are principally bound by chemical attraction through the formation of inner sphere complexes) than the non-specific (adsorbed ions are principally bound by electrostatic attraction through the formation of outer sphere complexes) adsorption. Hysteresis index (HI) value was greater for the WMP than the PMP (Table 3.5) indicating that the adsorbed phosphate in the WMP showed high persistence and was difficult to release back into the solution. The higher the value of HI, the lower is the reversibility (Ding *et al.*, 2019). Higher HI value for the S2 compared to that of the S1 (Table 3.5) suggested the lower desorption of adsorbed phosphate in the S2 than the S1. For all solid types (microplastics, soils, soil + microplastics) used in our experiment, phosphate adsorption data were well fitted to Freundlich isotherms and Freundlich fits suggest heterogeneous surfaces, which in turn would support hysteresis as suggested by Kan *et al.* (1994). Hingston *et al.* (1974) observed desorption hysteresis of phosphate with iron oxides and they suggested possible causes for this desorption hysteresis. The hysteresis may take place when the adsorption of phosphate changes from a monodentate complex to a binuclear bridging complex. In a monodentate complex, ligands are bound through one donor atom while a binuclear bridging complex contains two donor atoms which are connected by bridging ligands (Hingston *et al.*, 1974). Theoretically binuclear bridging complex is more stable than the monodentate complex since the ligands are bound to the phosphate at more adsorption sites and both atoms present in the binuclear complex need to be removed from the ligand to dissociate (Farzin *et al.*, 2019). Thus, adsorption of phosphate on the iron oxides through binuclear bridging complex results in the desorption hysteresis (Hingston *et al.*, 1974). In addition, desorption hysteresis can either be due to the physical entrapment of phosphate in the inner matrices (composite materials composed of a variety of short or continuous fibres bound together) of the chain structure of HDPE, or strong adsorptive interactions between phosphate and HDPE leading to irreversible binding of phosphate to the HDPE microplastics (Liu *et al.*, 2018; Qi *et al.*, 2014). In our study, both soils desorbed higher percentage of the adsorbed phosphate compared to the microplastics (Figure 3.6). This was consistent with Chen

et al. (2021) who found an order of magnitude higher desorption rate for the soil than the microplastics, however, Chen *et al.* (2021) was not able to explain the mechanism behind the desorption. Lower percentage of triclosan was desorbed from the microplastics than the soils in Chen's study could be due to the specific adsorption of all phosphate to the microplastics, whereas a higher percentage of phosphate was desorbed from the soil because of both specifically and non-specifically adsorbed phosphate. Non-specifically adsorbed phosphate tends to desorb phosphate more readily. Desorption from the weathered microplastic (WMP) was lower compared to the pristine microplastic (PMP) (Figure 3.6) which was possibly due to the charged surface of the WMP.

3.5. Conclusion

Phosphate adsorption and desorption phenomena are key aspects of the behaviour of phosphate that ultimately governs phosphate levels in soil required for the plant growth. In the present study, we examined the adsorption and desorption behaviours of phosphate to microplastics and soils. Our results showed the potential for microplastics to adsorb phosphate and UV weathering increased the adsorption to a greater extent. Both the pristine (PMP) and weathered (WMP) microplastics were likely to adsorb less phosphate than the soils and iron oxides. Comparatively higher phosphate adsorption exhibited by the high organic matter soil (S2) was most likely due to its higher organic matter content relative to the low organic matter soil (S1). Given the far lower adsorption of phosphate to the microplastics compared to the soils and iron oxides, microplastics were less likely to control the fate and behaviour of phosphate in soil. In addition, our data suggested that phosphate desorption was lower compared to the phosphate adsorption, and desorption isotherms do not coincide with the adsorption. The weathered microplastic (WMP) desorbed less than the pristine (PMP) one. Lower desorption was observed in the high organic matter soil (S2) than the low organic matter soil (S1). Both soils desorbed higher percentages of phosphate compared to the microplastics in our study. Although microplastics are less likely to control the fate and behaviour of phosphate, microplastics may have impact on the soil properties and growth of plants. Thus, our study highlights the need for a wide range of nutrients particularly essential nutrients like phosphate that plants require in large concentrations, together with a wider range of plastic feedstocks with potentially different surface chemistries and sorption characteristics, to be investigated (Chapter 5). Further, smaller particles than those investigated here will have a higher surface area to mass ratio which may impact on relative adsorption between soil and microplastics such that the impact of particle size also warrants further investigation (Chapter 6). Phosphate adsorption and desorption processes are highly dependent on pH and ionic strength of the soil solution which were investigated by several researchers. Phosphate adsorption and desorption on microplastic surfaces are likely to be impacted by pH and ionic strength of the soil solution and thus, we will focus on this in the next chapter.

3.6. References

- Ajmal, Z., Muhmood, A., Usman, M., Kizito, S., Lu, J., Dong, R., and Wu, S. (2018). Phosphate removal from aqueous solution using iron oxides: adsorption, desorption and regeneration characteristics. *Journal of Colloid and Interface Science*, 528, 145–155.
- Alimi, O. S., Budarz, J. F., Hernandez, L. M., and Tufenkji, N. (2018). Microplastics and nanoplastics in aquatic environments: aggregation, deposition, and enhanced contaminant transport. *Environmental Science and Technology*, 52, 1704-1724.
- Arai, Y. and Sparks, D. L. (2001). ATR–FTIR spectroscopic investigation on phosphate adsorption mechanisms at the ferrihydrite–water interface. *Journal of Colloid and Interface Science*, 241, 317–326.
- Arai, Y. and Sparks, D. L. (2007). Phosphate reaction dynamics in soils and soil minerals: a multiscale approach. *Advances in Agronomy*, 94, 135-179.
- Asensio, R. C., Moya, M. S. A., de la Roja, J. M., and Gómez, M. (2009). Analytical characterization of polymers used in conservation and restoration by ATR-FTIR spectroscopy. *Analytical and Bioanalytical Chemistry*, 395, 2081–2096.
- Asomaning, S. K. (2020). Processes and factors affecting phosphorus sorption in soils. In: Kyzas, G. and Lazaridis, N. (eds.) *Sorption in 2020s*. Germany: Books on Demand.
- Bai, J., Ye, X., Jia, J., Zhang, G., Zhao, Q., Cui, B., and Liu, X. (2017). Phosphorus sorption-desorption and effects of temperature, pH and salinity on phosphorus sorption in marsh soils from coastal wetlands with different flooding conditions. *Chemosphere*, 188, 677-688.
- Bakir, A., Rowland, S. J., and Thompson, R. C. (2014a). Enhanced desorption of persistent organic pollutants from microplastics under simulated physiological conditions. *Environmental Pollution*, 185, 16-23.

Bakir, A., Rowland, S. J., and Thompson, R. C. (2014b). Transport of persistent organic pollutants by microplastics in estuarine conditions. *Estuarine, Coastal and Shelf Science*, 140, 14-21.

Banihashemi, B. and Droste, R. L. (2014). Sorption–desorption and biosorption of bisphenol A, triclosan, and 17 α -ethinylestradiol to sewage sludge. *Science of the Total Environment*, 487, 813-821.

Barnes, D. K. A., Galgani, F., Thompson, R. C., and Barlaz, M. (2009). Accumulation and fragmentation of plastic debris in global environments. *Philosophical Transactions of the Royal Society of London: Biological Sciences*, 364, 1985-1998.

Barrow, N. J. (1984). Modelling the effects of pH on phosphate adsorption by soils. *Journal of Soil Science*, 35, 283-297.

Behera, S. K., Oh, S., and Park, H. (2010). Sorption of triclosan onto activated carbon, kaolinite and montmorillonite: effects of pH, ionic strength, and humic acid. *Journal of Hazardous Materials*, 179, 684-691.

Bolan, N. S., Syers, J. K., and Tillman, R. W. (1986). Ionic strength effects on surface charge and adsorption of phosphate and sulphate by soils. *Journal of Soil Science*, 37, 379-388.

Borggard, O. K., Jorgensen, S. S., Moberg, J. P., and Raben-Lange, B. (1990). Influence of organic matter on phosphate adsorption by aluminium and iron oxides in sandy soils. *Journal of Soil Science*, 41, 443-449.

Brant, J. A. (2011). *Fullerol clusters*. Boca Raton: Taylor and Francis.

Brennecke, D., Duarte, B., Paiva, F., Caçador, I., and Canning-Clode, J. (2016). Microplastics as vector for heavy metal contamination from the marine environment. *Estuarine, Coastal and Shelf Science*, 178, 189-195.

Briassoulis, D., Hiskakis, M., Scarascia, G., Picuno, P., Delgado, C., and Dejean, C. (2010). Labeling scheme for agricultural plastic wastes in Europe. *Quality Assurance and Safety of Crops and Foods*, 2, 93–104.

Browne, M. A., Crump, P., Niven, S. J., Teuten, E., Tonkin, A., and Galloway, T., and Thompson, R. (2011). Accumulation of microplastic on shorelines worldwide: sources and sinks. *Environmental Science and Technology*, 45, 9175–9179.

Carpentieri, I., Brunella, V., Bracco, P., Paganini, M. C., Del Prever, E. M. B., Luda, M. P., Bonomi, S., and Costa, L. (2011). Post irradiation oxidation of different polyethylenes. *Polymer Degradation and Stability*, 96, 624–629.

Cerozi, B. S. and Fitzsimmons, K. (2016). The effect of pH on phosphorus availability and speciation in an aquaponics nutrient solution. *Bioresource Technology*, 219, 778–781.

Charles, J. and Ramkumaar, G. R. (2009). Qualitative analysis of high density polyethylene using FTIR spectroscopy. *Asian Journal of Chemistry*, 21, 4477-4484.

Chen, X., Gu, X., Bao, L., Ma, S., and Mu, Y. (2021). Comparison of adsorption and desorption of triclosan between microplastics and soil particles. *Chemosphere*, 263, 1-8.

Coates, J. (2000). Interpretation of infrared spectra, a practical approach. In: Meyers, R. A. (ed.) *Encyclopedia of Analytical Chemistry*. Chichester: John Wiley and Sons Limited.

Debicka, M., Kocowicz, A., Weber, J., and Jamroz, E. (2016). Organic matter effects on phosphorus sorption in sandy soils. *Archives of Agronomy and Soil Science*, 62, 840–855.

Decho, A. W. (2000). Microbial biofilms in intertidal systems: an overview. *Continental Shelf Research*, 20, 1257–1273.

Ding, T., Huang, T., Wu, Z., Li, W., Guo, K., and Li, J. (2019). Adsorption–desorption behavior of carbendazim by sewage sludge-derived biochar and its possible mechanism. *The Royal Society of Chemistry*, 9, 35209–35216.

Dzombak, D. A. and Morel, F. M. (1990). *Surface complexation modeling: hydrous ferric oxides*. New York: John Wiley and Sons.

Edmeades, D. C., Wheeler, D. M., and Clinton, O. E. (1985). The chemical composition and ionic strength of soil solutions from New Zealand topsoils. *Australian Journal of Soil Research*, 23, 151 – 165.

Endo, S., Takizawa, R., Okuda, K., Takada, H., Chiba, K., Kanehiro, H., Ogi, H., Yamashita, R., and Date, T. (2005). Concentration of polychlorinated biphenyls (PCBs) in beached resin pellets: variability among individual particles and regional differences, *Marine Pollution Bulletin*, 50, 1103-1114.

Essington, M. E. (2003). *Soil and water chemistry: an integrative approach*. Boca Raton: CRC Press.

Farzin, M., Moeini, K., Mardani, Z., and Krautscheid, H. (2019). Spectral, structural and theoretical study of novel helical and linear structures of PbI₂ and PbBr₂ complexes with a triazine ligand. *Journal of Coordination Chemistry*, 72, 1876-1889.

Fei, W., Kai, M. S., and Xiao, Y. L. (2015). The partition behavior of perfluorooctanesulfonate (PFOS) and perfluorooctanesulfonamide (FOSA) on microplastics, *Chemosphere*, 119, 841-847.

Fu, Q., Negro, E., Chen, G., Law, D. C., Li, C. H., Hicks, R. F., and Raghavachari, K. (2002). Hydrogen adsorption on phosphorus-rich (2 × 1) indium phosphide (001). *Physical Review*, 65, 1-6.

Gardette, M., Perthue, A., Gardette, J. L., Janecska, T., Foldes, E., Pukanszky, B., and Therias, S. (2013). Photo and thermal oxidation of polyethylene: comparison of mechanisms and influence of unsaturated content. *Polymer Degradation and Stability*, 98, 2383–2390.

Gill, R. and Ramsey, M. H. (1997). What a geochemical analysis means. In: Gill, R. (ed.) *Modern analytical geochemistry: an introduction to quantitative chemical analysis techniques for earth, environment and materials scientists*. UK: Longman Geochemistry.

Gimsing, A. L. and Borggaard, O. K. (2001). Effect of KCl and CaCl₂ as background electrolytes on the competitive adsorption of glyphosate and phosphate on goethite. *Clays and Clay Minerals*, 49, 270–275.

Guedesa, R. S., Melob, L. C. A., Vergützc, L., Rodríguez-Vilad, A., Covelod, E. F., and Fernandes, A. R. (2016). Adsorption and desorption kinetics and phosphorus hysteresis in highly weathered soil by stirred flow chamber experiments. *Soil and Tillage Research*, 162, 46–54.

Guppy, C. N., Menzies, N. W., Moody, P. W., and Blamey, F. P. C. (2005). Competitive sorption reactions between phosphorus and organic matter in soil: a review. *Australian Journal of Soil Research*, 43, 189–202.

Han, Y., Byoungkoo, C., and Xiangwei, C. (2018). Adsorption and desorption of phosphorus in biochar-amended black soil as affected by freeze-thaw cycles in Northeast China. *Sustainability*, 10, 1-8.

Helsel, D. R. (2007). Fabricating data: how substituting values for nondetects can ruin results, and what can be done about it. *Chemosphere*, 65, 2434-2439.

Hingston, F. J., Posner, J. P., and Quirk, J. P. (1974). Anion adsorption by goethite and gibbsite: desorption of anions from hydrous oxide surfaces. *Journal of Soil Science*, 25, 16-26.

Hinsinger, P. (2001). Bioavailability of soil inorganic P in the rhizosphere as affected by root-induced chemical changes: a review. *Plant Soil*, 237, 173-195.

Hodson, M. E., Duffus-Hodson, C. A., Clark, A., Prendergast-Miller, M. T., and Thorpe, K. L. (2017). Plastic bag derived-microplastics as a vector for metal exposure in terrestrial invertebrates. *Environmental Science and Technology*, 51, 4714-4721.

Holmes, L. A., Turner, A., and Thompson, R. C. (2012). Adsorption of trace metals to plastic resin pellets in the marine environment. *Environmental Pollution*, 160, 42–48.

Hoogsteen, M. J. J., Lantinga, E. A., Bakker, E. J., and Tittonell, P. A. (2018). An evaluation of the loss-on-ignition method for determining the soil organic matter content of calcareous soils. *Communications in Soil Science and Plant Analysis*, 49, 1541–1552.

Horton, A. A., Walton, A., Spurgeon, D. J., Lahive, E., and Svendsen, C. (2017). Microplastics in freshwater and terrestrial environments: evaluating the current understanding to identify the knowledge gaps and future research priorities. *Science of the Total Environment*, 586, 127–141.

Huang, C. P. and Stumm, W. (1973). Specific adsorption of cations on hydrous Al₂O₃. *Journal of Colloid and Interface Science*, 43, 409-420.

Hüffer, T., Kah, M., Hofmann, T., and Schmidt, T. C. (2013). How redox conditions and irradiation affect sorption of PAHs by dispersed fullerenes (nC60). *Environmental Science and Technology*, 47, 6935-6942.

Hueffer, T. and Hofmann, T. (2016). Sorption of non-polar organic compounds by microsized plastic particles in aqueous solution. *Environmental Pollution*, 214, 194-201.

Hüffer, T., Weniger, A., and Hofmann, T. (2018). Sorption of organic compounds by aged polystyrene microplastic particles. *Environmental Pollution*, 236, 218-225.

ISO (International Organization for Standardization). (2013). ISO 21348 Definitions of solar irradiance spectral categories. *Space Weather*.

Jalali, M. and Peikam, E. N. (2013). Phosphorus sorption-desorption behaviour of riverbed sediments in the Abshineh river, Hamedan, Iran, related to their composition. *Environmental Monitoring and Assessment*, 185, 537-552.

Jambeck, J. R., Geyer, R., and Wilcox, C. (2015). Plastic waste inputs from land into the ocean. *Science*, 347, 769.

Jafvert, C. T. (1990). Sorption of organic acid compounds to sediments: Initial model development. *Environmental Toxicology and Chemistry*, 9, 959–968.

- Kan, A. T., Fu, G., and Tomson, M. B. (1994). Adsorption/ desorption hysteresis in organic pollutant and soil /sediment interaction. *Environmental Science and Technology*, 24, 859-867.
- Kanda, M., Nakajima, T., Hayashi, H., Hashimoto, T., Kanai, S., Nagano, C., Matsushima, Y., Tateishi, Y., Yoshikawa, S., Tsuruoka, Y., Sasamoto, T., and Takano, I. (2015). Multi-residue determination of polar veterinary drugs in livestock and fishery products by liquid chromatography/tandem mass spectrometry. *Journal of AOAC International*, 98, 230-247.
- Kreller, D. I., Gibson, G., Novak, W., Loon, G. W. V., and Horton, J. H. (2003). Competitive adsorption of phosphate and carboxylate with natural organic matter on hydrous iron oxides as investigated by chemical force microscopy. *Colloids and Surfaces*, 212, 249-264.
- Lalley, J., Han, C., Li, X., Dionysiou, D. D., and Nadagouda, M. N. (2016). Phosphate adsorption using modified iron oxide-based sorbents in lake water: Kinetics, equilibrium, and column tests. *Chemical Engineering Journal*, 284, 1386–1396.
- Lebreton, L., Egger, M., and Slat, B. (2019). A global mass budget for positively buoyant macroplastic debris in the ocean. *Scientific Reports*, 9, 1-10.
- Lee, H., Shim, W. J., and Kwon, J. H. (2014). Sorption capacity of plastic debris for hydrophobic organic chemicals. *Science of the Total Environment*, 470–471, 1545–1552.
- Li, C., Moore-Kucera, J., Lee, J., Corbin, A., Brodhagen, M., Miles, C., and Inglis, D. (2014). Effects of biodegradable mulch on soil quality. *Applied Soil Ecology*, 79, 59-69.
- Li, J., Zhang, K., and Zhang, H. (2018). Adsorption of antibiotics on microplastics. *Environmental Pollution*, 237, 460-467.
- Li, F., Fang, X., Zhou, Z., Liao, X., Zou, J., Yuan, B., and Sun, W. (2019). Adsorption of perfluorinated acids onto soils: kinetics, isotherms, and influences of soil properties. *Science of the Total Environment*, 649, 504-514.

Lin, J. H., Pan, Y. J., Liu, C. F., Huang, C. L., Hsieh, C. T., Chen, C. K., Lin, Z. I., and Lou, C. W. (2015). Preparation and compatibility evaluation of polypropylene/high density polyethylene polyblends. *Materials*, 8, 8850–8859.

Lin, J., Zhe, Z., and Zhan, Y. (2017). Effect of humic acid preloading on phosphate adsorption onto zirconium-modified zeolite. *Environmental Science and Pollution Research*, 24, 12195–12211.

Litaor, M. I., Reichmann, O., Belzer, M., Auerswald, K., Nishri, A. and Shenker, M. (2003). Spatial analysis of phosphorus sorption capacity in a semiarid altered wetland. *Journal of Environmental Quality*, 32, 335-343.

Liu, J., Ma, Y. N., Zhu, D. Q., Xia, T. J., Qi, Y., Yao, Y., Guo, X. R., Ji, R., and Chen, W. (2018). Polystyrene nanoplastics - enhanced contaminant transport: role of irreversible adsorption in glassy polymeric domain. *Environmental Science and Technology*, 52, 2677-2685.

Liu, G., Zhu, Z., Yang, Y., Sun, Y., Yu, F., and Ma, J. (2019a). Sorption behavior and mechanism of hydrophilic organic chemicals to virgin and aged microplastics in freshwater and seawater. *Environmental Pollution*, 246, 26-33.

Liu, P., Qian, L., Wang, H., Zhan, X., Lu, K., Gu, C., and Gao, S. (2019b). New insights into the aging behavior of microplastics accelerated by advanced oxidation processes. *Environmental Science and Technology*, 53, 3579-3588.

Lopez-Hernandez, D. and Burnham, C. P. (1974). The effect of pH on phosphate adsorption in soils. *Journal of Soil Science*, 25, 207-216.

Lozano, Y. M., Lehnert, T., Linck, L. T., Lehmann, A., and Rillig, M. C. (2020). Microplastic shape, polymer type and concentration affect soil properties and plant biomass. *Frontiers in Plant Science*, 12, 1-14.

Ma, J., Zhao, J., Zhu, Z., and Li, L., and Yu, F. (2019). Effect of microplastic size on the adsorption behavior and mechanism of triclosan on polyvinyl chloride. *Environmental Pollution*, 254, 1-10.

Machado, A. A. S., Lau, C. W., Kloas, W., Bergmann, J., Bachelier, J. B., Faltin, E., Becker, R., Görlich, A. S. and Rillig, M. C. (2019). Microplastics can change soil properties and affect plant performance. *Environmental Science and Technology*, 53, 6044 – 6052.

MacKay, A. A. and Canterbury, B. (2005). Oxytetracycline sorption to organic matter by metal-bridging. *Journal of Environmental Quality*, 34, 1964–1971.

Maheswari, C. U., Reddy, K. O., Muzenda, E., Shukla, M., and Rajulu, A. V. (2013). A comparative study of modified and unmodified high-density polyethylene/borassus fiber composites. *International Journal of Polymer Analysis and Characterization*, 18, 439-450.

Marc, L. G. (2005). *Organic chemistry*. New York: Oxford University Press.

Martínez-Romo, A., González, R. M., Bernal, J. J. S., Reyes, C. F., and Candelas, I. R. (2015). Effect of ultraviolet radiation in the photo-oxidation of high-density polyethylene and biodegradable polyethylene films. *Journal of Physics*, 582, 12026.

Massos, A. and Turner, A. (2017). Cadmium, lead and bromine in beached microplastics. *Environmental Pollution*, 227, 139–145.

Millero, F. J. (2001). *The Physical Chemistry of Natural Waters*. New York: Wiley-Interscience.

Moazed, H., Hoseini, Y., Naseri, A. A., and Abbasi, F. (2010). Determining phosphorus adsorption isotherm in soil and its relation to soil characteristics. *International Journal of Soil Science*, 5, 131-139.

Muller, A., Becker, R., Dorgerloh, U., Simon, F. G., and Braun, U. (2018). The effect of polymer aging on the uptake of fuel aromatics and ethers by microplastics. *Environmental Pollution*, 240, 639-646.

Nghiem, L. D. and Coleman, P. J. (2008). NF/RO filtration of the hydrophobic ionogenic compound triclosan: transport mechanisms and the influence of membrane fouling. *Separation and Purification Technology*, 62, 709-716.

Nishikida, K. and Coates, J. (2003). Infrared and Raman analysis of polymers. *In: Lobo, H. and Bonilla, J. V. (eds.) Handbook of Plastics Analysis*. New York: Marcel Dekker Inc.

Nizzetto, L., Futter, M., and Langaas, S. (2016a). Are agricultural soils dumps for microplastics of urban origin? *Environmental Science and Technology*, 50, 10777-10779.

Nizzetto, L., Bussi, G., Futter, M. N., Butterfield, D., and Whitehead, P. G. (2016b). A theoretical assessment of microplastic transport in river catchments and their retention by soils and river sediments. *Environmental Science: Processes and Impacts*, 18, 1050-1059.

Noda, I., Dowrey, A. E., Haynes, J. L., and Marcott, C. (2007). Group frequency assignments for major infrared bands observed in common synthetic polymers. *In: Mark, J. E. (ed.) Physical Properties of Polymers Handbook*. New York: Springer Science and Business Media.

Ouakouak, A. K. and Youcef, L. (2016). Phosphates removal by activated carbon, *Sensor Letters*, 14, 1-6.

Pignatello, J. J. (1998). Soil organic matter as a nanoporous sorbent of organic pollutants. *Advances in Colloid and Interface Science*, 75, 445-467.

PlasticsEurope (2008). *The compelling facts about plastics, analysis of plastics production, demand and recovery for 2006 in Europe*. Belgium: PlasticsEurope.

PlasticsEurope (2013). *Plastics – the facts 2013: an analysis of European latest plastics production, demand and waste data*. Belgium: PlasticsEurope.

PlasticsEurope (2017). *Plastics – the facts 2017: an analysis of European plastics production, demand and waste data*. Belgium: PlasticsEurope.

Qi, Z., Hou, L., Zhu, D., Ji, R., and Chen, W. (2014). Enhanced transport of phenanthrene and 1-naphthol by colloidal graphene oxide nanoparticles in saturated soil. *Environmental Science and Technology*, 48, 10136–10144.

Qi, Y. L., Yang, X. M., Pelaez, A. M., Lwanga, E. H., Beriot, N., Gertsen, H., Garbeva, P., and Geissen, V. (2018). Macro- and micro- plastics in soil-plant system: effects of plastic mulch film residues on wheat (*Triticum aestivum*) growth. *Science of the Total Environment*, 645, 1048–1056.

Ramalho, R. S. (1977). *Introduction to wastewater treatment processes*. New York: Academic Press.

Rochman, C. M., Hentschel, B. T., Teh, S. J., and The, S. J. (2014). Longterm sorption of metals is similar among plastic types: implications for plastic debris in aquatic environments. *PLOS One*, 9, 1-9.

Rodrigues, J. P., Duarte, A. C., Santos-Echeandía, J., and Rocha-Santos, T. (2019). Significance of interactions between microplastics and POPs in the marine environment: a critical overview. *Trac Trends in Analytical Chemistry*, 111, 252-260.

Rowell, D. L. (1994). *Soil science: methods and applications*. Essex: Longman Scientific and Technical.

Ruiz-Rosas, R., García-Mateos, F. J., Gutiérrez, M. C., Rodríguez-Mirasol, J., and Cordero, T. (2019). About the role of porosity and surface chemistry of phosphorus-containing activated carbons in the removal of micropollutants. *Frontiers in Materials*, 6, 1-14.

Schneider, C. A., Rasband, W. S., and Eliceiri, K.W. (2012). NIH image to ImageJ: 25 years of image analysis. *Nature Methods*. 9, 671–675.

Schwarz, J., Thiele-Bruhn, S., Eckhardt, K-U., and Schulten, H-R. (2012). Sorption of sulfonamide antibiotics to soil organic sorbents: batch experiments with model compounds and computational chemistry. *ISRN Soil Science*, 10, 1-9.

Singh, B. and Sharma, N. (2008). Mechanistic implications of plastic degradation. *Polymer Degradation and Stability*, 93, 561-584.

Sparks, D. L. (2003). *Environmental Soil Chemistry*. Michigan: Academic Press.

Spohn, M. and Kuzyakov, Y. (2013). Phosphorus mineralization can be driven by microbial need for carbon. *Soil Biology and Biochemistry*, 61, 69–75.

Sposito, G. (1989). *The Chemistry of Soils*. New York: Oxford University Press.

Stabnikov, V. B., Tay, S. T. L., Tay, D. K., and Ivanov, V. N. (2004). Effect of iron hydroxide on phosphate removal during anaerobic digestion of activated sludge. *Applied Biochemistry and Microbiology*, 40, 376-380.

Stumm, W. and Morgan, J. J. (1996). *Aquatic chemistry - chemical equilibria and rates in natural waters*. New York: Wiley.

Talvitie, J., Mikola, A., Setälä, O., Heinonen, M., and Koistinen, A. (2017). How well is microliter purified from wastewater? A detailed study on the stepwise removal of microliter in a tertiary level wastewater treatment plant. *Water Research*, 109, 164–172.

Telmo, O., Ana, F., Kátia, B., Emilene, D., Rodrigo, J., Fátima, B. and Flávio, C. (2011). Degradability of linear polyolefins under natural weathering. *Polymer Degradation and Stability*, 96, 703-707.

Tian, J. R., Zhou, P. J., He, C. Z., Fu, Y., and Song, L. R. (2006). Adsorption characters of phosphorus by floodplain sediments from the lower reaches (River section in Wuhan City) of Hangjiang River. *Wuhan University Journal of Natural Sciences*, 52, 717-722.

Tong, H., Hu, X., Zhong, X., and Jiang, Q. (2021). Adsorption and desorption of triclosan on biodegradable polyhydroxybutyrate microplastics. *Environmental Toxicology and Chemistry*, 40, 72–78.

Turner, A. and Holmes, L. A. (2015). Adsorption of trace metals by microplastic pellets in fresh water. *Environmental Chemistry*, 12, 600-608.

USDA (United States Department of Agriculture). (1951). Soil Survey Manual. Soil Survey Staff, Bureau of Plant Industry, Soils and Agricultural Engineering, United States Department of Agriculture, Washington, US.

Velzeboer, I., Kwadijk, C. J. A. F., and Koelmans, A. A. (2014). Strong sorption of PCBs to nanoplastics, microplastics, carbon nanotubes, and fullerenes. *Environmental Science and Technology*, 48, 4869-4876.

Verleye, G. A., Roeges, N. P., and De Moor, M. O. (2001). Easy Identification of plastics and rubbers. Shropshire: Rapra Technology Limited.

Walsh, J. N. (1997). Inductively coupled plasma-atomic emission spectrometry (ICP-AES). In: Gill, R. (ed.) *Modern analytical geochemistry: an introduction to quantitative chemical analysis techniques for earth, environment and materials scientists*. UK: Longman Geochemistry.

Wang, F., Shih, K. M., and Li, X. Y. (2015). The partition behavior of perfluorooctanesulfonate (PFOS) and perfluorooctanesulfonamide (FOSA) on microplastics. *Chemosphere*, 119, 841-847.

Wang, X., Li, W., Harrington, R., Liu, F., Parise, J. B., Feng, X., and Sparks, D. L. (2013). Effect of ferrihydrite crystallite size on phosphate adsorption reactivity. *Environmental Science and Technology*, 47, 10322–10331.

Weil, R., and Brady, N. C. (2016). *Nature and properties of soils*. London: Pearson New International Edition.

Westall, J. C., Chen, H., Zhang, W., and Brownawell, B. J. (1999). Sorption of linear alkylbenzenesulfonates on sediment materials. *Environmental Science and Technology*, 33, 3110–3118.

Wu, C., Spongberg, A. L., and Witter, J. D. (2009). Adsorption and degradation of triclosan and triclocarban in soils and biosolids-amended soils. *Journal of Agricultural and Food Chemistry*, 57, 4900-4905.

Wypych, G. (2003). *Handbook of Material Weathering*. Amsterdam: Elsevier.

Xiao, H., Gregory, D. F., Robert, V. H., and John, A. S. (2009). The maximum of phosphate adsorption at pH 4.0: why it appears on aluminum oxides but not on iron oxides. *Langmuir*, 25, 4450-4461.

Xu, B., Liu, F., Brookes, P. C., and Xu, J. (2018). Microplastics play a minor role in tetracycline sorption in the presence of dissolved organic matter. *Environmental Pollution*, 240, 87-94.

Yan, J., Jiang, T., Yao, Y., Lu, S., Wang, Q., and Wei, S. (2016). Preliminary investigation of phosphorus adsorption onto two types of iron oxide-organic matter complexes. *Journal of Environmental Sciences*, 42, 152-162.

Yang, W., Xiang, W., Bao, Z., Huang, C., Ma, M., Lu, X., Yao, L., and Wang, Y. (2022). Phosphorus sorption capacity of various iron-organic matter associations in peat soils. *Environmental Science and Pollution Research*, 29, 77580-77592.

Yang, X., Chen, X., and Yang, X. (2019). Effect of organic matter on phosphorus adsorption and desorption in a black soil from Northeast China. *Soil and Tillage Research*, 187, 85-91.

Yusran, F. H. (2010). The relationship between phosphate adsorption and soil organic carbon from organic matter addition. *Journal of Tropical Soils*, 15, 1-10.

Zeng, L., Li, X., and Liu, J. (2004). Adsorptive removal of phosphate from aqueous solutions using iron oxide tailings. *Water Research*, 38, 1318-1326.

Zhang, Z., Luo, X., Fan, Y., and Wu, Q. (2015). Cumulative effects of powders of degraded PE mulching-films on chemical properties of soil. *Environmental Science and Technology*, 38, 115-119.

Zhang, D., E. L. N., Wanli, H., Hongyuan, W., Pablo, G., Hude, Y., Wentao, S., Chongxiao, L., Xingwang, M., Bin, F., Peiyi, Z., Fulin, Z., Shuqin, J., Mingdong, Z., Lianfeng, D., Chang, P., Xuejun, Z., Zhiyu, X., Bin, X., Xiaoxia, L., Shiyou, S., Zhenhua, C., Lihua, J., Yufeng, W., Liang, G., Changlin, K., Yan, Li., Youhua, Ma., Dongfeng, H., Jian, Z., Jianwu, Y., Chaowen, L., Song, Q., Liuqiang, Z., Binghui, H., Deli, C., Huanchun, L., Limei, Z., Qiuliang, L., Shuxia, W., Yitao, Z., Juntong, P., Baojing, G., and Hongbin, L. (2020). Plastic pollution in croplands threatens long-term food security. *Global Change Biology*, 26, 3356–3367.

Zhao, T., Lozano, Y. M., and Rillig, M. C. (2021). Microplastics increase soil pH and decrease microbial activities as a function of microplastic shape, polymer type, and exposure time. *Frontiers in Environmental Science*, 9, 67-74.

Zhou, A. M., Tang, H. X., and Wang, D. S. (2005). Phosphorus adsorption on natural sediments: modeling and effects of pH and sediment composition. *Water Research*, 39, 1245-1254.

Zubris, K. A. V. and Richards, B. K. (2005). Synthetic fibers as an indicator of land application of sludge. *Environmental Pollution*, 2, 201–211.

Zuo, L. Z., Li, H. X., Lin, L., Sun, Y. X., Diao, Z. H., Liu, S., Zhang, Z. Y., and Xu, X. R. (2019). Sorption and desorption of phenanthrene on biodegradable poly (butylene adipate co-terephthalate) microplastics. *Chemosphere*, 215, 25–32.

Chapter 4

Effects of pH and concentration of background electrolyte on phosphate adsorption to the microplastic

4.1. Introduction

Chapter 3 showed that the HDPE microplastic can adsorb phosphate. Previous studies (Rodrigo *et al.*, 2019; Antelo *et al.*, 2005; Antelo *et al.*, 2010; Wang *et al.*, 2009, Gao and Mucci, 2003) reported that the adsorption of phosphate on the iron oxides, aluminium hydroxides, clay minerals and soil organic matter was significantly affected by the pH and concentration of the background electrolyte. This led to the investigations into the effects of pH and concentration of the background electrolyte on the phosphate adsorption to the microplastic surface. The current chapter explores the hypothesis that the phosphate adsorption to the microplastic is increased with the increasing ionic strength of the background electrolyte at the pH values above the point of zero charge (PZC) and the reverse occurs below the PZC. We conducted the present study with different concentrations of NaNO₃ which was a monovalent electrolyte. Theoretically ionic strength is the concentration of ions in a solution, and for the monovalent electrolyte, the ionic strength is equal to the concentration. This suggests that the phosphate adsorption is increased with the increasing concentration of the background electrolyte above the PZC and the adsorption decreases with the increasing concentration of the electrolyte below the PZC.

As far as the author is aware no study until today has studied the effects of pH and concentration of the background electrolyte on phosphate adsorption to the microplastic. Very few researches (Nan *et al.*, 2020; Sun *et al.*, 2022) have been conducted that investigated the effects of pH and concentration of the background electrolyte on the adsorption of other compounds to the microplastics. The findings of these researches are often contradictory. For example, Nan *et al.* (2020) reported that pH did not significantly affect the adsorption of strobilurin fungicides on microplastics while Sun *et al.* (2022) observed that adsorption of norfloxacin antibiotic on microplastics was first increased when the pH increased from 3 to 5 followed by a decrease at

the pH 7. According to Nan *et al.* (2020), an increase in the electrolyte concentration led to an increase in the adsorption of azoxystrobin and picoxystrobin fungicides to the microplastics, whereas no significant impact was found for the adsorption of pyraclostrobin fungicide.

Based on the above-mentioned hypothesis, the present study was conducted with different levels of pH (ranging from 2 to 12) and background matrices of varying concentrations of electrolyte (ranging from 0 to 0.1 M NaNO₃ solution) to determine whether the adsorption of phosphate to the microplastic surface can be impacted by the effects of pH and concentration of the background electrolyte. We used two types of microplastics: pristine and weathered, and two types of soils differing in organic matter content. A set of objectives for the present study is outlined below.

- To determine the phosphate adsorption to the microplastic with changes in the pH;
- To determine the phosphate adsorption to the microplastic with changes in the concentration of the background electrolyte;
- To determine the phosphate adsorption to the microplastic with the combined effects of pH and concentration of the background electrolyte.

4.2. Materials and methodology

4.2.1. Materials

Two types of soils were collected from York, UK with contrasting organic matter contents. Soil with low organic matter content (S1) was collected from an arable field and soil with high organic matter content (S2) was collected from a flower bed. Detailed description of the soils along with the processing and characterisation (USDA, 1951; Rowell, 1994) were reported in Chapter 3.

Commercial grade high-density polyethylene (HDPE) microplastics powder (Model No. SMHD-3006H) was purchased from Qingdao Sunsoar Tech. Co., Ltd. located in Shandong, China. The HDPE was produced using rotational molding technique (Sunsoar Tech, n.d.). The plastic was confirmed to be HDPE (Chapter 3). An UV lamp (Analytikjena PN 90-0019-01, USA) with a wavelength of 185 nm (ozone generating) was used to simulate weathering of HDPE. Detailed description of the procedure was given in Chapter 3.

4.2.2. Determination of point of zero charge (PZC)

The point of zero charge (PZC) of the solids (soil, microplastic, soil + microplastic) was determined according to the mass titration method outlined by Noh and Schwarz (1989). The experiment was conducted at room temperature with 0.1 M KCl as a background electrolyte. The experiment was carried out using an increasing mass of the solids which were added to a known volume of KCl in a centrifuge tube (50 ml) and allowed to equilibrate for about 24 hours to achieve optimal mixing and adsorption of ions onto the solids. A total of nine centrifuge tubes (50 ml) were used and each contained 40 ml of 0.1 M KCl solution. Increasing mass (0.01, 0.05, 0.10, 0.30, 0.50, 0.80, 1.00, 1.50, 2.00 g) of the solids were added to the centrifuge tubes containing 40 ml KCl solution. The centrifuge tubes were shaken using the horizontal shaker (IKA, KS 260 basic, Europe) for 24 hours, centrifuged at 2000 rpm for 10 minutes and filtered through Whatman filter paper (#42). After that the equilibrium pH of each solution was measured by a pH meter (Benchtop, Thermo Orion). We plotted the equilibrium pH versus the amount of the solid added, and we observed that the equilibrium pH was increased with the increasing amount of the solid. Finally we determined the PZC at the inflection point (no change in pH with the addition of solid).

4.2.3. Effects of pH and concentration of background electrolyte on phosphate adsorption

In the present study, we determined the total phosphorus content in our samples using the ICP-OES (Thermo Scientific ICAP 7000 Series, UK). We did not measure the speciation of P. As we measured the content of total P and did not measure its speciation in the following we refer to the adsorption of phosphate assuming that the majority of the P was present as PO_4^{3-} or related, e.g. HPO_4^{2-} ion (Chapter 3). Nonetheless, all concentrations reported are for total P.

Adsorption experiments were conducted using 0.2 to 200.0 mg/ L phosphorus solution with triplicate of all solids and solid-free control treatments (with different ranges of pH and background matrices of varying concentrations of electrolyte) at each concentration. Phosphorus solution was prepared by dissolving analytical grade potassium dihydrogen phosphate (KH_2PO_4) in a background electrolyte of varying concentrations (0 to 0.1 M) of NaNO_3 , to maintain a constant ionic strength in the solution. For the 0 M concentration, deionised water was used instead of NaNO_3 . For the 0.01 and 0.10 M concentrations, 0.01 and 0.10 M NaNO_3 solutions were used. At each concentration of background electrolyte, the pH of the solution was adjusted by adding 0.05 to 0.5 M HNO_3 or NaOH solutions until the pH was close to the desired value ranging from 2 to 12 and then allowed to drift (Liu *et al.*, 2011).

Both the pristine HDPE (PMP) and weathered HDPE (WMP) were washed with the analytical grade n-hexane (95 %) and methanol (99.85 %) for 24 hours each to remove any kind of impurities and then dried at room temperature. After that, 0.2 g HDPE (PMP, WMP) were placed into the screw-cap glass vials (50 ml) and 30 ml of phosphorus solution was added with different ranges of pH and different concentrations of background electrolyte. Aluminium foils were wrapped around the top of the vials before putting the lids on and then the vials were shaken for 24 hours on a flatbed shaker at 180 rpm at the room temperature (Moazed *et al.*, 2010). Control vials containing P solution with different values of pH and different concentrations of background electrolyte, but without the HDPE were also treated the same way. After 24 hours, triplicate sacrificial replicates were filtered through Whatman No. 42 filter paper and the supernatant was analyzed for P content using an Inductively Coupled Plasma Optical Emission Spectrometry (ICP-OES, Thermo Scientific ICAP 7000 Series, UK). Similar adsorption experiments were carried out using 0.2 g soil (S1, S2) and

also a mixture of soil and microplastics (S1 + PMP, S1 + WMP, S2 + PMP, S2 + WMP) in 30 ml of P solution. Regarding the mixture of soil and microplastics, 0.1 g soil and 0.1 g HDPE were mixed in 30 ml of P solution so that the total weight of the solid became 0.2 g.

4.2.4. Quality control and statistical analysis

Detection limits for the analytical instruments used were calculated as the mean plus six times the standard deviation of ten repeated measurements of the blank standard (Walsh, 1997). All data were above the detection limit. Accuracy of calibration was determined by analysis of an in-house certified reference material (CRM). Analytical precision was calculated from the coefficient of variation (CV) determined from the duplicate analysis of 10 % of the samples that were at least 100 times higher than the detection limit and determining the median of the difference between the duplicate measurements expressed as a percentage of their mean value (Gill and Ramsey, 1997). Quality control data for chemical analysis associated with each set of experiments are provided in Table B1. All calculations were done in the same way as outlined in Chapter 3 (Section 3.2.4). Three-way analysis of variance (ANOVA) tests were used to detect the significant differences in partition coefficient (K_d), maximum adsorption capacity (C_{SM}) and Freundlich constant ($\log K_f$) between the solid type (factor 1), pH (factor 2) and concentration of the background electrolyte (factor 3). Further analysis was made with post hoc test to know which solid type, pH and ionic strength groups are different from each other at 5 % level of significance using Tukey's Honestly Significant Difference (HSD) method.

All data were analyzed using IBM SPSS Statistics (version 25) software. Data were tested for normal distribution using the Shapiro-Wilk and Kolmogorov-Smirnov test and equal variance using Levene's mean test. Data were normally distributed for all analyses and thus no data transformation was required.

4.3. Results

4.3.1. Determination of point of zero charge (PZC)

The point of zero charge (PZC) of the pristine microplastic (PMP) was lower than the weathered (WMP) one (Table 4.1). Low organic matter soil (S1) had higher PZC compared to that of the high organic matter soil (S2). 95 % confidence intervals around the mean values of the PZC for the low organic matter soil + pristine microplastics (S1 + PMP) and the low organic matter soil + weathered microplastic (S1 + WMP) were overlapped and thus they were unlikely to be significantly different (Table 4.1). When the high organic matter soil was mixed with the weathered microplastic (S2 + WMP), PZC was comparatively higher than the mixture of soil and pristine microplastic (S2 + PMP).

Table 4.1. Point of zero charge (PZC) of the different solids (n = 2). The PZC was determined following the method in Section 4.2.2. Values of two replications are separated by comma (,).

Solid type	Point of zero charge (PZC)
PMP	6.30, 6.32
WMP	6.77, 6.79
S1	5.25, 5.27
S2	4.51, 4.51
S1 + PMP	4.51, 4.53
S1 + WMP	4.84, 4.84
S2 + PMP	3.44, 3.44
S2 + WMP	3.75, 3.76

*PMP = pristine HDPE, WMP = weathered HDPE, S1 = low organic matter soil, S2 = high organic matter soil, S1 + PMP = mixture of low organic matter soil and pristine HDPE, S1 + WMP = mixture of low organic matter soil and weathered HDPE, S2 + PMP = mixture of high organic matter soil and pristine HDPE, S2 + WMP = mixture of high organic matter soil and weathered HDPE.

4.3.2. Effects of pH and concentration of background electrolyte on partition coefficient

Our data indicated that the soil, microplastic and the mixture of both behaved in a similar pattern regarding the K_d values (Figure 4.1, Table B2). For all solids, K_d values were decreased with the increasing pH and with the reduced concentration of background electrolyte. Three-way ANOVA test indicated that the K_d varied significantly ($p \leq 0.05$) with the solid type, pH and concentration of the background electrolyte. Interactions of these three factors were also significant ($p \leq 0.05$). The weathered microplastic (WMP) had higher K_d than the pristine microplastic (PMP), and the high organic matter soil (S2) had higher K_d compared to the low organic matter soil (S1). There were no significant ($p \geq 0.05$) differences in K_d for the mixture of low organic matter soil and pristine microplastic (S1 + PMP) compared to that of the mixture of low organic matter soil and weathered microplastic (S1 + WMP). Likewise, no significant ($p \geq 0.05$) differences were observed in K_d for the mixture of high organic matter soil and pristine microplastic (S2 + PMP) compared to that of the mixture of high organic matter soil and weathered microplastic (S2 + WMP). Across the pH values K_d was significantly ($p \leq 0.05$) decreased from pH 2 to pH 5, from pH 5 to pH 7, from pH 7 to pH 9, and from pH 9 to pH 12. The solid type and pH showed significant ($p \leq 0.05$) interaction. Across the concentration of background electrolyte K_d was significantly greater in 0.10 M compared to the 0 and 0.01 M concentrations. There was no significant difference between 0 and 0.01 M concentrations. For the weathered microplastic (WMP), there were no significant ($p \geq 0.05$) differences in K_d between pH 5 and 7, and between pH 9 and 12 at the concentrations of 0 and 0.01 M (Figure 4.1b, Table B2). For the high organic matter soils (S2), there was no significant difference between 0.01 and 0.10 M concentrations at pH 7 (Figure 4.1d, Table B2). For the low organic matter soil and pristine microplastic (S1 + PMP), K_d decreased gradually with the increasing pH from 2 to 7 followed by a decrease at pH 12 for the 0 and 0.01 M concentrations (Figure 4.1e, Table B2). Mixture of low organic matter soil and weathered microplastic (S1 + WMP) followed the same trend as the S1 + PMP (Figure 4.1f, Table B2). The solid type and concentration of the background electrolyte showed significant ($p \leq 0.05$) interaction whilst the interaction between the pH and concentration of the background electrolyte was not significant ($p \geq 0.05$).

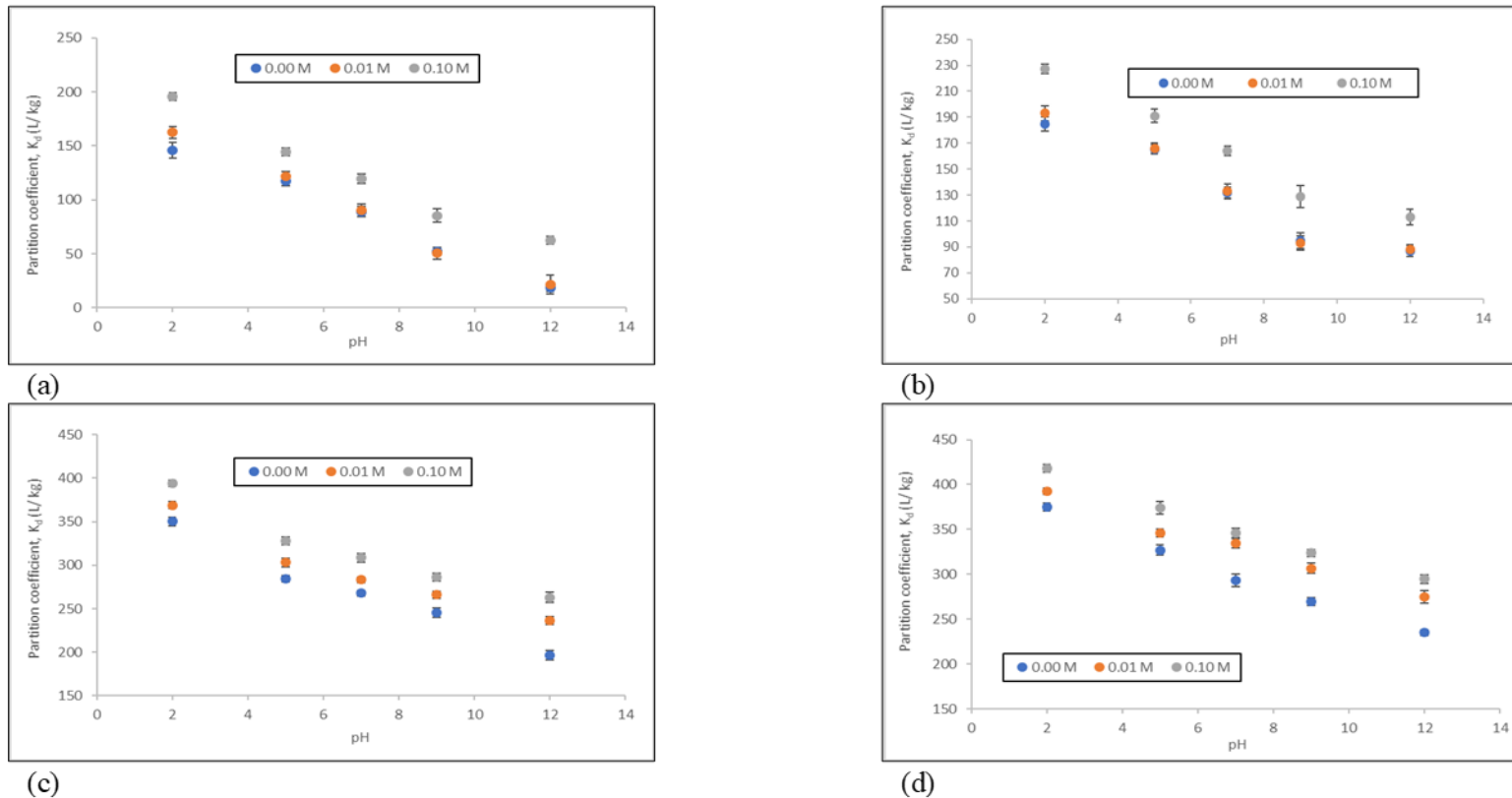
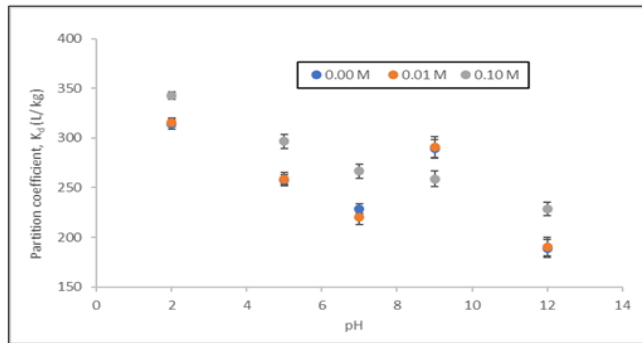
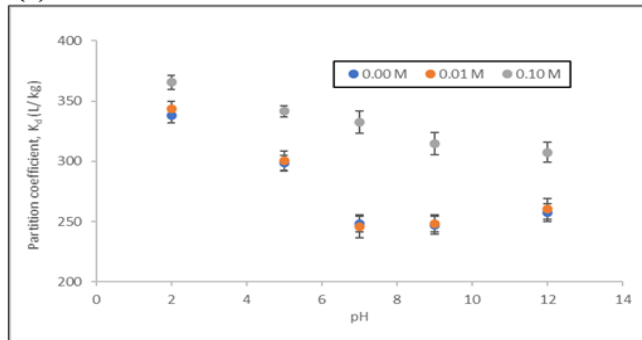


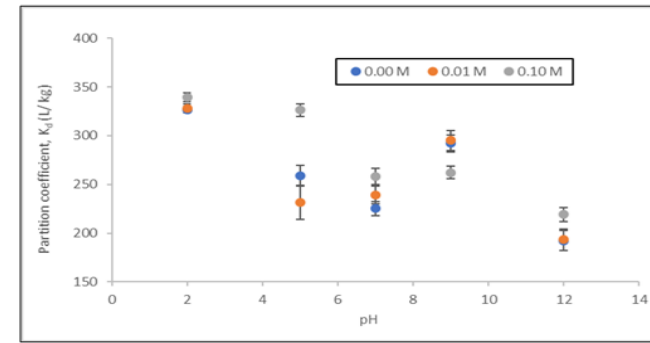
Figure 4.1. Partition coefficient, K_d for different solids: (a) PMP = pristine HDPE, (b) WMP = weathered HDPE, (c) S1 = low organic matter soil and (d) S2 = high organic matter soil for P adsorption at different values of pH and different concentrations of background electrolyte. Mass of solid used is 0.2 g and volume of solution is 30 ml. K_d values are calculated from the slope of linear regression (independent variable: P concentration present in the solution, C_{aq} ; dependent variable: P adsorbed to the solid, C_s). Error bars indicate standard deviations of means with three replicates ($n = 3$ for each set of data). Some data points are overlapping and thus all the replications are not visible. Some error bars are not visible as they are smaller than the symbols in the figure.



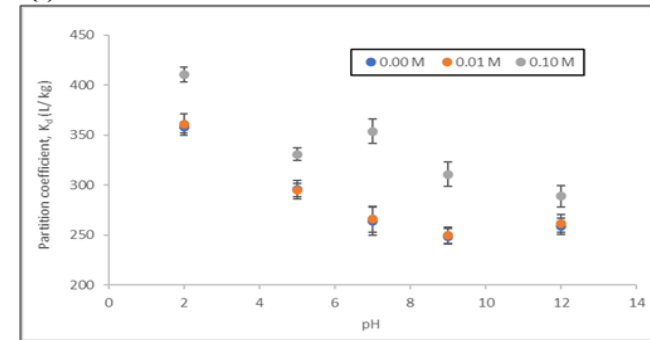
(e)



(g)



(f)



(h)

Figure 4.1. Partition coefficient, K_d for different solids: (e) S1 + PMP = mixture of low organic matter soil and pristine HDPE, (f) S1 + WMP = mixture of low organic matter soil and weathered HDPE, (g) S2 + PMP = mixture of high organic matter soil and pristine HDPE and (h) S2 + WMP = mixture of high organic matter soil and weathered HDPE for P adsorption at different values of pH and different concentrations of background electrolyte. Mass of solid used is 0.2 g and volume of solution is 30 ml. K_d values are calculated from the slope of linear regression (independent variable: P concentration present in the solution, C_{aq} ; dependent variable: P adsorbed to the solid, C_s). Error bars indicate standard deviations of means with three replicates ($n = 3$ for each set of data). Some data points are overlapping and thus all the replications are not visible. Some error bars are not visible as they are smaller than the symbols in the figure.

4.3.3. Effects of pH and concentration of background electrolyte on Langmuir parameters

Although Langmuir isotherms were not good fit for the solids at all ranges of pH and the concentration of the background electrolyte (Table B3), the fits to the Langmuir isotherms were used to determine the maximum adsorption capacities, C_{SM} and binding constants, b (Table B3). All solids followed a general trend in our study indicating that the C_{SM} were decreased with the increasing pH and with the reduced concentration of background electrolyte (Figure 4.2, Table B3). There were significant ($p \leq 0.05$) differences in the C_{SM} values between the solid type, pH and concentration of the background electrolyte. The weathered microplastic (WMP) had higher C_{SM} than the pristine microplastic (PMP). High organic matter soil (S2) had higher C_{SM} compared to the low organic matter soil (S1). There were no significant ($p \geq 0.05$) differences in C_{SM} for the mixture of soil and microplastic which was true for both soil types and both microplastics (S1 + PMP, S1 + WMP, S2 + PMP, S2 + WMP). No significant ($p \geq 0.05$) differences in C_{SM} were associated between the concentration of background electrolyte 0 and 0.01 M. Across the pH values maximum C_{SM} values were found for the pH 2 whilst minimum values for the pH 12. Values of pH were significantly ($p \leq 0.05$) decreased from the pH 2 to 5, from pH 5 to pH 7, from pH 7 to pH 9, and from the pH 9 to pH 12. There were no significant differences in C_{SM} between 0 and 0.01 M concentrations, with the C_{SM} showed maximum value in the 0.10 M concentration than the other two concentrations. We did not observe any significant ($p \geq 0.05$) interaction between the solid type and pH. Non-significant ($p \geq 0.05$) interactions were also found for the solid type and concentration of the background electrolyte, and for the pH and concentration of the background electrolyte. However, significant ($p \leq 0.05$) interaction was observed between the solid type, pH and concentration of the background electrolyte. Although all solids behaved in a similar pattern, mixture of high organic matter soil and weathered microplastic (S2 + WMP) showed a different pattern in C_{SM} with the increasing pH. At the highest concentration (0.10 M) of background electrolyte, C_{SM} were decreased with the increasing pH from 2 to 5 followed by an increase to pH 7 which was then decreased to the pH 9 (4.2h, Table B3).

95 % confidence intervals around the mean values of binding constants (b) for the solids (for each treatment) were overlapped (Table 4.2) and thus they were unlikely to be significantly different. Thus, we did not perform three-way ANOVA test for the binding constants and not plotted here.

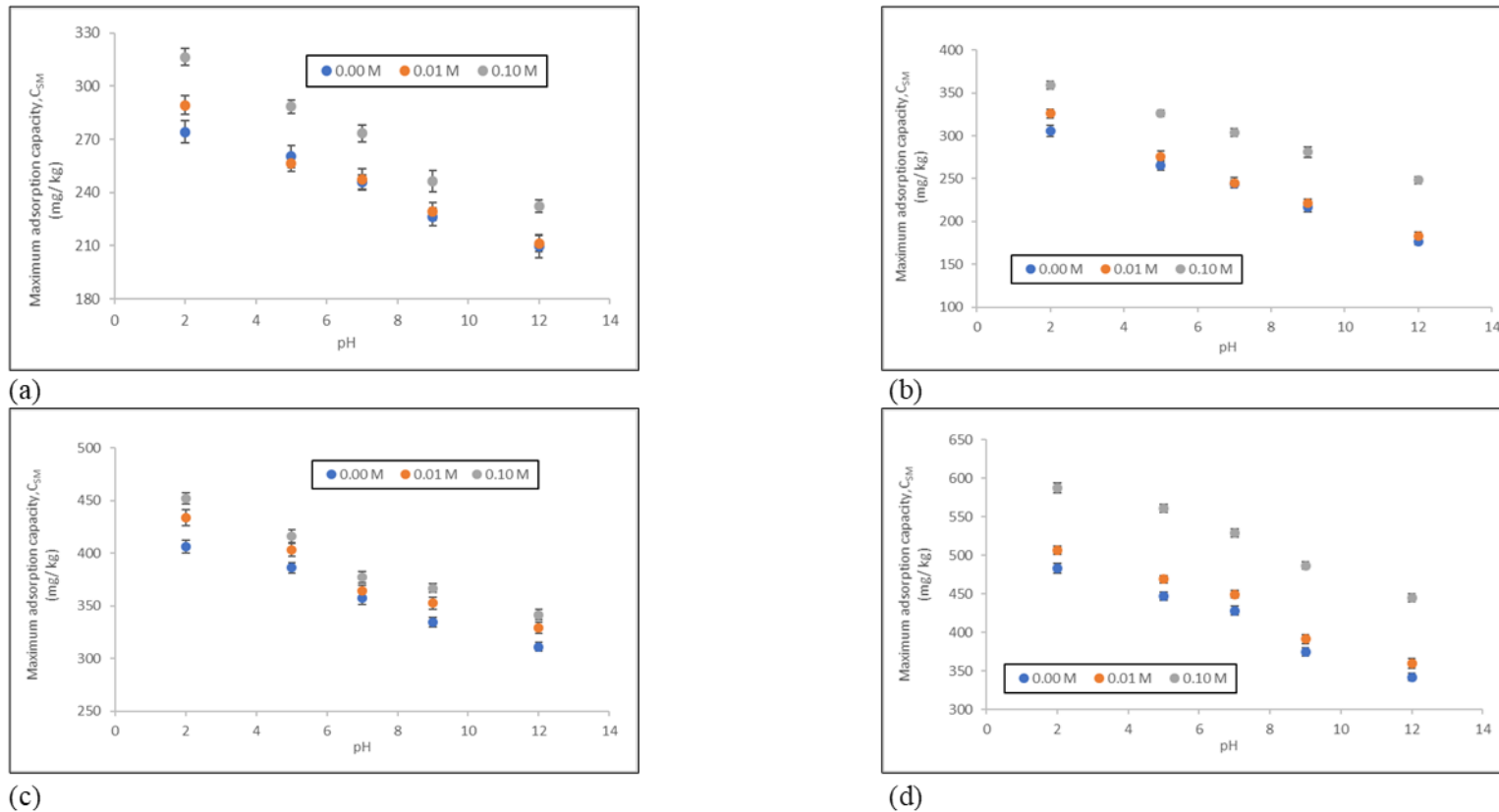
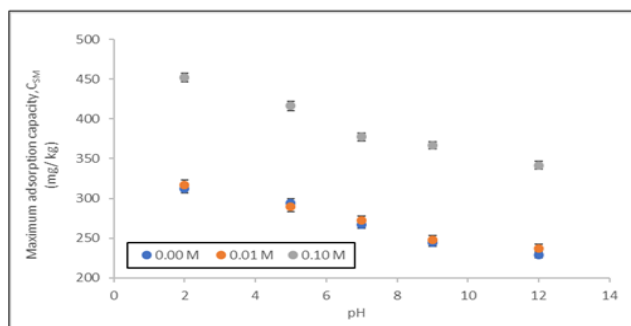
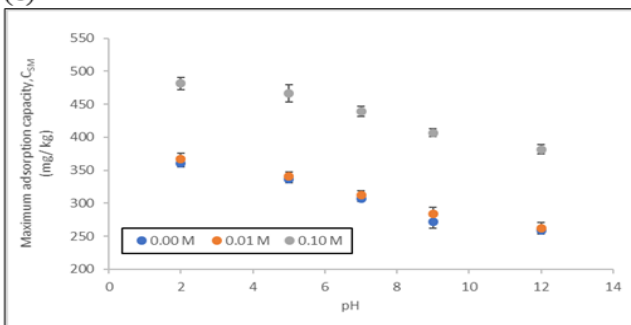


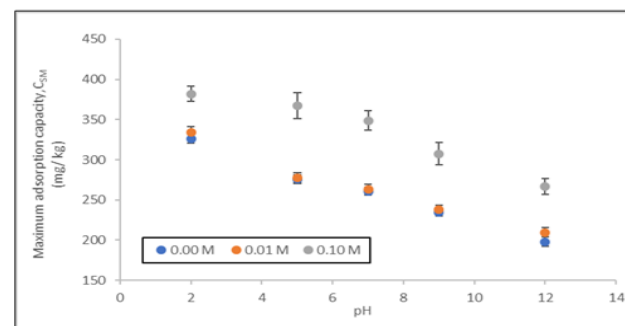
Figure 4.2. Maximum adsorption capacity, C_{SM} for different solids: (a) PMP = pristine HDPE, (b) WMP = weathered HDPE, (c) S1 = low organic matter soil and (d) S2 = high organic matter soil for P adsorption at different values of pH and different concentrations of background electrolyte. Mass of solid used is 0.2 g and volume of solution is 30 ml. C_{SM} values are calculated from the intercept ($1/C_{SM}$) of linear regression (independent variable: inverse of P concentration present in the solution, $1/C_{aq}$; dependent variable: inverse of P adsorbed to the solid, $1/C_s$). Error bars indicate standard deviations of means with three replicates ($n = 3$ for each set of data). Some data points are overlapping and thus all the replications are not visible. Some error bars are not visible as they are smaller than the symbols in the figure.



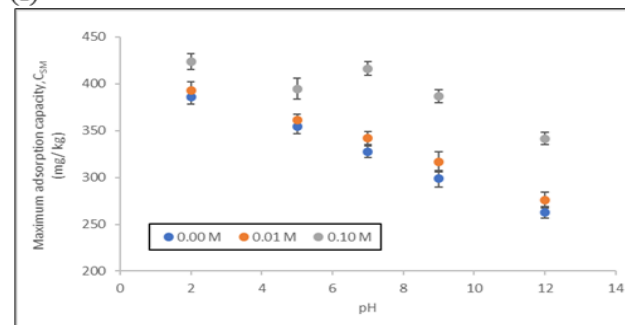
(e)



(g)



(f)



(h)

Figure 4.2. Maximum adsorption capacity, C_{SM} for different solids: (e) S1 + PMP = mixture of low organic matter soil and pristine HDPE, (f) S1 + WMP = mixture of low organic matter soil and weathered HDPE, (g) S2 + PMP = mixture of high organic matter soil and pristine HDPE and (h) S2 + WMP = mixture of high organic matter soil and weathered HDPE for P adsorption at different values of pH and different concentrations of background electrolyte. Mass of solid used is 0.2 g and volume of solution is 30 ml. C_{SM} values are calculated from the intercept ($1/C_{SM}$) of linear regression (independent variable: inverse of P concentration present in the solution, $1/C_{aq}$; dependent variable: inverse of P adsorbed to the solid, $1/C_s$). Error bars indicate standard deviations of means with three replicates ($n = 3$ for each set of data). Some data points are overlapping and thus all the replications are not visible. Some error bars are not visible as they are smaller than the symbols in the figure.

Table 4.2. Binding constants (L/ mg) for phosphorus adsorption at different values of pH (2 to 12) and different concentrations of background electrolyte (0 to 0.10 M NaNO₃). Mass of solid used is 0.2 g. Volume of solution is 30 ml. Binding constant (b) is determined from the slope (1/ bC_{SM}) of linear regression where C_{SM} = maximum adsorption capacity (mg/ kg). For the linear regression, 1/ C_{aq} (inverse of phosphorus concentration present in the solution) is the independent and 1/ C_s (inverse of phosphorus adsorbed to the solid) is the dependent variables. 95 % confidence intervals are calculated which are shown in brackets. Upper and lower limit of confidence intervals are separated by comma (,).

Values of pH and concentration of NaNO ₃	Solid types							
	PMP	WMP	S1	S2	S1+PMP	S1+WMP	S2+PMP	S2+WMP
pH 2, conc. 0.00 M	0.09 (0.05, 0.12)	0.12 (0.80, 1.02)	0.47 (0.22, 0.57)	0.82 (0.55, 0.97)	0.64 (0.32, 1.07)	0.79 (0.52, 1.11)	0.65 (0.33, 1.09)	0.81 (0.53, 1.12)
pH 5, conc. 0.00 M	0.09 (0.07, 0.11)	0.07 (0.04, 1.16)	0.49 (0.24, 0.61)	0.48 (0.20, 0.56)	0.49 (0.23, 0.58)	0.84 (0.54, 0.98)	0.49 (0.21, 0.59)	0.86 (0.58, 0.99)
pH 7, conc. 0.00 M	1.36 (1.05, 1.52)	1.29 (1.05, 1.42)	0.56 (0.29, 0.74)	0.61 (0.46, 0.86)	0.81 (0.57, 1.34)	0.83 (0.59, 1.36)	0.84 (0.61, 1.38)	0.82 (0.58, 1.35)
pH 9, conc. 0.00 M	1.46 (1.15, 1.72)	1.26 (1.04, 1.49)	0.89 (0.54, 1.09)	0.86 (0.61, 1.16)	0.64 (0.32, 1.07)	0.79 (0.52, 1.11)	0.65 (0.33, 1.09)	0.81 (0.53, 1.12)
pH 12, conc. 0.00 M	1.48 (1.21, 1.76)	1.36 (1.14, 1.56)	0.88 (0.55, 1.07)	0.87 (0.62, 1.18)	0.49 (0.23, 0.58)	0.84 (0.64, 0.98)	0.49 (0.21, 0.59)	0.86 (0.51, 0.99)
pH 2, conc. 0.01 M	0.08 (0.03, 1.16)	1.66 (1.12, 1.89)	0.64 (0.21, 0.96)	0.75 (0.31, 1.08)	0.68 (0.33, 1.16)	0.64 (0.38, 1.21)	0.79 (0.31, 1.26)	0.81 (0.41, 1.31)
pH 5, conc. 0.01 M	0.8 (0.05, 0.19)	1.79 (1.44, 2.01)	0.68 (0.35, 1.09)	0.86 (0.44, 1.25)	0.73 (0.43, 1.19)	0.74 (0.49, 1.21)	0.87 (0.51, 1.49)	0.88 (0.54, 1.42)
pH 7, conc. 0.01 M	1.09 (0.50, 1.12)	1.59 (1.25, 1.82)	0.67 (0.36, 1.11)	0.88 (0.46, 1.23)	0.49 (0.23, 0.68)	0.84 (0.64, 0.98)	0.49 (0.21, 0.59)	0.86 (0.51, 0.99)

Table 4.2 (continued). Binding constants (L/ mg) for phosphorus adsorption at different values of pH (2 to 12) and different concentrations of background electrolyte (0 to 0.10 M NaNO₃).

Values of pH and concentration of NaNO ₃	Solid types							
	PMP	WMP	S1	S2	S1+PMP	S1+WMP	S2+PMP	S2+WMP
pH 9, conc. 0.01 M	1.36 (1.09, 1.56)	1.09 (0.8, 1.14)	0.84 (0.46, 1.23)	0.85 (0.48, 1.28)	1.04 (0.79, 1.54)	1.14 (0.84, 1.68)	1.19 (0.81, 1.62)	1.21 (0.81, 1.48)
pH 12, conc. 0.01 M	1.29 (0.80, 1.46)	1.57 (1.24, 1.72)	0.74 (0.36, 1.41)	0.88 (0.46, 1.39)	1.24 (0.86, 1.64)	1.16 (0.87, 1.63)	1.22 (0.83, 1.64)	1.19 (0.79, 1.49)
pH 2, conc. 0.10 M	0.70 (0.30, 1.05)	1.36 (1.04, 1.72)	0.76 (0.38, 1.46)	0.78 (0.41, 1.49)	1.25 (0.87, 1.63)	1.04 (0.79, 1.54)	1.14 (0.84, 1.68)	1.19 (0.79, 1.49)
pH 5, conc. 0.10 M	1.59 (1.25, 1.84)	1.38 (1.12, 1.75)	0.91 (0.68, 1.26)	0.89 (0.61, 1.32)	1.24 (0.92, 1.74)	1.25 (0.94, 1.79)	1.32 (1.01, 1.82)	1.21 (0.81, 1.48)
pH 7, conc. 0.10 M	1.61 (1.47, 1.82)	1.41 (1.19, 1.82)	1.29 (0.90, 1.42)	1.46 (1.09, 1.82)	1.25 (0.87, 1.63)	1.04 (0.79, 1.54)	1.14 (0.84, 1.68)	1.19 (0.79, 1.49)
pH 9, conc. 0.10 M	1.59 (1.35, 1.78)	1.59 (1.24, 1.86)	1.28 (1.02, 1.46)	1.26 (1.09, 1.87)	1.04 (0.79, 1.54)	1.14 (0.84, 1.68)	1.19 (0.81, 1.62)	1.21 (0.81, 1.48)
pH 12, conc. 0.10 M	1.29 (0.90, 1.32)	1.54 (1.27, 1.92)	1.49 (1.12, 1.78)	1.52 (1.23, 1.84)	1.05 (0.77, 1.52)	1.17 (0.83, 1.68)	1.18 (0.81, 1.64)	1.22 (0.83, 1.46)

*PMP = Pristine microplastic, WMP = weathered microplastic, S1 = low organic matter soil, S2 = high organic matter soil, S1 + PMP = low organic matter soil + pristine microplastic, S1 + WMP = low organic matter soil + weathered microplastic, S2 + PMP = high organic matter soil + pristine microplastic, S2 + WMP = high organic matter soil + weathered microplastic. Langmuir equation is expressed as $\frac{C_s}{C_{aq}} = \frac{bC_{SM}}{1 + C_{aq}b}$, where, C_s = amount of P adsorbed on solid (mg/ kg), C_{aq} = concentration of P in equilibrium solution (mg/ L), C_{SM} = maximum adsorption capacity (mg/ kg), b = binding constant (L/ mg).

4.3.4. Effects of pH and concentration of background electrolyte on Freundlich parameters

Freundlich parameters were good fits for the solids for different ranges of pH and different concentrations of the background electrolyte (Table B4). There were significant ($p \leq 0.05$) differences in the $\log K_f$ values between the solid type, pH and concentration of the background electrolyte. The interactions of these three factors were also significant ($p \leq 0.05$). The weathered microplastic (WMP) had higher $\log K_f$ compared to the pristine microplastic (PMP). High organic matter soil (S2) had higher $\log K_f$ compared to the low organic matter soil (S1). There were no significant ($p \geq 0.05$) differences in $\log K_f$ for the mixture of soil and microplastic. This trend was followed by both soil types and microplastics (S1 + PMP, S1 + WMP, S2 + PMP, S2 + WMP). Across the pH values $\log K_f$ was significantly ($p \leq 0.05$) decreased from pH 2 to pH 5, from 5 to pH 7, and from the pH 7 to pH 9. There were no significant ($p \geq 0.05$) differences between the pH 9 and pH 12. Across the concentration of background electrolyte there were no significant ($p \geq 0.05$) differences in $\log K_f$ between the 0 and 0.01 M. Significant ($p \leq 0.05$) interactions were found between the solid type and pH whilst the interactions between the solid type and concentration of the background electrolyte was not significant. Interactions between the pH and concentration of the background electrolyte were not significant ($p \geq 0.05$). The microplastic, soil and mixture of both showed different trends regarding the $\log K_f$. The $\log K_f$ values for the PMP and the WMP increased with the increasing pH and with the increased concentration of the background electrolyte (Figure 4.3a, 4.3b, Table B4). The 0.10 M concentration showed higher $\log K_f$ for the PMP and WMP compared to the 0 and 0.01 M concentrations at all values of pH ranging from 2 to 12. The $\log K_f$ values for both soils (S1, S2) decreased with the increasing pH and with the increasing concentration of the background electrolyte (Figure 4.3b, 4.3c, Table B4). The $\log K_f$ for the mixture of low organic matter soil and pristine microplastic (S1 + PMP) followed the same trend as the soils (Figure 4.3e, Table B4). The $\log K_f$ for the mixture of low organic matter soil and weathered microplastic (S1 + WMP) showed similar trends as the S1 + PMP with the increasing pH. However, the S1 + WMP showed different trend for the $\log K_f$ with the increasing concentration of the background electrolyte indicating that the $\log K_f$ were decreased with the increasing concentration of the electrolyte (Figure 4.3f, Table B4). The mixture of high organic matter soil and microplastic (S2 + PMP, S2 + WMP) followed the same trend as the S1 + PMP (Figure 4.3g, 4.3h, Table B4).

95 % confidence intervals around the mean values of the heterogeneity factor ($1/n$) for all solids (for each treatment) were overlapped (Table 4.3) and thus they were unlikely to be significantly different. Thus, we did not perform three-way ANOVA test for the heterogeneity factors and not plotted here.

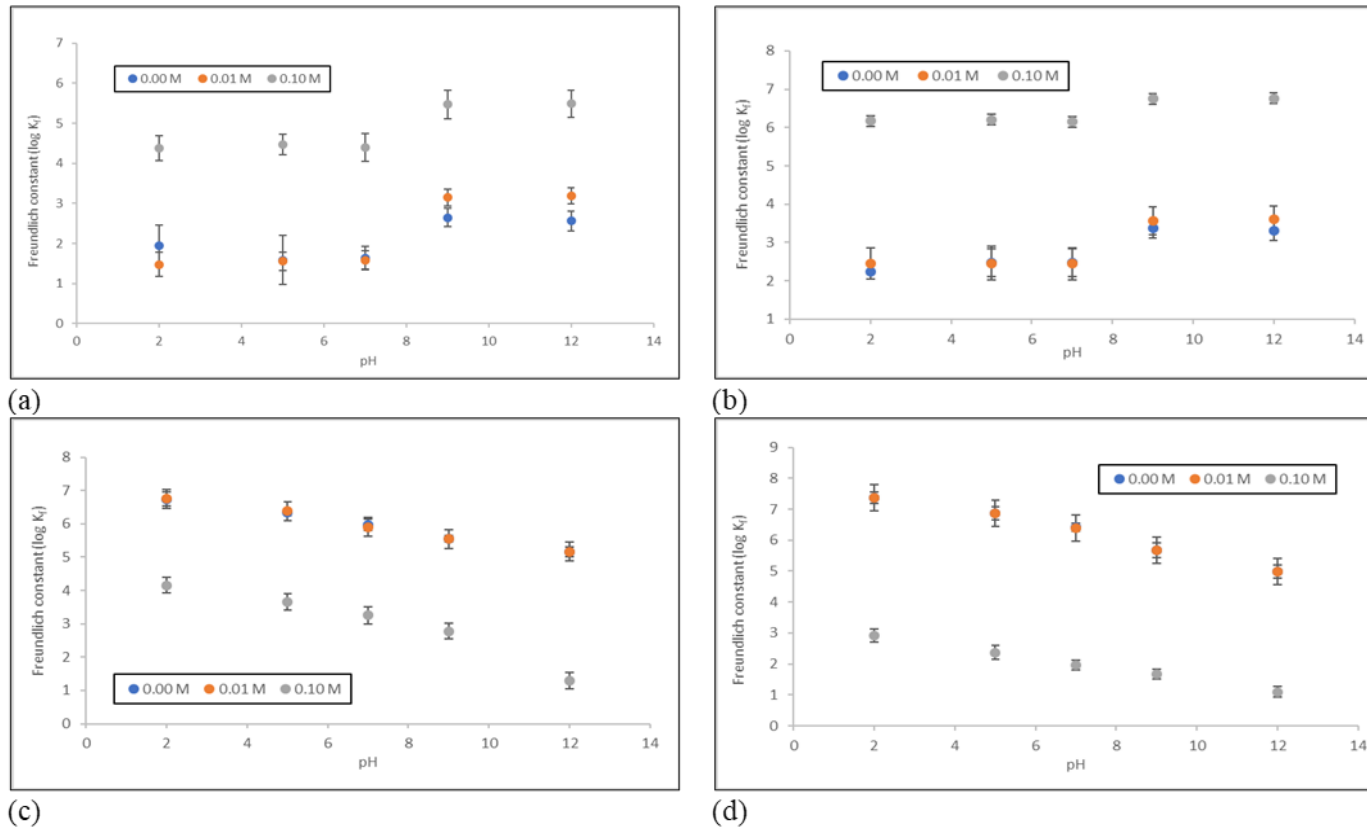


Figure 4.3. Freundlich constant, $\log K_f$ for different solids: (a) PMP = pristine HDPE, (b) WMP = weathered HDPE, (c) S1 = low organic matter soil and (d) S2 = high organic matter soil for P adsorption at different values of pH and different concentrations of background electrolyte. Mass of solid used is 0.2 g and volume of solution is 30 ml. $\log K_f$ is determined from the intercept of linear regression (independent variable: \log value of P concentration present in the solution, $\log C_{aq}$; dependent variable: \log value of P adsorbed to the solid, $\log C_s$). Error bars indicate standard deviations of means with three replicates ($n = 3$ for each set of data). Some data points are overlapping and thus all the concentrations of background electrolyte are not visible. Some error bars are not visible as they are smaller than the symbols in the figure.

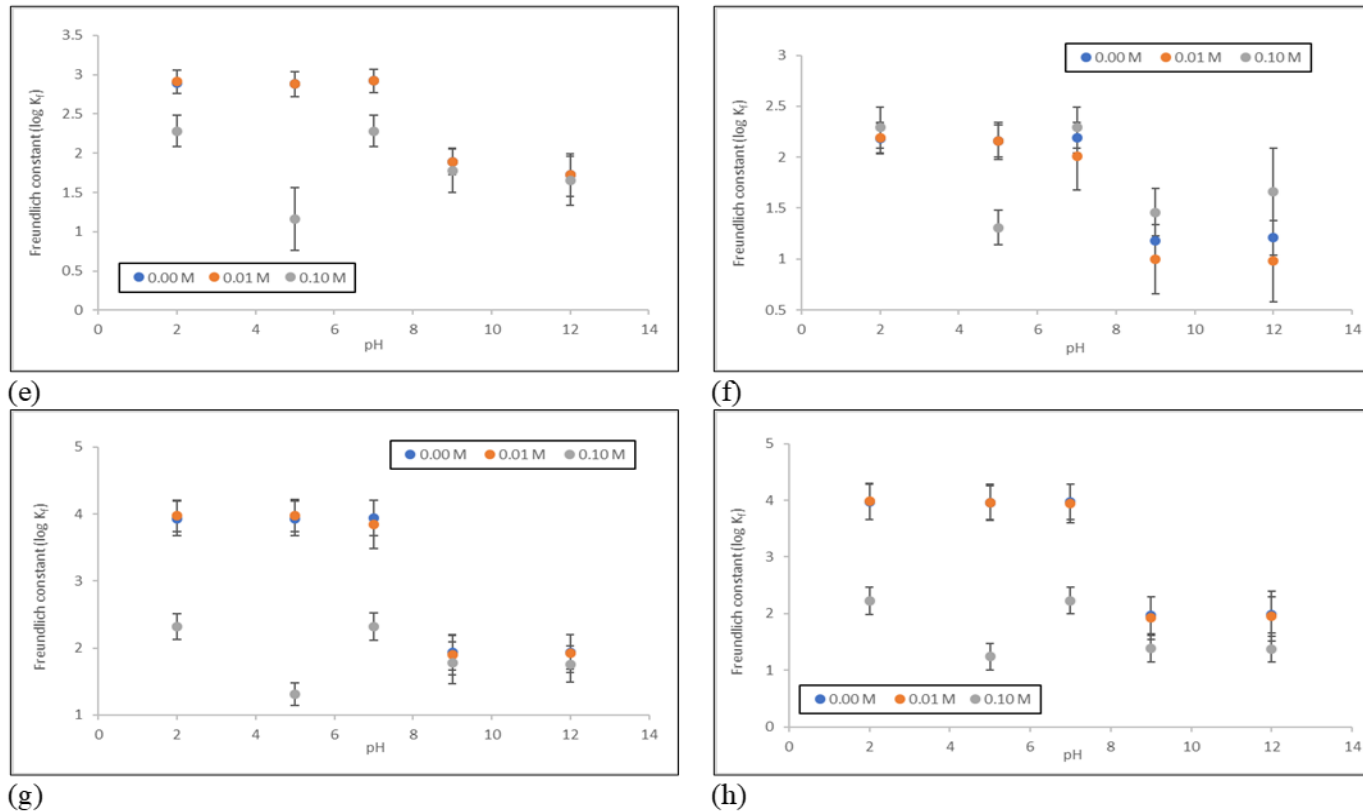


Figure 4.3. Freundlich constant, $\log K_f$ for different solids: (e) S1 + PMP = mixture of low organic matter soil and pristine HDPE, (f) S1 + WMP = mixture of low organic matter soil and weathered HDPE, (g) S2 + PMP = mixture of high organic matter soil and pristine HDPE and (h) S2 + WMP = mixture of high organic matter soil and weathered HDPE for P adsorption at different values of pH and different concentrations of background electrolyte. Mass of solid used is 0.2 g and volume of solution is 30 ml. $\log K_f$ is determined from the intercept of linear regression (independent variable: \log value of P concentration present in the solution, $\log C_{aq}$; dependent variable: \log value of P adsorbed to the solid, $\log C_s$). Error bars indicate standard deviations of means with three replicates ($n = 3$ for each set of data). Some data points are overlapping and thus all the concentrations of background electrolyte are not visible. Some error bars are not visible as they are smaller than the symbols in the figure.

Table 4.3. Heterogeneity factors ($1/n$) for phosphorus adsorption at different values of pH (2 to 12) and different concentrations of background electrolyte (0 to 0.10 M NaNO_3). Mass of solid used is 0.2 g. Volume of solution is 30 ml. $1/n$ is determined from the slope of linear regression (independent variable: log value of P concentration present in the solution, $\log C_{\text{aq}}$; dependent variable: log value of P adsorbed to the solid, $\log C_s$). 95 % confidence intervals are calculated which are shown in brackets. Upper and lower limit of confidence intervals are separated by comma (,).

Values of pH and concentration of NaNO_3	Solid types							
	PMP	WMP	S1	S2	S1+PMP	S1+WMP	S2+PMP	S2+WMP
pH 2, conc. 0.00 M	0.68 (0.54, 0.82)	0.64 (0.51, 0.79)	0.81 (0.75, 0.91)	0.89 (0.62, 1.06)	0.70 (0.52, 0.91)	0.78 (0.53, 0.97)	0.79 (0.61, 0.93)	0.75 (0.67, 0.96)
pH 5, conc. 0.00 M	0.84 (0.65, 1.15)	0.85 (0.72, 1.23)	0.83 (0.66, 0.99)	0.86 (0.55, 0.91)	0.72 (0.54, 0.94)	0.78 (0.53, 0.97)	0.81 (0.79, 0.95)	0.73 (0.65, 0.94)
pH 7, conc. 0.00 M	0.75 (0.46, 0.97)	0.67 (0.49, 0.93)	0.72 (0.45, 0.95)	0.71 (0.52, 0.90)	0.77 (0.56, 0.96)	0.70 (0.53, 0.94)	0.74 (0.46, 0.98)	0.70 (0.55, 0.95)
pH 9, conc. 0.00 M	0.77 (0.61, 0.84)	0.84 (0.76, 1.14)	0.75 (0.56, 0.95)	0.93 (0.79, 1.13)	0.69 (0.48, 0.86)	0.87 (0.73, 1.11)	0.79 (0.58, 0.83)	0.87 (0.72, 1.13)
pH 12, conc. 0.00 M	0.73 (0.64, 0.89)	0.74 (0.59, 1.03)	0.86 (0.67, 1.14)	0.85 (0.56, 1.21)	0.78 (0.63, 0.91)	0.83 (0.65, 1.16)	0.94 (0.76, 1.04)	0.95 (0.77, 1.18)
pH 2, conc. 0.01 M	0.64 (0.51, 0.79)	0.68 (0.54, 0.82)	0.89 (0.62, 1.06)	0.81 (0.75, 0.91)	0.79 (0.61, 0.93)	0.70 (0.52, 0.91)	0.78 (0.53, 0.97)	0.75 (0.67, 0.96)
pH 5, conc. 0.01 M	0.74 (0.59, 1.03)	0.73 (0.64, 0.89)	0.85 (0.56, 1.21)	0.86 (0.67, 1.14)	0.83 (0.65, 1.16)	0.94 (0.76, 1.04)	0.78 (0.63, 0.91)	0.83 (0.65, 1.16)
pH 7, conc. 0.01 M	0.68 (0.54, 0.82)	0.64 (0.51, 0.79)	0.61 (0.50, 0.71)	0.59 (0.42, 0.76)	0.70 (0.52, 0.91)	0.58 (0.43, 0.67)	0.79 (0.61, 0.94)	0.85 (0.67, 1.00)

Table 4.3 (continued). Heterogeneity factors ($1/n$) for phosphorus adsorption at different values of pH (2 to 12) and different concentrations of background electrolyte (0 to 0.10 M NaNO_3).

Values of pH and concentration of NaNO_3	Solid types							
	PMP	WMP	S1	S2	S1+PMP	S1+WMP	S2+PMP	S2+WMP
pH 9, conc. 0.01 M	0.68 (0.54, 0.82)	0.64 (0.51, 0.79)	0.81 (0.75, 0.91)	0.89 (0.62, 1.06)	0.70 (0.52, 0.91)	0.78 (0.53, 0.97)	0.79 (0.61, 0.93)	0.75 (0.67, 0.96)
pH 12, conc. 0.01 M	0.63 (0.51, 0.80)	0.66 (0.54, 0.82)	0.91 (0.76, 1.31)	0.93 (0.69, 1.39)	0.73 (0.54, 0.93)	0.76 (0.51, 0.96)	0.78 (0.62, 0.91)	0.74 (0.65, 0.93)
pH 2, conc. 0.10 M	0.79 (0.54, 1.32)	0.74 (0.51, 1.39)	0.83 (0.50, 1.41)	0.89 (0.52, 1.56)	0.67 (0.42, 0.81)	0.68 (0.43, 0.87)	0.79 (0.61, 0.94)	0.75 (0.67, 1.00)
pH 5, conc. 0.10 M	0.82 (0.55, 1.39)	0.84 (0.55, 1.43)	0.92 (0.65, 1.51)	0.94 (0.72, 1.66)	0.73 (0.55, 0.93)	0.57 (0.44, 0.68)	0.69 (0.41, 0.84)	0.65 (0.47, 0.89)
pH 7, conc. 0.10 M	0.76 (0.51, 1.30)	0.75 (0.50, 1.40)	0.84 (0.50, 1.42)	0.91 (0.53, 1.58)	0.68 (0.43, 0.87)	0.75 (0.67, 1.00)	0.79 (0.61, 0.94)	0.67 (0.42, 0.81)
pH 9, conc. 0.10 M	0.68 (0.54, 0.82)	0.64 (0.51, 0.79)	0.81 (0.50, 1.31)	0.89 (0.42, 1.36)	0.75 (0.56, 0.94)	0.77 (0.53, 0.98)	0.78 (0.63, 0.92)	0.75 (0.67, 0.95)
pH 12, conc. 0.10 M	0.68 (0.54, 0.82)	0.64 (0.51, 0.79)	0.93 (0.50, 1.57)	0.92 (0.42, 1.56)	0.73 (0.54, 0.93)	0.76 (0.51, 0.96)	0.78 (0.62, 0.91)	0.74 (0.65, 0.93)

*PMP = Pristine microplastic, WMP = weathered microplastic, S1 = low organic matter soil, S2 = high organic matter soil, S1 + PMP = low organic matter soil + pristine microplastic, S1 + WMP = low organic matter soil + weathered microplastic, S2 + PMP = high organic matter soil + pristine microplastic, S2 + WMP = high organic matter soil + weathered microplastic. Freundlich equation is expressed as $C_s = K_f C_{aq}^{1/n}$ where, C_s = amount of P adsorbed on solid (mg/ kg), C_{aq} = concentration of P in equilibrium solution (mg/ L), $\log K_f$ = Freundlich constant, $1/n$ = heterogeneity factor.

4.4. Discussion

Since the adsorption of phosphate ion (PO_4^{3-}) is likely to be dependent on the pH and concentration of the background electrolyte (Liu *et al.*, 2011; Chitrakar *et al.*, 2006; Bolan *et al.*, 1986), it was expected that the pH and concentration of background electrolyte would impact on the adsorption of phosphate to the HDPE microplastic, which was verified in our present study. As far as the present author is aware there are no published studies on the effects of pH and concentration of background electrolyte on the anion adsorption to the microplastic surface. There were few studies that studied the effects of pH and concentration of background electrolyte on the adsorption of cations (Holmes *et al.*, 2012; Binda *et al.*, 2021; Medynska-Juraszek and Jadhav, 2022) and organic compounds (Liu *et al.*, 2019; Deng *et al.*, 2012; You *et al.*, 2010).

4.4.1. Phosphate adsorption at point of zero charge (PZC)

The point of zero charge (PZC) of the pristine (PMP) and weathered (WMP) microplastics (Table 4.1) were higher than the reported literature value of 4.30 for the polyethylene (Xu *et al.*, 2018). This was probably due to the different methods used for the determination of the PZC and variations in the additives and dyes added during the manufacturing processes. We used the mass titration method (involving the use of an increasing mass of the solid to a known volume of the electrolyte) for the determination of the PZC, but Xu *et al.* (2018) used the potentiometric titration (determined the amounts of adsorbed H^+ / OH^- ions from the pH difference between the blank and acid/ base titrated suspensions at each different concentrations of the electrolyte) for the determination of the PZC in their study. It is worth noting that the PZC of the WMP (6.77, 6.79) was higher than the PMP (6.30, 6.32) in our study which could be due to the differences in surface chemistries and functional groups. The PZC values for different soils (ranging from 1.6 to 4.6) reported in the literatures are consistent with our findings of high organic matter soil (S2 = 4.51, 4.51). However, the PZC of the low organic matter soil, (S1 = 5.25, 5.27) was comparatively higher than the reported values (1.6 to 4.6) which was possibly due to the differences in origin, mineralogical composition and buffering capacity. The PZC of the S1 found in our study were higher than the PZC of the S2 which supported the observations of Wada and Okamura (1980) that the presence of organic matter tends to shift the PZC of the soil to lower values. The S2 had a higher organic matter content and therefore we would expect its PZC to be lower.

According to Ma *et al.* (2019), phosphate adsorption in the soil occurred at pH values below and above the point of zero charge (PZC) which was consistent with our study (Figure 4.1, 4.2, 4.3). Ma's study hypothesised that the adsorption was dominated either by chemisorption or through hydrogen bonding/ Van der Waals forces rather than the electrostatic interactions. This hypothesis contradicted the previous literatures (Wang *et al.*, 2015; Xu *et al.*, 2018) which stated that the electrostatic interaction was solely responsible for the decreases in phosphate adsorption with the increasing pH. Our findings of phosphate adsorption in the soil samples could be explained by Ma's hypothesis (2019). The PZC values of both soils (low organic matter soil, S1 = 5.25, 5.27; high organic matter soil, S2 = 4.51, 4.51) were lower than the pH 7. At the pH values below and above pH 7, phosphorus exists in the form of H_2PO_4^- and HPO_4^{2-} respectively (Parham *et al.*, 2002; Dunne *et al.*, 2011). The H_2PO_4^- and HPO_4^{2-} ions act as monodentate and bidentate ligands that have greater affinity for the soil surfaces (Tanuja *et al.*, 2021).

4.4.2. Effects of pH on phosphate adsorption

All the solid samples (microplastic, soil, soil + microplastic) showed decreases in phosphate adsorption (indicated by K_d and C_{SM} values) with the increasing pH (Figure 4.1, Figure 4.2, Table B2, Table B3). Our findings of continuous decreases in phosphate adsorption with increased pH for the solids were consistent with the reported results in the literatures (Wang *et al.*, 2015; Xu *et al.*, 2018). All these literatures indicated the role of electrostatic interaction for the decreases in adsorption with the increases in pH, although the authors (Wang *et al.*, 2015; Xu *et al.*, 2018) did not study the adsorption of phosphate. They did focus on the adsorption of metals and organic compounds to the microplastic surfaces. Solid surface is likely to develop positive charges at low pH (protonation) and negative charges at high pH (deprotonation) due to the behaviour of the protons (Stina *et al.*, 2006). Development of positive charge on the solids (microplastic, soil, soil + microplastic) could attract the negatively charged PO_4^{3-} ions leading to the increased adsorption of PO_4^{3-} at low pH. At high pH, adsorption of PO_4^{3-} decreased which could be due to the reduced attractions between negatively charged solid surface and negatively charged PO_4^{3-} ions. Previous studies (Holmes *et al.*, 2012; Zhang *et al.*, 2020; Dong *et al.*, 2020) reported that the adsorptions of Cr and As onto the high density polyethylene (HDPE) and polypropylene (PP) microplastics were decreased as the pH raised. Although Cr and As are cations, they exist in solution in the forms of oxyanions (Cr: $\text{HCrO}_4^- / \text{CrO}_4^{2-}$; As: AsO_2^-). As phosphate ion is an oxyanion, the

decreases in PO_4^{3-} adsorption with increasing pH were consistent with the adsorption behaviours of other oxyanions reported in the literatures.

Antelo *et al.* (2005) demonstrated that the higher phosphate adsorption on the goethite occurred in low pH at most ionic strengths, whereas lower phosphate adsorption occurred in high pH and low ionic strengths. Antelo *et al.* (2005) hypothesised that the phosphate adsorption might be due to the presence of three inner-sphere surface complexes (monodentate nonprotonated, bidentate nonprotonated, and bidentate protonated) suggesting that the phosphate ions were strongly bonded via ligand exchange (Russell *et al.*, 1974; Parfitt *et al.*, 1975). The binuclear bidentate $\text{Fe}_2\text{O}_2\text{PO}_2$ surface complex might be the dominant adsorbed phosphate species at neutral pH values and $\text{Fe}_2\text{O}_2\text{PO}_2$ might be protonated at low pH (Tejedor-Tejedor and Anderson, 1990). Our results were partially supported by Antelo's study (2005) since we found decreased phosphate adsorption with the increasing pH. Antelo's study was a theoretical modelling study and the authors used different spectroscopic techniques based on the molecular configuration of surface complex and the speciation of phosphorus. While Antelo's study determined the phosphorus adsorption directly on the synthesized iron oxides, our study determined the phosphate adsorption on the microplastic/soil/soil + microplastic samples.

Studies also showed that the adsorption of Cu on the polymethyl methacrylate (PMMA) microplastic increased at pH less than 7 but the adsorption decreased at pH above 7 (Demirata-Öztürk *et al.*, 1996; Yang *et al.*, 2019) which appeared to contradict our study. When the pH was less than 7, the PMMA surface could develop positive charges that could electrostatically repel Cu^{2+} ions preventing their approach to the PMMA. However, oxygen in the molecular structure of the PMMA had a strong attraction for the Cu^{2+} (arising from the negative charge of the oxygen) that could outweigh the repulsion between the positively charged PMMA and Cu^{2+} so that the Cu adsorption was seen to increase at low pH (less than 7) despite potential decrease in the electrostatic attraction between the PMMA and Cu^{2+} (Cruz-Lopes *et al.*, 2021). At the pH above 7, dissolved Cu moieties [CuOH^+ , $\text{Cu}_2(\text{OH})_2^{2+}$] could appear by reacting with the oxygen and hydrogen of the PMMA. Also, most Cu could be converted to hydroxide precipitates [$\text{Cu}(\text{OH})_2$] at the pH above 7. All these phenomena might reduce the concentration of Cu^{2+} leading to the decreased adsorption of Cu to the PMMA surface at the pH above 7 (Yang *et al.*, 2019; Tang *et al.*, 2021). Increases in adsorption at the low pH values reflect the differences in experimental systems between our study and others (Demirata-Öztürk *et al.*, 1996; Yang *et al.*, 2019) including our use of non-

polar HDPE microplastic with the carbon–carbon bonds compared to the polar polymethyl methacrylate (PMMA) microplastic having an ester group ($-\text{COO}-$) on the branched chain, and the presence of anion as an adsorbate in our experiment compared to the metal cation.

Contradictory results were also found by Sun *et al.* (2022) who demonstrated that the adsorption of norfloxacin (NOR) to the polybutylene succinate (PBS) microplastics increased at the initial stage (up to pH 7) and then decreased. Contradictory results between our study and Sun's study (2022) could be due to the dealing with the sorption of an anion compared to the sorption of a compound (NOR) that was a cation at pH less than 7 and an anion at pH greater than 7. At pH less than 7, negatively charged (due to the presence of oxygen in its structure) PBS forms an electric double layer with cations present in water to adsorb the NOR^+ which leads to the increased adsorption of NOR to the microplastic. When the pH is greater than 7, adsorption of NOR^- is inhibited by electrostatic repulsion (Sun *et al.*, 2022).

Moreover, another group of authors (Nan *et al.*, 2020) revealed that the changes in pH did not significantly affect the adsorption of fungicides on the microplastics. These fungicides (strobilurin) were reported to be neutral, organic compounds and thus, pH had little effect on their dissociation. Qi *et al.* (2019) reported that the changes in pH may lead to the dissociation of ionic compounds and affect their interaction with the surface charge of microplastic.

Although we found maximum phosphate adsorption at the same pH (pH value 2) for the pristine (PMP) and weathered microplastics (WMP), adsorption was significantly ($p \leq 0.05$) higher for the WMP as indicated by the three-way ANOVA test. This higher adsorption of the WMP was supported by our findings in Chapter 3. Oxygen containing functional groups (observed in Chapter 3) present on the WMP might affect the protonation which was likely to lead to more binding with the phosphate ions as suggested by Tang *et al.* (2020). However, Tang *et al.* (2020) could not able to explain the detailed mechanisms.

4.4.3. Effects of concentration of background electrolyte on phosphate adsorption

Phosphate adsorption to the solids (microplastic, soil, soil + microplastic) was reduced with the reduced concentration of the background electrolyte (Figure 4.1, 4.2, Table B2, B3). According to Liu *et al.* (2019), ionic strength influences the adsorption of anion in two ways: (a) by affecting the interfacial potentials and thus, the activity of the adsorbing anions, and (b) by affecting the competition between electrolyte ions and adsorbing anions for available surface sites. However, Liu *et al.* (2019) were not able to explain the mechanisms in details. As we mentioned earlier in this chapter (introduction: section 4.1) that the ionic strength is equal to the concentration of the background electrolyte for the NaNO_3 , the concentration of the background electrolyte influences the anion adsorption according to Liu's (2019) mechanisms.

Studies demonstrated that, depending on the point of zero charge (PZC), increasing the concentration of the background electrolyte can either decrease or increase phosphate adsorption, suggesting that the phosphate can be adsorbed when the potential in the plane of adsorption is either positive or negative (Bolan *et al.*, 1986; Barrow, 1984). Increasing the concentration of background electrolyte increases phosphate adsorption above the point of zero charge (PZC) and decreases adsorption below the PZC (Bolan *et al.*, 1986; Ryden *et al.*, 1977; Barrow *et al.*, 1980) which was partly supported by our study. This suggests that the effect of the concentration of background electrolyte on phosphate adsorption operates through its effect on the electrostatic potential in the plane of adsorption.

In our study, phosphate adsorption on the pristine (PMP) and weathered microplastics (WMP) increased with the increases in the concentrations of electrolyte at the pH values above and below 6.31 (PZC for the pristine microplastic) and 6.78 (PZC for the weathered microplastic) respectively (Figure 4.1, 4.2, Table B2, B3). Both soil types and the mixture of soil and microplastic showed the similar trends indicating that the adsorption was increased with the increasing concentration of the electrolyte above and below the respective PZC values (Table 4.1). However, we did not observe decreases in adsorption with the increasing concentration of the electrolyte below the PZC (Figure 4.1, 4.2, Table B2, B3). Our findings of increasing adsorption with the increasing concentration of the background electrolyte could be explained from the viewpoint of Wu *et al.* (2016). Although Wu *et al.* (2016) observed the adsorption of triclosan (a non-polar organic compound) on the microplastic in the marine sediments,

Wu's findings were in line with our study indicating that the gradual increases in the triclosan adsorption increased with the increases of the concentration of the background electrolyte. Increase in the concentration of the electrolyte could reduce the solubility which in turn could increase the adsorption of the triclosan as suggested by Soubaneh *et al.* (2014). The higher the concentration of the Na⁺ ions (provided by the NaNO₃ as the background electrolyte), the higher are the adsorption of phosphate.

According to Sparks (2003), the effect of the background electrolyte concentration on adsorption process depends on the type of complexes that the adsorbed ions can form with the surface. Our findings of increasing adsorption with the increasing concentration of the background electrolyte (Figure 4.1, 4.2, Table B2, B3) could be explained from the viewpoint of Sparks (2003). Phosphate ions directly coordinate to the surface of microplastic resulting in the formation of inner-sphere complexes. In the inner-sphere complex, phosphate ion does not compete or compete less with the ions of background electrolyte compared to the outer-sphere complex, which in turn increases the adsorption of phosphate with the increasing concentration of the background electrolyte (Sparks, 2003). With the increasing concentration of the background electrolyte the double layer thickness decreases enhancing the formation of complexes between the iron oxides and phosphate as suggested by Rodrigo *et al.* (2019) and Pardo *et al.* (1992). The soils (S1, S2) used in our study probably contains some iron oxides and the iron oxides are strongly adsorptive for phosphate (Ramalho, 1977; Borggard *et al.*, 1990). Thus, increased phosphate adsorption in the soils (S1, S2) with the increasing concentration of the background electrolyte could be explained by the complex formation.

Contradictory to our findings, studies (Liu *et al.*, 2019; Wang *et al.*, 2015; Sun *et al.*, 2022) found that the increased concentration of the background electrolyte was likely to decrease the adsorption of ciprofloxacin (CIP) to the microplastic, which might be due to the effects of cation exchange and salting in of the CIP. The CIP acts as a zwitterion that acquires a negative charge at high pH because of the deprotonation of the carboxylic group, whereas at low pH develops positive charge due to the protonation of the amine group (Wang *et al.*, 2015). The authors were not able to explain the effect of cation exchange. Although we observed decreases in the cation exchange due to the additions of microplastic treatments (Chapter 5), our findings did not support the previous literatures. Regarding the effect of salting in of the CIP, increased concentrations of background electrolyte inhibited the mass transfer from the aqueous to solid phase by increasing the viscosity and the density of the

solution (Wu *et al.*, 2018; Liu *et al.*, 2019). Thus, the adsorption of the CIP to the microplastic surface was decreased with the increasing concentrations of the background electrolyte.

Although Liu *et al.* (2011) did not find any effect for the pH, they observed that the phosphate adsorption was reduced with the increases in the concentration of the background electrolyte. This phenomenon could be explained by the preferential adsorption of the anions. Phosphate ions have higher binding affinity with the active sites than the chloride ions (Chitrakar *et al.*, 2006; Tian *et al.*, 2009). Cl⁻ ions would slow down the diffusion that may hinder the access of PO₄³⁻ to the active sites of the adsorbent (Keranen *et al.*, 2015; Tian *et al.*, 2006). Thus, increasing the concentration of the Cl⁻ ions (NaCl used as a background electrolyte) would restrict the access of PO₄³⁻ to the lanthanum-doped activated carbon fiber resulting in the decreased adsorption of PO₄³⁻ (Liu *et al.*, 2011). Our study and previous literatures (Liu *et al.*, 2019; Liu *et al.*, 2011; Wang *et al.*, 2015; Sun *et al.*, 2022) suggested that the adsorption of phosphate was likely to be highly dependent on the properties of the adsorbent and nature of the adsorbate.

4.4.4. Effects of interaction between pH and concentration of background electrolyte on phosphate adsorption

Previous studies found the effects of pH and concentration of the background electrolyte significant ($p \leq 0.05$) on the adsorption of cations (Holmes *et al.*, 2012; Binda *et al.*, 2021; Medynska-Juraszek and Jadhav, 2022) and organic compounds (Liu *et al.*, 2019; Deng *et al.*, 2012; You *et al.*, 2010). However, the interaction effect between the two factors was not significant ($p > 0.05$). In our study, we observed non-significant ($p > 0.05$) interaction effect between the pH and concentration of the background electrolyte for the partition coefficient (K_d), maximum adsorption capacity (C_{SM}) and Freundlich constant ($\log K_f$). However, there was a significant ($p \leq 0.05$) interaction between the solid type, pH and concentration of the background electrolyte for the partition coefficient (K_d), maximum adsorption capacity (C_{SM}) and Freundlich constant ($\log K_f$) as suggested by the three-way ANOVA.

Previous studies (Barrow *et al.*, 1980; Bowden *et al.*, 1980) looked at the adsorption variation with the pH or concentration of the background electrolyte with only one initial phosphorus concentration. Typically an ample range of phosphorus concentration is required to determine the P adsorption isotherms. Phosphate adsorption to different solid types was best described

by different types of linear and non-linear (Langmuir and Freundlich) isotherms (Table B2, Table B3, Table B4). All the solids except the S1, S1 + PMP and S2 + PMP were best fitted to the linear and Freundlich isotherms (Table B2, Table B4). All the solids except the PMP and WMP were best fitted to the Langmuir isotherms (Table B3). Both Langmuir and Freundlich isotherms indicated chemisorption which could imply that the reactions between the adsorbate (phosphate) and adsorbent (microplastic/ soil/ mixture of both) forms covalent bonds, and both the anions and cations compete for the adsorption sites (Sparks, 2003; Debicka *et al.*, 2016; Han *et al.*, 2018). Although the microplastic (non-polar, hydrophobic) and soil (polar, hydrophilic) had different physico-chemical properties, microplastic, soil and the soil + microplastic samples showed similar trends in the phosphate adsorption (indicated by K_d and C_{SM}) with the changes in pH, concentration of the background electrolyte and the interaction between the two factors.

Although all the solids (microplastic, soil, soil + microplastic) showed decreases in phosphate adsorption with the increasing pH and with the reduced concentration of background electrolyte (Figure 4.1, Figure 4.2, Table B2, Table B3) in the present study, there were few exceptions. For example, for the low organic matter soil and pristine microplastic (S1 + PMP), K_d decreased when the pH was increased from 2 to 7 followed by a sharp increase at pH 9 and then decreased at pH 12 for the 0 and 0.01 M concentrations (Figure 4.1e, Table B2). Mixture of low organic matter soil and weathered microplastic (S1 + WMP) followed the same trend as the S1 + PMP (Figure 4.1f, Table B2). It is worth noting that the K_d for the S1 + PMP and S1 + WMP at the pH 9 and at the background electrolyte concentration of 0.01 M indicated contamination in the solution. There would be a gradual downward slope without the data of pH 9 and 0.01 M concentration. We had tight error bars on the mean values (Figure 4.1e, 4.1f, Table B2) but if our background electrolyte was contaminated or we made the same mistake for those experiments then that could be expected. As our findings of continuous decreases in phosphate adsorption with increased pH were consistent with the reported results in the literatures (Wang *et al.*, 2015; Xu *et al.*, 2018), the bump at the pH 9 was more likely to be an error.

In broad terms, the mixture of soil and microplastic had the same trends as with the single solids suggesting a general decrease in the phosphate adsorption with the increasing pH and an increase in adsorption with the increasing concentration of the background electrolyte (Figure 4.1, 4.2, Table B2, B3). Although the general trends were similar for the mixture of

soil + microplastic and single solids (microplastic, soil), the soils had higher values for the K_d and C_{SM} (Figure 4.1, 4.2, Table B2, B3).

Data above suggested that the individual effects of pH and concentration of the background electrolyte were significant ($p \leq 0.05$) on the adsorption of phosphate to the microplastic surface but the interaction effects between the two factors were not significant ($p > 0.05$). We observed decreased phosphate adsorption with the increasing pH which was attributed to the electrostatic attractions. Depending on the PZC, microplastic could develop positive and negative charges leading to the adsorption of phosphate.

4.5. Conclusion

Although the fate and behaviour of the phosphate in the soil seems unlikely to be much impacted by the microplastics (Chapter 3), pH and concentration of the background electrolyte are likely to impact on the adsorption of phosphate to the microplastics in the soil. Our data showed that the adsorption of phosphate decreased with the increasing pH and with the reduced concentration of the background electrolyte. The results did not find any significant interaction between the pH and concentration of the background electrolyte although the interaction effects between the solid type, pH and concentration of the background electrolyte were significant. Thus, our study highlights the need for a wider range of plastic feedstocks with potentially different surface chemistries and sorption characteristics, to be investigated. On the basis of our findings it was not possible to know whether there was any desorption of the phosphate. Studies would be required to cast further light on the desorption of PO_4^{3-} at different ranges of pH and different concentrations of the background electrolyte which will help to determine whether the microplastic could release previously adsorbed PO_4^{3-} and to compare the release rates in different environmental conditions leading to different physico-chemical reactions of microplastics in the soil (Chapter 6). Since the phosphate adsorption to the microplastic was likely to be impacted by the changes in the pH and concentration of the background electrolyte, we will focus on how the microplastic will alter different soil properties and ultimately the growth of plants in the next chapter (Chapter 5).

4.6. References

Antelo, J., Marcelo, A., Fiol, S., López, R., and Arce, F. (2005). Effects of pH and ionic strength on the adsorption of phosphate and arsenate at the goethite–water interface. *Journal of Colloid and Interface Science*, 285, 476-486.

Antelo, J., Fiol, S., Perez, C., Marino, S., Arce, F., Gondar, D., and López, R. (2010). Analysis of phosphate adsorption onto ferrihydrite using the CD-MUSIC model. *Journal of Colloid and Interface Science*, 347, 112-119.

Barrow, N. J. (1984). Modelling the effects of pH on phosphate adsorption by soils. *Journal of Soil Science*, 35, 283-297.

Barrow, N. J., Bowden, J. W., Posner, A. M., and Quirk, J. P. (1980). Describing the effects of electrolyte on adsorption of phosphate by a variable charge surface. *Australian Journal of Soil Research*, 18, 395-404.

Binda, G., Spanu, D., Monticelli, D., Pozzi, A., Bellasi, A., Bettinetti, R., Carnati, S., and Nizzetto, L. (2021). Unfolding the interaction between microplastics and (trace) elements in water: a critical review. *Water Research*, 204, 1-9.

Bolan, N. S., Syers, J. K., and Tillman, R. W. (1986). Ionic strength effects on surface charge and adsorption of phosphate and sulphate by soils. *Journal of Soil Science*, 37, 379-388.

Borggard, O. K., Jorgensen, S. S., Moberg, J. P., and Raben-Lange, B. (1990). Influence of organic matter on phosphate adsorption by aluminium and iron oxides in sandy soils. *Journal of Soil Science*, 41, 443-449.

Bowden, J. W., Nagarajah, S., Barrow, N. J., Posner, A. M., and Quirk, J. P. (1980). Describing the adsorption of phosphate, citrate and selenite on a variable-charge mineral surface. *Australian Journal of Soil Research*, 18, 49–60.

Chitrakar, R., Tezuka, S., Sonoda, A., Sakane, K., Ooi, K., and Hirotsu, T. J. (2006). *Journal of Colloid and Interface Science*, 298, 602-608.

Cruz-Lopes, L. P., Macena, M., Esteves, B., and Guiné, R. P. F. (2021). Ideal pH for the adsorption of metal ions Cr^{6+} , Ni^{2+} , Pb^{2+} in aqueous solution with different adsorbent materials. *Open Agriculture*, 6, 115–123.

Debicka, M., Kocowicz, A., Weber, J., and Jamroz, E. (2016). Organic matter effects on phosphorus sorption in sandy soils. *Archives of Agronomy and Soil Science*, 62, 840–855.

Demirata-Öztürk, B., Gümüş, G., Öncül-Koc, A., and Catalgil-Giz, H. (1996). Preconcentration of copper ion in aqueous phase on methacrylate polymers. *Journal of Applied Polymer Science*, 62, 613–616.

Deng, S., Zhang, Q., Nie, Y., Wei, H., Wang, B., Huang, J., Yu, G., and Xing, B. (2012). Sorption mechanisms of perfluorinated compounds on carbon nanotubes. *Environmental Pollution*, 168, 138-144.

Dong, M., Luo, Z., Jiang, Q., Xing, X., Zhang, Q., and Sun, Y. (2020). The rapid increases in microplastics in urban lake sediments. *Scientific Reports*, 10, 1-11.

Dunne, E. J., Clark, M. W., Corstanje, R., and Reddy, K. R. (2011). Legacy phosphorus in subtropical wetland soils: influence of dairy, improved, and unimproved pasture land use. *Ecological Engineering*, 37, 1481–1491.

Gao, Y. and Mucci, A. (2003). Individual and competitive adsorption of phosphate and arsenate on goethite in artificial seawater. *Chemical Geology*, 199, 91 – 109.

Gill, R. and Ramsey, M. H. (1997). What a geochemical analysis means. In: Gill, R. (ed.) *Modern analytical geochemistry: an introduction to quantitative chemical analysis techniques for earth, environment and materials scientists*. UK: Longman Geochemistry.

Han, Y., Byoungkoo, C., and Xiangwei, C. (2018). Adsorption and desorption of phosphorus in biochar-amended black soil as affected by freeze-thaw cycles in Northeast China. *Sustainability*, 10, 1-8.

Holmes L. A., Turner, A., and Thompson R. C. (2012). Adsorption of trace metals to plastic resin pellets in the marine environment. *Environmental Pollution*, 160, 42–48.

Keranen, A., Leiviska, T., Hormi, O., and Tanskanen, J. (2015). Removal of nitrate by modified pine sawdust: effects of temperature and co-existing anions. *Journal of Environmental Management*, 147, 46–54.

Liu, J., Wan, L., Zhang, L., and Zhou, Q. (2011). Effect of pH, ionic strength, and temperature on the phosphate adsorption onto lanthanum-doped activated carbon fiber. *Journal of Colloid and Interface Science*, 364, 490-496.

Liu, G. Z., Zhu, Z. L., Yang, Y. X., Sun, Y. R., Yu, F., and Ma, J. (2019). Sorption behavior and mechanism of hydrophilic organic chemicals to virgin and aged microplastics in freshwater and seawater. *Environmental Pollution*, 246, 26-33.

Ma, J., Zhao, J., Zhu, Z., and Li, L., and Yu, F. (2019). Effect of microplastic size on the adsorption behavior and mechanism of triclosan on polyvinyl chloride. *Environmental Pollution*, 254, 1-10.

Medynska-Juraszek, A. and Jadhav, B. (2022). Influence of different microplastic forms on pH and mobility of Cu^{2+} and Pb^{2+} in soil. *Molecules*, 1-11.

Moazed, H., Hoseini, Y., Naseri, A. A., and Abbasi, F. (2010). Determining phosphorus adsorption isotherm in soil and its relation to soil characteristics. *International Journal of Soil Science*, 5, 131-139.

Nan, H., Liu, X., Li, Y., Kong, F., Zhang, Y., and Fang, S. (2020). Effects of microplastics on the adsorption and bioavailability of three strobilurin fungicides. *ACS Omega*, 5, 30679–30686.

- Noh, J. S. and Schwarz, J. A. (1989). Estimation of the point of zero charge of simple oxides by mass titration. *Journal of Colloid and Interface Science*, 130, 157–164.
- Pardo, M. T., Guadalix, M. E., and Garcia-Gonzalez, M. T. (1992). Effect of pH and background electrolyte on P sorption by variable charge soils. *Geoderma*, 54, 275-284.
- Parfitt, R. L., Atkinson, R. J., and Smart, R. S. C. (1975). The mechanism of phosphate fixation by iron oxides. *Soil Science Society of America Journal*, 39, 837-841.
- Parham, J. A., Deng, S. P., Raun, W. R., and Johnson, G. V. (2002). Long-term cattle manure application in soil. I. Effect on soil phosphorus levels, microbial biomass C, and dehydrogenase and phosphatase activities. *Biology and Fertility of Soils*, 35, 328-337.
- Qi, X., Chen, M., Qian, Y., Liu, M., Li, Z., Shen, L., Qin, T., Zhao, S., Zeng, Q., and Shen, J. (2019). Construction of macroporous salectan polysaccharide-based adsorbents for wastewater remediation. *International Journal of Biological Macromolecules*, 132, 429-438.
- Ramalho, R. S. (1977). *Introduction to wastewater treatment processes*. New York: Academic Press.
- Rodrigo C. P., Pedro, R. A., Eduardo, D. M., Daniel, F. V., Antonio, C. S. C., Cássia, T. B., and Dimas A. M. (2019). The effect of pH and ionic strength on the adsorption of glyphosate onto ferrihydrite. *Geochemical Transactions*, 20, 1-14.
- Rowell, D. L. (1994). *Soil science: methods and applications*. Essex: Longman Scientific and Technical.
- Russell, J. D., Parfitt, L. R., Fraser, A. R., and Farmer, V. C. (1974). Surface structures of gibbsite goethite and phosphated goethite. *Nature*, 248, 220-221.
- Ryden, J. C., Syers, J. K., and Mclaughlin, J. R. (1977). Effects of ionic strength on chemisorption and potential-determining sorption of phosphate by soils. *Journal of Soil Science*, 28, 62-71.

Soubaneh, Y. D., Gagné, J. P., Lebeuf, M., Gouteux, B., Nikiforov, V., and Awaleh, M. O. (2014). Sorption behaviors of a persistent toxaphene congener on marine sediments under different physicochemical conditions. *Chemosphere*, 114, 310–316.

Sparks, D. L. (2003). *Environmental Soil Chemistry*. Michigan: Academic Press.

Stina L., Wei-Feng X., Olga, S., Bauer, M. C., Hanna, N., and Sara, L. (2006). Salting the charged surface: pH and salt dependence of protein g b1 stability. *Biophysical Journal*, 90, 2911–2921.

Sun, M., Yang, Y., Huang, M., Fu, S., Hao, Y., Hu, S., Lai, D., and Zhao, L. (2022). Adsorption behaviors and mechanisms of antibiotic norfloxacin on degradable and nondegradable microplastics. *Science of the Total Environment*, 807, 1-10.

Tang, S., Lin, L., Wang, X., Feng, A., and Yu, A. (2020). Pb (II) uptake onto nylon microplastics: Interaction mechanism and adsorption performance. *Journal of Hazardous Materials*, 386, 1-9.

Tang, S., Lin, L., Wang, X., Yu, A., and Sun, X. (2021). Interfacial interactions between collected nylon microplastics and three divalent metal ions (Cu(II), Ni(II), Zn(II)) in aqueous solutions. *Journal of Hazardous Materials*, 403, 1-11.

Tanuja, T., Rohit, K., Chandanshive, A. C., and Chikkali, S. H. (2021). Phosphorus ligands in hydroformylation and hydrogenation: a personal account. *The Chemical Record*, 21,1182– 1198.

Tejedor-Tejedor, M. I. and Anderson, M. A. (1990). The protonation of phosphate on the surface of goethite as studied by CIR-FTIR and electrophoretic mobility. *Langmuir*, 6, 602-611.

Tian, J. R., Zhou, P. J., He, C. Z., Fu, Y., and Song, L. R. (2006). Adsorption characters of phosphorus by floodplain sediments from the lower reaches (River section in Wuhan City) of Hangjiang River. *Wuhan University Journal of Natural Sciences*, 52, 717-722.

Tian, S., Jiang, P., Ning, P., and Su, Y. (2009). Enhanced adsorption removal of phosphate from water by mixed lanthanum/ aluminum pillared montmorillonite. *Chemical Engineering Journal*, 151, 141-148.

USDA (United States Department of Agriculture). (1951). Soil Survey Manual. Soil Survey Staff, Bureau of Plant Industry, Soils and Agricultural Engineering, United States Department of Agriculture, Washington, US.

Wada, K. and Okamura, Y. (1980). Electric charge characteristics of Ando A, and buried A, horizon soils. *Journal of Soil Science*, 31, 307-314.

Walsh, J. N. (1997). Inductively coupled plasma-atomic emission spectrometry (ICP-AES). In: Gill, R. (ed.) *Modern analytical geochemistry: an introduction to quantitative chemical analysis techniques for earth, environment and materials scientists*. UK: Longman Geochemistry.

Wang, Y., Jiang, J., Xu, R. K., and Tiwari, D. (2009). Phosphate adsorption at variable charge soil/ water interfaces as influenced by ionic strength. *Australian Journal of Soil Research*, 47, 529–536.

Wang, F., Shih, K. M., and Li, X. Y. (2015). The partition behavior of perfluorooctanesulfonate (PFOS) and perfluorooctanesulfonamide (FOSA) on microplastics. *Chemosphere*, 119, 841-847.

Wu, C., Zhang, K., Huang, X., and Liu, J. (2016). Sorption of pharmaceuticals and personal care products to polyethylene debris. *Environmental Science and Pollution Research*, 23, 8819–8826.

Wu, G., Ma, J., Li, S., Guan, J., Jiang, B., Wang, L., Li, J., Wang, X., and Chen, L. (2018). Magnetic copper-based metal organic framework as an effective and recyclable adsorbent for removal of two fluoroquinolone antibiotics from aqueous solutions. *Journal of Colloid and Interface Science*, 528, 360-371.

Xu, B., Liu, F., Brookes, P. C., and Xu, J. (2018). The sorption kinetics and isotherms of sulfamethoxazole with polyethylene microplastics. *Marine Pollution Bulletin*, 131, 191-196.

Yang, J., Cang, L., Sun, Q., Dong, G., Ata-Ul-Karim, S. T., and Zhou, D. (2019). Effects of soil environmental factors and UV aging on Cu²⁺ adsorption on microplastics. *Environmental Science and Pollution Research*, 26, 23027–23036.

You, C., Jia, C., and Pan, G. (2010). Effect of salinity and sediment characteristics on the sorption and desorption of perfluorooctane sulfonate at sediment-water interface. *Environmental Pollution*, 158, 1343-1347.

Zhang, D., E. L. N., Wanli, H., Hongyuan, W., Pablo, G., Hude, Y., Wentao, S., Chongxiao, L., Xingwang, M., Bin, F., Peiyi, Z., Fulin, Z., Shuqin, J., Mingdong, Z., Lianfeng, D., Chang, P., Xuejun, Z., Zhiyu, X., Bin, X., Xiaoxia, L., Shiyou, S., Zhenhua, C., Lihua, J., Yufeng, W., Liang, G., Changlin, K., Yan, Li., Youhua, Ma., Dongfeng, H., Jian, Z., Jianwu, Y., Chaowen, L., Song, Q., Liuqiang, Z., Binghui, H., Deli, C., Huanchun, L., Limei, Z., Qiuliang, L., Shuxia, W., Yitao, Z., Junting, P., Baojing, G., and Hongbin, L. (2020). Plastic pollution in croplands threatens long-term food security. *Global Change Biology*, 26, 3356–3367.

Chapter 5

Impacts of microplastic on soil properties and plant growth

5.1. Introduction

To date only scant attention has been paid to investigating sources, fate and transport of microplastics in terrestrial ecosystems, although microplastics have recently been detected in agricultural fields (Habib *et al.*, 1998; Zubris and Richards, 2005; Zhang *et al.*, 2019; Zhang and Liu, 2018), cities, industrialized areas (Huerta Lwanga *et al.*, 2017; Fuller and Gautam, 2016), and remote areas (Scheurer and Bigalke, 2018). In European agricultural land, microplastic loadings have been estimated at between 63,000 and 430,000 tonnes per year (Nizzetto *et al.*, 2016a); with studies reporting anywhere between 700 and 4000 plastic particles per kg of soil (Barnes *et al.*, 2009); and, in roadside soils near industrial areas, up to 7% microplastic fragments have been reported (Fuller and Gautam, 2016). Once deposited at the soil surface via a variety of input routes (Bläsing and Amelung, 2018), microplastics can be persistent; for example, one study showed that synthetic microfibres could be identified 15 years after sewage sludge application (Zubris and Richards, 2005). It has been hypothesized that high-density polyethylene (HDPE) is not biodegradable and can persist in the natural soil for decades resulting from the high molecular weight of the plastic and its content of antioxidants and stabilisers (Lambert *et al.*, 2017). Due to their persistence characteristics, microplastic is thought to accumulate in soils with sources of microplastic typically derived from diverse sources, such as landfills (Nizzetto *et al.*, 2016b), plastic mulch used in agricultural activities (Kasirajan and Ngouajio, 2012; Li *et al.*, 2018), virgin plastic flakes, pre-production plastic pellets (Foitzik *et al.*, 2018), sewage sludge and laundry dust (Carr *et al.*, 2016; Mahon *et al.*, 2017; Mathalon and Hill, 2014).

Generally adsorption occurs on the surface of microplastics because of the large surface area and hydrophobicity of microplastic, although the adsorption depends on several factors, such as, microplastic characteristics, adsorbate characteristics and surrounding environment (Zhang *et al.*, 2019; Zhang and Liu, 2018). Adsorption by microplastics was evident in Chapter 3 where P was adsorbed by HDPE microplastics; the current chapter explores the hypothesis that HDPE limits plant growth by reducing the amount of available phosphate.

Microplastic can alter the properties of soil by changing its texture and structure, with consequences for functional changes in soil, that may directly/ indirectly influence growth and development of plants. Comparable studies on the impacts of microplastics on plants are remarkably scarce and still very sketchy. For example, Qi *et al.* (2018) observed poor growth of wheat while Zhang *et al.* (2015) observed improved crop quality for corn plants. Machado *et al.* (2019) mentioned that polyester (PES) and polyamide (PA) triggered significant increases in plant traits and metabolic functions, while weaker effects were observed in plants exposed to high-density polyethylene (PEHD), polyethylene terephthalate (PET) and polypropylene (PP).

Plants that have not been exposed to the application of plastic mulches may still come into contact with microplastics during irrigation, with some microplastics bypassing the treatment process at wastewater treatment works. With this current study, we aimed to take the first steps towards filling the gaps left by past studies and focused on the previously neglected area of research concerning microplastics in the soil-plant system. Based on the above-mentioned hypothesis, the present study was conducted with different levels of microplastic for a period of 30 days (incubation phase) followed by growth of plant in that soil (greenhouse phase). Therefore, the overarching aim of this study is to determine the impacts of microplastics on plant growth. To address this overarching aim, a set of objectives was outlined below.

Objectives of this study are:

- To determine the potential for high-density polyethylene (HDPE) microplastic to impact soil properties and plant growth;
- To determine soil chemical and biological properties after incubation with microplastic and again after subsequent plant growth;
- To observe plant growth parameters in presence of microplastic in the soil.

5.2. Materials and methodology

5.2.1. Materials

Two types of soils were collected from York, UK with contrasting organic matter contents. Soil with low organic matter content was collected from an arable field at grid reference 53° 52' 25.2" N and 1° 19' 47.0" W, located in Big Substation East field at the University of Leeds experimental farm; soil with high organic matter content was collected from a flower bed which is located at grid reference 53° 56' 41.0" N and 1° 3' 04.9" W on the University of York campus. The soils were air-dried, visible roots and plant debris were discarded and the soils were ground gently to break up larger soil aggregates. After that the soils were sieved at 2 mm, thoroughly homogenized and finally characterized. Soil texture was determined manually (USDA, 1951). A ball of soil was placed between thumb and forefinger, gently pushing the soil with the thumb and working it upward to make a ribbon. The ribbon was allowed to emerge and extend over the forefinger, breaking from its own weight, and finally the texture of the soil was determined from the length and strength of the ribbon. pH of the soil was determined by mixing air-dried soil and deionised water at a ratio of 1:2.5 followed by shaking for 15 minutes. The suspension was allowed to settle and pH was measured using an Accumet AB150 pH meter calibrated with pH 4.0, 7.0 and 10.0 buffers (Rowell, 1994). Soil organic matter was determined by heating 20 g of air-dried soil overnight at 105 °C, reweighed and then combusted at 350 °C overnight. Mass loss on ignition (LOI) was determined and used as a proxy for organic matter content (Hoogsteen *et al.*, 2018; Rowell, 1994). Low organic matter soil had a silty loam texture with a pH of 7.63 ± 0.13 and organic matter content of 3.58 ± 0.15 %; high organic matter soil had a loamy texture having a pH of 7.11 ± 0.09 and organic matter content of 4.62 ± 0.13 % (Table C1; n = 5, \pm standard deviation).

Commercial grade high-density polyethylene (HDPE) microplastics powder (Model No. SMHD-3006H) was purchased from Qingdao Sunsoar Tech. Co., Ltd. located in Shandong, China. The plastic was confirmed to be HDPE by comparing its spectra with other reported analyses of untreated HDPE (Hodson *et al.*, 2017; Anu and Pillai, 2022) using Fourier Transform Infrared Spectroscopy (FTIR) equipped with an ATR platinum diamond attenuated total reflectance accessory and a potassium bromide beam splitter. The spectra were scanned in the range of 400 to 4000 cm^{-1} . Each spectrum comprised 144 scans with a 4 cm^{-1} resolution and were background corrected.

5.2.2. Incubation experiment

An incubation experiment (Figure 5.1) was conducted following a randomized block design (Figure 5.2) to investigate the impacts of HDPE on soil physico-chemical properties.

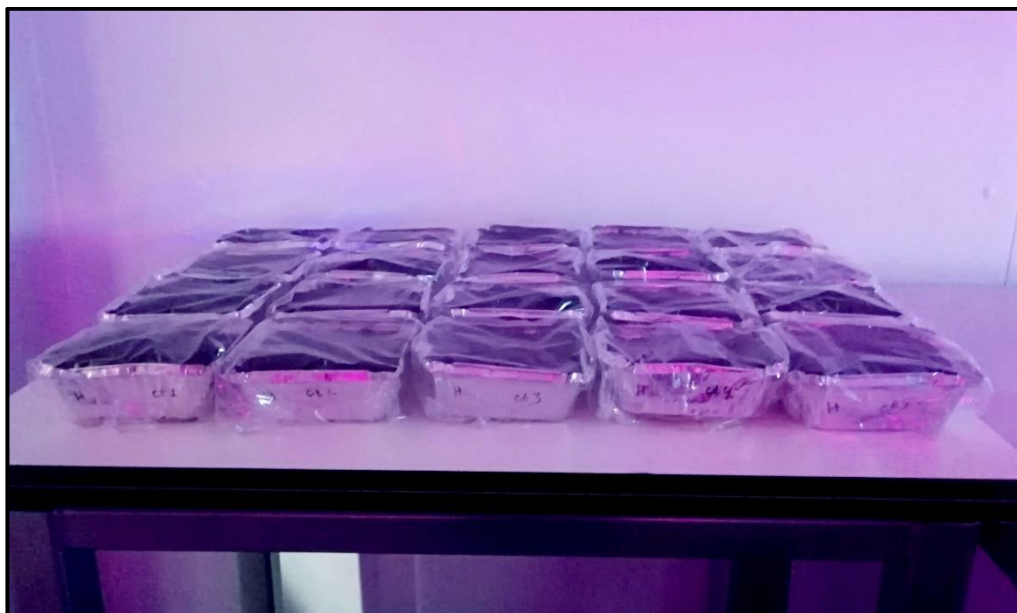


Figure 5.1. Incubation experiment conducted in a controlled temperature room for a period of 30 days. Temperature 25 °C and relative air humidity 80 %. Two types of soils (low and high organic matter soil) and four treatments (control, 0.05 %, 0.50 % and 5.00 % HDPE) were used in the experiment. Each treatment had four replicates.

The incubation experiment was based on four groups of microplastic treatments *viz.*, control, 0.05 %, 0.50 % and 5.00 % (w/w) which were selected on the basis of values of microplastics found in arable soil (Nizzetto *et al.*, 2016a; Machado *et al.*, 2018; Qi *et al.*, 2018). All treatments were replicated four times giving a total of 32 (16 for each soil) aluminum containers (4.1 cm deep, 14.1 cm long, 11.6 cm wide). Each container contained 400 ± 0.05 g air-dried soil. HDPE was added to the soil according to the treatments: control, 0.05 % (0.2 g HDPE), 0.50 % (2 g HDPE) and 5.00 % (20 g HDPE). Thus, four treatments are produced for each soil: i) low organic matter soil not treated with microplastics (L0) (n = 4), ii) low organic matter soil treated with 0.05 % microplastics (L0.05) (n = 4), iii) low organic matter soil treated with 0.50 % microplastics (L0.5) (n = 4), iv) low organic matter soil treated with 5.00 % microplastics (L5.0) (n = 4), v) high organic matter soil not treated with microplastics (H0) (n = 4), vi) high organic matter soil treated with 0.05 % microplastics (H0.05) (n = 4),

vii) high organic matter soil treated with 0.50 % microplastics (H0.5) (n = 4) and viii) high organic matter soil treated with 5.00 % microplastics (H5.0) (n = 4).

Block 1	L0.05	H0.05	L0	H0	L5.0	H5.0	L0.5	H0.5
Block 2	L5.0	H5.0	L0.5	H0.5	L0	H0	L0.05	H0.05
Block 3	L5.0	H5.0	L0.05	H0.05	L0.5	H0.5	L0	H0
Block 4	L0.5	H0.5	L5.0	H5.0	L0.05	H0.05	L0	H0

Figure 5.2. Experimental design for both incubation and greenhouse experiments. Two types of soils and four treatments (each treatment had four replicates) were used following a randomized block design. Low organic matter control soil = L0, low organic matter soil with 0.05 % HDPE = L0.05, low organic matter soil with 0.50 % HDPE = L0.5, low organic matter soil with 5.00 % HDPE = L5.0, high organic matter control soil = H0, high organic matter soil with 0.05 % HDPE = H0.05, high organic matter soil with 0.50 % HDPE = H0.5, high organic matter soil with 5.00 % HDPE = H5.0.

After adding microplastics to the soil, the soils were thoroughly mixed and homogenized with a glass rod to distribute the microplastics as evenly as possible. 100 ml of deionised water was added to each container and thoroughly mixed into the soil to establish a soil water content of 25 % w/w. The containers were wrapped within plastic film to prevent evaporation. Finally, all containers were kept at 25 °C in a controlled temperature room and a relative air humidity of 80 % at the Department of Environment and Geography, University of York, UK for an incubation period of 30 days. The moisture content of the soil was determined by mass loss and deionised water was added (0.5 – 1.0 g) on a weekly basis to maintain a constant water content. After 30 days c. 100 g soil was removed to test biological (respiration rate and enzyme activity) and chemical (soil pH, exchangeable cations, cation exchange capacity (CEC), cold and hot water extractable carbon, Olsen phosphorus, ammonium, nitrate, soil water holding capacity, water stable aggregates and phosphorus in soil pore water) parameters

of the incubated soil. Remaining c. 300 g soil was transferred to the plant pots for greenhouse experiment.

5.2.3. Greenhouse experiment

A greenhouse experiment (Figure 5.3) was conducted in order to observe the interaction of soil, plant and HDPE. For the greenhouse experiment, clean, opaque plastic plant pots with a 1.3 litre capacity (height = 13.0 cm, top diameter = 12.5 cm, bottom diameter = 10.1 cm) were used. According to the treatments, each plant pot was filled with soil/ mixture of soil and HDPE directly from the incubation experiment.

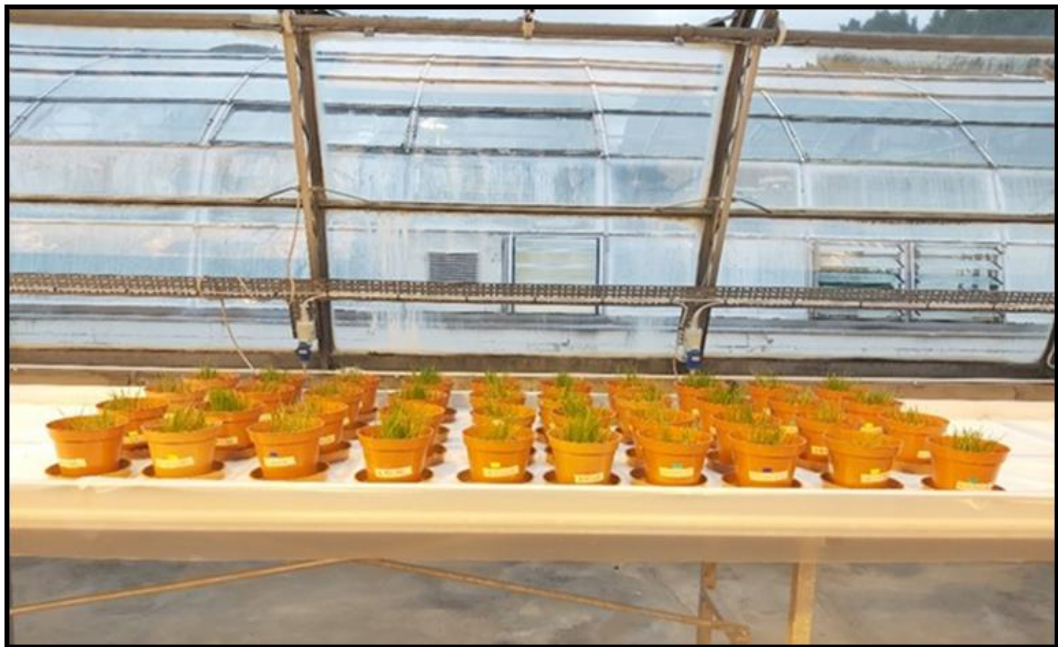


Figure 5.3. Greenhouse experiment with ryegrass (*Lolium perenne*) conducted for a total period of seven weeks. Minimum day/night temperature of 20 °C day/ 15 °C, with vents opening at 18 °C. Relative humidity was ambient, ranging from 30 – 85 %. Two types of soils (low and high organic matter soil) and four treatments (control, 0.05 %, 0.50 % and 5.00 % HDPE) were used in the experiment. Each treatment had four replicates. Pots were rearranged every week to minimize the effects of variation.

Ryegrass (*Lolium perenne*) was chosen as the plant to grow in the experiment on the basis that it is one of the most common, native grass species in Europe, providing high yields and quality forage throughout a wide range of environmental conditions (Jung *et al.*, 1996). Seeds of diploid ryegrass were purchased from Wilko Seed Company and mesocosms in which ryegrass was grown received 200 seeds (approximately 0.37 g) giving a density of 27.5 kg ha⁻¹. Seeding rates were chosen based on studies on optimal seeding rates for ryegrass (Lee *et al.*, 2016). The seeds were distributed evenly on the soil surface of each pot. This experiment ran for seven weeks within a greenhouse with minimum day and night temperatures of 20 °C and 15 °C respectively. Relative humidity in the greenhouse was ambient, ranging from 30 to 85 %. The plant pots were randomly placed in a greenhouse and after that the position of the pots were changed randomly every week in order to provide the plants with equivalent lighting. Throughout the experiment, plants were watered twice a week with 120 ml tap water to keep the soil moist. The seeds began to germinate after one week of sowing, which was indicated by the emergence of a radicle. At the end of the experimental period, plant parameters (plant height, leaf chlorophyll content, shoot biomass, root biomass, root: shoot ratio) were determined. Roots were removed from the soil as much as possible and then homogenized the soil prior to subsampling. After that, soil samples were divided into two subsamples for further chemical analyses. One group (c. 100 g soil) was used to test soil biological (respiration rate and enzyme activity) and another group (c. 200 g soil) chemical parameters (soil pH, exchangeable cations, cation exchange capacity (CEC), cold and hot water extractable carbon, Olsen phosphorus, ammonium, nitrate, soil water holding capacity, water stable aggregates and phosphorus in soil pore water).

5.2.4. Measurements of plant growth parameters

At the end of the greenhouse experiment different plant growth parameters *viz.*, plant height, total chlorophyll content, root and shoot biomass, root: shoot ratio as well as phosphorus content in plants, were determined to investigate whether plant growth is affected by HDPE. Plant height was measured from the base to the tip of the highest fully expanded leaf using a ruler. For determining chlorophyll concentration, three fully expanded leaves were randomly selected and three measurements per leaf were done (Richardson *et al.*, 2002; Pinkard *et al.*, 2006), using an atLEAF CHL PLUS chlorophyll meter (Minolta, USA). The chlorophyll meter measured atLEAF CHL value which was then converted to total chlorophyll using the equation $y = 0.0247x - 0.0615$, where y = total chlorophyll (mg/ cm²) and x = atLEAF CHL PLUS index value obtained from the chlorophyll meter. Finally, all the values were averaged

for the determination of chlorophyll concentration. Shoots of ryegrass were cut half a centimetre above the base of the soil and then weighed to determine the shoot biomass on a fresh weight basis. After that, the shoots were oven-dried at 60 °C to constant mass for determining the dry weight of shoot. In our case, the shoots reached a constant mass after 48 hours. Fresh roots were carefully collected from each plant and then washed thoroughly with deionised water on a 2 mm sieve to remove any excess soil. They were dried on a blue paper and root biomass (fresh weight) was determined. Roots were then oven dried at 60 °C to constant mass (roots did not lose any more mass after 48 hours) to determine dry weight of the root (Boots *et al.*, 2019). Phosphorus in plants was determined using the manual hydraulic press followed by analysing with P-XRF (Portable X-Ray Fluorescence Spectrometry). The instrument was calibrated using a Si-spiked synthetic methyl cellulose (Sigma-Aldrich, product no. 274429) and validated using Certified Reference Materials of NCS DC73349 ‘bush branches and leaves’ obtained from China National Analysis Centre for Iron and Steel (Reidinger *et al.*, 2012). Oven dried shoot materials were finely ground with a ball mill. Fine powder was pressed at 10 tons into a 13 mm diameter pellets with a manual hydraulic press using a 13 mm die (Specac, Orpington, United Kingdom) to produce homogenous sample pellets (McLarnon *et al.*, 2017). After that, P in shoots was measured using a P-XRF (Nitron XL3t900 GOLDD analyser: Thermo Scientific Winchester, UK) held in a test stand (SmartStand, Thermo Scientific, Winchester, UK). Two readings (measuring both sides of the pellet; each side took approximately 20 seconds for measurement) were taken for each pellet and the average P (%) was calculated (Reidinger *et al.*, 2012).

5.2.5. Determination of soil parameters

Both the incubated and greenhouse soils were analysed in the laboratory to investigate whether soil parameters were affected by HDPE. Respiration rate was determined as it is considered a good proxy of the microbial activity in soil (Anderson and Domsch, 1978). For soil microbial respiration air-dried soil from each treatment was moistened with 10 g water per 100 g of air-dry soil and stored for one week in a polyethylene bag which was shaken every day to aerate the soil. The soil was transferred to a glass jar and a glass vial containing 10 ml of 0.3 M sodium hydroxide (NaOH) was placed in the jar, which was then made air-tight by using vaseline and parafilm. After one week of incubation in the dark at 15 °C, the concentration of carbon dioxide dissolved in the NaOH was determined by a titration using 1 M barium chloride (BaCl₂·2H₂O) and phenolphthalein indicator. Blank corrections were performed in the same way with 50 g of sand instead of soil. Water content of the moist soil

was determined at the time the glass jars were made ready for the experiment. Finally respiration rate was expressed on a per mass of air-dried soil basis (Rowell, 1994).

Phosphatase enzyme activity in soil was determined by colorimetric estimation of the *p*-nitrophenol released by phosphatase activity. 1 ± 0.05 g (≤ 2 mm) fresh soil was placed into a 50 ml Erlenmeyer flask, 4 ml of Modified Universal Buffer (MUB) (pH 6.5), 0.25 ml of toluene and 1 ml of *p*-nitrophenol (PNP) solution were added, then the flask was swirled for a few seconds to mix the contents. After wrapping the mouth of the flasks with parafilm, they were placed in an incubator at 37° C for an hour. 1 ml of 0.5 M calcium chloride (CaCl₂) and 4 ml of 0.5 M sodium hydroxide (NaOH) were added to the soil suspension, swirled for a few seconds, and filtered through Whatman filter paper (#2). The filtrate was then transferred to a 4 ml plastic cuvette and colour intensity was measured at 410 nm using a Jenway 6300 UV/vis spectrophotometer. The *p*-nitrophenol content of the filtrate was calculated by reference to a calibration graph obtained with standards containing 0, 10, 20, 30, 40 and 50 µg of *p*-nitrophenol. Control experiments were performed by adding 1 ml of PNP solution after the additions of 0.5 M CaCl₂ and 0.5 M NaOH immediately before filtration of the soil suspension (Tabatabai and Bremner, 1969; Kramer and Yerdei, 1958).

Soil pH was determined by a pH meter (Benchtop, Thermo Orion). Air-dried soil was placed in a 50 ml centrifuge tube, ultra-pure was added at a ratio of 1:2.5, then placed on a shaker for 15 minutes. pH of the samples was determined after necessary calibrations with pH 4.00, 7.00 and 10.00 buffer solutions (Lankinen, 2000).

Exchangeable cations (Na, K, Mg, Ca and Al) were determined by placing 2.00 ± 0.05 g air-dried soil in a 50 ml centrifuge tube with 0.2 M barium chloride. It was then placed on a horizontal shaker for 2 hours at 220 rpm, followed by centrifugation (Hettich Rotanta 460) for 5 minutes. The supernatant was filtered and analysed for exchangeable cations (Na⁺, K⁺, Mg²⁺, Ca²⁺ and Al³⁺) using ICP-OES (Thermo Scientific ICAP 7000 Series, UK). Residual soil was rinsed off the Whatman filter paper (#42) into a new 50 ml centrifuge tube using 0.01 M barium chloride, shaken for one hour and this procedure was repeated three times (Hendershot and Duquette, 1986). The supernatant was discarded each time and after the third decantation of 0.01 M barium chloride, 0.025 M MgSO₄ was added. After that, it was shaken overnight on a horizontal shaker, filtered through Whatman filter paper (#42) and the supernatant was analysed using ICP-OES for Mg content in soil. Finally, cation exchange capacity (CEC) in soil was calculated (Hendershot and Daquette, 1986).

Cold and hot water extractable carbon was determined after extracting the soil with cold and hot water followed by analysing with TOC Analyser (Elementar Vario TOC Select, UK) for measuring the dissolved organic carbon (DOC) of the extractant, according to the method outlined by Haynes and Francis (1993) modified by Ghani *et al.* (2003). 3 ± 0.05 g air-dried soil was put into a 50 ml polypropylene centrifuge tube, 30 ml of ultra-pure water was added, then placed on a horizontal shaker for 30 min at 20 °C. After extraction, the suspension was centrifuged at 3500 rpm for 20 minutes. The supernatant was filtered through a 0.45 micron cellulose nitrate filter which was analysed with TOC Analyser for determining DOC which was referred to as cold water extractable carbon (CWEC). CWEC is classified as labile and water soluble carbon (Ghani *et al.*, 2003). The soil was then resuspended using ultra-pure water, shaken vigorously for 10 seconds, and placed in an 80 °C water bath for 16 hours. The suspension was centrifuged, filtered and the solution was analysed with TOC Analyser as described before for DOC which indicated the hot water extractable carbon (HWEC). HWEC tends to correlate strongly with microbial biomass carbon and concentration of soil micro-aggregates (Ghani *et al.*, 2003).

Olsen phosphorus in the soil was determined by adding 5 ± 0.05 g air-dried soil to 100 ml of 0.5 M sodium hydrogen carbonate at pH 8.5, shaken for 30 minutes at 30 rpm, and the supernatant was filtered through Whatman filter paper (#2) (Almodares *et al.*, 2008; Rowell, 1994; Barrow and Shaw, 1974). Concentration of extractable phosphorus was determined using Autoanalyser (SEAL AutoAnalyzer 3 High Resolution, Germany).

Contents of ammonium and nitrate were determined using Autoanalyser (SEAL AutoAnalyzer 3 High Resolution, Germany) after mixing the fresh soil and 1 M potassium chloride at a ratio of 1:5. Samples were shaken on a horizontal shaker for one hour and filtered through GF/ A 15 cm filter paper (Gałka *et al.*, 2016; Rowell, 1994).

For determining P content in the soil pore water, pore water was extracted by centrifuging the soil (Richards and Weaver, 1944) followed by analysing with Autoanalyser (SEAL AutoAnalyzer 3 High Resolution, Germany). Around 40 g air-dried soil was moistened with 10 g of deionised water to maintain the soil water content of 25 % (w/ w) and left for one week at room temperature in an aluminium container. The soil was then transferred to a 20 ml disposable syringe. Glass wool (acted as a filter) was placed in a 2 mm deep layer that covered the bottom of the syringe. The syringe was placed in a 50 ml polypropylene centrifuge tube using a lid with a 25 mm hole in such a way that the syringe was fitted tightly

into the tube. After that, the samples were centrifuged for 10 minutes at 3500 rpm. Supernatant was pressure filtered through the glass wool which was further analysed with Autoanalyser (SEAL AutoAnalyzer 3 High Resolution, Germany) for determining P content in soil pore water.

Water holding capacity (WHC) of the soils were measured following the method of ISO 11274 (2019). In brief, approximately 50 g of air-dried soil was placed into open tubes of 3.5 cm diameter and 5 cm length with nylon mesh bases. The filled tubes were placed in a container of water and allowed to wet up by capillary action. When the soil surface had a glossy appearance, the cores were removed from the water and allowed to drain until they stopped dripping. The soil in the cores was then gently removed and weighed. The water holding capacity of the cores was determined as the weight of water held in the soil cores compared with the 105 °C oven dry weight of the sample (Milleret *et al.*, 2009).

Water stable aggregate (%WSA) was measured manually using wet sieving method (Boots *et al.*, 2019) following the protocol by Kemper and Chepil (1965); 4.0 g air-dried soils were sieved through a 2 mm sieve and the soils were placed into sieves for capillary rewetting in deionised water for 5 min. We used 250 µm sieves to test the stability of the soil fraction > 250 µm (macroaggregates) against water as a disintegrating force. For the test, the soils were sieved manually by moving the sieve up and down for a period of three minutes. The %WSA was calculated, after correction for the mass of soil > 250 µm, as the weight of aggregates remaining on the sieve relative to the total initial weight of aggregates (Milleret *et al.*, 2009).

5.2.6. Quality control and statistical analysis

Detection limits for all analytical instruments used were calculated as the mean plus six times the standard deviation of ten repeated measurements of the blank standard (Gill and Ramsey, 1997). For statistical analysis of solution data value below detection limit was given a value equal to the detection limit (Gill, 1997). Accuracy of calibration was determined by analysis of a certified reference material (CRM) or an in-house reference material. Analytical precision was calculated from the coefficient of variation (CV) determined from duplicate analysis of 10 % of the samples that were at least 100 times higher than the detection limit and determining the median of the difference between the duplicate measurements expressed as a percentage of their mean value (Gill and Ramsey, 1997; Walsh, 1997). Quality control data for chemical analysis associated with each set of experiments are provided in Table C2.

All data were analyzed using MINITAB (version 19) or SigmaPlot (version 14) software. Data were tested for normal distribution using the Shapiro-Wilk and Kolmogorov-Smirnov test; and equal variance using Levene's mean test. A two-way analysis of variance (ANOVA; soil type and treatment) was used to detect the differences in respiration rate, phosphatase enzyme activity, pH, exchangeable cations (Na, K, Mg, Ca and Al), effective and total cation exchange capacity, cold and hot water extractable carbon, Olsen phosphorus, ammonium, nitrate, soil water holding capacity, water stable aggregates, phosphorus in pore water, plant height, total chlorophyll content, shoot biomass (fresh and dry weight), root biomass (fresh and dry weight), root: shoot ratio (fresh and dry) and phosphorus in plant, across two soil types and four treatments. Data were normally distributed for all analyses except Mg content and effective cation exchange capacity (ECEC). Thus, within the Mg and ECEC datasets, data were square root transformed. Further analysis was made with post hoc test to know which treatment groups are different from each other at 5 % level of significance using Tukey's method. Pearson correlations were performed to determine how respiration rate, pH, and water extractable carbon across all soil types and treatments related to each other.

5.3. Results

5.3.1. Soil parameters

5.3.1.1. Respiration rate

Rate of respiration was determined for both incubated and greenhouse soils at the end of their experimental periods. For incubated soil, soil type and treatment had a significant ($p \leq 0.05$) influence on respiration rate; however, their interaction effect was not significant ($p \geq 0.05$). Respiration rate was significantly ($p \leq 0.05$) greater for high organic matter soil than for low organic matter soil. For both soils the 5.00 % treatment has a significantly ($p \leq 0.05$; $n = 4$) greater respiration rate than the other treatments (Figure 5.4a). No significant ($p \geq 0.05$) variation was found between control, 0.05 % and 0.50 % treatments for both soil types.

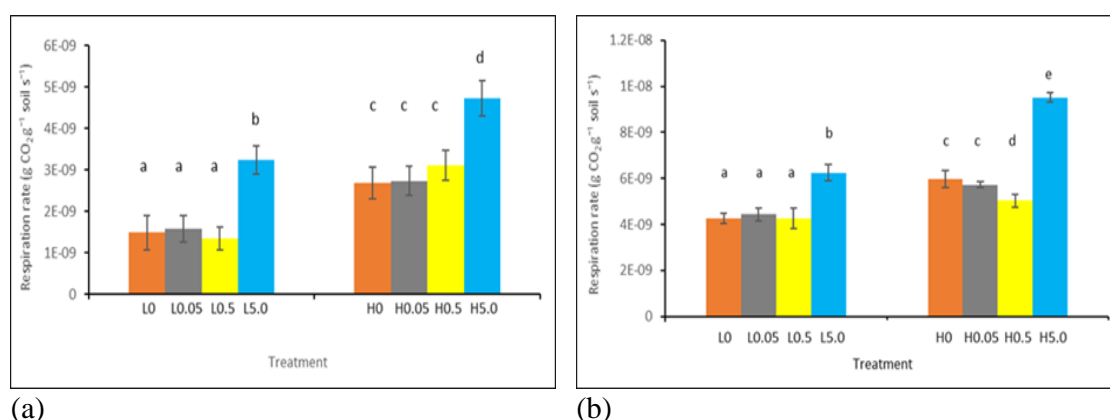


Figure 5.4. Respiration rate for (a) incubated and (b) greenhouse soil following HDPE treatments. Bars indicate standard deviations of means with four replicates ($n = 4$). Low organic matter control soil = L0, low organic matter soil with 0.05 % HDPE treatment = L0.05, low organic matter soil with 0.50 % HDPE treatment = L0.5, low organic matter soil with 5.00 % HDPE = L5.0, high organic matter control soil = H0, high organic matter soil with 0.05 % HDPE = H0.05, high organic matter soil with 0.50 % HDPE = H0.5, high organic matter soil with 5.00 % HDPE = H5.0. The letters indicate significant ($p \leq 0.05$) differences between treatment means as determined by post hoc tests.

Significant ($p \leq 0.05$) differences were found between soil type, treatment and their interaction for greenhouse experiment soils. High organic matter soil had significantly ($p \leq 0.05$) greater respiration rate than the low organic matter soil (Figure 5.4b). L5.0 had significantly ($p \leq 0.05$) higher respiration rate than L0, L0.05 and L0.5 treatments. No

significant ($p \geq 0.05$) difference was observed between L0, L0.05 and L0.5 treatments. Respiration rate in H0.5 was significantly ($p \leq 0.05$) lower than the H0 and H0.05. H5.0 had the highest respiration rates ($p \leq 0.05$; Figure 5.4b).

5.3.1.2. Phosphatase enzyme activity

Figure 5.5a and Figure 5.5b show the changes in phosphatase enzyme activity due to microplastics addition for both incubated and greenhouse experiments. Two-way ANOVA of the incubation study indicates that there were significant ($p \leq 0.05$) differences between soil types, HDPE treatments and their interaction. High organic matter soils had significantly ($p \leq 0.05$) greater respiration rate than the low organic matter ones. The addition of microplastics significantly increased the enzyme activity in the 5.00 % treatments compared to the controls which was applicable for both soil types (Figure 5.5a). L0, L0.05 and L0.5 were not significantly different from each other ($p \geq 0.05$). Also, no significant ($p \geq 0.05$) difference was found between H0, H0.05 and H0.5 (Figure 5.5a).

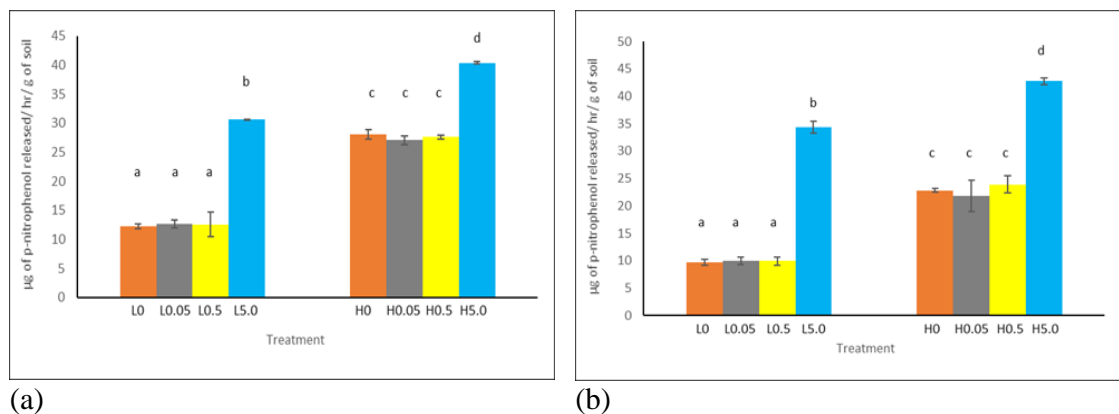


Figure 5.5. Phosphatase enzyme activity for (a) incubated and (b) greenhouse soil following HDPE treatments. Bars indicate standard deviations of means with four replicates ($n = 4$). Control, 0.05 %, 0.50 % and 5.00 % indicated HDPE application rates: low organic matter control soil = L0, low organic matter soil with 0.05 % HDPE = L0.05, low organic matter soil with 0.50 % HDPE = L0.5, low organic matter soil with 5.00 % HDPE = L5.0, high organic matter control soil = H0, high organic matter soil with 0.05 % HDPE = H0.05, high organic matter soil with 0.50 % HDPE = H0.5, high organic matter soil with 5.00 % HDPE = H5.0. The letters indicate significant ($p \leq 0.05$) differences between treatment means as determined by post hoc tests.

Greenhouse soils (Figure 5.5b) responded in a similar way to the treatments as the incubated soils for the phosphatase enzyme activity. Enzyme activity was significantly ($p \leq 0.05$) greater in L5.0 compared to other three (L0, L0.05 and L0.5) treatments. Pairwise comparison indicated that these three treatments (L0, L0.05 and L0.5) were not significantly different from each other. Same trend was observed for the high organic matter soils; H5.0 had the highest enzyme activity; H0, H0.05 and H0.5 were not significantly different from each other (Figure 5.5b).

5.3.1.3. Soil pH

Soil type, treatment and their interaction showed significant ($p \leq 0.05$) influence on soil pH for the incubation study. High organic matter soils had higher pH than the low organic matter soils. The maximum value of soil pH was recorded in the L5.0 treatments. Soil pH was significantly ($p \leq 0.05$) lower in the L0 compared to the L0.5 and L5.0. L0.5 and L5.0 were significantly ($p \leq 0.05$) different from each other whereas no significant ($p \geq 0.05$) difference was found between L0 and L0.05 (Figure 5.6a). Soil pH was lower in H0 which was significantly ($p \leq 0.05$) increased in H0.5 and H5.0. Both H0.5 and H5.0 were significantly ($p \geq 0.05$) different from each other. No significant ($p \geq 0.05$) variation was found between H0 and H0.05 (Figure 5.6a).

Like the incubated soils, high organic matter greenhouse soils had higher soil pH than the low organic matter ones. For both low and high organic matter soils, the pH was significantly ($p \leq 0.05$) higher in the 0.5 % and 5.0 % microplastic treatments than in the 0.05 % treatments and controls (Figure 5.6b). All these treatments (control, 0.5 % and 5.0 %) were significantly ($p \leq 0.05$) different from each other, although no difference was found between control and 0.05 % treatments.

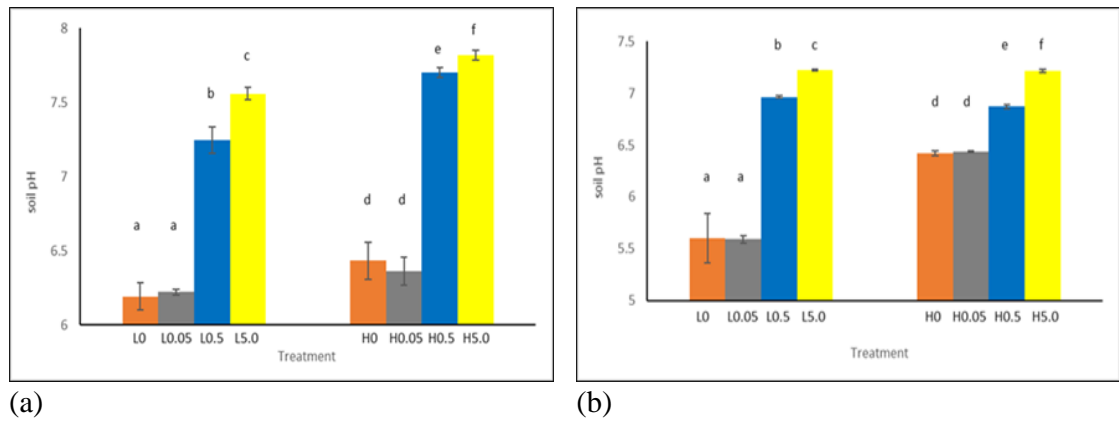


Figure 5.6. Soil pH for (a) incubated and (b) greenhouse soil following HDPE treatments. The bars indicate standard deviations of means with four replicates ($n = 4$). Control, 0.05 %, 0.50 % and 5.00 % indicated HDPE application rates: low organic matter control soil = L0, low organic matter soil with 0.05 % HDPE = L0.05, low organic matter soil with 0.50 % HDPE = L0.5, low organic matter soil with 5.00 % HDPE = L5.0, high organic matter control soil = H0, high organic matter soil with 0.05 % HDPE treatment = H0.05, high organic matter soil with 0.50 % HDPE = H0.5, high organic matter soil with 5.00 % HDPE = H5.0. The letters indicate significant ($p \leq 0.05$) differences between treatment means as determined by post hoc tests.

5.3.1.4. Exchangeable cations

For incubation experiment, the outcomes of two-way ANOVA tests performed between the soil type and treatment for exchangeable cations (Na^+ , K^+ , Mg^{2+} , Ca^{2+} and Al^{3+}) are summarised in Table 5.1. Different cations behaved differently in the experiment. There was a significant effect of the soil type for exchangeable K^+ , Mg^{2+} and Ca^{2+} . Mean concentrations of K^+ and Ca^{2+} were greater in high organic matter soils compared to the low organic matter soils whereas concentrations of Mg^{2+} were lower in high organic matter soils than the low organic matter soils. Treatment effect was significant for all exchangeable cations *viz.*, K^+ , Mg^{2+} , Ca^{2+} and Al^{3+} , except Na^+ (Table 5.1). Interaction effect was not found for Na^+ and Al^{3+} . No significant ($p \geq 0.05$) variation was found for the mean concentrations of exchangeable Na^+ , K^+ and Ca^{2+} when considering the incubated low organic matter soils as shown in [Figure 5.7 (a, b and c)]. Mg^{2+} and Al^{3+} decreased significantly in the L5.0 treated soils from the L0 [Figure 5.7 (c and h)]. Mean concentrations of Na^+ was decreased significantly only in the H5.0 [Figure 5.7 (a)] whereas concentrations of K^+ , Mg^{2+} and Ca^{2+}

reduced in both H0.5 and H5.0 amended soils [Figure 5.7 (b, c and g)] compared to that of the H0.

In contrast to the incubation experiment, greenhouse experiment showed a slightly different response for the exchangeable cations. Significant ($p \leq 0.05$) effect was found for the soil type for all exchangeable cations (K^+ , Mg^{2+} , Ca^{2+} and Al^{3+}), except Na^+ (Table 5.2). Mean concentrations of Mg^{2+} and Al^{3+} were higher in the low organic matter soils compared to that of the high organic matter ones. Opposite findings were found for K^+ and Ca^{2+} ; higher concentrations were found in the high organic matter soils. Treatment effect was not found for Na^+ and Al^{3+} . Interaction (soil type * treatment) effect was not associated with Al^{3+} (Table 5.2). Mean concentrations of Na^+ , Mg^{2+} and Ca^{2+} were decreased significantly ($p \leq 0.05$) in the L5.0 treatments [Figure 5.7 (d, f and i)] compared to the L0. No significant difference ($p \geq 0.05$) was associated with K^+ (Figure 5.7e) and Al^{3+} (Figure 5.7j) for the low organic matter soils. Regarding high organic matter soils, mean concentrations of K^+ and Ca^{2+} were declined significantly ($p \leq 0.05$) in both H0.5 and H5.0 soils [Figure 5.7 (e and i)] whereas concentrations of Na^+ and Mg^{2+} were decreased in only H5.0 [Figure 5.7 (d and f)] compared to the H0.

Table 5.1. Effects of different factors on exchangeable cations for incubated soils. There are two factors: soil type and treatment. Two types of soils differing in organic matter contents and four treatments (control, 0.05 %, 0.50 % and 5.00 % HDPE) were used. For all cases, n = 4.

Factor	Na ⁺		K ⁺		Mg ²⁺		Ca ²⁺		Al ³⁺	
	F value	P value	F value	P value	F value	P value	F value	P value	F value	P value
Soil type	3.952	≥ 0.05	11.339	≤ 0.05	5.517	≤ 0.05	165.070	≤ 0.05	0.866	≥ 0.05
Treatment	10.022	≥ 0.05	59.381	≤ 0.05	63.843	≤ 0.05	90.758	≤ 0.05	7.401	≤ 0.05
Soil type × Treatment	4.814	≥ 0.05	32.920	≤ 0.05	31.200	≤ 0.05	104.511	≤ 0.05	0.448	≥ 0.05

Table 5.2. Effects of different factors on exchangeable cations for greenhouse soils. There are two factors: soil type and treatment. Two types of soils differing in organic matter contents and four treatments (control, 0.05 %, 0.50 % and 5.00 % HDPE) were used. For all cases, n = 4.

Factor	Na ⁺		K ⁺		Mg ²⁺		Ca ²⁺		Al ³⁺	
	F value	P value	F value	P value	F value	P value	F value	P value	F value	P value
Soil type	3.952	≥ 0.05	100.687	≤ 0.05	351.475	≤ 0.05	175.616	≤ 0.05	15.447	≤ 0.05
Treatment	2.689	≥ 0.05	33.631	≤ 0.05	41.133	≤ 0.05	80.104	≤ 0.05	1.929	≥ 0.05
Soil type × Treatment	8.915	≤ 0.05	27.822	≤ 0.05	12.863	≤ 0.05	51.499	≤ 0.05	0.868	≥ 0.05

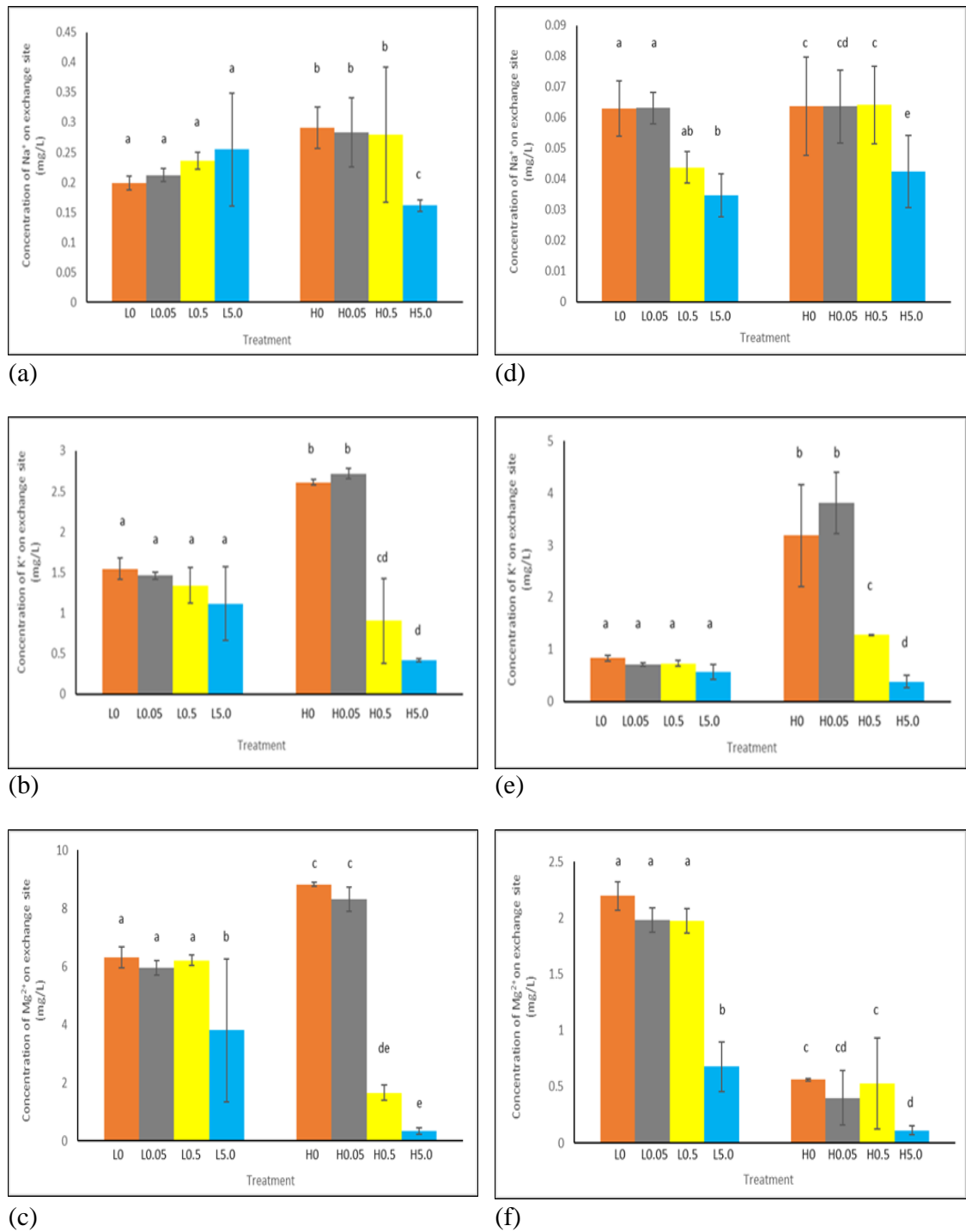
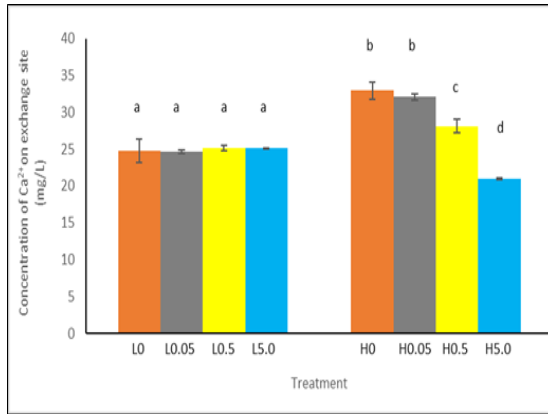
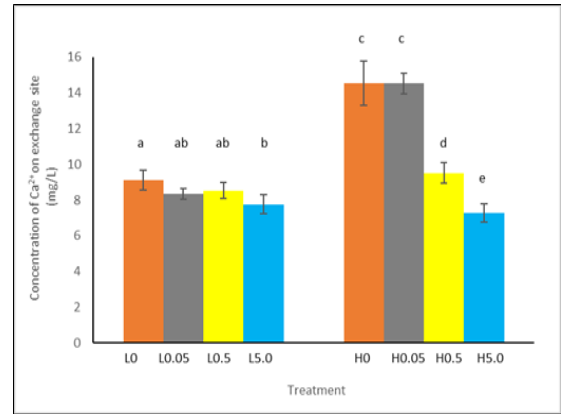


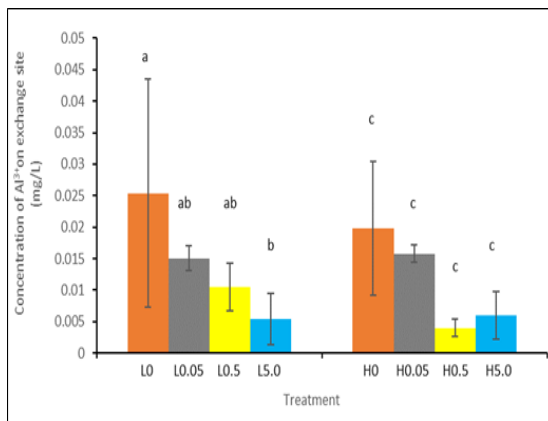
Figure 5.7. Concentration of exchangeable cations: (a) Na⁺, (b) K⁺, (c) Mg²⁺ for the incubated soil, (d) Na⁺, (e) K⁺, (f) Mg²⁺ for the greenhouse soil following HDPE treatments. Bars indicate standard deviations of means with four replicates (n = 4). The letters indicate significant (p ≤ 0.05) differences between treatment means as determined by post hoc tests. Control, 0.05 %, 0.50 % and 5.00 % indicated HDPE application rates.



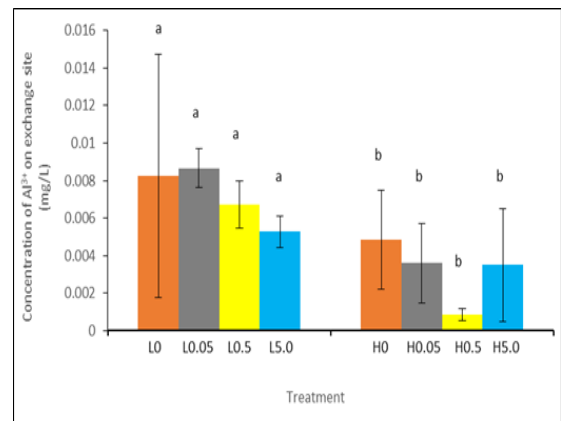
(g)



(i)



(h)



(j)

Figure 5.7 (continued). Concentration of exchangeable cations: (g) Ca²⁺, (h) Al³⁺ for the incubated soil, (i) Ca²⁺, (j) Al³⁺ for the greenhouse soil following HDPE treatments. Bars indicate standard deviations of means with four replicates (n = 4). Control, 0.05 %, 0.50 % and 5.00 % indicated HDPE application rates: low organic matter control soil = L0, low organic matter soil with 0.05 % HDPE = L0.05, low organic matter soil with 0.50 % HDPE = L0.5, low organic matter soil with 5.00 % HDPE = L5.0, high organic matter control soil = H0, high organic matter soil with 0.05 % HDPE treatment = H0.05, high organic matter soil with 0.50 % HDPE = H0.5, high organic matter soil with 5.00 % HDPE = H5.0. The letters indicate significant ($p \leq 0.05$) differences between treatment means as determined by post hoc tests.

5.3.1.5. Effective cation exchange capacity (ECEC) and total cation exchange capacity (TCEC)

Significant ($p \leq 0.05$) differences were found between soil type, treatment and their interaction for incubated soils. High organic matter soils had significantly ($p \leq 0.05$) greater ECEC than the low organic matter soils. There was a significant ($p \leq 0.05$) decrease in ECEC in the L5.0 by 33 % compared to the L0. Significant ($p \leq 0.05$) decreases were also found in H0.5 and H5.0 treatments by 38 % and 47 % respectively (Figure 5.8a) from the H0. ECEC of the H0, H0.5 and H5.0 treatments were significantly different from each other (Figure 5.8a). For both soil types, there was no difference between control and 0.05 % treatments.

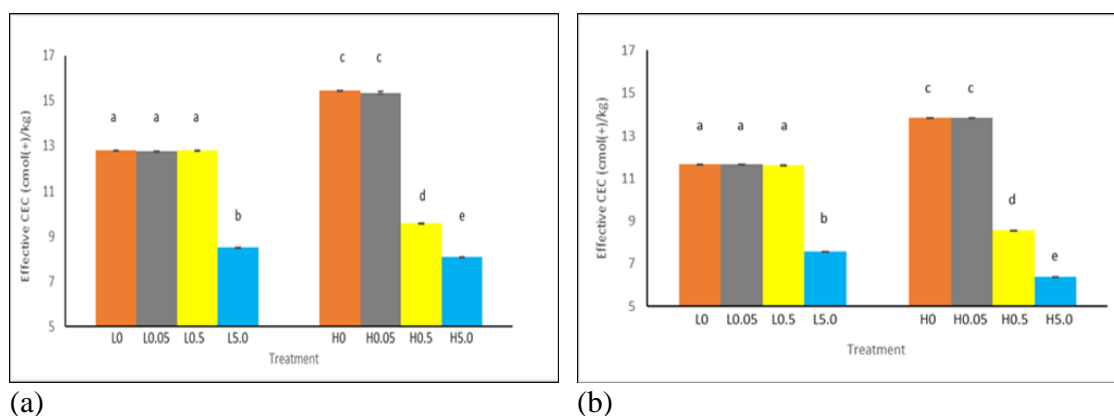


Figure 5.8. ECEC for (a) incubated and (b) greenhouse soil following HDPE treatments. Bars indicate standard deviations of means with four replicates ($n = 4$). Control, 0.05 %, 0.50 % and 5.00 % indicated HDPE application rates: low organic matter control soil = L0, low organic matter soil with 0.05 % HDPE = L0.05, low organic matter soil with 0.50 % HDPE = L0.5, low organic matter soil with 5.00 % HDPE = L5.0, high organic matter control soil = H0, high organic matter soil with 0.05 % HDPE treatment = H0.05, high organic matter soil with 0.50 % HDPE = H0.5, high organic matter soil with 5.00 % HDPE = H5.0. The letters indicate significant ($p \leq 0.05$) differences between treatment means as determined by post hoc tests.

Like the incubated soils, there were significant ($p \leq 0.05$) differences between soil type, treatment and their interaction for the greenhouse soils. ECEC was significantly ($p \leq 0.05$) greater in high organic matter soils than in the low organic matter soils. The ECEC was significantly ($p \leq 0.05$) decreased by 35 % in L5.0 treatments from the L0. H0.5 and H5.0 showed significantly ($p \leq 0.05$) lower ECEC by 38 % and 54 % respectively when compared

with the H0 (Figure 5.8b). No significant ($p \geq 0.05$) difference was observed between control and 0.05 % treatments for both soil types.

While significantly ($p \leq 0.05$) lower total cation exchange capacity (TCEC) was observed in incubated L5.0 treatments compared to the L0, there were significantly ($p \leq 0.05$) lower TCECs in H0.5 and H5.0 treatments when comparing with the H0 treatments (Figure 5.9a). There was no significant ($p \geq 0.05$) difference between L0, L0.05 and L0.5 whereas significant ($p \leq 0.05$) difference was seen between H0.5 and H5.0 (Figure 5.9a).

Both soil types showed similar trend in the greenhouse study. L0.5 and L5.0 had significantly ($p \leq 0.05$) lower TCEC than the L0 (Figure 5.9b). H0.5 and H5.0 had significantly ($p \leq 0.05$) lower TCEC as compared with the H0; H0, H0.5 and H5.0 were significantly ($p \leq 0.05$) different from each other (Figure 5.9b). For both soil types, no difference was found between control and 0.05 % treatments.

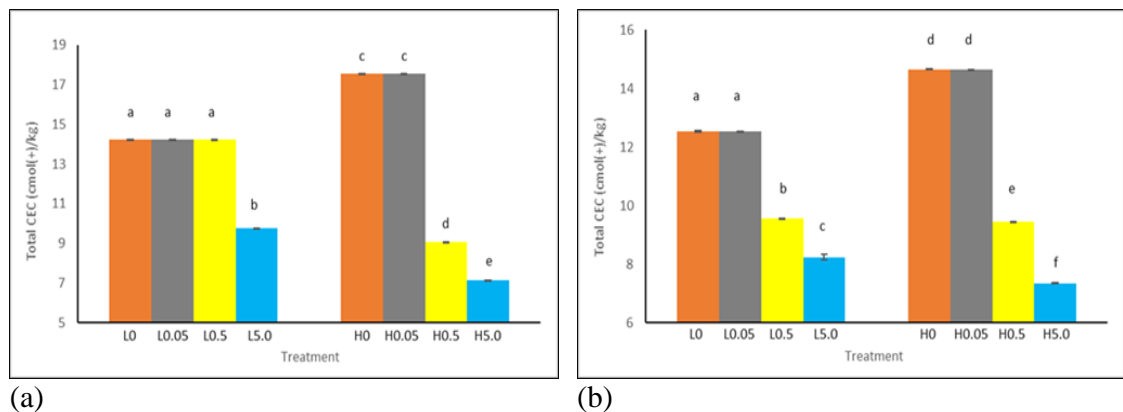


Figure 5.9. TCEC for (a) incubated and (b) greenhouse soil following HDPE treatments. Bars indicate standard deviations of means with four replicates ($n = 4$). Control, 0.05 %, 0.50 % and 5.00 % indicated HDPE application rates: low organic matter control soil = L0, low organic matter soil with 0.05 % HDPE = L0.05, low organic matter soil with 0.50 % HDPE = L0.5, low organic matter soil with 5.00 % HDPE = L5.0, high organic matter control soil = H0, high organic matter soil with 0.05 % HDPE treatment = H0.05, high organic matter soil with 0.50 % HDPE = H0.5, high organic matter soil with 5.00 % HDPE = H5.0. The letters indicate significant ($p \leq 0.05$) differences between treatment means as determined by post hoc tests.

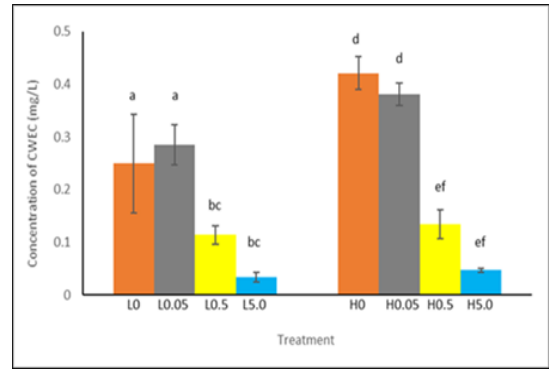
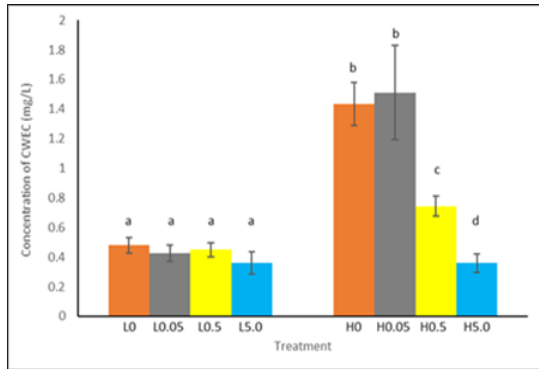
5.3.1.6. Water extractable carbon (WEC)

Two functional pools of water extractable carbon (WEC) were studied in our study: a) cold water extractable carbon (CWEC) and b) hot water extractable carbon (HWEC). CWEC is highly mobile and quantitatively is very close to the dissolved organic carbon in soil. Compared to the CWEC, HWEC gives indications of microbial activity, microbial biomass C, C cycling and microaggregate concentration (Ghani *et al.*, 2003). Effects of soil, treatment and their interaction were significant for the incubation study regarding concentrations of CWEC. Concentrations of CWEC were significantly ($p \leq 0.05$) higher in the incubated high organic matter soils compared to the low organic matter ones. No difference was observed between L0, L0.05, L0.5 and L5.0. CWEC was reduced in H0.5 and H5.0 treatments by 6 % and 25 % respectively compared to the H0. Significant ($p \leq 0.05$) difference was observed between the H0.5 and H5.0 treatments also (Figure 5.10a).

Effects of soil and treatment had significant ($p \leq 0.05$) impacts on CWEC, but their interaction had no impact ($p \geq 0.05$) in the greenhouse study. CWEC was higher in the high organic matter soils than the low organic matter ones. CWEC was decreased significantly in L0.5 and L5.0 by 54 % and 86 % respectively from the L0, although L0.5 and L5.0 were not significantly ($p \geq 0.05$) different from each other (Figure 5.10b). Likewise, CWEC was decreased significantly by 68 % in the H0.5 treatments and 88 % in H5.0 treatments relative to the H0 (Figure 5.10b). However, no difference was associated between H0.5 and H5.0. There was no variation in control and 0.05 % treatments for both soil types.

Soil type and treatment had a significant ($p \leq 0.05$) influence on HWEC; however, their interaction effect was not significant ($p \geq 0.05$) for the incubation study. HWEC was significantly ($p \leq 0.05$) higher in the high organic matter soils than the low organic matter soils. For both soils, HWEC was significantly ($p \leq 0.05$) declined in 0.50 % and 5.00 % treatments (Figure 5.11a).

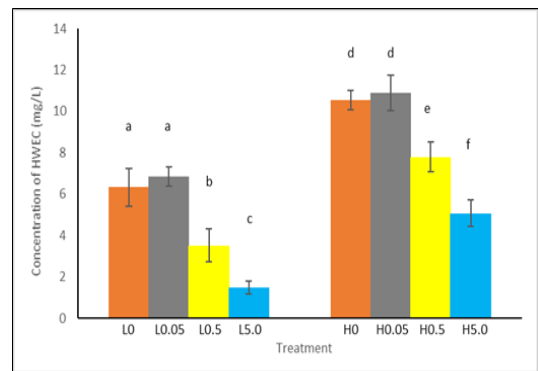
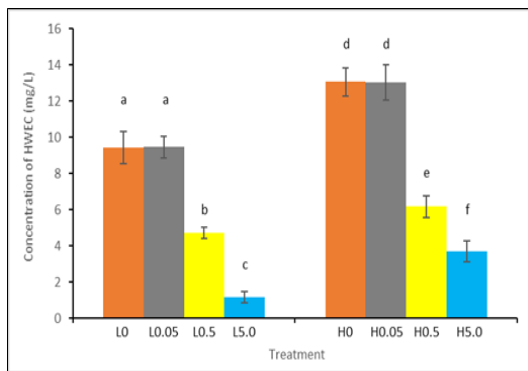
Similar findings were observed from the two-way ANOVA tests for the greenhouse study. Concentrations of HWEC were significantly ($p \leq 0.05$) higher in the high organic matter soils than the low organic matter ones. For both soil types, 0.50 % and 5.00 % treatments showed reductions in HWEC (Figure 5.11b).



(a)

(b)

Figure 5.10. CWEC for (a) incubated and (b) greenhouse soil following HDPE treatments. The bars indicate standard deviations of means with four replicates ($n = 4$). Control, 0.05 %, 0.50 % and 5.00 % indicated HDPE application rates: low organic matter control soil = L0, low organic matter soil with 0.05 % HDPE = L0.05, low organic matter soil with 0.50 % HDPE = L0.5, low organic matter soil with 5.00 % HDPE = L5.0, high organic matter control soil = H0, high organic matter soil with 0.05 % HDPE treatment = H0.05, high organic matter soil with 0.50 % HDPE = H0.5, high organic matter soil with 5.00 % HDPE = H5.0. The letters indicate significant ($p \leq 0.05$) differences between treatment means as determined by post hoc tests.



(a)

(b)

Figure 5.11. HWEC for (a) incubated and (b) greenhouse soil following HDPE treatments. Bars indicate standard deviations of means with four replicates ($n = 4$). Control, 0.05 %, 0.50 % and 5.00 % indicated HDPE application rates: low organic matter control soil = L0, low organic matter soil with 0.05 % HDPE = L0.05, low organic matter soil with 0.50 % HDPE = L0.5, low organic matter soil with 5.00 % HDPE = L5.0, high organic matter control soil = H0, high organic matter soil with 0.05 % HDPE = H0.05, high organic matter soil with 0.50 % HDPE = H0.5, high organic matter soil with 5.00 % HDPE = H5.0. The letters indicate significant ($p \leq 0.05$) differences between treatment means as determined by post hoc tests.

5.3.1.7. Olsen phosphorus (P)

In both incubation and greenhouse experiments, outcomes of two-way ANOVA are similar, indicating that soil types, treatments and their interaction showed significant ($p \leq 0.05$) differences in the concentration of Olsen P. High organic matter soils had higher Olsen P than the low organic matter soils which was true for both experiments. Incubated L5.0 treatments contained significantly ($p \leq 0.05$) less Olsen P compared to the L0. There were no significant differences between the L0, L0.05 and L0.5 treatments (Figure 5.12a). Concentrations of Olsen P in the H0.5 and H5.0 treatments were significantly ($p \leq 0.05$) reduced from the H0 treatments (Figure 5.12a). H0.5 and H5.0 treatments were significantly ($p \leq 0.05$) different from each other though no variation was found between H0 and H0.05.

For greenhouse studies, no significant ($p \geq 0.05$) interaction effect was found between the low organic matter soils and treatments (L0, L0.05, L0.5 and L5.0; Figure 5.12b). Olsen P concentrations were found to be decreased in H0.5 and H5.0 compared with the H0 (Figure 5.12b). H0, H0.5 and H5.0 treatments were significantly different from one another. No significant variation was seen between H0 and H0.05.

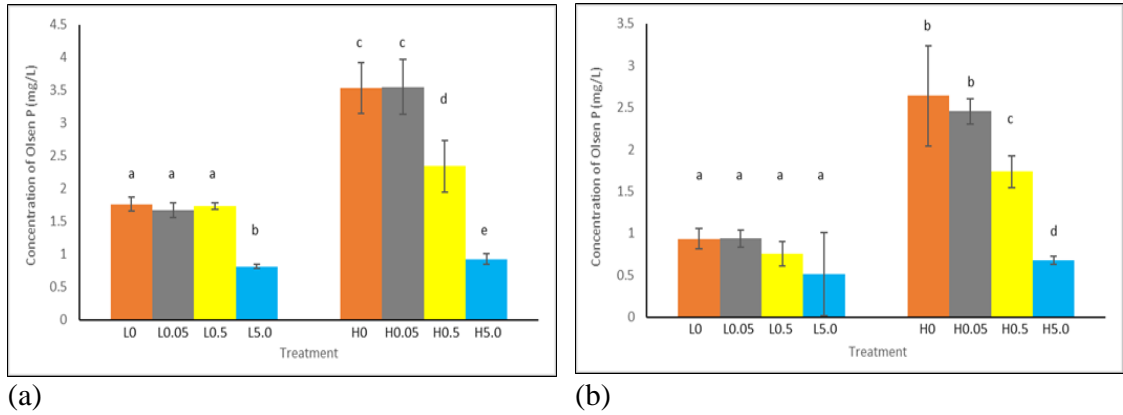


Figure 5.12. Olsen phosphorus for (a) incubated and (b) greenhouse soil following HDPE treatments. Bars indicate standard deviations of means with four replicates ($n = 4$). Control, 0.05 %, 0.50 % and 5.00 % indicated HDPE application rates: low organic matter control soil = L0, low organic matter soil treated with 0.05 % HDPE = L0.05, low organic matter soil with 0.50 % HDPE = L0.5, low organic matter soil with 5.00 % HDPE = L5.0, high organic matter control soil = H0, high organic matter soil with 0.05 % HDPE = H0.05, high organic matter soil with 0.50 % HDPE = H0.5, high organic matter soil with 5.00 % HDPE = H5.0. The letters indicate significant ($p \leq 0.05$) differences between treatment means as determined by post hoc tests.

5.3.1.8. Ammonium (NH_4^+) and nitrate (NO_3^-)

Concentration of NH_4^+ showed similar results in both incubation (Figure 5.13a) and greenhouse (Figure 5.13b) studies. Effects of treatment was significant ($p \leq 0.05$), but effects of soil and interaction between soil and treatment were not significant ($p \leq 0.05$). NH_4^+ concentration was significantly ($p \leq 0.05$) lower in the L5.0 than in the L0, L0.05 and L0.5 treatments. There was no significant ($p \geq 0.05$) variation between L0, L0.05 and L0.5 treatments. The same trend was seen for the high organic matter soils.

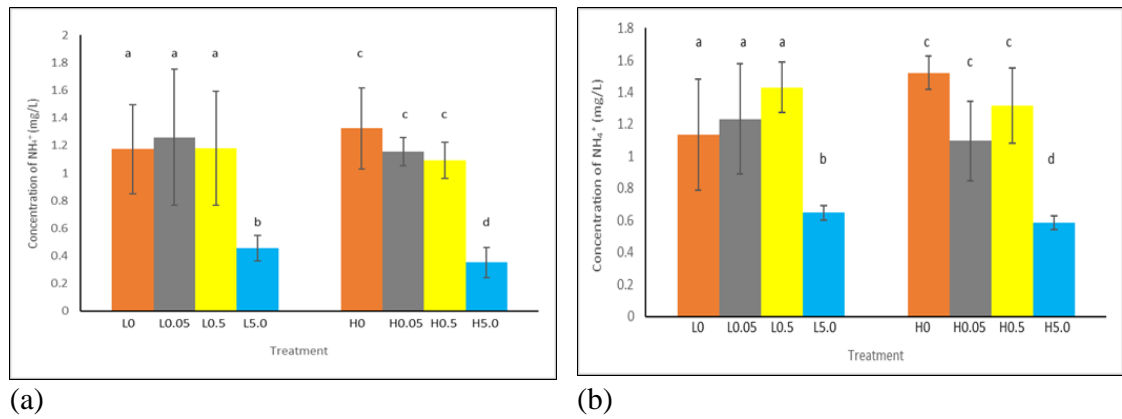


Figure 5.13. NH_4^+ for (a) incubated and (b) greenhouse soil following HDPE treatments. Bars indicate standard deviations of means with four replicates ($n = 4$). Control, 0.05 %, 0.50 % and 5.00 % indicated HDPE application rates: low organic matter control soil = L0, low organic matter soil with 0.05 % HDPE = L0.05, low organic matter soil with 0.50 % HDPE = L0.5, low organic matter soil with 5.00 % HDPE = L5.0, high organic matter control soil = H0, high organic matter soil with 0.05 % HDPE treatment = H0.05, high organic matter soil with 0.50 % HDPE = H0.5, high organic matter soil with 5.00 % HDPE = H5.0. The letters indicate significant ($p \leq 0.05$) differences between treatment means as determined by post hoc tests.

Soil and treatment had significant impacts on NO_3^- concentrations in the incubation study. Incubated high organic matter soils had significantly ($p \leq 0.05$) higher NO_3^- concentrations when compared to the low organic matter soils. For both soil types, NO_3^- in control, 0.05 % and 0.5 % treatments were not significantly ($p \geq 0.05$) different from one another but were significantly ($p \leq 0.05$) greater than the NO_3^- concentrations in the L5.0 (Figure 5.14a).

Soil, treatment and their interaction showed significant influence on NO_3^- concentrations in the greenhouse study. NO_3^- concentrations were significantly ($p \leq 0.05$) higher in high organic matter soils than in the low organic matter soils. Comparisons of the L0 with other treatments (L0.05, L0.5 and L5.0) indicated significant ($p \leq 0.05$) decreases in the concentrations of NO_3^- in the L5.0 from the L0. No significant ($p \geq 0.05$) difference was recorded between L0.5 and L5.0. Concentrations of NO_3^- was significantly reduced in L5.0 than the L0.05 treatments (Figure 5.14b). No significant difference was associated between L0, L0.05 and L0.5. NO_3^- concentrations was decreased significantly ($p \leq 0.05$) in the H5.0 treatments when comparing to the H0. There was no significant difference between H0, H0.05 and H0.5 (Figure 5.14b).

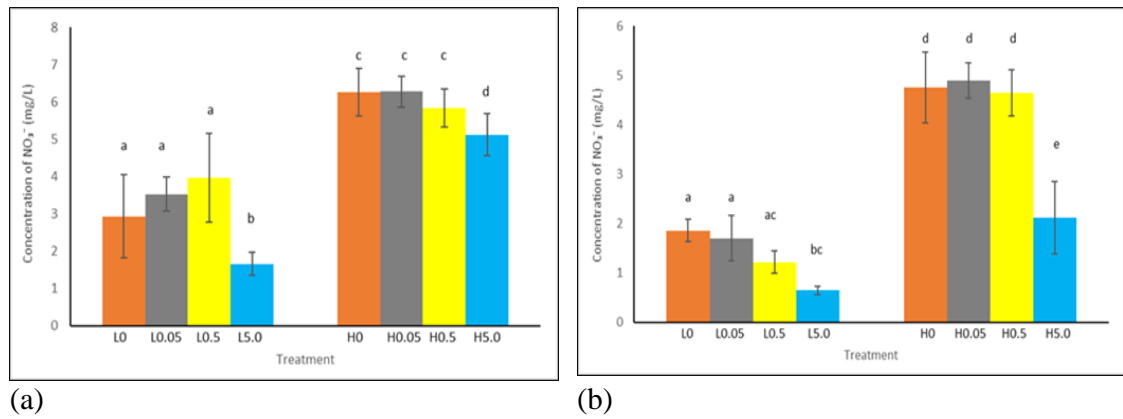


Figure 5.14. NO_3^- for (a) incubated and (b) greenhouse soil following HDPE treatments. Bars indicate standard deviations of means with four replicates ($n = 4$). Control, 0.05 %, 0.50 % and 5.00 % indicated HDPE application rates: low organic matter control soil = L0, low organic matter soil with 0.05 % HDPE = L0.05, low organic matter soil with 0.50 % HDPE = L0.5, low organic matter soil with 5.00 % HDPE = L5.0, high organic matter control soil = H0, high organic matter soil with 0.05 % HDPE treatment = H0.05, high organic matter soil with 0.50 % HDPE = H0.5, high organic matter soil with 5.00 % HDPE = H5.0. The letters indicate significant ($p \leq 0.05$) differences between treatment means as determined by post hoc tests.

5.3.1.9. Phosphorus in soil pore water

Soil type, treatment and their interaction had significant ($p \leq 0.05$) influences on P content in soil pore water for the incubation experiment. Significantly ($p \leq 0.05$) lower P content was found in low organic matter soils compared to the high organic matter ones. P content was significantly lower in the L5.0 than in L0. No significant ($p \geq 0.05$) differences among other treatments (L0, L0.05 and L0.5) were observed (Figure 5.15a). H0.5 and H5.0 had significantly ($p \leq 0.05$) lower P contents compared to the H0. Significant ($p \leq 0.05$) differences were also found between H0.5 and H5.0. There was no difference between H0 and H0.05 treatments.

In the greenhouse experiment, P contents in the pore water showed significant differences across soil type, treatment and their interaction. P content is greater in high organic matter soils than in the low organic matter ones. No difference ($p \geq 0.05$) was observed in L0, L0.05, L0.5 and L5.0, while significant ($p \leq 0.05$) differences were found in H0.5 and H5.0 (Figure

5.15b) compared to that of the H0. Both H0.5 and H5.0 were significantly ($p \leq 0.05$) different from each other (Figure 5.17b). However, no variation was found between H0 and H0.05.

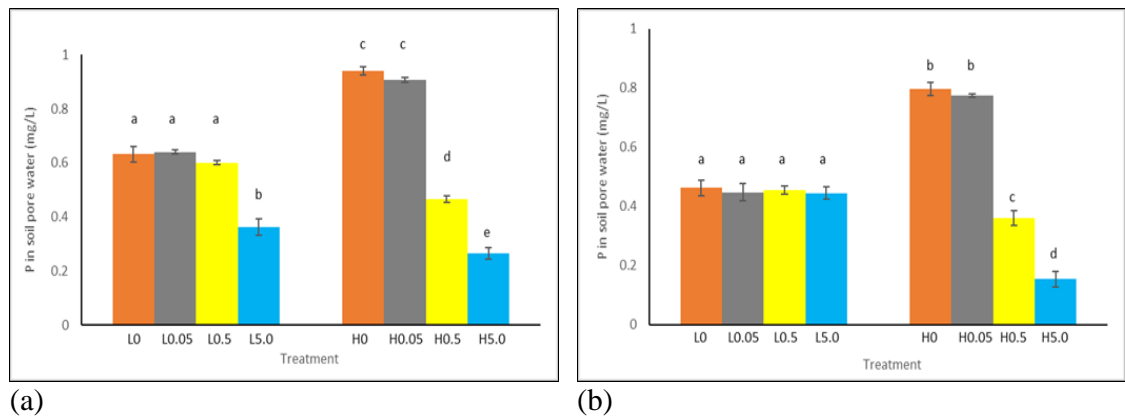


Figure 5.15. Phosphorus in soil pore water for (a) incubated and (b) greenhouse soil following HDPE treatments. Bars indicate standard deviations of means with four replicates ($n = 4$). Control, 0.05 %, 0.50 % and 5.00 % indicated HDPE application rates: low organic matter control soil = L0, low organic matter soil with 0.05 % HDPE = L0.05, low organic matter soil with 0.50 % HDPE = L0.5, low organic matter soil with 5.00 % HDPE = L5.0, high organic matter control soil = H0, high organic matter soil with 0.05 % HDPE = H0.05, high organic matter soil with 0.50 % HDPE = H0.5, high organic matter soil with 5.00 % HDPE = H5.0. The letters indicate significant ($p \leq 0.05$) differences between treatment means as determined by post hoc tests.

5.3.1.10. Water holding capacity (WHC) of soil

WHC was significantly ($p \leq 0.05$) influenced by soil type, treatment and their interaction in the incubation study. WHC is significantly ($p \leq 0.05$) greater in high organic matter soils than the low organic matter ones. WHC was significantly ($p \leq 0.05$) decreased in L5.0 compared to the L0 treatments. There was no significant ($p \geq 0.05$) difference between L0, L0.05 and L0.5 (Figure 5.16a). WHC of H0.5 and H5.0 was significantly lower than that of H0 treatments. However, H0.5 and H5.0 were not significantly ($p \geq 0.05$) different from each other.

In the greenhouse study, soil type, treatment and their interaction showed significant ($p \leq 0.05$) influences on WHC. High organic matter soils had higher WHC than the low organic matter soils. WHC of L5.0 was significantly lower than the L0 treatments. There was no

significant ($p \geq 0.05$) difference between L0, L0.05 and L0.5 (Figure 5.16b). However, WHC was significantly ($p \leq 0.05$) decreased in H0.5 and H5.0 compared to the H0 treatments. H0, H0.5 and H5.0 were significantly different from each other (Figure 5.16b), but there was no difference between H0 and H0.05 treatments.

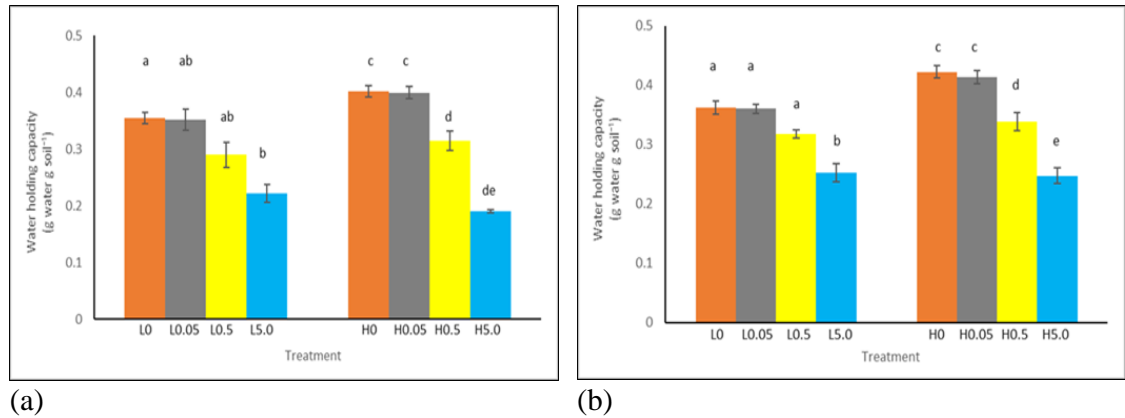


Figure 5.16. Soil water holding capacity for (a) incubated and (b) greenhouse soil following HDPE treatments. Bars indicate standard deviations of means with four replicates ($n = 4$). Control, 0.05 %, 0.50 % and 5.00 % indicated HDPE application rates: low organic matter control soil = L0, low organic matter soil with 0.05 % HDPE = L0.05, low organic matter soil with 0.50 % HDPE = L0.5, low organic matter soil with 5.00 % HDPE = L5.0, high organic matter control soil = H0, high organic matter soil with 0.05 % HDPE = H0.05, high organic matter soil with 0.50 % HDPE = H0.5, high organic matter soil with 5.00 % HDPE = H5.0. The letters indicate significant ($p \leq 0.05$) differences between treatment means as determined by post hoc tests.

5.3.1.11. Water stable aggregates (WSA)

For both incubation (Figure 5.17a) and greenhouse (Figure 5.17b) experiments, soil type and treatment had significant ($p \leq 0.05$) impacts on %WSA, but no interaction effect ($p \geq 0.05$) was found. 0.5 % and 5.00 % treatments had significantly ($p \leq 0.05$) lower %WSA compared to the controls. Although there was no variation ($p \geq 0.05$) between control and 0.05 % treatments, 0.5 % and 5.00 % treatments were significantly ($p \leq 0.05$) different from each other (Figure 5.17a, 5.17b). Both soil types behaved similarly in the incubation and greenhouse studies.

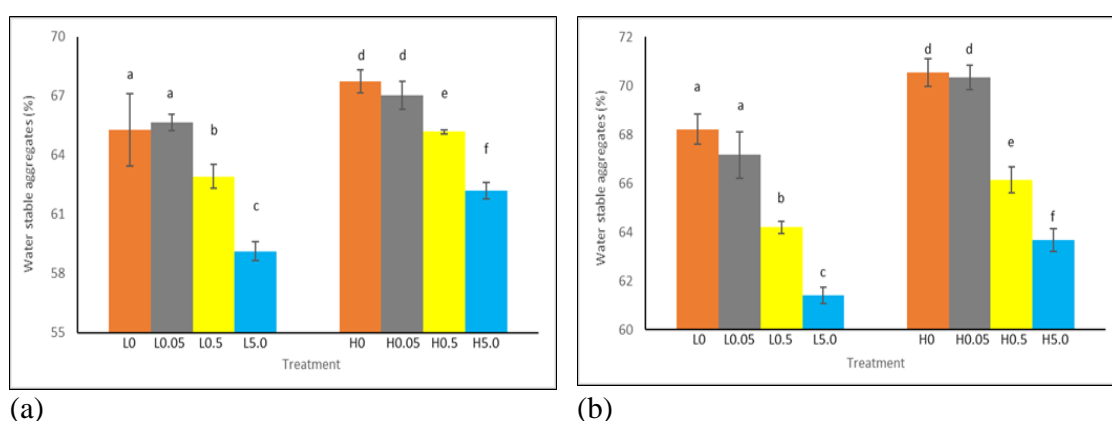


Figure 5.17. Water stable aggregates for (a) incubated and (b) greenhouse soil following HDPE treatments. Bars indicate standard deviations of means with four replicates ($n = 4$). Control, 0.05 %, 0.50 % and 5.00 % indicated HDPE application rates: low organic matter control soil = L0, low organic matter soil with 0.05 % HDPE = L0.05, low organic matter soil with 0.50 % HDPE = L0.5, low organic matter soil with 5.00 % HDPE = L5.0, high organic matter control soil = H0, high organic matter soil with 0.05 % HDPE = H0.05, high organic matter soil with 0.50 % HDPE = H0.5, high organic matter soil with 5.00 % HDPE = H5.0. The letters indicate significant ($p \leq 0.05$) differences between treatment means as determined by post hoc tests.

5.3.1.12. Relationship of respiration rate, pH and water extractable carbon

For both incubation (Table 5.3a) and greenhouse (Table 5.3b) experiments, positive correlations were observed between cold water extractable carbon (CWEC) and hot water extractable carbon (HWEC), total water extractable carbon (WEC) and hot water extractable carbon (HWEC), total water extractable carbon (WEC) and cold water extractable carbon

(CWEC), and between respiration rate and pH. Negative correlations were observed between pH and hot water extractable carbon (HWEC), pH and cold water extractable carbon (CWEC), and between pH and total water extractable carbon (WEC). In contrast hot water extractable carbon (HWEC), cold water extractable carbon (CWEC) and total water extractable carbon (WEC) had no significant relationship ($p > 0.05$) with the respiration rate (Table 5.3a, 5.3b).

Table 5.3. Correlations of respiration rate, pH and water extractable carbon for (a) incubation and (b) greenhouse experiments. Two types of soils (low and high organic matter soil) and four microplastic treatments (control, 0.05 %, 0.50 % and 5.00 % HDPE) were considered. Upper values indicate Pearson correlation coefficients; lower values indicate p values. Values in italic, red color are significant at $p \leq 0.01$ and those in italic, blue color at $p \leq 0.05$.

(a)

	HWEC				
CWEC	<i>0.970</i>				
	<i>0.000</i>				
		CWEC			
TWEC	<i>0.998</i>	<i>0.998</i>			
	<i>1.12×10^{-36}</i>	<i>1.12×10^{-36}</i>			
			TWEC		
pH	<i>-0.806</i>	<i>-0.806</i>	<i>-0.782</i>		
	<i>2.64×10^{-8}</i>	<i>2.64×10^{-8}</i>	<i>1.23×10^{-7}</i>		
				pH	
Respiration rate	-0.344	-0.344	-0.316	<i>0.634</i>	
	0.064	0.064	0.078	<i>9.74×10^{-5}</i>	

(b)

	HWEC				
CWEC	<i>0.812</i>				
	<i>1.66×10^{-8}</i>				
		CWEC			
TWEC	<i>0.997</i>	<i>0.882</i>			
	<i>9.91×10^{-49}</i>	<i>5.17×10^{-9}</i>			
			TWEC		
pH	<i>-0.177</i>	<i>-0.256</i>	<i>-0.159</i>		
	<i>0.027</i>	<i>0.023</i>	<i>0.027</i>		
				pH	
Respiration rate	-0.0941	-0.325	-0.106	<i>0.764</i>	
	0.068	0.069	0.565	<i>3.69×10^{-7}</i>	

*CWEC = cold water extractable carbon, HWEC = hot water extractable carbon, WEC = total water extractable carbon.

5.3.2. Plant parameters

All plant parameters (plant height, leaf chlorophyll content, shoot biomass, root biomass, root: shoot ratio and plant P) were measured at the end of the seven week growth period. Two-way ANOVA test showed that for all parameters, the patterns were similar for both soil types (Table 5.4). Values of controls and 0.05 % microplastic treatments had higher values for all parameters. There was no significant ($p \geq 0.05$) difference between control and 0.05 % treatments. There were significant reductions on the parameters with 0.50 % and 5.00 % treatments compared to the controls. 5.00 % treatments had significantly ($p \leq 0.05$) lower values for the parameters than the 0.50 % treatments.

Table 5.4. Plant height (cm), leaf chlorophyll content (g/ m^2), fresh and dry weight of shoot biomass (g), fresh and dry weight of root biomass (g), fresh and dry root: shoot ratio and plant P (%). Values are expressed as means of four replicates ($n = 4$). There are two types of soil and four HDPE treatments: low organic matter control soil = L0, low organic matter soil with 0.05 % HDPE = L0.05, low organic matter soil with 0.50 % HDPE = L0.5, low organic matter soil with 5.00 % HDPE = L5.0, high organic matter control soil = H0, high organic matter soil with 0.05 % HDPE = H0.05, high organic matter soil with 0.50 % HDPE = H0.5, high organic matter soil with 5.00 % HDPE = H5.0. Means of HDPE application rates that do not share a letter are significantly ($p \leq 0.05$) different which was indicated by post-hoc tests (showed which treatment groups are different from each other).

Measured parameters	Treatments							
	L0	L0.05	L0.5	L5.0	H0	H0.05	H0.5	H5.0
Plant height (cm)	22.16 ± 0.24 a	22.23 ± 0.33 a	19.11 ± 0.13 b	15.75 ± 0.21 c	25.65 ± 0.21 d	25.53 ± 0.15 d	23.88 ± 0.21 e	19.62 ± 0.24 f
Chlorophyll content (g/ m^2)	0.87 ± 0.03 a	0.84 ± 0.03 a	0.56 ± 0.01 b	0.31 ± 0.03 c	0.95 ± 0.01 d	0.95 ± 0.004 d	0.63 ± 0.04 e	0.30 ± 0.08 f
Fresh weight of shoot biomass (g)	6.61 ± 0.09 a	6.45 ± 0.13 a	4.59 ± 0.09 b	2.86 ± 0.09 c	7.44 ± 0.04 d	7.53 ± 0.11 d	5.64 ± 0.09 e	3.78 ± 0.13 f
Dry weight of shoot biomass (g)	1.50 ± 0.05 a	1.53 ± 0.08 a	1.33 ± 0.03 b	1.02 ± 0.006 c	1.87 ± 0.09 d	1.86 ± 0.02 d	1.57 ± 0.02 e	1.18 ± 0.05 f
Fresh weight of root biomass (g)	6.06 ± 0.09 a	5.89 ± 0.13 a	4.05 ± 0.08 b	2.31 ± 0.09 c	6.89 ± 0.04 d	6.98 ± 0.10 d	5.09 ± 0.09 e	3.23 ± 0.13 f
Dry weight of root biomass (g)	1.10 ± 0.05 a	1.13 ± 0.08 a	0.93 ± 0.03 b	0.62 ± 0.006 c	1.47 ± 0.09 d	1.46 ± 0.02 d	1.17 ± 0.02 e	0.78 ± 0.05 f
Root: shoot ratio (fresh)	0.92 ± 0.001 a	0.91 ± 0.002 a	0.88 ± 0.002 b	0.81 ± 0.008 c	0.93 ± 0.0003 d	0.93 ± 0.00 d	0.90 ± 0.002 e	0.85 ± 0.005 f
Root: shoot ratio (dry)	0.73 ± 0.009 a	0.74 ± 0.01 a	0.69 ± 0.006 b	0.61 ± 0.002 c	0.76 ± 0.01 d	0.79 ± 0.002 d	0.70 ± 0.003 e	0.66 ± 0.02 f
Plant P (%)	0.23 ± 0.0003 a	0.23 ± 0.0003 a	0.15 ± 0.0019 b	0.12 ± 0.0002 c	0.36 ± 0.0001 d	0.36 ± 0.0002 d	0.22 ± 0.0002 e	0.19 ± 0.0002 f

Plant height was 22.16 ± 0.24 cm ($n = 4$; \pm standard deviation) in L0 treatments which was not significantly ($p \geq 0.05$) different from the L0.05 treatments. L0.5 and L5.0 treatments were significantly ($p \leq 0.05$) different from each other. Plant height was significantly ($p \leq 0.05$) declined by 13 % in the L0.5 and 29 % in L5.0 treatments relative to L0 (Table 5.4). Same trend was followed in high organic matter soils. Plant height was 22.65 ± 0.21 cm ($n = 4$) in the H0 which was not significantly ($p \geq 0.05$) different from the H0.05 treatments. Plant height was reduced by 7 % in H0.5 and 24 % in H5.0 treatments compared to the H0 treatments. Both H0.5 and H5.0 treatments were significantly ($p \leq 0.05$) different from each other (Table 5.4). Chlorophyll content was 0.87 ± 0.03 g/ m² for the plants grown in the L0 treatments and no significant difference was associated between L0 and L0.05 treatments. Chlorophyll content was decreased in L0.5 and L5.0 treatments by 36 % and 64 % respectively when compared with the L0; L0.5 and L5.0 treatments were significantly ($p \leq 0.05$) different from each other. Reduction in chlorophyll content was 34 % with the H0.5 and 68 % with the H5.0 than that of the H0 treatments which had a chlorophyll content of 0.95 ± 0.01 g/ m² ($n = 4$; \pm standard deviation). No significant ($p \geq 0.05$) variation was found between H0 and H0.05. In both high and low organic matter soils, fresh and dry weight of shoot biomass were significantly declined in 0.50 % and 5.00 % treatments when compared with the control. Both 0.50 % and 5.00 % treatments were significantly different from each other. There was no significant difference found between control and 0.05 % treatments. Similar pattern was followed by fresh and dry weight of root biomass and root: shoot ratio. Plant P content was recorded 0.23 ± 0.0003 % ($n = 4$; \pm standard deviation) in L0 which showed 35 % and 48 % reductions in L0.5 and L5.0 treatments respectively. L0.5 and L5.0 treatments were significantly different from each other but no significant difference was observed between L0 and L0.05. H0 treatments had P content of 0.36 ± 0.0001 % which was declined by 39 % in H0.5 and 47 % in H5.0 treatments. H0.5 and H5.0 treatments were significantly different from each other but no significant difference was observed between H0 and H0.05 (Table 5.4).

5.4. Discussion

Our initial hypothesis was HDPE would limit plant growth by reducing the amount of available P. By the end of our experiment, our data supported part of our hypothesis. It was observed in our study that P concentrations were reduced in the presence of microplastics, and it is possible that this is due to the sorption of P to the microplastics as discussed in our adsorption experiment (Chapter 3) and/ or it was due to the precipitation of P. Respiration rate, phosphatase enzyme activity and soil pH had higher values in the higher microplastic treatments than in the controls. However, exchangeable cations (Na, K, Mg, Ca and Al), effective cation exchange capacity (ECEC), total cation exchange capacity (TCEC), cold (CWEC) and hot water extractable carbon (HWEC), Olsen P, pore water P, NH_4^+ , NO_3^- , water holding capacity (WHC), aggregate stability, plant height, chlorophyll content, biomass (shoot and root), root: shoot ratio as well as plant P were decreased with the higher microplastic treatments than the controls. Reductions in some parameters (e.g. exchangeable cations, ECEC, TCEC, CWEC, HWEC, Olsen P, pore water P, NH_4^+ and NO_3^-) were more than a factor of 0.95 indicating that the greater reductions could be explained by dilution due to the microplastic additions. Some of these trends (decreases/ increases in soil parameters) were consistent with decreased plant growth. Thus, changes (decreases/ increases) in all soil parameters together or a single parameter alone might explain the decreased growth of plant in our study.

5.4.1. Microplastics impact on soil properties and plant growth

In the incubation experiments, there were no significant differences in the respiration rate (Figure 5.4a) or enzyme activity (Figure 5.5a) between the treatments except the 5.00 %. Respiration rate was significantly ($p \leq 0.05$) increased by approximately 119 % and 76 % for the L5.0 and H5.0 treatments respectively (Figure 5.4a) compared to the controls. Enzyme activity was significantly ($p \leq 0.05$) increased by approximately 150 % and 44 % for the L5.0 and H5.0 treatments respectively (Figure 5.5a) relative to the control treatments. In the greenhouse experiments, respiration rate was significantly ($p \leq 0.05$) increased by approximately 46 % in L5.0 than L0. Respiration was decreased by about 15 % in the H0.5 relative to H0 treatments (Figure 5.4b). However, respiration was increased by 59 % in the H5.0 treatment relative to the H0 (Figure 5.4b). Enzyme activity was significantly ($p \leq 0.05$) increased by approximately 150 % and 44 % for the incubated L5.0 and H5.0 treatments

respectively (Figure 5.5b) compared to controls. Increased enzyme activity in our study was consistent with previous studies (Huang *et al.*, 2019; Fei *et al.*, 2020; Liu *et al.*, 2017; Yang *et al.*, 2018; Zhao *et al.*, 2021; Aciego and Brookes, 2009) where authors recorded an increase in enzyme activity in the presence of microplastics. Authors suggested that the relatively high content of carbon (typically around 80 %; Rillig, 2018) in microplastics could feed the soil microbes causing a priming effect which led to increased microbial activity with potential increases in enzyme activity. Another reason for enhanced enzyme activity with high doses of microplastic treatments as suggested by Machado *et al.* (2019) was release of compounds from the microplastics into the soil solution (added during manufacturing process) which could provide a food source for the soil microbes. Production of microplastic involves polymerisation of organic compounds and the remaining monomers (atoms/ small molecules that bond together to form polymer) loosely interacting with the polymer matrix can leach into the soil. For instance, HDPE production involves polymerisation of ethene and the remaining monomers were aliphatic hydrocarbons (C₁₄, C₁₆, C₁₈, C₂₀, and C₂₂) that leach into the soil solution (Browne *et al.*, 2008).

Salazar *et al.* (2011) stated that increased microbial activity is linked with an increased enzyme activity, which is in turn positively correlated with increased soil respiration. Increased respiration in soil is typically linked to rapid decomposition of labile C (Eliasson *et al.*, 2005), increases in soil pH and enzyme activity (Aciego and Brookes, 2008; Allison and Vitousek, 2005). Both our incubation and greenhouse experiments observed positive correlations between cold water extractable carbon (CWEC) and hot water extractable carbon (HWEC), total water extractable carbon (WEC) and hot water extractable carbon (HWEC), total water extractable carbon (WEC) and cold water extractable carbon (CWEC), and between respiration rate and pH (Table 5.3a, 5.3b). These types of positive correlations were observed for both soil types. It was apparent from our study that high doses of microplastics tended to reduce the concentration of WEC (Figure 5.10, 5.11), increase phosphatase enzyme activity (Figure 5.5) and increase soil pH (Figure 5.6). Soil pH does not influence respiration directly, rather it controls nutrient solubility and availability which impacts on soil microbes responsible for soil organic matter decomposition which is evident by soil respiration. The pH range 5.5 – 6.5 is optimal for the survival and multiplication of microbes as the availability of nutrients is optimal at this pH range. Soil pH was found 7.6 and 7.8 for the incubated L5.0 and H5.0 treatments respectively which was significantly ($p \leq 0.05$) higher than the controls (6.2 in L0; 6.4 in H0; Figure 5.6a). For the greenhouse study, pH was 7.0 and 7.2 in the L0.5 and L5.0 treatments respectively whereas 6.9 and 7.2 in the H0.5 and H5.0 respectively

(Figure 5.6b). All these values were significantly ($p \leq 0.05$) higher than the controls (5.5 in L0; 6.4 in H0). These increases in pH supported our findings of higher soil respiration (Figure 5.4). Changes in soil pH may affect the solubility and availability of nutrients by changing chemical speciation processes within soils (Machado *et al.*, 2019) which in turn affect plant growth. More divalent anion (HPO_4^{2-}) is taken up by plants at higher soil pH (typically above 6.5) whereas at low pH (less than 6.5), monovalent anion (H_2PO_4^-) is the dominant ion for the plants (Parham *et al.*, 2002). HPO_4^{2-} was more likely to be uptaken by the plants in high microplastic treated soils since the pH values were more than 6.5 (Figure 5.6). However, H_2PO_4^- was more likely to be taken up by the plants in control soils as the soils had pH values less than 6.5 (Figure 5.6). Previous studies (Ren *et al.*, 2020; Liu *et al.*, 2017; Boots *et al.*, 2019) observed increased CO_2 fluxes in microplastic treated soils and it can be assumed that these increases reflect increases in respiration. These findings were supported by our data since we observed higher rate of respiration due to the addition of microplastics (Figure 5.4).

It is worth noting that the soil pH was decreased (from 7.6 to 6.2 in L0 and 7.1 to 6.4 in H0; Section 5.2.1; Figure 5.6) after incubating in the controlled temperature room for a period of 30 days. Incubation at 25 °C (Figure 5.1) encourages growth of microbes and these microbes could produce more organic acids leading to decreases in soil pH (Fu and Mathews, 1999; Ratzke and Gore, 2018). Increased microbial biomass resulting from the incubation experiment would have increased the decomposition of soil organic matter that could result in the formation of soluble organic acids in the soil and, as a result, soil pH was decreased (Weil and Brady, 2016). Decreased pH after incubating the soil could be due to speeding up the nitrification process. The nitrification process significantly decreases soil pH by producing H^+ ions (Weil and Brady, 2016). The nitrifying bacteria (responsible for nitrification), being aerobic, require oxygen to oxidize NH_4^+ to NO_2^- and then NO_3^- , and thus are favoured in well aerated, moist soils (Weil and Brady, 2016; Schaefer and Hollibaugh, 2017). The nitrifying bacteria perform best when temperatures are between 20 and 30 °C (Weil and Brady, 2016). We maintained a soil water content of 25 % (w/w) and a temperature of 25 °C throughout the incubation experiment which could be attributed to speeding up the nitrification in soil.

It was apparent from our study that high doses of microplastics tended to reduce microbial biomass C as suggested by the HWEC (Figure 5.11) since concentration of HWEC is linked to the microbial biomass (Ghani *et al.*, 2003). Microbes present in the soil could be more active but their numbers were not increased. In addition, decrease in the concentrations of

WEC (Figure 5.10, 5.11) due to higher decomposition (Figure 5.4) could outweigh any increase in microbial biomass so that HWEC was seen to decrease despite potential increase in microbial numbers to accompany the increase in microbial activity. It is noteworthy that the higher respiration in the soil is likely to reduce the concentration of WEC (both CWEC and HWEC; Figure 5.10, 5.11) as it is converted into CO₂. There could be some additional sources of C present in soil that were not extracted by the cold and hot water extraction methods.

Studies also showed that microplastics in the soil can decrease enzymatic activity and respiration (Zhao *et al.*, 2021; Fei *et al.*, 2020) which appeared to contradict our study. The decrease was attributed to the incorporation of microplastics into the dynamic structure of aggregates introducing fracture points into the aggregates, and thus decreasing aggregate stability. Reduced concentration of HWEC (Figure 5.11) which was used as an index of microaggregates (Ghani *et al.*, 2003) would indicate fewer microaggregates and ultimately fewer macroaggregates (as these are built of microaggregates) resulting in the decrease of aggregate stability (Figure 5.17) in our high microplastic treated soils which were consistent with previous studies (Machado *et al.*, 2018; Machado *et al.*, 2019 and Zhang *et al.*, 2018). These studies showed a declining trend in aggregate stability with the increasing level of microplastics. However, it was apparent from the studies (Lehmann *et al.*, 2021; Rillig, 2018; Machado *et al.*, 2018; Machado *et al.*, 2019; Zhang *et al.*, 2018) that microplastic type and shape are not always likely to be the dominant factor for influencing aggregate stability, and that the characteristics and concentration of the additives present in microplastic are more likely to be the factors affecting aggregates. Effect of microplastics on aggregate stability may decrease water flows (Six *et al.*, 2004) in the soil that may explain the decreases in enzymatic activities as observed by Zhao *et al.* (2021) and Fei *et al.* (2020). Decreased flow of water reduces the rate of reactions at which the complex molecules are broken down to release plant available nutrients by reducing the transportation of substrate (molecule upon which an enzyme acts) to the active site of the enzyme. As a result, enzyme activity is decreased in the soil (Wallenstein and Burns, 2011). Although we observed poor aggregate stability (Figure 5.17), findings of enzyme activity (Figure 5.5) in presence of higher levels of microplastics were opposite compared to the other study (Zhao *et al.*, 2021). The study by Zhao *et al.* (2021) was conducted in leaching columns, thus water flow could be affected and it would be reduced by the presence of microplastics which explained the observed decrease in enzyme activity. In our experiment, water flow was not affected as we had a constant water content which could explain the opposite trends in the enzyme activity. Moreover, Zhao *et*

al. (2021) used dry and nutrient deficient grassland soil whereas we used two types of agricultural soils in our study. We were not able to explain the effect of poor aggregate stability on water flows like Zhao *et al.* (2021) and Fei *et al.* (2020) as soil moisture was held constant throughout our experimental period (no other edaphic conditions were altered).

Reduced concentrations of Olsen P (Figure 5.12) and pore water P (Figure 5.15) were in line with our data as presented in Chapter 3 where we found that the microplastics had the ability to adsorb P. These findings were also consistent with the findings of our phosphatase enzyme activity and reduced nutrient contents. When the nutrient contents in the soil are limited, soil microbes struggle and they may produce more enzymes to try and obtain sufficient nutrients for their survival and normal function of the metabolic processes (Aneja *et al.*, 2006). Experiments have shown that although C is the most essential nutrient for soil microbes, other nutrients (e.g. NH_4^+ , NO_3^- , K^+ , Mg^{2+} , Ca^{2+} , P) are also required by the microbes to some extent for their growth and survival (Waring, 2012). For instance, NH_4^+ and NO_3^- are required for the formation of proteins, nucleic acids and coenzymes required for the microbes (Kim and Gadd, 2008). K^+ helps to activate different enzymes by physically changing the shape of the enzyme molecule, releasing nutrients from the complex compounds for the microbes. Mg^{2+} is involved as cofactor (non-protein ion acted as a catalyst for the activity of enzyme) of different enzymes required for the microbes and Ca^{2+} is involved in microbial cell structure (Kim and Gadd, 2008). Thus, decreases in WEC (Figure 5.10, 5.11), NH_4^+ (Figure 5.13), NO_3^- (Figure 5.14), K [Figure 5.7 (b and c)], Mg [Figure 5.7 (c and f)] and Ca [Figure 5.7 (g and i)] resulting from the high microplastic treatments were likely to affect microbes. Microbes are likely to affect plants since microbes are involved in breaking down complex, organic molecules into simple, inorganic form that are easily uptaken by the plants. Lower values of WEC (Figure 5.10, 5.11) and water holding capacity (Figure 5.16) together with reduced contents of P, NH_4^+ , NO_3^- , Na^+ , K^+ , Mg^{2+} and Ca^{2+} in presence of high microplastics would have affected different physiological processes (e.g. photosynthesis) in plants leading to decreased growth of plants (Table 5.4). Our findings supported previous studies (Qi *et al.*, 2018; Zhou *et al.*, 2021; Lozano and Rillig, 2020; Zhang *et al.*, 2020). These studies demonstrated that high levels of microplastics caused reductions in different plant parameters (plant height, shoot biomass and root biomass) which was possibly due to the interaction between microplastics and soil nutrients (Galloway *et al.*, 2017). However, authors (Qi *et al.*, 2018; Zhou *et al.*, 2021; Lozano and Rillig, 2020; Zhang *et al.*, 2020) were not able to explain the mechanism of this interaction. Contradictory to our findings, studies (Tao *et al.*, 2012; Zhang *et al.*, 2015) found that low density polyethylene (LDPE) was likely to improve plant

growth. Tao *et al.* (2012) and Zhang *et al.* (2015) suggested that microplastic has the potential to increase soil organic matter resulting in increased contents of available nutrients that leads to increased growth of plants.

High pH in soil is due to the reductions in exchangeable cations, soil C and increased enzyme activity (Sharpley, 1991). Increased respiration in high microplastic treated soils could break down potentially acidic organic molecules present in the soil resulting in an increase in pH (Ren *et al.*, 2020). As pH increases above 7.0 in microplastic treated soils compared to the controls (pH of both incubated and greenhouse soils were less than 7.0 which was applicable for high and low organic matter soils), most of the dissolved P reacts with Ca forming calcium phosphates (Parham *et al.*, 2002). Gradually, reactions occur in which the dissolved free phosphate species form insoluble compounds (precipitates) that cause both Olsen P (and also pore water P) and Ca to become unavailable. At high pH, Ca is the dominant cation that reacts with Olsen P. A general sequence of reactions at high pH condition involves the formation of dibasic calcium phosphate dihydrate, octacalcium phosphate, and hydroxyapatite (Parham *et al.*, 2002; Smith *et al.*, 1998). Each phosphate product formation results in the decreases of Olsen P and Ca (Siebielec *et al.*, 2014). Olsen P (Figure 5.12) (and also pore water P; Figure 5.15) along with Ca [Figure 5.7(g and i)] was observed to decrease in our high microplastic treated soils. Our findings were paralleled with Zhang *et al.* (2020), who found that Olsen P declined by up to 5 % with every 100 kg/ ha addition of LDPE (low density polyethylene) plastic film residue, although this study differed from our study in many aspects. They conducted the experiment for a relatively longer period of time in a field and found that decline in Olsen P was likely associated with reduced soil water infiltration rate (decreased by 8 % from the control). Similar types of insoluble Mg compounds could be formed resulting from the chemical reactions between Mg and Olsen P present in soil solution at high pH (Parham *et al.*, 2002) leading to the decreased concentrations of extractable Mg [Figure 5.7(c and f)] and Olsen P in the soil (Parham *et al.*, 2002). Furthermore, at increased pH, soil minerals are populated by multivalent cations (charge greater than +1; Ca^{2+} , Mg^{2+} , Al^{3+}) which promotes the formation of mineral–organic associations through cation bridging (Muneer and Oades, 1989). The cation bridging could be another reason for decreased concentrations of exchangeable Ca, Mg and Al in high microplastic treated soils. The solubility of exchangeable K could be depressed in alkaline soil, as high concentrations of H^+ ions began to occupy cation exchange sites, making it difficult for K to find places to attach (Weil and Brady, 2016; Nye *et al.*, 1968) which could result in decreased concentrations of extractable K [Figure 5.7(b and e)]. It is noteworthy that the concentrations

of exchangeable Na (Figure 5.7a), K [Figure 5.7(b and e)] and Ca (Figure 5.7g) showed non-significant differences in the low organic matter soils. It is possible that lower content of negative charges (assuming organic matter is negatively charged) on soil (Sparks, 2003) reduces the soil's ability to attract and retain positively charged cations on their exchange sites leading to a reduction in the concentrations of exchangeable Na, K and Ca. Organic matter is likely to develop negative charge at pH values greater than 3.0 (point of zero charge) although the effect depends on soil characteristics. As the pH increases above point of zero charge, the degree of negative charge increases in soil due to the deprotonation of H^+ from functional groups (Sparks, 2003). We found pH values higher than 3.0 in all our treatments (L0, L0.05, L0.5 and L5.0; Figure 5.6) that could be the reason for non-significant differences between the treatments in low organic matter soils. Concentration of exchangeable Al showed non-significant differences in the high organic matter soils for both incubation and greenhouse studies which could be due to the complexes of Al with organic matter resulting in decreased Al availability on exchange sites (Bloom *et al.*, 1979; Mulder *et al.*, 1989).

The pH and soil C are negatively correlated under natural circumstances as stated by Zhou *et al.* (2019), with higher pH values associated with lower contents of soil C, although this seems to be highly dependent on the soil characteristics and agricultural practices (Ritchie and Dolling, 1985). Although our soils differed with Zhou's soil (2019) in texture and organic matter content, we found negative correlations between pH and hot water extractable carbon (HWEC), cold water extractable carbon (CWEC) and total water extractable carbon (WEC) (Table 5.3a, 5.3b). Lower soil C together with lower WEC (Figure 5.10, 5.11) were consistent with higher pH values (Figure 5.6). Previous study (Zhao *et al.*, 2021) observed that pH in high microplastic treated soils was increased with a change in the soil physical properties that could in turn affect the activity of soil bacteria (Fei *et al.*, 2020; Cole *et al.*, 2011). Soil bacteria converts the soil organic compounds into inorganic, plant available forms by consuming H^+ and consequently soil pH is increased. We did not determine bacterial activity in our study, however, increased respiration and enzyme activity could be an indicator of higher bacterial activity. A study by Boots *et al.* (2019) found decreased soil pH in presence of microplastics which contradicts our study. The lower pH reflects differences in experimental systems between our study and other including the presence of plant and soils in our experiment compared to a combination of soil, plant and earthworms. Reasons behind the low pH in Boot's study (2019) was probably due to the changes in soil organic matter although the mechanism was not explained by the authors. Despite the lower values of soil water holding capacity (Figure 5.16) and aggregate stability (Figure 5.17), enzyme activity

(Figure 5.5) was seen to increase with the high microplastic treatments that resulted in higher values of soil pH (Figure 5.6). Low water holding capacity together with poor aggregates could reduce microbial numbers which was found to increase the enzyme activity. Under natural circumstances, typical water holding capacity of soil helps to maintain physiological state (normal functions of cell) of soil microbes and good soil structure is crucial for the availability of C substrates required by the microbes (Gupta, 2011). Lack of C substrates was evident by the lower concentrations of WEC (Figure 5.10, 5.11) in our study that resulted in poor soil structure. Lower water holding capacity (Figure 5.16) along with poor soil structure (Figure 5.17) in high microplastic treated soils would have affected the amount of water available for plant uptake. Lower content of plant available water together with increased soil pH (Figure 5.6) and lower content of Mg on exchange sites [Figure 5.7(c and f)] would have inhibited the formation of chlorophyll (Table 5.4). Previous studies showed that under natural circumstances, chlorophyll in the plant leaf was significantly declined due to changes in soil pH (Kerwin *et al.*, 2017) and Mg content (Zhou, 2003). Formation of a chlorophyll molecule begins with the chelation of porphyrin (N containing ring structure) which is mediated by Mg (Scheer, 2006). Decline in chlorophyll concentration with higher soil pH was observed by Bryan *et al.* (1989), although this effect is likely to be highly dependent on plant species and soil characteristics. Although P had no direct effect on chlorophyll synthesis, decreased contents of phosphorus (Figure 5.12; Figure 5.17) and higher soil pH (Figure 5.6) could result in reduced uptake of N that in turn led to reduced chlorophyll production (Graciano *et al.*, 2006). Contrary to our results, Kalcíkov *et al.* (2017) and Boots *et al.* (2019) found no significant impact on the chlorophyll content among microplastic treatments. Kalcíkov *et al.* (2017) conducted the experiment on the freshwater plant duckweed (*Lemna minor*) and different finding was probably due to large variation in the physiology of duckweed and ryegrass. Duckweed plant has a specialised root system which tends to lengthen when the plants are deficient in nutrients (Landesman *et al.*, 2002). The extended root systems help to uptake nutrients from the water. Although Boots *et al.* (2019) found that the contents of chlorophyll a and b did not significantly differ between any microplastic treatments, chlorophyll-a/ chlorophyll-b ratio was significantly different between the treatments, which was probably due to the reduction in the availability of nutrients (Mg and N) which had cascading effects on the photosynthetic capacity as measured by chlorophyll. Nevertheless, Boots *et al.* (2019) did not study nutrient contents in their study. It is possible that high organic matter content (approximately 19 %) of the soil used in Boot's study provided N for chlorophyll synthesis.

High microplastic treatments had lower values of effective (ECEC) and total cation exchange capacities (TCEC) as shown in Figure 5.8 and 5.9. ECEC is positively correlated with exchangeable cations, pH (Weil and Brady, 2016) and soil C content (Fang *et al.*, 2017). Reductions in exchangeable cations (Figure 5.7) was explained by the lower CEC values (Figure 5.8 for ECEC; Figure 5.9 for TCEC). Additionally, exchangeable cations form organo-metal complexes where cations (acted as metals) and organic compounds are bound together, which causes physical protection of soil organic matter (Kunhi Mouvenchery *et al.*, 2012). Physically protected soil organic matter (SOM) protects it from decomposition resulting in the reduced concentrations of plant available nutrients (Rasmussen *et al.*, 2018; Rowley *et al.*, 2018). Reductions in the available nutrients ultimately decreased plant growth which was evident in our data (Table 5.4). Although we did not study the sorption of exchangeable cations, we have demonstrated sorption of P in our study (Chapter 3) and other studies (Holmes *et al.*, 2012; Rochman *et al.*, 2014; Hodson *et al.*, 2017; Massos and Turner, 2017; Lee *et al.*, 2014) have shown sorption of other cations (Al, Cr, Mn, Fe, Co, Ni, Zn, Cd and Pb). Similar to our findings [Figure 5.7 (c and f), 5.7 (b and e), Table 5.4], Boots *et al.* (2019) also reported lower contents of exchangeable Mg and K that resulted in decreased plant growth. Boots *et al.* (2019) hypothesised that the decreases in exchangeable Mg and K was due to a decrease in aggregate stability leading to decreased growth of plants which was consistent with our study (Figure 5.17, Table 5.4). In contrast to our study and Boots's study (2019), Wang *et al.* (2021) found no negative effect of microplastics on exchangeable cations. High soil temperature due to the use of plastic mulching would have induced higher rate of decomposition of soil organic matter leading to increased contents of K in soil solution (Wang *et al.*, 2021). A part of K in soil solution could be adsorbed by the exchange sites leading to increased contents of exchangeable K. Differences in findings between our study (also Boot's study) and Wang's study could be due to the application of HDPE powder compared to plastic (polybutylene adipate terephthalate) mulching, the use of controlled laboratory condition in our study compared to in situ study, and the presence of ryegrass in our study compared to *Caragana erinacea* capable of surviving in extreme drought. One of the major findings of our study was that soil ECEC in presence of microplastics was declined despite of increased pH. Theoretically, increasing soil pH (decreasing the concentration of H⁺) increases variable charges on exchange sites that results in higher ECEC (Luo *et al.*, 2015; Weil and Brady, 2016), although this relationship between pH and ECEC is likely governed by the buffering capacity of soil, retention of cations (Jiang *et al.*, 2018) and soil properties (Weil and Brady, 2016). Low soil C together with low WEC (Figure 5.10, 5.11) could lead to a reduction in ECEC across high microplastic treatments since ECEC is positively related to soil C (Fang

et al., 2017). Soils with CEC (both ECEC and TCEC) values lower than 10.0 cmol(+)/ kg were not able to hold nutrient cations by electrostatic attraction (Cai and Ma, 1988) and consequently plants are likely to develop nutrient deficiencies which lead to decreased plant biomass. The low CEC of our high microplastic soils [control treatments had CEC values higher than 10.0 cmol(+)/ kg] resulting in low plant growth (Table 5.4) was due to the low availability of nutrients held on CEC sites is consistent with Cai and Ma's study.

Significantly lower concentrations of NH_4^+ (Figure 5.13) and NO_3^- (Figure 5.14) were found in the high microplastic treatments compared to the controls. No study till today was focused on the impacts of microplastics on the contents of NH_4^+ and NO_3^- present in the soil although studies by Liu *et al.* (2017) and Machado *et al.* (2019) reported positive impacts of microplastics addition on dissolved organic nitrogen (DON) and plant N respectively. Nevertheless, these studies are not consistent with our study due to differences in experimental design and plastic type. Liu *et al.* (2017) showed 28 % (w/ w) microplastic treatments stimulated the activity of phenoloxidase (PO) enzyme involved in the degradation of recalcitrant compounds (such as lignin) present in soil resulting in the decomposition of insoluble/ poorly dissolved high molecular weight compounds into easily dissolved low-molecular-weight compounds and thus increased the accumulation of dissolved organic matter (DOM). The DOM led to the release of dissolved organic nitrogen (DON) into the soil solution (Liu *et al.*, 2017). Different trends in our study compared to Liu's (2017) and Machado's (2019) studies could be due to the use of a more fertile soil, presumably such that N wasn't limiting and/ or there was a large reservoir of N to tap into or use of a nitrogen bearing plastic. The polyamide (PA) used in Machado's (2019) study was composed of a long, multiple-unit molecules and the molecular chains are linked together by the amide groups. Amide group is characterised by a carbonyl group linked to a nitrogen atom (John *et al.*, 2011). Machado *et al.* (2019) stated that nearly two-fold increase in leaf N content after the addition of PA since PA released N into the soil that could be taken up by the plants.

We observed decreased concentrations of NH_4^+ (Figure 5.13) and NO_3^- (Figure 5.14) in our study which were probably due to the reductions in WHC of soil, oxygen levels, C content and changes in pH. WHC of soil, oxygen levels, C content and pH are responsible for the activities of ammonifying and nitrifying bacteria involved in ammonification and nitrification processes respectively which can affect nitrogen cycling (Bouwman *et al.*, 2002). Ammonifying and nitrifying bacteria prefer moist soil with an adequate supply of air (Thangarajan *et al.*, 2015; San Francisco *et al.*, 2011) and sufficient quantities of C (nutrient

and energy source for the bacteria) (McDonald *et al.*, 2008). When the bacteria are active enough, ammonifying bacteria breaks down the organic nitrogen and releases them back into the soil as NH_4^+ (ammonification), and nitrifying bacteria oxidises NH_4^+ to NO_2^- and then to NO_3^- (nitrification) (Thangarajan *et al.*, 2015; San Francisco *et al.*, 2011). In addition, availability of nitrogen substrate is another factor for the formation of NH_4^+ and NO_3^- through ammonification and nitrification respectively. Availability of N could be limited through the sorption/ fixation of N compounds. Microplastics are capable of adsorbing NH_4^+ as evident by Li *et al.* (2021), although the experiment was conducted in a water body. Li *et al.* (2021) hypothesised that microplastics could strongly adsorb NH_4^+ in soil also. However, no study was conducted till today on the impacts of microplastics on NO_3^- adsorption. Relatively high microplastic treatments showed reductions in the water holding capacity of soil (Figure 5.16) and labile C (Figure 5.10, 5.11) that would have affected ammonifying and nitrifying bacteria resulting in the decreased concentrations of NH_4^+ (Figure 5.13) and NO_3^- (Figure 5.14). Soil with a low water holding capacity was more likely to be closer to saturation for a given water content and thus more likely to be oxygen limited (Weil and Brady, 2016) leading to decreased contents of NH_4^+ and NO_3^- . It is worth noted that contents of NO_3^- in high microplastic treated soils were declined at the end of experimental periods (30 days for incubation; 45 days for greenhouse experiment) despite of increased pH. Under natural circumstances (without any microplastic addition), formation of NO_3^- through nitrification is higher at increased pH (typically around 8.5; Sahrawat, 1996), although this seems to be highly dependent on properties of soil (depth and texture) and surrounding environment (temperature, light and humidity). Liu *et al.* (2017) observed that microplastic addition immediately contributed to the suppression of NO_3^- but the effect was transient. The content of NH_4^+ in natural soil is typically low; microplastic addition stimulated soil microbial activity which urged microbes to fiercely compete for the limited NH_4^+ , therefore limiting the nitrification process as described by Liu *et al.* (2017). Jones *et al.* (2004) mentioned that microplastics increased C-substrates that enables heterotrophic microbial growth (NH_4^+ immobilization) dominating over autotrophic growth (NH_4^+ oxidation), thus inhibiting the NO_3^- accumulation.

All the soil parameters (respiration rate, phosphatase enzyme activity, pH, exchangeable Na, K, Mg, Ca, Al, effective cation exchange capacity, total cation exchange capacity, water extractable C, Olsen P, NH_4^+ , NO_3^- , P in pore water, soil water holding capacity as well as aggregate stability) and plant parameters (plant height, leaf chlorophyll content, shoot biomass, root biomass, root: shoot ratio and plant P) discussed above showed lack of

differences between the control and 0.05 % HDPE treatments for both soil types. It seems most likely that these levels of HDPE were too low to have a detectable impact on those parameters. For most parameters, both low and high organic matter soils followed the same trend in response to the 5.0 % microplastic treatments. For a few parameters, high organic matter soils showed significant differences in both 0.5 % and 5.0 % treatments compared to controls which was probably due to the high content of organic matter, whereas low organic matter soils only showed differences between the controls and the 5.0 % treatments.

Some of the parameters observed in our study are a function of organic matter content. For instance, WHC and aggregate stability is a function of organic matter content (Hillel, 1980; Hillel, 2008). High content of organic matter typically contributes to larger WHC (Boyle *et al.*, 1997) and improves soil aggregation by binding soil particles together into aggregates (Hillel, 1980). In our study, it may be the case that the rate of reactions occurring within the soil has been controlled by the organic matter content to an extent. High organic matter would have magnified the rate of interaction between soil and microplastic, and microbial activity resulting in significant differences even in lower microplastic concentration (0.5 %). We have demonstrated higher level of P adsorption exhibited by the high organic matter soils relative to the low organic matter ones in our study (Chapter 3) and other study (Hodson *et al.*, 2017) have shown higher Zn adsorption in high organic matter soils. Liang *et al.* (2021) observed that microplastic fibres had no effect on aggregate stability and enzyme activities in the soil without organic matter addition. In microplastic treated soils, aggregate stability and enzyme activities were significantly decreased in the presence of organic matter indicating that effects of microplastic fibres on soil aggregation and enzyme activities are organic matter dependent (Liang *et al.*, 2021). However, Liang *et al.* (2021) could not explain the role of organic matter on decreased aggregate stability and enzyme activities in presence of microplastics. The impacts of microplastics on soil properties and plant growth thus not only depend on the concentration levels of microplastics, but also on the soil type.

5.5. Conclusion

Soil and plant can come in contact with microplastics easily as the content of microplastics are increasing in the soil due to the continued application of biosolids as a fertilizer, plastic mulching and irrigation. This study examined how the microplastics impact on soil physico-chemical properties and plant growth. The experiment was designed with four levels of microplastic treatments which is considered environmentally relevant for soils exposed to high human pressure and industrialisation. This study shows that although HDPE microplastic did not show any negative effects on soil and plant when applied at a small rate (0.05 %), application rate of 0.50 % and 5.00 % did cause negative responses related to general soil health and plant performance. Overall, this study revealed that HDPE microplastics led to significant reductions in the exchangeable Na, K, Mg, Ca, Al, CEC, Olsen P, pore water P, NH_4^+ , NO_3^- , WHC, aggregate stability as well as increases in the soil pH, respiration rate and phosphatase enzyme activity. Reductions in the concentrations of exchangeable Na, K, Mg, Ca, Al, CEC, Olsen P, pore water P, NH_4^+ , NO_3^- were more than a factor of 0.95 that could be accounted for by the dilution caused by the microplastic additions. Some changes (decreases/ increases) in soil parameters were consistent with decreased plant growth. Our findings were able to confirm that our data are consistent with plant growth being reduced due to the reduced P availability. However, we have not proved that in our present study. Reduction in available P could be due to the adsorption to microplastics (discussed in Chapter 3) or precipitation with exchangeable cations or simply due to the soil pH effect. A more detailed investigation into the soil properties and plant parameters would be required coupled with different doses of P fertilizers to cast further light on this (Chapter 6). High organic matter soils showed significant differences in both 0.5 % and 5.0 % treatments compared to controls which was probably due to the high content of organic matter, whereas low organic matter soils only showed differences between the controls and the 5.0 % treatments. It is possible that high content of organic matter magnified the interaction between soil and microplastics, and microbial activity. Our findings imply that pervasive microplastic impacts may have consequences for agroecosystems and terrestrial ecosystems. These impacts not only depend on the concentration levels of HDPE, but also on the soil type. Given the negative impacts of HDPE, there is a need to better understand whether those impacts are only temporary and how they change in the long term particularly in the field environment. Future studies should therefore focus on (a) quantifying HDPE in global terrestrial environments; and (b) determining HDPE effects in different environmental conditions, as different environmental conditions lead to different physico-chemical reactions and

biochemistry of HDPE, using different types and shapes of HDPE. Possible future studies will be discussed in the next chapter (Chapter 6) in order to comprehensively assess the environmental risk of HDPE microplastic pollution.

5.6. References

- Aciego, J. C. P. and Brookes, P. C. (2008). Relationships between soil pH and microbial properties in a UK arable soil. *Soil Biology and Biochemistry*, 40, 1856-1861.
- Aciego, J. C. P. and Brookes, P. C. (2009). Substrate inputs and pH as factors controlling microbial biomass, activity and community structure in an arable soil. *Soil Biology and Biochemistry*, 41, 1396-1405.
- Allison, S. D. and Vitousek, P. M. (2005). Responses of extracellular enzymes to simple and complex nutrient inputs. *Soil Biology and Biochemistry*, 37, 937-944.
- Almodares, A., Taheri, R., Chung, I. M., and Fathi, M. (2008). The effect of nitrogen and potassium fertilizers on growth parameters and carbohydrate contents of sweet sorghum cultivars. *Journal of Environmental Biology*, 29, 849-852.
- Anderson, J. P. E. and Domsch, K. H. (1978). A physiological method for the quantitative measurement of microbial biomass in soils. *Soil Biology and Biochemistry*, 10, 215-221.
- Aneja, M. K., Shilpi, S., Frank, F., Susanne, S., Werner, H., Gunther, B., Jean, C. M., and Michael, S. (2006). Microbial colonization of beech and spruce litter: influence of decomposition site and plant litter species on the diversity of microbial community. *Microbial Ecology*, 52, 127-135.
- Anu, M. A. and Pillai, S. S. (2022). Structure, thermal, optical and dielectric properties of SnO₂ nanoparticles-filled HDPE polymer. *Solid State Communications*, 341, 1-10.
- Arthur, E., Moldrup, P., Holmstrup, M., Schjonning, P., Winding, A., Mayer, P., and de Jonge, L.W. (2012). Soil microbial and physical properties and their relations along a steep copper gradient. *Agriculture, Ecosystems and Environment*, 159, 9-18.

Barnes, D. K. A., Galgani, F., Thompson, R. C., and Barlaz, M. (2009). Environmental accumulation and fragmentation of plastic debris in global. *Philosophical Transactions of the Royal Society of London B: Biological Sciences*, 364, 1985-1998.

Barrow, N. J. and Shaw, T. C. (1974). Factors affecting the long-term effectiveness of phosphate and molybdate fertilizers. *Soil Science and Plant Analysis*, 5, 355-364.

Bläsing, M. and Amelung, W. (2018). Plastics in soil: analytical methods and possible sources. *Science of the Total Environment*, 612, 422–435.

Bloom, P. R., McBride, M. B., and Weaver, R. M. (1979). Aluminum organic matter in acid soils: buffering and solution aluminum activity. *Soil Science Society of America Journal*, 43, 488–493.

Boots, B., Russell, C. W., and Green, D. S. (2019). Effects of microplastics in soil ecosystems: above and below ground. *Environmental Science and Technology*, 53, 11496 – 11506.

Bouwman, A. F., Boumans, L. J. M., and Batjes, N. H. (2002). Estimation of global NH₃ volatilization loss from synthetic fertilizers and animal manure applied to arable lands and grasslands. *Global Biogeochemical Cycles*, 16, 1-8.

Boyle, K. E., Curry, J. P., and Farrell, E. P. (1997). Influence of earthworms on soil properties and grass production in reclaimed cutover peat. *Biology and Fertility of Soils*, 25, 20-26.

Browne, M. A., Dissanayake, A., Galloway, T. S., Lowe, D. M., and Thompson, R. C. (2008). Ingested microscopic plastic translocate to the circulatory system of the mussel, *Mytilus edulis* (L) *Environmental Science and Technology*, 42, 5026-5031.

Bryan, J. A., Sieler, J. R., and Wright, R. D. (1989). Influence of growth medium pH on growth of container-grown Fraser fir seedlings. *Journal of Environmental Horticulture*, 7, 62-64.

Cai, Z. and Ma, Y. (1988). The relationship between soil organic matter and soil cation exchange capacity. *Progress in soil science*, 16, 10-15.

- Carr, S.A., Liu, J., and Tesoro, A.G. (2016). Transport and fate of microplastic particles in wastewater treatment plants. *Water Research*, 91, 174-182.
- Cole, M., Lindeque, P., Halsband, C., and Galloway, T. S. (2011). Microplastics as contaminants in the marine environment: a review. *Marine Pollution Bulletin*, 62, 2588-2597.
- Connolly, E. L. and Walker, E. L. (2008). Time to pump iron: iron-deficiency-signaling mechanisms of higher plants. *Current Opinion in Plant Biology*, 11, 530-535.
- Eliasson, P. E., Mcmurtrie, R. E., Pepper, D. A., Stromgren, M., Linder, S., and Argren, G. I. (2005). The response of heterotrophic CO₂ flux to soil warming. *Global Change Biology*, 11, 167–181.
- Fang, K., Kou, D., Wang, G., Chen, L., Ding, J., Li, F., ... Yang, G., Qin, S., Liu, L., Zhang, Q., and Yang, Y. (2017). Decreased soil cation exchange capacity across northern China's grasslands over the last three decades. *Journal of Geophysical Research: Biogeosciences*, 122, 3088–3097.
- Fei, Y., Huang, S., Zhang, H., Tong, Y., Wen, D., Xia, X., Wang, H., Luo, Y., and Barcelo, D. (2020). Response of soil enzyme activities and bacterial communities to the accumulation of microplastics in an acid cropped soil. *Science of the Total Environment*, 707, 1-9.
- Flessa, H., Ludwig, B., Heil, B., and Merbach, W. (2000). The origin of soil organic C, dissolved organic C and respiration in a long-term maize experiment in Halle, Germany, determined by ¹³C natural abundance. *Journal of Plant Nutrition and Soil Science*, 163, 157– 163.
- Foitzik, M.-J., Unrau, H.-J., Gauterin, F., Dörnhöfer, J., and Koch, T. (2018). Investigation of ultra fine particulate matter emission of rubber tires. *Wear*, 394–395, 87-95,
- Fu, W. and Mathews, A. P. (1999). Lactic acid production from lactose by *Lactobacillus plantarum*: kinetic model and effects of pH, substrate, and oxygen. *Biochemical Engineering Journal*, 3, 163–170.

Fuller, S. and Gautam, A. (2016). A procedure for measuring microplastics using pressurized fluid extraction. *Environmental Science and Technology*, 50, 5774–80.

Gałka, B., Kabała, C. Karczewska, A. Sowiński, J., and Jakubiec, J. (2016). Variability of soil properties in an intensively cultivated experimental field. *Soil Science Annual*, 67, 10–16.

Galloway, T. S., Cole, M., and Lewis, C. (2017). Interactions of microplastic debris throughout the marine ecosystem. *Nature Ecology and Evolution*, 1, 0116.

Ghani, A., Dexter, M., and Perrott, K. W. (2003). Hot-water extractable carbon in soils; a sensitive measurement for determining impacts of fertilisation, grazing and cultivation. *Soil Biology and Biochemistry*, 35, 1231–1243.

Gill, R. (1997). *Modern analytical geochemistry*. UK: Routledge Publishers.

Gill, R. and Ramsey, M. H. (1997). What a geochemical analysis means. In: Gill, R. (ed.) *Modern analytical geochemistry: an introduction to quantitative chemical analysis techniques for earth, environment and materials scientists*. UK: Longman Geochemistry.

Graciano, C., Goya, J. F., Frangi J. L., and Guiamet, J. J. (2006). Fertilization with phosphorus increases soil nitrogen absorption in young plants of *Eucalyptus grandis*. *Forest Ecology and Management*, 236, 202–210.

Gupta, V. (2011). Microbes and soil structure. In: Gliński J., Horabik J., and Lipiec J. (eds.) *Encyclopedia of Agrophysics*. Dordrecht: Springer.

Habib, D., Locke, D. C., and Cannone, L. J. (1998). Synthetic fibres as indicators of municipal sewage sludge, sludge products, and sewage treatment plant effluents. *Water Air Soil Pollution*, 103, 1-8.

Haynes, R. J. and Francis, G. S. (1993). Changes in microbial biomass C, soil carbohydrate composition and aggregate stability induced by growth of selected crop and forage species under field conditions. *Journal of Soil Science*, 44, 665– 675.

Hendershot, W. H. and Duquette, M. (1986). A simple barium chloride method for determining cation exchange capacity and exchangeable cations. *Soil Science Society of America Journal*, 50, 605-608.

Herbert, B. E. and Bertsch, P. M. (1995). Characterization of dissolved and colloidal organic matter in soil solution: a review. *In: McFee, W. W. and Kelly, J. M. (eds.) Carbon forms and functions in forest soils*. USA: Soil Science Society of America.

Hillel, D. (1980). 7 - Soil water: content and potential. *In: Hillel, D. (ed.) Fundamentals of soil physics*. San Diego: Academic Press.

Hillel, D. (2008). 7 - Soil water: content and potential. *In: Hillel, D. (ed.) Soil in the Environment*. San Diego: Academic Press.

Hodson, M. E., Duffus-Hodson, C. A., Clark, A., Prendergast-Miller, M. T., and Thorpe, K. L. (2017). Plastic bag derived-microplastics as a vector for metal exposure in terrestrial invertebrates. *Environmental Science and Technology*, 51, 4714-4721.

Holmes, L. A., Turner, A., and Thompson, R. C. (2012). Adsorption of trace metals to plastic resin pellets in the marine environment. *Environmental Pollution*, 160, 42-48.

Hoogsteen, M. J. J., Lantinga, E. A., Bakker, E. J., and Tittonell, P. A. (2018). An evaluation of the loss-on-ignition method for determining the soil organic matter content of calcareous soils. *Communications in Soil Science and Plant Analysis*, 49, 1541-1552.

Huang, Y., Zhao, Y., Wang, J., Zhang, M., Jia, W., and Qin, X. (2019). LDPE microplastic films alter microbial community composition and enzymatic activities in soil. *Environmental Pollution*, 254, 1-10.

Huerta Lwanga, E., Gertsen, H., Gooren, H., Peters, P., Salanki, T., van der Ploeg, M., Besseling, E., Koelmans, A.A., and Geissen, V. (2017). Incorporation of microplastics from litter into burrows of *Lumbricus terrestris*. *Environmental Pollution*, 220, 523-531.

International Organization for Standardization (ISO). (2019). *Soil quality-determination of water retention characteristics–Laboratory methods No. 11274*. Geneva: ISO Central Secretariat.

Jiang, J., Wang, Y. P., Yu, M., Cao, N., and Yan, J. (2018). Soil organic matter is important for acid buffering and reducing aluminum leaching from acidic forest soils. *Chemical Geology*, 501, 86–94.

John, R. B., Chao, W., Jianwei, B., and Joseph, M. R. (2011). Enantioselective Total Synthesis of (–)-Kibdelone C. *Journal of the American Chemical Society*, 133, 9956-9959.

Jones, D. L., Shannon, D., Murphy, D. V., and Farrar, J. (2004). Role of dissolved organic nitrogen (DON) in soil N cycling in grassland soils. *Soil Biology and Biochemistry*, 36, 749-756.

Jung, G. A., Van Wijk, A. J. P., Hunt, W. F., and Watson, C. E. (1996). Ryegrasses. In: Moser, L. E., Buxton, D. R., and Casler, M. D. (eds). *Cool-Season Forage Grasses*. USA: Soil Science Society of America.

Kalcikov, G., Zgajnar Gotvajn, A., Kladnik, A., and Jemec, A. (2017). Impact of polyethylene microbeads on the floating freshwater plant duckweed *Lemna minor*. *Environmental Pollution*, 230, 1108 – 1115.

Kasirajan, S. and Ngouajio, M. (2012). Polyethylene and biodegradable mulches for agricultural applications: a review. *Agronomy for Sustainable Development*, 32, 501-529.

Kerwin, L., Charles, P. L., Patrick, A. N., and Felix, N. (2017). Effects of pH and phosphorus concentrations on the chlorophyll responses of *Salvia chamelaeagnea* (Lamiaceae) grown in hydroponics. In: Eduardo, J. L., Leila, Q. Z., and Maria, I. Q. (eds.) *Chlorophyll*. UK: IntechOpen.

Kim, B. H. and Gadd, G. M. (2008). *Bacterial physiology and metabolism*. Cambridge: Cambridge University Press.

Kunhi Mouvenchery, Y., Kucerik J., Diehl, D., and Schaumann, G. E. (2012). Cation-mediated cross-linking in natural organic matter: a review. *Reviews in Environmental Science and Bio/Technology*, 11, 41-54.

Kramer, M. and Yerdei, G. (1958). Application of the method of phosphatase activity determination in agriculture chemistry. *Soviet Soil Science*, 9, 1100-1103.

Lambert, S., Scherer, C., and Wagner, M. (2017). Ecotoxicity testing of microplastics: considering the heterogeneity of physicochemical properties. *Integrated Environmental Assessment and Management*, 13, 470-475.

Landesman, L., Chang, J., Yamamoto, Y., and Goodwin, J. (2002). Nutritional value of wastewater grown duckweed for fish and shrimp feed. *World Aquaculture*, 33, 39–40.

Lankinen, A. (2000). Effects of soil pH and phosphorus on *in vitro* pollen competitive ability and sporophytic traits in clones of *Viola tricolor*. *International Journal of Plant Science*, 161, 885–893.

Lee, H., Shim, W. J., and Kwon, J. H. (2014). Sorption capacity of plastic debris for hydrophobic organic chemicals. *Science of the Total Environment*, 470–471, 1545–1552.

Lee, J. M., Thom, E. R., Wynn, K., Waugh, D., Rossi, L., and Chapman, D. F. (2016). High perennial ryegrass seeding rates reduce plant size and survival during the first year after sowing: does this have implications for pasture sward persistence? *Grass Forage Science*, 72, 382–400.

Lehmann, A., Leifheit, E. F., Gerdawischke, M., and Rillig, M. C. (2021). Microplastics have shape and polymer dependent effects on soil aggregation and organic matter loss – an experimental and meta-analytical approach. *Microplastics and Nanoplastics*, 1, 1-14.

Li, J., Zhang, K., and Zhang, H. (2018). Adsorption of antibiotics on microplastics. *Environmental Pollution*, 237, 460-467.

Li, X., Jiang, X., Song, Y., and Chang, S. X. (2021). Coexistence of polyethylene microplastics and biochar increases ammonium sorption in an aqueous solution. *Journal of Hazardous Materials*, 405, 1-9.

Liang, Y., Lehmann, A., Yang, G., Leifheit, E. F., and Rillig, M. C. 2021. Effects of microplastic fibers on soil aggregation and enzyme activities are organic matter dependent. *Frontiers in Environmental Science*, 9, 1-11.

Lin, D., Yang, G., Dou, P., Qian, S., Zhao, L., Yang, Y., and Fanin, N. (2020). Microplastics negatively affect soil fauna but stimulate microbial activity: insights from a field-based microplastic addition experiment. *Proceedings of the Royal Society B: Biological Sciences*, 287, 1-9.

Liu, H., Yang, X., Liu, G., Liang, C., Xue, S., Chen, H., Ritsema, C. J., and Geissen, V. (2017). Response of soil dissolved organic matter to microplastic addition in Chinese loess soil. *Chemosphere*, 185, 907-917.

Lozano, Y. M. and Rillig, M.C. (2020). Effects of microplastic fibers and drought on plant communities. *Environmental Science and Technology*, 54, 6166–6173.

Lozano, Y. M., Lehnert, T., Linck, L. T., Lehmann, A., and Rillig, M. C. (2020). Microplastic shape, polymer type and concentration affect soil properties and plant biomass. *Frontiers in Plant Science*, 12, 1-14.

Luo, Y., Wan, S., Hui, D., and Wallace L. L. (2001). Acclimatisation of soil respiration to warming in a tall grass prairie. *Nature*, 413, 622–625.

Luo, W. T., Nelson, P. N., Li, M. H., Cai, J. P., Zhang, Y. Y., Zhang, Y. G., Yang, S., Wang, R. Z., Wang, Z. W., Wu, Y. N., Han, X. G., and Jiang, Y. (2015). Contrasting pH buffering patterns in neutral-alkaline soils along a 3600 km transect in northern China. *Biogeosciences*, 12, 7047–7056.

Machado, A. A. S., Lau, C. W., Till, J., Kloas, W., Lehmann, A., Becker, R., and Rillig, M. C. (2018). Impacts of microplastics on the soil biophysical environment. *Environmental Science and Technology*, 52, 9656–9665.

Machado, A. A. S., Lau, C. W., Kloas, W., Bergmann, J., Bachelier, J. B., Faltin, E., Becker, R., Görlich, A. S. and Rillig, M. C. (2019). Microplastics can change soil properties and affect plant performance. *Environmental Science and Technology*, 53, 6044 – 6052.

Mahon, A. M., O'Connell, B., Healy, M. G., O'Connor, I., Officer, R., Nash, R., and Morrison, L. (2017). Microplastics in sewage sludge: effects of treatment. *Environmental Science and Technology*, 51, 810–818.

Martin, H. C. (2003). Dissolved and water-extractable organic matter in soils: a review on the influence of land use and management practices. *Geoderma*, 113, 357– 380.

Massos, A. and Turner, A. (2017). Cadmium, lead and bromine in beached microplastics. *Environmental Pollution*, 227, 139–145.

Mathalon, A. and Hill, P. (2014). Microplastic fibres in the intertidal ecosystem surrounding Halifax Harbor. *Nova Scotia Marine Pollution Bulletin*, 81, 69–79.

McDonald, I. R., Bodrossy, L., Chen, Y., and Murrell, J. C. (2008). Molecular techniques for the study of aerobic methanotrophs. *Applied and Environmental Microbiology*, 74, 1305–1315.

McGill, W. B., Cannon, K. R., Robertson, J. A., and Cook, F. D. (1986). Dynamics of soil microbial biomass and water soluble organic C in Breton L after 50 years of cropping to rotations. *Canadian Journal of Soil Science*, 66, 1–19.

McLarnon, E., McQueen-Mason, S., Lenk, I., and Hartley, S. E. (2017). Evidence for active uptake and deposition of Si-based defenses in tall fescue. *Frontiers in Plant Science*, 8, 1-11.

Milleret, R., Le, B. R-C., and Gobat, J-M. (2009). Root, mycorrhiza and earthworm interactions: their effects on soil structuring processes, plant and soil nutrient concentration and plant biomass. *Plant Soil*, 316, 1–12.

Mulder, J., van Breemen, N., and Eijck, H. C. (1989). Depletion of soil aluminium by acid deposition and implications for acid neutralization. *Nature*, 337, 247–249.

Muneer, M. and Oades, J. M. (1989). The role of Ca-organic interactions in soil aggregate stability: mechanisms and models. *Australian Journal of Soil Research*, 27, 411–423.

Nizzetto, L., Bussi, G., Futter, M. N., Butterfield, D., and Whitehead, P. G. (2016a). A theoretical assessment of microplastic transport in river catchments and their retention by soils and river sediments. *Environmental Science: Processes and Impacts*, 18, 1050-1059.

Nizzetto, L., Futter, M., and Langaas, S. (2016b). Are agricultural soils dumps for microplastics of urban origin? *Environmental Science and Technology*, 50, 10777–10779.

Nye, P. H. (1968). Processes in the root Environment, *Journal of Soil Science*, 19, 205–215.

Oechel, W. C., Vourlitis, G. L., Hastings, S. J., Zulueta, R. C., Hinzman, L., and Kane, D. (2000). Acclimation of ecosystem CO₂ exchange in the Alaskan Arctic in response to decadal climate warming. *Nature*, 406, 978–981.

Parham, J. A., Deng, S. P., Raun, W. R., and Johnson, G. V. (2002). Long-term cattle manure application in soil. I. Effect on soil phosphorus levels, microbial biomass C, and dehydrogenase and phosphatase activities. *Biology and Fertility of Soils*, 35, 328-337.

Pinkard, E. A., Patel, V., and Mohammed, C. (2006). Chlorophyll and nitrogen determination for plantation-grown *Eucalyptus nitens* and *E. globulus* using a non-destructive meter. *Forest Ecology and Management*, 223, 211-217.

Qi, Y. L., Yang, X. M., Pelaez, A. M., Lwanga, E. H., Beriot, N., Gertsen, H., Garbeva, P., and Geissen, V. (2018). Macro- and micro- plastics in soil-plant system: effects of plastic mulch film

residues on wheat (*Triticum aestivum*) growth. *Science of the Total Environment*, 645, 1048–1056.

Rasmussen, C., Heckman, K., Wieder, W. R., Keiluweit, M., Lawrence, C. R., Berhe, A. A., Blankinship, J. C., Crow, S. E., Druhan, J. L., Hicks Pries C. E., Marin-Spiotta, E., Plante, A. F., Schädel, C., Schimel, J. P., Sierra, C. A., Thompson, A., and Wagai, R. (2018). Beyond clay: towards an improved set of variables for predicting soil organic matter content. *Biogeochemistry*, 137, 297–306.

Ratzke, C. and Gore, J. (2018). Modifying and reacting to the environmental pH can drive bacterial interactions. *PLOS Biology*, 16, 1-20.

Reidinger, S., Ramsey, M. H., and Hartley, S. E. (2012). Rapid and accurate analyses of silicon and phosphorus in plants using a portable X-ray fluorescence spectrometer. *New Phytologist*, 195, 699–706.

Ren, X., Tang, J., Liu, X., and Liu, Q. (2020). Effects of microplastics on greenhouse gas emissions and the microbial community in fertilized soil. *Environmental Pollution*, 256, 113347.

Richards, L. A., and Weaver, L. R. (1944). Moisture retention by some irrigated soils as related to soil moisture tension. *Journal of Agricultural Research*, 69, 215–235.

Richardson, A. D., Duigan, S. P., and Berlyn, G. P. (2002). An evaluation of noninvasive methods to estimate foliar chlorophyll content. *New Phytologist*, 153, 185 – 194.

Rillig, M. C. (2018). Microplastic disguising as soil carbon storage. *Environmental Science and Technology*, 52, 6079–6080.

Rillig, M.C., Lehmann, A., Machado, A. A. D. S., and Yang, G. (2019). Microplastic effects on plants. *New Phytologist*, 223, 1066–1070.

Ritchie, G. S. P. and Dolling, P. J. (1985). The Role of Organic Matter in Soil Acidification. *Soil Research*, 23, 569 – 576.

Rochman, C. M., Hentschel, B. T., Teh, S. J., and The, S. J. (2014). Longterm sorption of metals is similar among plastic types: implications for plastic debris in aquatic environments. *PLOS One*, 9, 1-10.

Romera-Castillo, C., Pinto, M., Langer, T. M., Álvarez-Salgado, X. A., and Herndl, G. J. (2018). Dissolved organic carbon leaching from plastics stimulates microbial activity in the ocean. *Nature Communications*, 9, 1-7.

Rowell, D. L. (1994). *Soil science: methods and applications*. Longman Scientific and Technical, Essex, UK.

Rowley, M. C., Grand, S., and Verrecchia, E. P. (2018). Calcium-mediated stabilisation of soil organic carbon. *Biogeochemistry*, 137, 27–49.

Sahrawat, K. L. (1996). Nitrification inhibitors, with emphasis on natural products, and the persistence of nitrogen in the soil. In: Ahmad, N. (ed.) *Nitrogen Economy in Tropical Soils*. The Netherlands: Kluwer Academic Publishers.

Salazar, S., Sánchez, L. E., Alvarez, J., Valverdea, A., Galindoc, P., Igual, J. M., Peixa, A., and Santa-Reginaa, I. (2011). Correlation among soil enzyme activities under different forest system management practices, *Ecological Engineering*, 37, 1123–1131.

San Francisco, S., Urrutia, O., Martin, V., Peristeropoulos, A., and Garcia-Mina, J. M. (2011). Efficiency of urease and nitrification inhibitors in reducing ammonia volatilization from diverse nitrogen fertilizers applied to different soil types and wheat straw mulching. *Journal of the Science of Food and Agriculture*, 91, 1569-1575.

Sardans, J., Peñuelas, J., and Ogaya, R. (2008). Experimental drought reduced acid and alkaline phosphatase activity and increased organic extractable P in soil in a *Quercus ilex* Mediterranean forest. *European Journal of Soil Biology*, 44, 509–520.

Schaefer, S. C. and Hollibaugh, J. T. (2017). Temperature decouples ammonium and nitrite oxidation in coastal waters. *Environmental Science and Technology*, 51, 3157-3164.

Scheer, H. (2006). An overview of chlorophylls and bacteriochlorophylls: biochemistry, biophysics, functions and applications. chlorophylls and bacteriochlorophylls. *In: Grim, B., Porra, R. J., Rudiger, W., and Scheer, H. (eds.) Advances in photosynthesis and respiration.* Dordrecht: Springer.

Scheurer, M. and Bigalke, M. (2018). Microplastics in Swiss floodplain soils. *Environmental Science and Technology*, 52, 3591-3598.

Sharpley, A. N. (1991). Effect of soil pH on cation and anion solubility. *Communications in Soil Science and Plant Analysis*, 22, 827-841.

Siebielec, G., Ukalska-Jaruga, A., and Kidd, P. (2014). Bioavailability of trace elements in soils amended with high-phosphate materials. *In: Selim, M. (ed.) Phosphate in soils: interaction with micronutrients, radionuclides and heavy metals.* USA: CRC Press.

Six, J., Bossuyt, H., Degryze, S., and Deneff, K. A. (2004). History of research on the link between (micro)aggregates, soil biota, and soil organic matter dynamics. *Soil and Tillage Research*, 79, 7-31.

Smagin, A. V. and Prusak, A. V. (2008). The effect of earthworm coprolites on the soil water retention curve. *Eurasian Soil Science*, 41, 618-622.

Smith, K. A., Chalmers, A. G., Chambers, B. J., and Christie, P. (1998). Organic manure phosphorus accumulation, mobility and management. *Soil Use and Management*, 14, 154-159.

Sparks, D. L. (2003). *Environmental soil chemistry.* Michigan: Academic Press.

Tabatabai, M. A. and Bremner, J. M. (1969). Use of p-nitrophenylphosphate for assay of soil phosphatase activity. *Soil Biology and Biochemistry*, 1, 301-307.

Thangarajan, R., Bolan, N. S., Naidu, R., and Surapaneni, A. (2015). Effects of temperature and amendments on nitrogen mineralization in selected Australian soils. *Environmental Science and Pollution Research*, 22, 8843-8854.

Tribedi, P. and Sil, A. K. (2013). Low-density polyethylene degradation by *Pseudomonas sp.* AKS2 biofilm. *Environmental Science and Pollution Research*, 20, 4146-4153.

USDA (United States Department of Agriculture). (1951). Soil Survey Manual. Soil Survey Staff, Bureau of Plant Industry, Soils and Agricultural Engineering, United States Department of Agriculture, Washington, US.

Walsh, J. N. (1997). Inductively coupled plasma-atomic emission spectrometry (ICP-AES). In: Gill, R. (ed.) *Modern analytical geochemistry: an introduction to quantitative chemical analysis techniques for earth, environment and materials scientists*. USA: Longman Geochemistry Series.

Wallenstein, M. D. and Burns, R. G. (2011). Ecology of extracellular enzyme activities and organic matter degradation in soil: a complex community-driven process. In: Dick, R. P (ed.) *Methods of soil enzymology*. USA: Soil Science Society of America.

Wang, X., Sun, H., Tan, C., Wang, X., and Xia, M. (2021). Effects of film mulching on plant growth and nutrients in artificial soil: a case study on high altitude slopes. *Sustainability*, 13, 1-15.

Waring, B. G. (2012). A meta-analysis of climatic and chemical controls on leaf litter decay rates in tropical forests. *Ecosystems*, 15, 999–1009.

Weil, R., and Brady, N. C. (2016). *Nature and properties of soils*. London: Pearson New International Edition.

Yang, X., Bento, C. P. M., Chen, H., Zhang, H., Xue, S., Huerta Lwanga, E., Zomer, P., Ritsema, C. J., and Geissen, V. (2018). Influence of microplastic addition on glyphosate decay and soil microbial activities in Chinese loess soil. *Environmental Pollution*, 242, 338-347.

Zang, H., Zhou, J., Marshall, M. R., Chadwick, D. R., Wen, Y., and Jones, D. L. (2020). Microplastics in the agroecosystem: are they an emerging threat to the plant-soil system. *Soil Biology and Biochemistry*, 148, 1-10.

Zhang, Z., Luo, X., Fan, Y., and Wu, Q. (2015). Cumulative effects of powders of degraded PE mulching-films on chemical properties of soil. *Environmental Science and Technology*, 38, 115-119.

Zhang, G. and Liu, Y. (2018). The distribution of microplastics in soil aggregate fractions in southwestern China. *Science of the Total Environment*, 642, 12-20.

Zhang, S., Xiaomei, Y., Hennie, G., Piet, P., Tamás, S., and Violette, G. (2018). A simple method for the extraction and identification of light density microplastics from soil. *Science of the Total Environment*, 616–617, 1056–1065.

Zhang, Y., Gao, T., Kang, S., and M. Sillanpaa. (2019). Impacts of atmospheric transport for microplastics deposited in remote areas. *Environmental Pollution*, 24, 11-23.

Zhang, D., E. L. N., Wanli, H., Hongyuan, W., Pablo, G., Hude, Y., Wentao, S., Chongxiao, L., Xingwang, M., Bin, F., Peiyi, Z., Fulin, Z., Shuqin, J., Mingdong, Z., Lianfeng, D., Chang, P., Xuejun, Z., Zhiyu, X., Bin, X., Xiaoxia, L., Shiyou, S., Zhenhua, C., Lihua, J., Yufeng, W., Liang, G., Changlin, K., Yan, Li., Youhua, Ma., Dongfeng, H., Jian, Z., Jianwu, Y., Chaowen, L., Song, Q., Liuqiang, Z., Binghui, H., Deli, C., Huanchun, L., Limei, Z., Qiuliang, L., Shuxia, W., Yitao, Z., Juntong, P., Baojing, G., and Hongbin, L. (2020). Plastic pollution in croplands threatens long-term food security. *Global Change Biology*, 26, 3356–3367.

Zhao, T., Lozano, Y. M., and Rillig, M. C. (2021). Microplastics increase soil pH and decrease microbial activities as a function of microplastic shape, polymer type, and exposure time. *Frontiers in Environmental Science*, 9, 67-74.

Zhou, G. S. (2003). Effect of water stress on photochemical activity of chloroplast from wheat. *Journal of Beijing Agricultural College*, 18, 188–190.

Zhou, W., Han, G., Liu, M., and Li, X. (2019). Effects of soil pH and texture on soil carbon and nitrogen in soil profiles under different land uses in Mun River Basin, Northeast Thailand. *PeerJ*, 7, 1-15.

Zhou, J., Wen, Y., Marshall, M. R., Zhao, J., Gui, H., Yang, Y. D., Zeng, Z. H., Jones, D. L., and Zang, H. D. (2021). Microplastics as an emerging threat to plant and soil health in agroecosystems. *Science of the Total Environment*, 787, 1-12.

Zubris, K. A. V. and Richards, B. K. (2005). Synthetic fibres as an indicator of land application of sludge. *Environmental Pollution*, 2, 201–211.

Chapter 6

General discussion and future research

6.1. Introduction

The primary aim of this thesis was to understand the interactions between microplastics, soils and plants, and to examine how the interactions directly/ indirectly influence soil properties and growth of plants. The present thesis shows the crucial benefits in integrating plant science, and rye grass (*Lolium perenne*) in particular. Laboratory and greenhouse pot experiments were carried out to answer the abovementioned research aim. The first laboratory experiment (Chapter 3) was carried out, before taking further steps, to verify our initial hypothesis mentioning the potential of microplastic to adsorb the essential plant nutrient, phosphate, which is required in large concentrations for the plants. In this experiment, we tested the potential of HDPE microplastic used extensively in industrial and packaging sectors to adsorb the phosphate that underpin many of the biochemical processes of plants (Chapter 3). We used the pristine and UV weathered microplastics and also two different soils differing in organic matter content for the initial adsorption experiment. Once the potential of microplastics to adsorb phosphate was verified, we studied the effects of pH and concentration of the background electrolyte on the adsorption of phosphate to the surfaces of microplastics (Chapter 4). We observed different trends in the phosphate adsorption for the microplastics and soils with the changes in pH and concentration of the background electrolyte. For this, we used a range of pH (2 – 12) and concentrations of the background electrolyte (0 – 0.10 M). After that, we investigated the impacts of microplastic on soil properties and whether the impacts on soil properties were different in the presence of plants which microplastics interacted with (Chapter 5); then determined whether the interaction effects of microplastics, soils and plants were different for the different soil types and how did they change with different levels of microplastics (Chapter 5). An incubation experiment was conducted for a period of 30 days to determine the effects of microplastic on the soil biological (respiration rate and enzyme activity), chemical (soil pH, exchangeable cations, cation exchange capacity, cold and hot water extractable carbon, Olsen phosphorus, ammonium, nitrate and phosphorus in soil pore water) and physical (soil water holding capacity and water stable aggregates) properties using four different microplastic treatments

(0 %, 0.05 %, 0.50 % and 5.00 %) and two types of soil samples (low and high organic matter soils). The incubation experiment was followed by a greenhouse pot experiment using the incubated soils (similar doses of microplastics and same types of soils). We used a higher than environmentally relevant dose of microplastic (5.00 % w/ w) to establish possible microplastic effects in our study.

6.2. Main findings

The thesis made the following contributions: it has (1) examined for the first-time how microplastics adsorb phosphate ion which is one of the key nutrients for the soil fertility; (2) assessed the effects of pH and concentration of the background electrolyte on the adsorption of phosphate; and (3) explored how microplastics affect the soils and plants. The key outputs are: (1) determination of the potential of microplastic to adsorb the phosphate; (2) determination of the difference in the phosphate adsorption between the microplastic and soil; (3) determination of the desorption from the microplastic and soil; (4) determination of the adsorption of phosphate on the microplastic with varying ranges of pH and different concentrations of the background electrolyte; (5) determination of the adsorption of phosphate on the microplastic with the combined effects of pH and concentration of the background electrolyte; (6) measurement of the soil physico-chemical and biological properties in the incubation experiment with different doses of microplastic; (7) measurement of the soil physico-chemical and biological properties in the greenhouse pot experiment with different doses of microplastic; (8) estimation of the plant growth in response to varying doses of microplastic treatments.

In the first laboratory experiment (Chapter 3), commercial grade high-density polyethylene (HDPE) microplastic powder was purchased from a Chinese company in order to determine the potential of the microplastic for the adsorption of phosphate in the soil. Weathered microplastic (WMP) was obtained by treating the pristine microplastic (PMP) with an artificial UV light having a wavelength of 185 and 365 nm. The UV light with 365 nm wavelength was not able to weather the microplastic and thus it was not used further in the kinetic and adsorption experiments. The kinetic experiment was carried out to establish the time to equilibrium prior to running the full adsorption experiment. Post hoc Tukey test confirmed the time at which the microplastics and soils reached the steady state. For the convenience of our study, we performed the adsorption experiments for 24 hours. Linear and

non-linear models (Langmuir and Freundlich) were used to fit the adsorption isotherms of phosphorus. Linear, Langmuir and Freundlich isotherms were used to determine the partition coefficient (K_d), maximum adsorption capacity (C_{SM}) and heterogeneity factor ($1/n$) respectively. Our results showed the potential for the microplastic to adsorb phosphate. HDPE microplastic used in the study was polar (developing charge at the pH value above and below the point of zero charge, PZC) and the phosphate was also charged indicating that the adsorption of PO_4^{3-} (Chapter 3, Figure 3.4, Figure 3.5) was either by specific adsorption or through hydrogen bonding / Van der Waals forces. The K_d , C_{SM} , and $1/n$ for the PMP were similar to those reported for the HDPE particles in the existing literatures (Table 3.3, Table 3.4). Higher value of $1/n$ for the WMP compared to that of the PMP (Chapter 3, Table 3.4) was related to the increased polarity due to the presence of C = O functional groups into the polymer structure. Our data showed that the phosphate adsorption was significantly higher with the WMP compared to that of the PMP. Values of K_d , C_{SM} and $1/n$ of both the PMP and WMP were significantly lower compared to the values of soils. Comparatively higher adsorption of PO_4^{3-} on the soil could result from the stronger electrostatic attraction between the charged surfaces of the soil and negatively charged PO_4^{3-} ion. Our results suggested that the microplastics are less likely than the iron oxides to control the fate and behaviour of phosphate in the soil. Regression analysis was done on the percentage of desorption to detect whether there were different regression results for the different solids. Our data indicated that the desorption of phosphate from the microplastic and soil was quite low compared to the phosphate adsorption, and desorption isotherms did not coincide with the adsorption (Chapter 3, Figure 3.6). Values of the Hysteresis Index (HI) were greater for the PMP and WMP compared to the soils indicating that the adsorbed phosphate in both microplastics showed high persistence and was difficult to release back into the solution.

The experiments on the pH and concentration of the background electrolyte (Chapter 4) were carried out to clarify contradictory literature findings about the impacts of the pH and background electrolyte concentration on phosphate adsorption to the microplastic. Adsorption experiments were conducted using 0.2 to 200.0 mg/ L phosphorus solution with the solids and solid-free control treatments (with different ranges of pH and background matrices of varying concentrations of electrolyte) at each concentration. Three-way ANOVA tests indicated that the K_d , C_{SM} and $\log K_f$ values varied significantly ($p \leq 0.05$) with the solid type, pH and concentration of the background electrolyte. Interactions of these three factors were also significant ($p \leq 0.05$). However, interactions between the pH and concentration of the background electrolyte were not significant ($p \geq 0.05$). The experiments showed that the

K_d and C_{SM} for the microplastic and soil were decreased with the increasing pH and with the reduced concentration of the background electrolyte. However, $\log K_f$ showed different trends with the increasing pH and with the reducing background electrolyte concentration. The $\log K_f$ values for the microplastics increased with the increasing pH and with the increased concentration of the background electrolyte (Chapter 4, Figure 4.3). The $\log K_f$ values for the soils decreased with the increasing pH and with the increasing concentration of the background electrolyte (Chapter 4, Figure 4.3). Three-way ANOVA tests revealed that the weathered microplastic (WMP) had higher K_d than the pristine microplastic (PMP), and the high organic matter soil (S2) had higher K_d compared to the low organic matter soil (S1). There were no significant ($p \geq 0.05$) differences in K_d for the mixture of low organic matter soil and pristine microplastic (S1 + PMP) compared to that of the mixture of low organic matter soil and weathered microplastic (S1 + WMP). Likewise, no significant ($p \geq 0.05$) differences were observed in K_d for the mixture of high organic matter soil and pristine microplastic (S2 + PMP) compared to that of the mixture of high organic matter soil and weathered microplastic (S2 + WMP). Similar findings were found for the C_{SM} and $\log K_f$. For the K_d and C_{SM} , values of pH were significantly ($p \leq 0.05$) decreased from the pH 2 to 5, from pH 5 to pH 7, from pH 7 to pH 9, and from the pH 9 to pH 12. Regarding the $\log K_f$, pH values were significantly ($p \leq 0.05$) decreased from the pH 2 to 5, from pH 5 to pH 7, from pH 7 to pH 9, whilst no significant ($p \geq 0.05$) differences were found between the pH 9 and pH 12. Across the concentration of background electrolyte, there were no significant ($p \geq 0.05$) differences between the 0 and 0.01 M for the K_d , C_{SM} and $\log K_f$. The results suggested that the pH and concentration of the background electrolyte are likely to exert significant impacts on the adsorption of phosphate to the microplastic in the soil, and could have role to play in influencing the soil properties and plant growth. In Chapters 3 and 4, the soil with higher organic matter content had higher phosphate adsorption on the microplastic compared to the soil with lower organic matter content.

The incubation and greenhouse experiments were carried out to better understand the impact of microplastic on the soil properties using a range of environmentally relevant to higher than environmentally relevant concentration of microplastic, whilst considering the relative effects of plants (Chapter 5). The incubation experiment was conducted in a controlled temperature room (temperature 25 °C, relative humidity 80 %) for a period of 30 days following a randomized block design with four groups of microplastic treatments (0, 0.05, 0.50 and 5.00 % w/ w), four replications and two types of soils. The incubation experiment was then followed by a greenhouse pot experiment (day/ night temperature was 20 °C/ 15 °C, relative

humidity 30 to 85 %) with the ryegrass (*Lolium perenne*) for seven weeks. Our data showed that although microplastic did not show any negative effects on soil and plant when applied at a small rate (0.05 %), application rate of 0.50 % and 5.00 % did cause negative responses for the soils and plants. For all parameters of the soil and plant, there were no significant ($p \geq 0.05$) differences between the control and 0.05 % treatments. The soil parameters *viz.*, respiration rate, phosphatase enzyme activity and soil pH had higher values in the higher microplastic treatments than in the controls and 0.05 % treatments (Chapter 5, Figure 5.4 – 5.6). However, exchangeable cations (Na, K, Mg, Ca and Al), effective cation exchange capacity (ECEC), total cation exchange capacity (TCEC), cold (CWEC) and hot water extractable carbon (HWEC), Olsen P, pore water P, NH_4^+ , NO_3^- , water holding capacity (WHC) and aggregate stability were decreased with the higher microplastic treatments compared to the controls and 0.05 % treatments (Chapter 5, Figure 5.7 – 5.17). The plant parameters *viz.*, plant height, chlorophyll content, shoot biomass, root biomass, root: shoot ratio and plant P were decreased with the higher microplastic treatments than the controls and 0.05 % treatments (Chapter 5, Table 5.4). Reductions in some soil parameters (exchangeable cations, ECEC, TCEC, CWEC, HWEC, Olsen P, pore water P, NH_4^+ and NO_3^-) were more than a factor of 0.95 in spite of the dilution caused by the microplastic additions. Our findings imply that pervasive microplastic impacts may have consequences for agroecosystems and terrestrial ecosystems. These impacts not only depend on the concentration levels of HDPE, but also on the soil type.

Our findings showed that comparatively higher level of phosphate adsorption was exhibited by the high organic matter soil than the low organic matter soil. At a specific pH and concentration of the background electrolyte, the partition coefficient and maximum phosphate adsorption capacity for the high organic matter soils were greater than the low organic matter ones. Our incubation and greenhouse data (Chapter 5) suggested that the high organic matter soils showed significant ($p \leq 0.05$) differences in the soil and plant parameters with both 0.5 % and 5.0 % treatments whereas low organic matter soils only showed differences in the 5.0 % treatments. It is possible that high content of organic matter magnified the interaction between the soil and microplastic, and also microbial activity. Thus, our findings suggested that the soils with high organic matter content were more likely (compared to the low organic matter soil) to be impacted by the microplastic present in the soil that could affect the soil properties leading to a reduction in plant growth.

Overall, we observed that microplastic has the potentiality to adsorb the phosphate and plant growth was reduced due to the limitations in available phosphate. Limitation in available phosphate was possibly due to the phosphate adsorption to the microplastic surface. However, adsorption might not be the dominant process in our study. Phosphate could be precipitated with soil particles also. We measured other soil properties that might be responsible for the reduced growth of plant rather than the adsorption/ precipitation of phosphate.

6.3. Research limitations

While the experiments described in Chapters 3, 4 and 5 each addressed some aspects of the questions posed at the end of literature review, there were limitations to each experiment. Across the whole thesis, perhaps the key limitation of all the experiments was the small-scale laboratory experiments. While these allowed controls of many environmental factors (temperature, precipitation, relative humidity and lighting), they did not necessarily represent what may occur in the soils and plants in presence of microplastics in the field.

In all experiments we used raw (free from any kind of contaminant) HDPE microplastic which was directly purchased from an industry. Typically this raw microplastic is stronger and more durable when compared to the highly processed microplastic (Schyns and Shaver, 2021). During the processing of microplastic for various purposes, the quality and durability decreases every time as the long chains of atoms get broken down and shortened (Schyns and Shaver, 2021). The microplastic used in our experiments did not represent the field microplastic. Our experiments could be better if we could collect soil samples from the field, extract the microplastics and then use them in our experiments. At the initial stage of our experiments, we tried to break down the plastic bottles using the liquid nitrogen to obtain the microplastics. However, we were not able to do that. It could be overcome if we left the microplastic and the liquid nitrogen for longer periods of time. We did not wait for the microplastic to degrade using the liquid nitrogen due to our time limitations.

In the Chapters 3, 4 and 5, we measured the total phosphate concentration. Reduction in available phosphate could be due to the adsorption and/ or precipitation of phosphate. We were not able to differentiate the adsorption/ precipitation of phosphate in our present study. We could observe the adsorption of phosphate with the batch experiments (using a range of

phosphate concentrations) whilst we could observe the phosphate precipitation using the microscopy/ spectroscopy techniques.

In Chapter 5, we investigated the impacts of pristine microplastic (PMP) on the soil properties and growth of plants. However, this was not our planned experimental design. Our initial plan was to compare the impacts of both pristine (PMP) and weathered microplastics (WMP) on the soils and plants. We were not able to conduct the experiment with the WMP since we did not have sufficient WMP. We used the UV lamp with 185 nm wavelength (ozone producing) to obtain the WMP, but this lamp was only capable of weathering small amounts of microplastic (approximately 10 g). The attempt to make a UV exposure box to degrade about 180 g microplastics (required for the total 32 treatments) was not successful due to the Covid pandemic. Our order of the UV box was cancelled since the laboratories were closed down. In our experiments, only 185 nm wavelength UV light was able to weather the microplastics whilst the UV light with 365 nm wavelength was not able to weather the microplastics (Chapter 3, Section 3.2.2). The reason could be due to the absence of ozone in the 365 nm wavelength or it could be due to the insufficient exposure time to the microplastic. Ozone has high reactivity and every ozone molecules react with a chain of plastic molecules leading to the breakdown of the chain (Nijjaawan and Nijjaawan, 2010). Our experiments also only considered grass (ryegrass, *Lolium perenne*). While this plant was chosen for a number of reasons, such as availability of its seeds, fast growing and capable of providing high yields and quality forage, it is not a plant that a farmer willingly grows in the agricultural soils. The ryegrass is mainly used for the silage, hay and grazing. This limitation could be overcome if we planted any agricultural crop (e.g. wheat, cabbage, etc.) typically grows in agricultural soils. Our findings in Chapter 5 were able to confirm that our data are consistent with the plant growth being reduced due to the reduced phosphate availability. However, we have not proved that in our present study. Reduction in available phosphate could be due to the adsorption/ precipitation of phosphate/ simply due to the soil pH effect.

Initially we had planned to conduct field work in which the soil samples were collected from different locations across the UK. Our plan was to extract the microplastics from the soils, determine the type, shape, size of the microplastics and finally determine the concentrations of microplastics in the soils. We were not able to conduct the field work due to the Covid restrictions.

6.4. Future researches

There is the potential for further work derived from each of the experimental chapters.

Section 3.5 (Chapter 3) discussed the need for future work investigating a wider range of plant nutrients particularly essential nutrients, such as nitrogen, potassium, sulphur, which are required by the plants in large concentrations to find out if similar adsorptions (similar to phosphate) occur on the microplastic surface, and for further investigations into the effects of nutrient adsorptions in the microplastic contaminated soils. Future work could involve adsorption experiments for different nutrient ions (cations/ anions) to examine ion specific adsorptions to a wider range of plastic feedstocks with potentially different molecular compositions, surface chemistries, sorption characteristics and presence of additives. Particle size is an important factor for the adsorption process (Muller, 2010) and previous works related to the microplastic observed that different sizes of microplastics had different adsorption patterns for the metals and organic molecules. Phosphate adsorption on the smaller/ bigger microplastic particles than those investigated in the present study (diameter approximately 238.11 μm) warrants further investigation. Further studies could use potential technologies to prove/ disprove the existing hypotheses on microplastics. For example, microplastics with larger specific surface areas and pore volumes accumulate more adsorbates (Zhou *et al.*, 2020). Rate of adsorption of the adsorbates by the microplastics decrease by increasing the grade of the crystallinity (Mato *et al.*, 2001; Karapanagioti *et al.*, 2008). Surface morphology of the microplastic using the scanning electron microscope (SEM), specific surface area, pore volume and pore size using the surface area analyser (SAA) and crystallinity using the X-ray diffractometer (XRD) could be determined which will provide useful insights on the properties of microplastic and microplastic-nutrient interaction.

Although not done in Chapter 4, future experiments could study the impacts of the pH and concentration of the background electrolyte on the desorption of phosphate from the microplastic that will help to determine whether the microplastic could release previously adsorbed PO_4^{3-} and to compare the release rates with those from the soil. This information will help to better understand the fate and behaviour of PO_4^{3-} in presence of the microplastic in the soil. Since both the pH and concentration of the background electrolyte change over time, there is a need to better understand whether those impacts are only temporary and how they change in the long term. Future studies on the impacts of pH and background electrolyte

concentration in different environmental conditions such as acid soil, calcareous soil, etc, would be required coupled with the possible phosphate adsorption mechanisms, which will help to manage the soil phosphate level leading to a better plant growth.

Section 5.5 (Chapter 5) discussed the need for a more detailed investigation into the soil properties and plant parameters coupled with different doses of phosphate fertilisers. This is important to understand whether the reduced phosphate concentration is due to the adsorption or precipitation of phosphate to the microplastics or simply due to the soil pH effect. A wide range of soils differing in clay content, moisture percentage and nutrient concentrations may show different impacts on phosphate adsorption to the microplastic such that the impact of soil type warrants further investigation. Existing literatures quantified microplastics in the global terrestrial environments. However, as far as the author is aware there is no quantification of the HDPE microplastic in the terrestrial environments. Future studies should focus on quantifying the HDPE microplastic in the terrestrial environments particularly in the agricultural soils. Most studies until today related to the impacts of microplastics have performed separately for soil – plant (Anderson *et al.*, 2018a; Anderson *et al.*, 2018b; Yu *et al.*, 2022; Qi *et al.*, 2018; Zhang *et al.*, 2015; Machado *et al.*, 2019) and soil – soil organisms (Rodriguez-Seijo *et al.*, 2017; Huerta Lwanga *et al.*, 2016; Huerta Lwanga *et al.*, 2017; Hodson *et al.*, 2017; Rillig *et al.*, 2017), studying their interaction remains to be done. Although not done in our experiments, further experiments should focus on the combination of soil, plant and soil organisms in a single experiment to better mimic the field conditions. Section 5.3.1 and 5.4.1 (Chapter 5) discussed the changes in soil parameters due to the different levels of microplastic additions, of which some of the trends (decreases/ increases in soil parameters) were consistent with the reduced growth of plants. Decreases/ increases in all soil parameters together or a single parameter alone might be the reason for reduced growth of plant. Future studies should try to find out the reasons for the reductions in plant growth which will help to improve plant growth in the presence of microplastics. We could conduct a greenhouse experiment with fertilisation (e.g. phosphorus, nitrate, ammonium, potassium) or adding elemental sulphur/ sulfuric acid or treating the soils with appropriate measures. After that, we could compare the plant responses on treated and untreated soils. Fertilisation improves the soil nutrient levels for an optimum growth of plants. Elemental sulphur/ sulfuric acid is used to decrease the soil pH (Reeves and Leibig, 2016). Different measures are adopted for treating different soil problems, such as low water holding capacity of the soil is improved by adding organic matter/ manure/ compost (Sui *et al.*, 2012).

The natural progression for future work from this thesis, beyond those discussed at the end of each chapter, would be field scale studies. These studies would aim to understand how the microplastic alters the soil and plant in the natural environment. This would help to better understand whether the plant resulting from the recovery of the changed (decreases/increases) soil parameters differs from the plant grown in the untreated soils. When considering the thesis as a whole, future work is needed to consider the four elements together *viz.*, microplastic, phosphate, soil and plant. Further work should examine the impacts of microplastic differing in size, shape and type on the plant differing in physiology and rooting strategy.

6.5. References

Anderson, A. S. M., Kloas, W., Zarfl, C., Hempel, S., and Rillig, M. C. (2018a). Microplastics as an emerging threat to terrestrial ecosystems. *Global Change Biology*, 24, 1405–1416.

Anderson, A. M., Chung, W. L., Jennifer, T., Werner, K., Anika, L., Roland, B., and Matthias, C. R. (2018b). Impacts of microplastics on the soil biophysical environment. *Environmental Science and Technology*, 52, 9656-9665.

Hodson, M.E., Duffus-Hodson, C.A., Clark, A., Prendergast-Miller, M.T., and Thorpe, K.L. (2017). Plastic bag derived-microplastics as a vector for metal exposure in terrestrial invertebrates. *Environmental Science and Technology*, 51, 4714-4721.

Huerta Lwanga, E., Gertsen, H., Gooren, H., Peters, P., Salanki, T., van der Ploeg, M., Besseling, E., Koelmans, A. A., and Geissen, V. (2016). Microplastics in the terrestrial ecosystem: implications for *Lumbricus terrestris* (Oligochaeta, Lumbricidae). *Environmental Science and Technology*, 50, 2685-2691.

Huerta Lwanga, E., Gertsen, H., Gooren, H., Peters, P., Salanki, T., van der Ploeg, M., Besseling, E., Koelmans, A.A., and Geissen, V. (2017). Incorporation of microplastics from litter into burrows of *Lumbricus terrestris*. *Environmental Pollution*, 220, 523-531.

Karapanagioti, H. K. and Klontza, I. (2008). Testing phenanthrene distribution properties of virgin plastic pellets and plastic eroded pellets found on Lesvos island beaches (Greece). *Marine Environmental Research*, 65, 283–290.

Machado, A. A. S., Lau, C. W., Kloas, W., Bergmann, J., Bachelier, J. B., Faltin, E., Becker, R., Görlich, A. S. and Rillig, M. C. (2019). Microplastics can change soil properties and affect plant performance. *Environmental Science and Technology*, 53, 6044 – 6052.

Mato, Y., Isobe, T., Takada, H., Kanehiro, H., Ohtake, C., and Kaminuma, T. (2001). Plastic resin pellets as a transport medium for toxic chemicals in the marine environment. *Environmental Science and Technology*, 35, 318–324.

Muller, B. R. (2010). Effect of particle size and surface area on the adsorption of albumin-bonded bilirubin on activated carbon. *Carbon*, 48, 3607-3615.

Nijjaawan, N. and Nijjaawan, R. (2010). Need of maintenance. In: Nijjaawan, N. and Nijjaawan, R. (eds). *Modern approach to maintenance in spinning*. India: Woodhead Publishing.

Qi, Y. L., Yang, X. M., Pelaez, A. M., Lwanga, E. H., Beriot, N., Gertsen, H., Garbeva, P., and Geissen, V. (2018). Macro- and micro- plastics in soil-plant system: effects of plastic mulch film residues on wheat (*Triticum aestivum*) growth. *Science of the Total Environment*, 645, 1048–1056.

Reeves, J. L. and Liebig, M. A. (2016). Depth Matters: Soil pH and dilution effects in the Northern Great Plains. *Nutrient Management and Soil and Plant Analysis Note*, 80, 1424–1427.

Rillig, M. C., Ziersch, L., and Hempel, S. (2017). Microplastic transport in soil by earthworms. *Scientific Reports*, 7, 1-6.

Rodriguez-Seijo, A., Lourenço, J., Rocha-Santos, T.A.P., da Costa, J., Duarte, A.C., Vala, H., and Pereira, R. (2017). Histopathological and molecular effects of micro-plastics in *Eisenia andrei* Bouche. *Environmental Pollution*, 220, 495-503.

Schyns, Z. O. G. and Shaver, M. P. (2021). Mechanical recycling of packaging plastics: a review. *Macromolecular Rapid Communications*, 42, 1-27.

Sui, Y.-Y., Jiao, X.-G., Liu, X.-B., Zhang, X.-Y., and Ding, G.-W. (2012). Water-stable aggregates and their organic carbon distribution after five years of chemical fertilizer and manure treatments on eroded farmland of Chinese Mollisols. *Canadian Journal of Soil Science*, 92, 551–557.

Yu, H., Ying, Z., Tan, W. and Zhang, Z. (2022). Microplastics as an emerging environmental pollutant in agricultural soils: effects on ecosystems and human health. *Frontiers in Environmental Science*, 6, 1-18.

Zhang, Z., Luo, X., Fan, Y., and Wu, Q. (2015). Cumulative effects of powders of degraded PE mulching-films on chemical properties of soil. *Environmental Science and Technology*, 38, 115-119.

Zhou, Y., Yang, Y., Liu, G., He, G., and Liu, W. (2020). Adsorption mechanism of cadmium on microplastics and their desorption behavior in sediment and gut environments: the roles of water pH lead ions, natural organic matter and phenanthrene. *Water Research*, 184, 1-14.

Appendix A

Appendices of Chapter 3

Figures

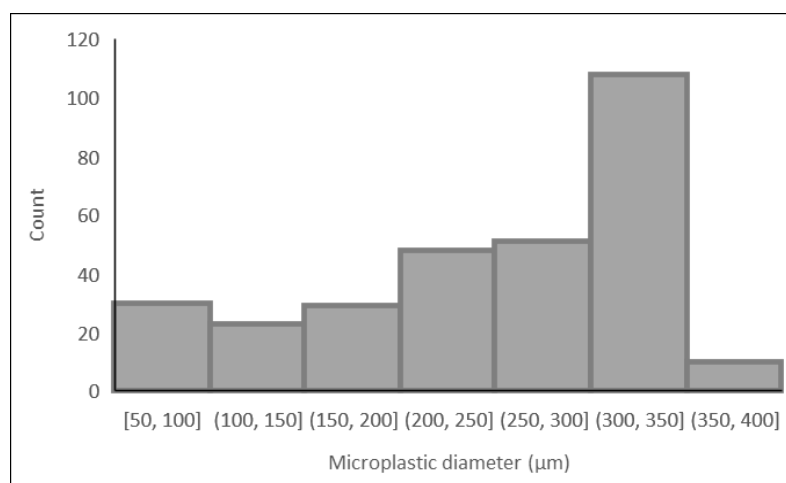


Figure A1. HDPE microplastic diameter distributions (n = 300).

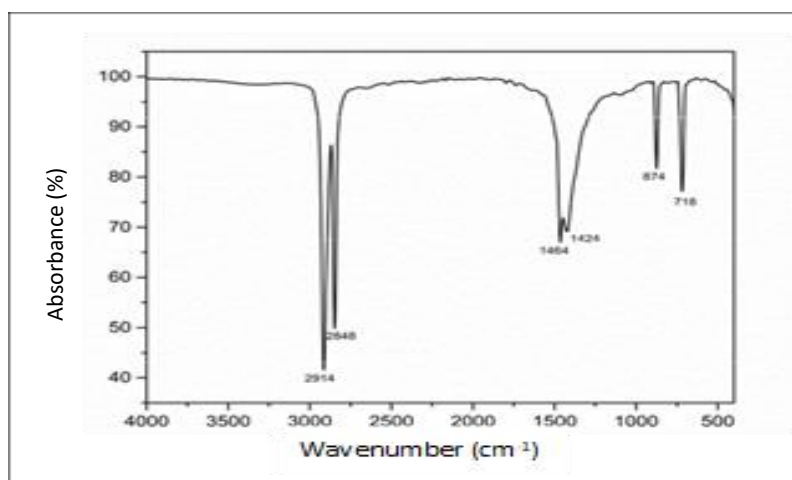


Figure A2. FTIR spectrum of untreated HDPE reported in other studies (Lin *et al.*, 2015; Maheswari *et al.*, 2013).



Figure A3. Unweathered HDPE particles under microscope. Particles were scattered on a slide, flattened by over-laying a piece of glass and images captured with a Zeiss PlanNeoFluar Microscope at 33.5 magnification. Microplastic particles which were treated (four hours per day over a period of five months) with UV radiation having 365 nm wavelength looks like the unweathered HDPE particles.

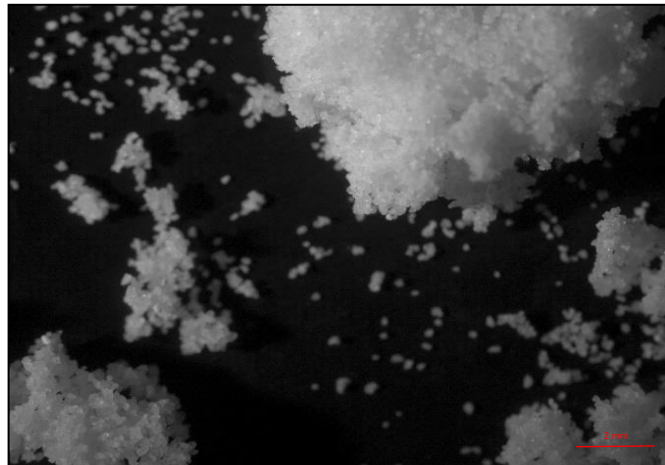


Figure A4. HDPE particles after exposure to the UV radiation with 185 nm wavelength under microscope. Particles showed a tendency to clump together. Particles were scattered on a slide, flattened by over-laying a piece of glass and images captured with a Zeiss PlanNeoFluar Microscope at 33.5 magnification. Particles were exposed to the UV radiation four hours per day over a period of five months.

A1. Basic operational principles of Inductively Coupled Plasma Optical Emission Spectrometry (ICP-OES)

Inductively Coupled Plasma Optical Emission Spectrometry (ICP-OES, Thermo Scientific ICAP 7000 Series, UK) typically derives its analytical data from the emission spectra of elements excited within a high-temperature plasma. The purpose of the ICP-OES is to separate element-specific wavelengths of light emitted from the excited sample and to focus the resolved light onto the detector as efficiently as possible (Homazava *et al.*, 2007; Thompson, 2011). The spectrometer provides comprehensive, virtually continuous wavelength coverage in the range of 166.4 to 847.0 nm, allowing the option of alternate wavelength selection in the presence of spectral interferences. The echelle spectrometer (with 383 mm effective focal length, 9.5° UV fused silica cross dispersion prism and echelle grating) fitted with an autosampler and Thermo Scientific™ Qtegra™ Intelligent Scientific Data Solution™ (ISDS) software is comprised of two sections: the fore-optics and either a mono- or polychromator (Drava and Minganti, 2020; Cherevko and Mayrhofer, 2018). When the light exits the mono- or polychromator, it is focused on to the detector and the derived signals are processed to quantify the elemental composition. The polychromator is designed to enhance stability and extend analytical run times without the need for calibration. The high resolution echelle spectrometer increases accuracy by reducing spectral overlap and exceptional sensitivity is ensured by high transmission (Drava and Minganti, 2020).

A simplified diagram of ICP-OES is presented in Figure A5. Typically, a liquid sample is pumped by a peristaltic pump into the sample introduction system of the ICP-OES (Cherevko and Mayrhofer, 2018). The sample introduction system consists of a nebulizer and a spray chamber. In the nebulizer, argon gas flow is used to break the liquid–gas interface forming an aerosol (nebula). Within the spray chamber, the aerosol is separated by droplet size, allowing only a small part of the liquid to proceed further into the plasma. The latter is formed when argon gas is inserted into a strong electromagnetic field. Aerosol particles are consequently vapourized and ionized after transferring to the plasma (Cherevko and Mayrhofer, 2018).

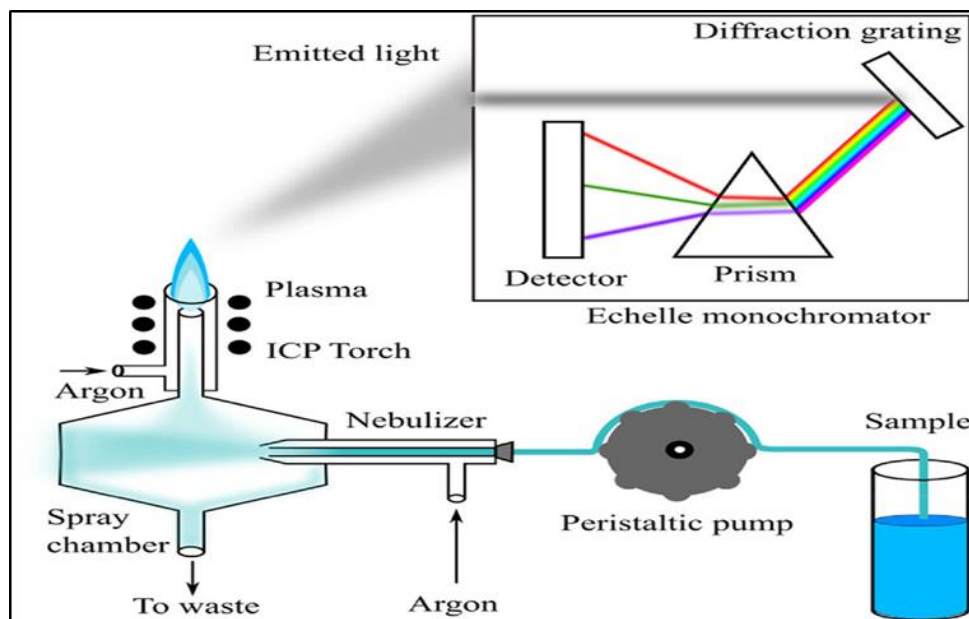


Figure A5. A simplified diagram showing the basic operational principles of Inductively Coupled Plasma Optical Emission Spectrometry (ICP-OES, Thermo Scientific ICAP 7000 Series, UK). The diagram was adapted from Cherevko and Mayrhofer (2018).

The plasma is typically composed of argon gas, although nitrogen gas and mixed gas compositions have also been reported (Thompson, 2011). Generation of the plasma is performed in the plasma torch that consists of three quartz tubes: (a) outer torch tube, (b) auxiliary tube and (c) injector tube. Between the outer tube and the auxiliary tube, a tangential cool gas flow is introduced. This gas contains the plasma and keeps it away from the outer torch tube, protecting it from melting down. The auxiliary gas flow is used to elevate the bottom of the plasma from the injector tube. The sample aerosol is introduced into the plasma via a thin injector tube that typically has an aperture of 1 to 2 mm. Through this opening, a thin jet of sample aerosol is emitted and punches a hole into the centre of the plasma (Thompson, 2011).

In the ICP-OES, the plasma can usually be observed in two ways: (a) radially (observation of the plasma cross-section from the side) and (b) axially (observation of the plasma from the end and along the entire length of the plasma). The radial plasma view offers less sensitivity than the axial view. The radial view is preferable when analyzing samples containing high amounts of dissolved solid matrices, as the plasma viewing position can be optimized to reduce background emissions

(Silva *et al.*, 2003). The axially viewed plasma configuration offers greater sensitivity than the radial configuration, but has higher susceptibility to spectral interferences. As the entire plasma is viewed, the quantity of light observed from both analyte and background emissions are increased (Silva *et al.*, 2003).

The plasma has high electron density and temperature which is used for the excitation-emission of the sample (Klemm *et al.*, 2011; Thompson, 2011). The plasma energy is given to an analysis sample from outside to excite the component atoms. ICP-OES possesses an excitation temperature of 5000 to 7000 K which efficiently excite elements. When the excited atoms return to low energy position, ions emit photons of characteristic wavelengths unique for each element. Emitted light containing numerous wavelengths is focused on a diffraction grating and prism, which are used to split and separate the spectra into its component wavelengths. Finally the concentration of certain elements in the initial liquid sample is measured by counting the emitted photons. For measuring the concentration of element, photomultipliers or photodetectors can be used. Currently, solid-state charge transfer devices (CTDs) are used as the detectors of the ICP-OES. CTDs have almost completely replaced the photomultiplier tubes (Homazava *et al.*, 2007).

Tables

Table A1. Quality control for chemical analyses of different solids for the kinetic, adsorption and desorption studies. Detection limits were calculated from the mean plus six times the standard deviation of ten repeated measurements of the blank standard. In-house certified reference material (CRM) was used having a concentration of 0.5 mg/L PO₄-P (total) in water for determining accuracy. Precision was calculated from coefficient of variation (CV) determined from duplicate analysis of 10 % of the samples. Values were averaged when there were more than one instrumental runs. Instrument used for the analysis was ICP-OES (Thermo Scientific ICAP 7000 Series, UK). Accuracy and precision are expressed in percentage (%). Detection limit is expressed in mg/ L.

Parameters	Name of experiment	Accuracy (%)	Precision (%)	Detection limit (mg/ L)
Phosphorus	Kinetic	98.19	0.78	0.07
Phosphorus	Adsorption	98.60	2.38	0.77
Phosphorus	Desorption	97.92	1.92	0.61

*PMP = Pristine microplastic, WMP = weathered microplastic, S1 = low organic matter soil, S2 = high organic matter soil, S1 + PMP = low organic matter soil + pristine microplastic, S1 + WMP = low organic matter soil + weathered microplastic, S2 + PMP = high organic matter soil + pristine microplastic, S2 + WMP = high organic matter soil + weathered microplastic.

Table A2. Time required for reaching steady state for different solids in the kinetic experiments. 0.2 g solid was added to 30 ml of 5 mg/ L KH_2PO_4 solution in a background electrolyte of 0.1 M NaNO_3 . The samples were shaken at 180 rpm at 20 °C. Number of replications was three in all cases.

Materials	Time required to reach steady state (hours)
PMP	24
WMP	14
S1	24
S2	24
S1 + PMP	24
S1 + WMP	14
S2 + PMP	24
S2 + WMP	14

*PMP = Pristine microplastic, WMP = weathered microplastic, S1 = low organic matter soil, S2 = high organic matter soil, S1 + PMP = low organic matter soil + pristine microplastic, S1 + WMP = low organic matter soil + weathered microplastic, S2 + PMP = high organic matter soil + pristine microplastic, S2 + WMP = high organic matter soil + weathered microplastic.

Appendix B

Appendices of Chapter 4

Tables

Table B1. Quality control for chemical analyses of different solids for the studies on the pH and concentration of the background electrolyte. Detection limits were calculated from the mean plus six times the standard deviation of ten repeated measurements of the blank standard. In-house certified reference material (CRM) was used having a concentration of 0.5 mg/ L PO₄-P (total) in water for determining accuracy. Precision was calculated from coefficient of variation (CV) determined from duplicate analysis of 10 % of the samples. Values were averaged when there were more than one instrumental runs. Instrument used for the analysis was ICP-OES (Thermo Scientific ICAP 7000 Series, UK). Accuracy and precision are expressed in percentage (%). Detection limit is expressed in mg/ L.

Parameters	Name of experiment	Accuracy (%)	Precision (%)	Detection limit (mg/ L)
Phosphorus	pH	98.26	0.81	0.05
Phosphorus	Concentration of background electrolyte	97.54	0.39	0.06

Table B2. Partition coefficient (K_d) values for phosphorus adsorption at different values of pH and different concentrations of background electrolyte. Mass of solid used is 0.2 g and volume of solution is 30 ml. Equilibrium time for the adsorption experiment is 24 hours. Values of pH range from 2 to 12 and concentration of background electrolyte from 0 to 0.1 M NaNO_3 . Reported values are calculated from the linear regression of 30 values ($n = 3$ for each set of data). K_d is determined from the slope of linear regression (independent variable: phosphorus concentration present in the solution, C_{aq} ; dependent variable: phosphorus adsorbed to the solid, C_s). 95 % confidence interval is calculated which are shown in brackets. Upper and lower limit of confidence intervals are separated by comma (,). Unit of K_d is L/ kg for all solid types.

pH	Value	Solid types							
		PMP	WMP	S1	S2	S1+PMP	S1+WMP	S2+PMP	S2+WMP
2	NaNO_3 Conc. (M)	0.00	0.00	0.00	0.00	0.00	0.00	0.00	0.00
	K_d	146.18 (138.93, 153.41)	184.56 (179.18, 190.60)	350.10 (345.42, 354.02)	374.81 (370.82, 379.82)	313.87 (309.19, 318.19)	326.88 (323.26, 330.46)	337.92 (332.84, 343.64)	357.64 (352.81, 363.81)
	R^2	0.90	0.57	0.76	0.57	0.66	0.74	0.50	0.72
	p	≤ 0.05	≤ 0.05	≤ 0.05	≤ 0.05	≤ 0.05	≤ 0.05	≤ 0.05	≤ 0.05
5	NaNO_3 Conc. (M)	0.00	0.00	0.00	0.00	0.00	0.00	0.00	0.00
	K_d	117.44 (113.47, 121.87)	165.38 (161.87, 169.07)	284.39 (280.52, 287.52)	326.98 (321.05, 332.85)	258.18 (253.19, 263.19)	259.19 (248.32, 269.72)	298.39 (291.42, 305.42)	295.32 (286.09, 304.09)
	R^2	0.88	0.97	0.51	0.78	0.81	0.91	0.61	0.76
	p	≤ 0.05	≤ 0.05	≤ 0.05	≤ 0.05	≤ 0.05	≤ 0.05	≤ 0.05	≤ 0.05
7	NaNO_3 Conc. (M)	0.00	0.00	0.00	0.00	0.00	0.00	0.00	0.00
	K_d	88.89 (84.98, 93.78)	131.72 (127.36, 136.76)	267.88 (264.76, 270.76)	293.04 (286.16, 299.16)	228.735 (223.36, 233.96)	225.13 (217.04, 232.04)	248.39 (241.02, 255.22)	264.03 (250.39, 278.39)
	R^2	0.93	0.79	0.66	0.90	0.63	0.81	0.81	0.32
	p	≤ 0.05	≤ 0.05	≤ 0.05	≤ 0.05	≤ 0.05	≤ 0.05	≤ 0.05	≤ 0.05

Table B2 (continued). Partition coefficient (K_d) values for phosphorus adsorption at different values of pH and concentration of background electrolyte.

pH	Value	Solid types							
		PMP	WMP	S1	S2	S1+PMP	S1+WMP	S2+PMP	S2+WMP
9	NaNO ₃ Conc. (M)	0.00	0.00	0.00	0.00	0.00	0.00	0.00	0.00
	K_d	52.21 (48.66, 56.06)	94.79 (88.11, 100.91)	245.19 (239.99, 250.43)	269.25 (264.71, 273.51)	289.51 (280.01, 298.21)	292.18 (283.74, 300.34)	246.95 (239.44, 254.64)	248.24 (240.65, 256.05)
	R^2	0.90	0.93	0.30	0.84	0.64	0.99	0.62	0.87
	p	≤ 0.05	≤ 0.05	≤ 0.05	≤ 0.05	≤ 0.05	≤ 0.05	≤ 0.05	≤ 0.05
12	NaNO ₃ Conc. (M)	0.00	0.00	0.00	0.00	0.00	0.00	0.00	0.00
	K_d	18.47 (15.79, 21.39)	87.07 (82.46, 91.66)	196.42 (190.39, 202.45)	234.85 (232.15, 237.55)	188.60 (179.04, 197.84)	192.28 (181.57, 202.97)	257.50 (250.67, 264.67)	258.68 (250.29, 266.49)
	R^2	0.84	0.95	0.30	0.96	0.87	0.64	0.94	0.55
	p	≤ 0.05	≤ 0.05	≤ 0.05	≤ 0.05	≤ 0.05	≤ 0.05	≤ 0.05	≤ 0.05
2	NaNO ₃ Conc. (M)	0.01	0.01	0.01	0.01	0.01	0.01	0.01	0.01
	K_d	162.47 (157.79, 167.39)	193.07 (187.46, 198.66)	369.10 (365.42, 372.02)	392.81 (389.82, 396.82)	315.60 (310.04, 320.84)	328.28 (323.57, 332.97)	343.50 (337.67, 349.67)	360.68 (349.29, 371.49)
	R^2	0.89	0.82	0.77	0.58	0.67	0.76	0.54	0.74
	p	≤ 0.05	≤ 0.05	≤ 0.05	≤ 0.05	≤ 0.05	≤ 0.05	≤ 0.05	≤ 0.05

Table B2 (continued). Partition coefficient (K_d) values for phosphorus adsorption at different values of pH and concentration of background electrolyte.

pH	Value	Solid types							
		PMP	WMP	S1	S2	S1+PMP	S1+WMP	S2+PMP	S2+WMP
5	NaNO ₃ Conc. (M)	0.01	0.01	0.01	0.01	0.01	0.01	0.01	0.01
	K_d	121.47 (116.79, 126.39)	166.07 (162.46, 169.66)	303.12 (297.03, 308.66)	346.19 (341.29, 350.47)	258.60 (251.04, 265.84)	231.28 (214.57, 248.97)	300.50 (292.67, 308.67)	294.68 (288.29, 301.49)
	R^2	0.82	0.95	0.56	0.77	0.83	0.92	0.63	0.77
	p	≤ 0.05	≤ 0.05	≤ 0.05	≤ 0.05	≤ 0.05	≤ 0.05	≤ 0.05	≤ 0.05
7	NaNO ₃ Conc. (M)	0.01	0.01	0.01	0.01	0.01	0.01	0.01	0.01
	K_d	90.47 (84.79, 96.39)	133.16 (127.59, 138.66)	283.11 (279.59, 286.48)	334.59 (329.28, 340.94)	220.60 (213.04, 228.84)	239.28 (229.57, 248.97)	245.50 (236.67, 254.67)	265.68 (252.29, 278.49)
	R^2	0.91	0.78	0.67	0.88	0.71	0.83	0.82	0.46
	p	≤ 0.05	≤ 0.05	≤ 0.05	≤ 0.05	≤ 0.05	≤ 0.05	≤ 0.05	≤ 0.05
9	NaNO ₃ Conc. (M)	0.01	0.01	0.01	0.01	0.01	0.01	0.01	0.01
	K_d	50.4724 (44.79, 56.39)	93.07 (87.46, 98.66)	266.10 (261.42, 270.02)	306.81 (301.63, 312.82)	290.60 (279.04, 301.84)	295.28 (284.57, 305.97)	248.50 (241.67, 255.67)	249.68 (241.29, 257.49)
	R^2	0.86	0.91	0.31	0.86	0.65	0.96	0.66	0.89
	p	≤ 0.05	≤ 0.05	≤ 0.05	≤ 0.05	≤ 0.05	≤ 0.05	≤ 0.05	≤ 0.05

Table B2 (continued). Partition coefficient (K_d) values for phosphorus adsorption at different values of pH and concentration of background electrolyte.

pH	Value	Solid types							
		PMP	WMP	S1	S2	S1+PMP	S1+WMP	S2+PMP	S2+WMP
12	NaNO ₃ Conc. (M)	0.01	0.01	0.01	0.01	0.01	0.01	0.01	0.01
	K_d	21.47 (12.79, 30.39)	88.07 (84.46, 91.66)	236.10 (231.42, 240.02)	274.81 (267.63, 281.82)	190.60 (180.04, 200.84)	193.28 (182.57, 204.97)	260.50 (251.67, 269.67)	261.68 (252.29, 270.49)
	R ²	0.85	0.92	0.55	0.94	0.88	0.65	0.93	0.53
	p	≤ 0.05	≤ 0.05	≤ 0.05	≤ 0.05	≤ 0.05	≤ 0.05	≤ 0.05	≤ 0.05
2	NaNO ₃ Conc. (M)	0.10	0.10	0.10	0.10	0.10	0.10	0.10	0.10
	K_d	195.47 (191.79, 199.39)	227.07 (223.46, 230.66)	394.10 (390.42, 398.02)	417.81 (413.82, 422.82)	342.60 (338.04, 346.84)	339.28 (334.57, 343.97)	365.50 (359.67, 371.67)	410.68 (403.29, 418.49)
	R ²	0.86	0.84	0.73	0.63	0.69	0.78	0.56	0.73
	p	≤ 0.05	≤ 0.05	≤ 0.05	≤ 0.05	≤ 0.05	≤ 0.05	≤ 0.05	≤ 0.05
5	NaNO ₃ Conc. (M)	0.10	0.10	0.10	0.10	0.10	0.10	0.10	0.10
	K_d	144.47 (140.79, 148.39)	191.07 (185.46, 196.66)	327.63 (322.54, 332.85)	374.14 (367.46, 380.09)	296.60 (289.04, 303.84)	326.28 (319.57, 332.97)	341.50 (336.67, 346.67)	330.68 (324.29, 337.49)
	R ²	0.83	0.94	0.57	0.79	0.89	0.94	0.68	0.73
	p	≤ 0.05	≤ 0.05	≤ 0.05	≤ 0.05	≤ 0.05	≤ 0.05	≤ 0.05	≤ 0.05

Table B2 (continued). Partition coefficient (K_d) values for phosphorus adsorption at different values of pH and concentration of background electrolyte.

pH	Value	Solid types							
		PMP	WMP	S1	S2	S1+PMP	S1+WMP	S2+PMP	S2+WMP
7	NaNO ₃ Conc. (M)	0.10	0.10	0.10	0.10	0.10	0.10	0.10	0.10
	K_d	119.47 (115.79, 123.39)	164.07 (160.46, 167.66)	308.58 (303.55, 313.59)	345.95 (340.58, 351.16)	266.60 (259.04, 273.84)	258.28 (250.57, 266.97)	332.50 (323.67, 341.67)	353.68 (341.29, 365.49)
	R^2	0.92	0.79	0.67	0.89	0.76	0.85	0.84	0.59
	p	≤ 0.05	≤ 0.05	≤ 0.05	≤ 0.05	≤ 0.05	≤ 0.05	≤ 0.05	≤ 0.05
9	NaNO ₃ Conc. (M)	0.10	0.10	0.10	0.10	0.10	0.10	0.10	0.10
	K_d	85.47 (79.79, 91.39)	129.07 (120.46, 137.66)	286.10 (281.42, 290.02)	323.81 (319.82, 327.82)	258.60 (250.04, 266.84)	262.28 (255.57, 269.97)	314.50 (305.67, 323.67)	310.68 (298.29, 322.49)
	R^2	0.86	0.91	0.31	0.86	0.65	0.96	0.66	0.89
	p	≤ 0.05	≤ 0.05	≤ 0.05	≤ 0.05	≤ 0.05	≤ 0.05	≤ 0.05	≤ 0.05
12	NaNO ₃ Conc. (M)	0.10	0.10	0.10	0.10	0.10	0.10	0.10	0.10
	K_d	62.47 (59.79, 65.39)	113.07 (107.46, 118.66)	263.10 (257.42, 268.02)	294.81 (289.82, 299.82)	228.60 (221.04, 235.84)	219.28 (212.57, 226.97)	307.50 (299.67, 315.67)	288.68 (277.29, 299.49)
	R^2	0.85	0.92	0.55	0.94	0.88	0.65	0.93	0.53
	p	≤ 0.05	≤ 0.05	≤ 0.05	≤ 0.05	≤ 0.05	≤ 0.05	≤ 0.05	≤ 0.05

*PMP = Pristine microplastic, WMP = weathered microplastic, S1 = low organic matter soil, S2 = high organic matter soil, S1 + PMP = low organic matter soil + pristine microplastic, S1 + WMP = low organic matter soil + weathered microplastic, S2 + PMP = high organic matter soil + pristine microplastic, S2 + WMP = high organic matter soil + weathered microplastic.

Table B3. Langmuir adsorption isotherm parameters for phosphorus adsorption at different values of pH and different concentrations of background electrolyte. Mass of solid used is 0.2 g. Volume of solution is 30 ml. Equilibrium time for the adsorption experiment is 24 hours. Values of pH range from 2 to 12 and concentration of background electrolyte from 0 to 0.1 M NaNO₃. C_{SM} and b are determined from the intercept (1/ C_{SM}) and slope (1/ bC_{SM}) of linear regression (independent variable: inverse of phosphorus concentration present in the solution, 1/ C_{aq}; dependent variable: inverse of phosphorus adsorbed to the solid, 1/ C_s) respectively. 95 % confidence interval is calculated which are shown in brackets. Upper and lower limit of confidence intervals are separated by comma (,).

pH	Value	Solid types							
		PMP	WMP	S1	S2	S1+PMP	S1+WMP	S2+PMP	S2+WMP
2	NaNO ₃ Conc. (M)	0.00	0.00	0.00	0.00	0.00	0.00	0.00	0.00
	C _{SM} (mg/ kg)	274.18 (267.93, 280.41)	305.56 (299.18, 311.60)	406.19 (400.42, 412.02)	483.29 (477.82, 489.82)	312.19 (307.19, 317.19)	326.19 (320.26, 331.46)	360.19 (355.84, 365.64)	386.19 (378.81, 394.81)
	b (L/ mg)	0.09 (0.05, 0.12)	0.12 (0.80, 1.02)	0.47 (0.22, 0.57)	0.82 (0.55, 0.97)	0.64 (0.32, 1.07)	0.79 (0.52, 1.11)	0.65 (0.33, 1.09)	0.81 (0.53, 1.12)
	R ²	0.66	0.67	0.78	0.69	0.76	0.74	0.75	0.72
	p	≤ 0.05	≤ 0.05	≤ 0.05	≤ 0.05	≤ 0.05	≤ 0.05	≤ 0.05	≤ 0.05
5	NaNO ₃ Conc. (M)	0.00	0.00	0.00	0.00	0.00	0.00	0.00	0.00
	C _{SM} (mg/ kg)	260.33 (254.47, 266.87)	265.38 (260.87, 270.07)	386.16 (380.52, 391.52)	447.36 (442.05, 452.85)	294.16 (289.19, 299.19)	275.55 (270.32, 280.72)	336.16 (331.42, 341.42)	354.16 (347.09, 361.09)
	b (L/ mg)	0.09 (0.07, 0.11)	0.07 (0.04, 1.16)	0.49 (0.24, 0.61)	0.48 (0.20, 0.56)	0.49 (0.23, 0.58)	0.84 (0.54, 0.98)	0.49 (0.21, 0.59)	0.86 (0.58, 0.99)
	R ²	0.66	0.67	0.71	0.78	0.61	0.62	0.91	0.86
	p	≤ 0.05	≤ 0.05	≤ 0.05	≥ 0.05	≤ 0.05	≤ 0.05	≤ 0.05	≥ 0.05

Table B3 (continued). Langmuir adsorption isotherm parameters for phosphorus at different values of pH and concentration of background electrolyte.

pH	Value	Solid types							
		PMP	WMP	S1	S2	S1+PMP	S1+WMP	S2+PMP	S2+WMP
7	NaNO ₃ Conc. (M)	0.00	0.00	0.00	0.00	0.00	0.00	0.00	0.00
	C _{SM} (mg/ kg)	245.89 (241.98, 250.78)	243.72 (239.36, 248.76)	357.19 (351.76, 362.76)	428.39 (422.16, 434.16)	267.19 (262.36, 272.96)	260.89 (255.04, 266.04)	307.19 (302.02, 312.22)	327.19 (321.39, 333.39)
	b (L/ mg)	1.36 (1.05, 1.52)	1.29 (1.05, 1.42)	0.56 (0.29, 0.74)	0.61 (0.46, 0.86)	0.81 (0.57, 1.34)	0.83 (0.59, 1.36)	0.84 (0.61, 1.38)	0.82 (0.58, 1.35)
	R ²	0.73	0.69	0.76	0.78	0.73	0.81	0.82	0.62
	p	≤0.05	≤0.05	≥0.05	≤0.05	≤0.05	≤0.05	≤0.05	≤0.05
9	NaNO ₃ Conc. (M)	0.00	0.00	0.00	0.00	0.00	0.00	0.00	0.00
	C _{SM} (mg/ kg)	226.21 (221.66, 231.06)	216.79 (210.11, 222.91)	334.57 (329.99, 339.43)	374.67 (368.71, 380.51)	244.57 (239.01, 249.21)	234.41 (230.74, 238.34)	271.57 (261.44, 281.64)	298.57 (289.65, 307.05)
	b (L/ mg)	1.46 (1.15, 1.72)	1.26 (1.04, 1.49)	0.89 (0.54, 1.09)	0.86 (0.61, 1.16)	0.64 (0.32, 1.07)	0.79 (0.52, 1.11)	0.65 (0.33, 1.09)	0.81 (0.53, 1.12)
	R ²	0.62	0.63	0.67	0.74	0.74	0.88	0.82	0.87
	p	≤0.05	≤0.05	≤0.05	≥0.05	≤0.05	≤0.05	≥0.05	≤0.05

Table B3 (continued). Langmuir adsorption isotherm parameters for phosphorus at different values of pH and concentration of background electrolyte.

pH	Value	Solid types							
		PMP	WMP	S1	S2	S1+PMP	S1+WMP	S2+PMP	S2+WMP
12	NaNO ₃ Conc. (M)	0.00	0.00	0.00	0.00	0.00	0.00	0.00	0.00
	C _{SM} (mg/ kg)	209.47 (203.79, 215.39)	176.07 (172.46, 179.66)	311.08 (306.39, 315.45)	341.91 (336.15, 347.55)	229.08 (224.04, 233.84)	198.09 (191.57, 204.97)	259.08 (254.67, 263.67)	263.08 (256.29, 269.49)
	b (L/ mg)	1.48 (1.21, 1.76)	1.36 (1.14, 1.56)	0.88 (0.55, 1.07)	0.87 (0.62, 1.18)	0.49 (0.23, 0.58)	0.84 (0.64, 0.98)	0.49 (0.21, 0.59)	0.86 (0.51, 0.99)
	R ²	0.74	0.65	0.71	0.96	0.87	0.74	0.94	0.75
	p	≥0.05	≤0.05	≤0.05	≤0.05	≤0.05	≤0.05	≤0.05	≤0.05
	2	NaNO ₃ Conc. (M)	0.01	0.01	0.01	0.01	0.01	0.01	0.01
C _{SM} (mg/ kg)	289.26 (284.79, 294.39)	326.07 (320.46, 331.66)	433.78 (426.42, 441.02)	506.39 (501.82, 511.82)	316.78 (310.04, 323.84)	333.63 (326.57, 341.97)	366.78 (357.67, 376.67)	392.78 (383.29, 401.49)	
b (L/ mg)	0.08 (0.03, 1.16)	1.66 (1.12, 1.89)	0.64 (0.21, 0.96)	0.75 (0.31, 1.08)	0.68 (0.33, 1.16)	0.64 (0.38, 1.21)	0.79 (0.31, 1.26)	0.81 (0.41, 1.31)	
R ²	0.69	0.62	0.67	0.68	0.68	0.76	0.74	0.74	
p	≤0.05	≤0.05	≤0.05	≤0.05	≥0.05	≤0.05	≤0.05	≤0.05	

Table B3 (continued). Langmuir adsorption isotherm parameters for phosphorus at different values of pH and concentration of background electrolyte.

pH	Value	Solid types							
		PMP	WMP	S1	S2	S1+PMP	S1+WMP	S2+PMP	S2+WMP
5	NaNO ₃ Conc. (M)	0.01	0.01	0.01	0.01	0.01	0.01	0.01	0.01
	C _{SM} (mg/ kg)	256.46 (252.79, 260.39)	276.07 (269.46, 282.66)	403.16 (397.42, 409.02)	468.94 (464.63, 473.82)	289.16 (283.04, 295.84)	277.39 (271.57, 283.97)	341.16 (335.67, 347.67)	361.16 (355.29, 367.49)
	b (L/ mg)	0.8 (0.05, 0.19)	1.79 (1.44, 2.01)	0.68 (0.35, 1.09)	0.86 (0.44, 1.25)	0.73 (0.43, 1.19)	0.74 (0.49, 1.21)	0.87 (0.51, 1.49)	0.88 (0.54, 1.42)
	R ²	0.66	0.74	0.71	0.86	0.74	0.96	0.76	0.89
	p	≤0.05	≤0.05	≤0.05	≤0.05	≤0.05	≤0.05	≤0.05	≤0.05
	NaNO ₃ Conc. (M)	0.01	0.01	0.01	0.01	0.01	0.01	0.01	0.01
7	C _{SM} (mg/ kg)	247.47 (241.79, 253.39)	245.16 (239.46, 250.66)	364.19 (358.42, 369.02)	449.59 (445.63, 454.82)	272.19 (266.04, 277.84)	263.39 (257.57, 269.97)	312.19 (305.67, 318.67)	342.19 (335.29, 349.49)
	b (L/ mg)	1.09 (0.50, 1.12)	1.59 (1.25, 1.82)	0.67 (0.36, 1.11)	0.88 (0.46, 1.23)	0.49 (0.23, 0.68)	0.84 (0.64, 0.98)	0.49 (0.21, 0.59)	0.86 (0.51, 0.99)
	R ²	0.66	0.61	0.68	0.86	0.65	0.96	0.86	0.69
	p	≤0.05	≤0.05	≤0.05	≤0.05	≤0.05	≤0.05	≤0.05	≤0.05
	NaNO ₃ Conc. (M)	0.01	0.01	0.01	0.01	0.01	0.01	0.01	0.01
	C _{SM} (mg/ kg)	247.47 (241.79, 253.39)	245.16 (239.46, 250.66)	364.19 (358.42, 369.02)	449.59 (445.63, 454.82)	272.19 (266.04, 277.84)	263.39 (257.57, 269.97)	312.19 (305.67, 318.67)	342.19 (335.29, 349.49)
b (L/ mg)	1.09 (0.50, 1.12)	1.59 (1.25, 1.82)	0.67 (0.36, 1.11)	0.88 (0.46, 1.23)	0.49 (0.23, 0.68)	0.84 (0.64, 0.98)	0.49 (0.21, 0.59)	0.86 (0.51, 0.99)	
R ²	0.66	0.61	0.68	0.86	0.65	0.96	0.86	0.69	
p	≤0.05	≤0.05	≤0.05	≤0.05	≤0.05	≤0.05	≤0.05	≤0.05	

Table B3 (continued). Langmuir adsorption isotherm parameters for phosphorus at different values of pH and concentration of background electrolyte.

pH	Value	Solid types							
		PMP	WMP	S1	S2	S1+PMP	S1+WMP	S2+PMP	S2+WMP
9	NaNO ₃ Conc. (M)	0.01	0.01	0.01	0.01	0.01	0.01	0.01	0.01
	C _{SM} (mg/ kg)	229.47 (224.79, 234.39)	221.07 (215.46, 266.66)	352.57 (346.42, 358.02)	391.36 (385.63, 397.82)	247.57 (242.04, 253.84)	238.03 (232.57, 243.97)	283.57 (273.67, 294.67)	316.57 (305.29, 327.49)
	b (L/ mg)	1.36 (1.09, 1.56)	1.09 (0.8, 1.14)	0.84 (0.46, 1.23)	0.85 (0.48, 1.28)	1.04 (0.79, 1.54)	1.14 (0.84, 1.68)	1.19 (0.81, 1.62)	1.21 (0.81, 1.48)
	R ²	0.66	0.61	0.71	0.86	0.73	0.94	0.77	0.88
	p	≤0.05	≤0.05	≤0.05	≤0.05	≤0.05	≤0.05	≤0.05	≤0.05
12	NaNO ₃ Conc. (M)	0.01	0.01	0.01	0.01	0.01	0.01	0.01	0.01
	C _{SM} (mg/ kg)	211.47 (206.79, 216.39)	183.07 (178.46, 187.66)	329.08 (323.42, 334.02)	359.46 (353.63, 365.82)	237.08 (231.04, 242.84)	209.36 (203.57, 215.97)	262.08 (253.67, 270.67)	276.08 (267.29, 284.49)
	b (L/ mg)	1.29 (0.80, 1.46)	1.57 (1.24, 1.72)	0.74 (0.36, 1.41)	0.88 (0.46, 1.39)	1.24 (0.86, 1.64)	1.16 (0.87, 1.63)	1.22 (0.83, 1.64)	1.19 (0.79, 1.49)
	R ²	0.66	0.71	0.71	0.76	0.65	0.66	0.86	0.69
	p	≤0.05	≤0.05	≤0.05	≤0.05	≤0.05	≤0.05	≤0.05	≤0.05

Table B3 (continued). Langmuir adsorption isotherm parameters for phosphorus at different values of pH and concentration of background electrolyte.

pH	Value	Solid types							
		PMP	WMP	S1	S2	S1+PMP	S1+WMP	S2+PMP	S2+WMP
2	NaNO ₃ Conc. (M)	0.10	0.10	0.10	0.10	0.10	0.10	0.10	0.10
	C _{SM} (mg/ kg)	316.47 (311.79, 321.39)	359.07 (354.46, 363.66)	452.19 (446.42, 457.02)	587.92 (581.82, 594.82)	452.19 (446.04, 457.84)	382.06 (372.57, 391.97)	481.67 (472.29, 491.49)	423.67 (415.29, 432.49)
	b (L/ mg)	0.70 (0.30, 1.05)	1.36 (1.04, 1.72)	0.76 (0.38, 1.46)	0.78 (0.41, 1.49)	1.25 (0.87, 1.63)	1.04 (0.79, 1.54)	1.14 (0.84, 1.68)	1.19 (0.79, 1.49)
	R ²	0.69	0.62	0.77	0.78	0.77	0.76	0.84	0.74
	p	<0.05	<0.05	<0.05	<0.05	<0.05	<0.05	<0.05	<0.05
5	NaNO ₃ Conc. (M)	0.10	0.10	0.10	0.10	0.10	0.10	0.10	0.10
	C _{SM} (mg/ kg)	288.47 (284.79, 292.39)	326.07 (322.42, 329.02)	416.16 (409.87, 422.45)	561.37 (556.82, 566.82)	416.16 (409.04, 422.84)	367.16 (350.57, 383.97)	466.78 (453.29, 480.49)	394.68 (383.29, 405.49)
	b (L/ mg)	1.59 (1.25, 1.84)	1.38 (1.12, 1.75)	0.91 (0.68, 1.26)	0.89 (0.61, 1.32)	1.24 (0.92, 1.74)	1.25 (0.94, 1.79)	1.32 (1.01, 1.82)	1.21 (0.81, 1.48)
	R ²	0.69	0.62	0.67	0.65	0.87	0.76	0.78	0.74
	p	<0.05	<0.05	≥0.05	<0.05	<0.05	<0.05	<0.05	<0.05

Table B3 (continued). Langmuir adsorption isotherm parameters for phosphorus at different values of pH and concentration of background electrolyte.

pH	Value	Solid types							
		PMP	WMP	S1	S2	S1+PMP	S1+WMP	S2+PMP	S2+WMP
7	NaNO ₃ Conc. (M)	0.10	0.10	0.10	0.10	0.10	0.10	0.10	0.10
	C _{SM} (mg/ kg)	273.47 (268.79, 278.39)	304.07 (299.46, 308.66)	377.29 (372.42, 382.02)	529.18 (524.82, 534.82)	377.29 (372.04, 382.84)	348.79 (336.57, 360.97)	439.29 (431.67, 447.67)	416.29 (409.29, 423.49)
	b (L/ mg)	1.61 (1.47, 1.82)	1.41 (1.19, 1.82)	1.29 (0.90, 1.42)	1.46 (1.09, 1.82)	1.25 (0.87, 1.63)	1.04 (0.79, 1.54)	1.14 (0.84, 1.68)	1.19 (0.79, 1.49)
	R ²	0.67	0.66	0.67	0.71	0.77	0.76	0.61	0.74
	p	≤ 0.05	≤ 0.05	≤ 0.05	≤ 0.05	≤ 0.05	≤ 0.05	≤ 0.05	≤ 0.05
9	NaNO ₃ Conc. (M)	0.10	0.10	0.10	0.10	0.10	0.10	0.10	0.10
	C _{SM} (mg/ kg)	246.47 (240.79, 252.39)	281.07 (275.46, 287.66)	366.78 (362.42, 370.02)	486.75 (481.82, 491.82)	366.78 (362.04, 370.84)	307.46 (293.57, 321.97)	406.78 (400.67, 412.67)	386.78 (380.29, 393.49)
	b (L/ mg)	1.59 (1.35, 1.78)	1.59 (1.24, 1.86)	1.28 (1.02, 1.46)	1.26 (1.09, 1.87)	1.04 (0.79, 1.54)	1.14 (0.84, 1.68)	1.19 (0.81, 1.62)	1.21 (0.81, 1.48)
	R ²	0.69	0.62	0.87	0.78	0.81	0.86	0.84	0.84
	p	≤ 0.05	≤ 0.05	≤ 0.05	≤ 0.05	≤ 0.05	≤ 0.05	≤ 0.05	≤ 0.05

Table B3 (continued). Langmuir adsorption isotherm parameters for phosphorus at different values of pH and concentration of background electrolyte.

pH	Value	Solid types							
		PMP	WMP	S1	S2	S1+PMP	S1+WMP	S2+PMP	S2+WMP
12	NaNO ₃ Conc. (M)	0.10	0.10	0.10	0.10	0.10	0.10	0.10	0.10
	C _{SM} (mg/ kg)	232.47 (229.79, 235.39)	248.07 (243.46, 252.66)	1.209 (1.003, 1.438)	1.361 (1.066, 1.792)	341.67 (336.04, 346.84)	266.34 (256.57, 276.97)	381.67 (374.67, 388.67)	341.67 (335.29, 348.49)
	b (L/ mg)	1.29 (0.90, 1.32)	1.54 (1.27, 1.92)	1.49 (1.12, 1.78)	1.52 (1.23, 1.84)	1.05 (0.77, 1.52)	1.17 (0.83, 1.68)	1.18 (0.81, 1.64)	1.22 (0.83, 1.46)
	R ²	0.66	0.61	0.67	0.68	0.87	0.86	0.74	0.76
	p	≤0.05	≤0.05	≤0.05	≤0.05	≤0.05	≤0.05	≤0.05	≤0.05

*PMP = Pristine microplastic, WMP = weathered microplastic, S1 = low organic matter soil, S2 = high organic matter soil, S1 + PMP = low organic matter soil + pristine microplastic, S1 + WMP = low organic matter soil + weathered microplastic, S2 + PMP = high organic matter soil + pristine microplastic, S2 + WMP = high organic matter soil + weathered microplastic. Langmuir equation is expressed as $\frac{C_s}{C_{aq}} = \frac{bC_{SM}}{1 + C_{aq}b}$, where, C_s = amount of P adsorbed on solid (mg/ kg), C_{aq} = concentration of P in equilibrium solution (mg/ L), C_{SM} = maximum adsorption capacity (mg/ kg), b = binding constant (L/ mg).

Table B4. Freundlich adsorption isotherm parameters for phosphorus at different values of pH and concentration of background electrolyte. Mass of solid used is 0.2 g. Volume of solution is 30 ml. Equilibrium time for the adsorption experiment is 24 hours. Values of pH range from 2 to 12 and concentration of background electrolyte from 0 to 0.1 M NaNO₃. Log K_f and 1/ n are determined from the intercept and slope of linear regression (independent variable: log value of P concentration present in the solution, log C_{aq}; dependent variable: log value of P adsorbed to the solid, log C_s) respectively. 95 % confidence interval is calculated which are shown in brackets. Upper and lower limit of confidence intervals are separated by comma (,).

pH	Value	Solid types							
		PMP	WMP	S1	S2	S1+PMP	S1+WMP	S2+PMP	S2+WMP
2	Conc. of NaNO ₃ (M)	0.00	0.00	0.00	0.00	0.00	0.00	0.00	0.00
	log K _f	1.94 (1.44, 2.32)	2.23 (2.13, 2.26)	6.74 (6.51, 6.93)	7.37 (7.18, 7.52)	2.89 (2.64, 3.02)	2.18 (1.89, 2.31)	3.93 (2.62, 4.17)	3.97 (3.68, 4.26)
	1/ n	0.68 (0.54, 0.82)	0.64 (0.51, 0.79)	0.81 (0.75, 0.91)	0.89 (0.62, 1.06)	0.70 (0.52, 0.91)	0.78 (0.53, 0.97)	0.79 (0.61, 0.93)	0.75 (0.67, 0.96)
	R ²	0.95	0.94	0.94	0.91	0.89	0.94	0.85	0.81
	p	≤ 0.05	≤ 0.05	≤ 0.05	≤ 0.05	≤ 0.05	≤ 0.05	≤ 0.05	≤ 0.05
5	Conc. of NaNO ₃ (M)	0.00	0.00	0.00	0.00	0.00	0.00	0.00	0.00
	log K _f	1.59 (1.19, 2.19)	2.48 (2.11, 2.81)	6.35 (6.21, 6.43)	6.86 (6.72, 7.05)	2.88 (2.63, 3.02)	2.16 (1.91, 2.32)	3.93 (2.62, 4.17)	3.96 (3.67, 4.27)
	1/ n	0.84 (0.65, 1.15)	0.85 (0.72, 1.23)	0.83 (0.66, 0.99)	0.86 (0.55, 0.91)	0.72 (0.54, 0.94)	0.78 (0.53, 0.97)	0.81 (0.79, 0.95)	0.73 (0.65, 0.94)
	R ²	0.88	0.97	0.31	0.78	0.81	0.91	0.61	0.76
	p	≤ 0.05	≤ 0.05	≤ 0.05	≤ 0.05	≤ 0.05	≤ 0.05	≤ 0.05	≤ 0.05

Table B4 (continued). Freundlich adsorption isotherm parameters for phosphorus at different values of pH and concentration of background electrolyte.

pH	Value	Solid types							
		PMP	WMP	S1	S2	S1+PMP	S1+WMP	S2+PMP	S2+WMP
7	Conc. of NaNO ₃ (M)	0.00	0.00	0.00	0.00	0.00	0.00	0.00	0.00
	log K _f	1.64 (1.41, 1.91)	2.48 (2.11, 2.81)	5.97 (5.81, 6.13)	6.41 (6.28, 6.52)	2.92 (2.64, 3.03)	2.19 (1.89, 2.32)	3.94 (2.65, 4.18)	3.97 (3.68, 4.26)
	1/ n	0.75 (0.46, 0.97)	0.67 (0.49, 0.93)	0.72 (0.45, 0.95)	0.71 (0.52, 0.90)	0.77 (0.56, 0.96)	0.70 (0.53, 0.94)	0.74 (0.46, 0.98)	0.70 (0.55, 0.95)
	R ²	0.93	0.79	0.66	0.90	0.63	0.81	0.81	0.32
	p	≤0.05	≤0.05	≤0.05	≤0.05	≤0.05	≤0.05	≤0.05	≤0.05
9	Conc. of NaNO ₃ (M)	0.00	0.00	0.00	0.00	0.00	0.00	0.00	0.00
	log K _f	2.65 (2.48, 2.87)	3.37 (3.13, 3.59)	5.55 (5.41, 5.63)	5.67 (5.48, 5.88)	1.89 (1.64, 2.02)	1.18 (0.89, 1.31)	1.93 (1.62, 2.17)	1.97 (1.68, 2.26)
	1/ n	0.77 (0.61, 0.84)	0.84 (0.76, 1.14)	0.75 (0.56, 0.95)	0.93 (0.79, 1.13)	0.69 (0.48, 0.86)	0.87 (0.73, 1.11)	0.79 (0.58, 0.83)	0.87 (0.72, 1.13)
	R ²	0.90	0.93	0.30	0.84	0.64	0.99	0.62	0.87
	p	≤0.05	≤0.05	≤0.05	≤0.05	≤0.05	≤0.05	≤0.05	≤0.05

Table B4 (continued). Freundlich adsorption isotherm parameters for phosphorus at different values of pH and concentration of background electrolyte.

pH	Value	Solid types							
		PMP	WMP	S1	S2	S1+PMP	S1+WMP	S2+PMP	S2+WMP
12	Conc. of NaNO ₃ (M)	0.00	0.00	0.00	0.00	0.00	0.00	0.00	0.00
	log K _f	2.56 (2.34, 2.81)	3.32 (3.19, 3.56)	5.16 (4.92, 5.28)	4.98 (4.89, 5.18)	1.72 (1.58, 1.96)	1.21 (0.96, 1.36)	1.94 (1.62, 2.18)	1.98 (1.67, 2.27)
	1/ n	0.73 (0.64, 0.89)	0.74 (0.59, 1.03)	0.86 (0.67, 1.14)	0.85 (0.56, 1.21)	0.78 (0.63, 0.91)	0.83 (0.65, 1.16)	0.94 (0.76, 1.04)	0.95 (0.77, 1.18)
	R ²	0.84	0.95	0.30	0.96	0.87	0.64	0.94	0.55
	p	≤ 0.05	≤ 0.05	≤ 0.05	≤ 0.05	≤ 0.05	≤ 0.05	≤ 0.05	≤ 0.05
2	Conc. of NaNO ₃ (M)	0.01	0.01	0.01	0.01	0.01	0.01	0.01	0.01
	log K _f	1.48 (1.13, 1.76)	2.45 (2.14, 2.84)	6.74 (6.51, 6.93)	7.37 (7.18, 7.52)	2.91 (2.63, 3.03)	2.19 (1.91, 2.32)	3.97 (2.62, 4.18)	3.98 (3.69, 4.28)
	1/ n	0.64 (0.51, 0.79)	0.68 (0.54, 0.82)	0.89 (0.62, 1.06)	0.81 (0.75, 0.91)	0.79 (0.61, 0.93)	0.70 (0.52, 0.91)	0.78 (0.53, 0.97)	0.75 (0.67, 0.96)
	R ²	0.89	0.82	0.77	0.58	0.67	0.76	0.54	0.74
	p	≤ 0.05	≤ 0.05	≤ 0.05	≤ 0.05	≤ 0.05	≤ 0.05	≤ 0.05	≤ 0.05

Table B4 (continued). Freundlich adsorption isotherm parameters for phosphorus at different values of pH and concentration of background electrolyte.

pH	Value	Solid types							
		PMP	WMP	S1	S2	S1+PMP	S1+WMP	S2+PMP	S2+WMP
5	Conc. of NaNO ₃ (M)	0.01	0.01	0.01	0.01	0.01	0.01	0.01	0.01
	log K _f	1.56 (1.35, 1.79)	2.46 (2.17, 2.87)	6.39 (6.26, 6.49)	6.86 (6.72, 7.05)	2.88 (2.63, 3.02)	2.16 (1.91, 2.32)	3.98 (2.62, 4.17)	3.96 (3.67, 4.27)
	1/ n	0.74 (0.59, 1.03)	0.73 (0.64, 0.89)	0.85 (0.56, 1.21)	0.86 (0.67, 1.14)	0.83 (0.65, 1.16)	0.94 (0.76, 1.04)	0.78 (0.63, 0.91)	0.83 (0.65, 1.16)
	R ²	0.86	0.91	0.31	0.86	0.65	0.96	0.66	0.89
	p	≤ 0.05	≤ 0.05	≤ 0.05	≤ 0.05	≤ 0.05	≤ 0.05	≤ 0.05	≤ 0.05
7	Conc. of NaNO ₃ (M)	0.01	0.01	0.01	0.01	0.01	0.01	0.01	0.01
	log K _f	1.59 (1.31, 1.82)	2.45 (2.14, 2.84)	5.91 (5.76, 6.10)	6.40 (6.26, 6.51)	2.92 (2.64, 3.03)	2.01 (1.89, 2.32)	3.84 (2.65, 4.18)	3.94 (3.68, 4.26)
	1/ n	0.68 (0.54, 0.82)	0.64 (0.51, 0.79)	0.61 (0.50, 0.71)	0.59 (0.42, 0.76)	0.70 (0.52, 0.91)	0.58 (0.43, 0.67)	0.79 (0.61, 0.94)	0.85 (0.67, 1.00)
	R ²	0.86	0.91	0.31	0.86	0.65	0.96	0.66	0.89
	p	≤ 0.05	≤ 0.05	≤ 0.05	≤ 0.05	≤ 0.05	≤ 0.05	≤ 0.05	≤ 0.05

Table B4 (continued). Freundlich adsorption isotherm parameters for phosphorus at different values of pH and concentration of background electrolyte.

pH	Value	Solid types							
		PMP	WMP	S1	S2	S1+PMP	S1+WMP	S2+PMP	S2+WMP
9	Conc. of NaNO ₃ (M)	0.01	0.01	0.01	0.01	0.01	0.01	0.01	0.01
	log K _f	3.15 (2.96, 3.36)	3.57 (3.26, 3.89)	5.55 (5.41, 5.63)	5.68 (5.47, 5.87)	1.89 (1.64, 2.02)	1.00 (0.89, 1.31)	1.90 (1.62, 2.17)	1.92 (1.68, 2.26)
	1/ n	0.68 (0.54, 0.82)	0.64 (0.51, 0.79)	0.81 (0.75, 0.91)	0.89 (0.62, 1.06)	0.70 (0.52, 0.91)	0.78 (0.53, 0.97)	0.79 (0.61, 0.93)	0.75 (0.67, 0.96)
	R ²	0.86	0.91	0.31	0.86	0.65	0.96	0.66	0.89
	p	≤ 0.05	≤ 0.05	≤ 0.05	≤ 0.05	≤ 0.05	≤ 0.05	≤ 0.05	≤ 0.05
12	Conc. of NaNO ₃ (M)	0.01	0.01	0.01	0.01	0.01	0.01	0.01	0.01
	log K _f	3.19 (2.95, 3.38)	3.61 (3.28, 3.92)	5.16 (4.92, 5.28)	4.98 (4.89, 5.18)	1.72 (1.58, 1.96)	0.98 (0.76, 1.36)	1.92 (1.62, 2.18)	1.95 (1.67, 2.37)
	1/ n	0.63 (0.51, 0.80)	0.66 (0.54, 0.82)	0.91 (0.76, 1.31)	0.93 (0.69, 1.39)	0.73 (0.54, 0.93)	0.76 (0.51, 0.96)	0.78 (0.62, 0.91)	0.74 (0.65, 0.93)
	R ²	0.86	0.91	0.31	0.86	0.65	0.96	0.66	0.89
	p	≤ 0.05	≤ 0.05	≤ 0.05	≤ 0.05	≤ 0.05	≤ 0.05	≤ 0.05	≤ 0.05

Table B4 (continued). Freundlich adsorption isotherm parameters for phosphorus at different values of pH and concentration of background electrolyte.

pH	Value	Solid types							
		PMP	WMP	S1	S2	S1+PMP	S1+WMP	S2+PMP	S2+WMP
2	Conc. of NaNO ₃ (M)	0.10	0.10	0.10	0.10	0.10	0.10	0.10	0.10
	log K _f	4.37 (4.06, 4.63)	6.17 (5.96, 6.46)	4.16 (3.92, 4.38)	2.92 (2.72, 3.12)	2.28 (2.18, 2.46)	2.29 (2.17, 2.47)	2.32 (2.21, 2.49)	2.23 (2.13, 2.44)
	1/ n	0.79 (0.54, 1.32)	0.74 (0.51, 1.39)	0.83 (0.50, 1.41)	0.89 (0.52, 1.56)	0.67 (0.42, 0.81)	0.68 (0.43, 0.87)	0.79 (0.61, 0.94)	0.75 (0.67, 1.00)
	R ²	0.89	0.82	0.77	0.58	0.67	0.76	0.54	0.74
	p	≤ 0.05	≤ 0.05	≤ 0.05	≤ 0.05	≤ 0.05	≤ 0.05	≤ 0.05	≤ 0.05
5	Conc. of NaNO ₃ (M)	0.10	0.10	0.10	0.10	0.10	0.10	0.10	0.10
	log K _f	4.47 (4.16, 4.71)	6.21 (5.98, 6.51)	3.66 (3.52, 3.78)	2.37 (2.26, 2.52)	1.16 (1.08, 2.36)	1.31 (1.19, 2.46)	1.31 (2.19, 2.46)	1.24 (2.15, 2.45)
	1/ n	0.82 (0.55, 1.39)	0.84 (0.55, 1.43)	0.92 (0.65, 1.51)	0.94 (0.72, 1.66)	0.73 (0.55, 0.93)	0.57 (0.44, 0.68)	0.69 (0.41, 0.84)	0.65 (0.47, 0.89)
	R ²	0.89	0.82	0.77	0.58	0.67	0.76	0.54	0.74
	p	≤ 0.05	≤ 0.05	≤ 0.05	≤ 0.05	≤ 0.05	≤ 0.05	≤ 0.05	≤ 0.05

Table B4 (continued). Freundlich adsorption isotherm parameters for phosphorus at different values of pH and concentration of background electrolyte.

pH	Value	Solid types							
		PMP	WMP	S1	S2	S1+PMP	S1+WMP	S2+PMP	S2+WMP
7	Conc. of NaNO ₃ (M)	0.10	0.10	0.10	0.10	0.10	0.10	0.10	0.10
	log K _f	4.39 (4.12, 4.71)	6.15 (5.94, 6.43)	3.26 (3.02, 3.42)	1.97 (1.89, 2.18)	2.28 (2.18, 2.46)	2.29 (2.17, 2.47)	2.32 (2.21, 2.49)	2.23 (2.13, 2.44)
	1/ n	0.76 (0.51, 1.30)	0.75 (0.50, 1.40)	0.84 (0.50, 1.42)	0.91 (0.53, 1.58)	0.68 (0.43, 0.87)	0.75 (0.67, 1.00)	0.79 (0.61, 0.94)	0.67 (0.42, 0.81)
	R ²	0.89	0.82	0.77	0.58	0.67	0.76	0.54	0.74
	p	≤0.05	≤0.05	≤0.05	≤0.05	≤0.05	≤0.05	≤0.05	≤0.05
9	Conc. of NaNO ₃ (M)	0.10	0.10	0.10	0.10	0.10	0.10	0.10	0.10
	log K _f	5.47 (5.19, 5.79)	6.75 (6.49, 7.02)	2.78 (2.52, 2.92)	1.67 (1.51, 1.82)	1.78 (1.54, 2.04)	1.46 (1.27, 1.67)	1.78 (1.47, 2.07)	1.38 (1.19, 1.59)
	1/ n	0.68 (0.54, 0.82)	0.64 (0.51, 0.79)	0.81 (0.50, 1.31)	0.89 (0.42, 1.36)	0.75 (0.56, 0.94)	0.77 (0.53, 0.98)	0.78 (0.63, 0.92)	0.75 (0.67, 0.95)
	R ²	0.89	0.82	0.77	0.58	0.67	0.76	0.54	0.74
	p	≤0.05	≤0.05	≤0.05	≤0.05	≤0.05	≤0.05	≤0.05	≤0.05

Table B4 (continued). Freundlich adsorption isotherm parameters for phosphorus at different values of pH and concentration of background electrolyte.

pH	Value	Solid types							
		PMP	WMP	S1	S2	S1+PMP	S1+WMP	S2+PMP	S2+WMP
12	Conc. of NaNO ₃ (M)	0.10	0.10	0.10	0.10	0.10	0.10	0.10	0.10
	log K _f	5.49 (5.21, 5.80)	6.76 (6.48, 7.02)	1.29 (1.03, 1.48)	1.09 (0.84, 1.24)	1.65 (1.36, 1.94)	1.66 (1.28, 2.07)	1.76 (1.42, 2.01)	1.37 (1.17, 1.58)
	1/ n	0.68 (0.54, 0.82)	0.64 (0.51, 0.79)	0.93 (0.50, 1.57)	0.92 (0.42, 1.56)	0.73 (0.54, 0.93)	0.76 (0.51, 0.96)	0.78 (0.62, 0.91)	0.74 (0.65, 0.93)
	R ²	0.89	0.82	0.77	0.58	0.67	0.76	0.54	0.74
	p	< 0.05	< 0.05	< 0.05	< 0.05	< 0.05	< 0.05	< 0.05	< 0.05

*PMP = Pristine microplastic, WMP = weathered microplastic, S1 = low organic matter soil, S2 = high organic matter soil, S1 + PMP = low organic matter soil + pristine microplastic, S1 + WMP = low organic matter soil + weathered microplastic, S2 + PMP = high organic matter soil + pristine microplastic, S2 + WMP = high organic matter soil + weathered microplastic. Freundlich equation is expressed as $C_s = K_f C_{aq}^{1/n}$ where, C_s = amount of P adsorbed on solid (mg/ kg), C_{aq} = concentration of P in equilibrium solution (mg/ L), log K_f = Freundlich constant, 1/ n = heterogeneity factor.

Appendix C

Appendices of Chapter 5

Tables

Table C1. Chemical and physical properties of soils used in the study. Two types of soil samples were arable and flower bed soil. Units of the parameters are shown in parentheses. For all parameters, n = 5, \pm standard deviation.

Parameters	Arable soil	Flower bed soil
Respiration rate (g CO ₂ g ⁻¹ soil s ⁻¹)	$2.1 \times 10^{-9} \pm 0.05$	$3.2 \times 10^{-9} \pm 0.09$
Phosphatase enzyme activity (μ g of p-nitrophenol/ hr/ g of soil)	16.0 ± 0.82	31.0 ± 0.61
Soil pH	7.6 ± 0.13	7.1 ± 0.09
Exchangeable Na (mg/ L)	3.4 ± 0.63	3.6 ± 0.63
Exchangeable K (mg/ L)	4.1 ± 0.78	5.4 ± 0.57
Exchangeable Mg (mg/ L)	9.5 ± 0.29	11.2 ± 0.38
Exchangeable Ca (mg/ L)	10.0 ± 0.78	12.2 ± 0.78
Exchangeable Al (mg/ L)	1.9 ± 0.78	2.4 ± 0.78
Effective cation exchange capacity (cmol(+)/ kg)	14.6 ± 0.93	17.8 ± 0.91
Total cation exchange capacity (cmol(+)/ kg)	15.6 ± 0.79	18.8 ± 0.36
Cold water extractable carbon (mg/ L)	1.1 ± 0.09	2.6 ± 0.19
Hot water extractable carbon (mg/ L)	12.2 ± 0.85	17.9 ± 0.94
Organic matter content (%)	3.5 ± 0.11	4.6 ± 0.78
Olsen phosphorus (mg/ L)	2.6 ± 0.03	5.1 ± 0.42
Ammonium (mg/ L)	2.8 ± 0.79	3.1 ± 1.63
Nitrate (mg/ L)	4.2 ± 1.64	7.9 ± 1.13
Water holding capacity (g water g soil ⁻¹)	1.2 ± 0.12	2.4 ± 0.19
water stable aggregates (%)	73.8 ± 0.17	81.6 ± 0.18
Pore water P (mg/ L)	1.5 ± 0.14	1.9 ± 0.15

Table C2. Quality control for chemical analyses of soils amended with different levels of microplastics. Detection limits were calculated from the mean plus six times the standard deviation of ten repeated measurements of the blank standard. Precision was calculated from coefficient of variation (CV) determined from duplicate analysis of 10 % of the samples. Values were averaged when there were more than one instrumental runs. Values of accuracy and precision are expressed in percentage (%). Detection limit is expressed in mg/ L.

Parameters	Instrument used	Certified Reference Material (CRM)	Accuracy (%)	Precision (%)	Detection limit (mg/ L)
Extractable Na	ICP-OES	In-house 0.5 mg/ L multi-element standard	91.04	6.07	0.01
Extractable K	ICP-OES	In-house 0.5 mg/ L multi-element standard	120.74	2.12	0.01
Extractable Mg	ICP-OES	In-house 0.5 mg/ L multi-element standard	116.51	1.50	0.03
Extractable Ca	ICP-OES	In-house 0.5 mg/ L multi-element standard	105.15	0.09	0.15
Extractable Al	ICP-OES	In-house 0.5 mg/ L multi-element standard	136.07	20.01	1.9×10^{-6}
Cold water extracted C (as dissolved organic C)	TOC Analyser	50.0 mg/ L TOC standard	101.90	2.16	0.01
Hot water extracted C (as dissolved organic C)	TOC Analyser	50.0 mg/ L TOC standard	101.90	2.16	0.01
Olsen P (as PO_4^{3-}P)	Autoanalyser	0.4 mg/ L PO_4^{3-}P standard	Not found due to matrix issue	1.12	0.05
Pore water P (as PO_4^{3-}P)	Autoanalyser	0.4 mg/ L PO_4^{3-}P standard	100	1.96	0.08
NH_4^+	Autoanalyser	1.0 mg/ L ammonium standard	108.40	0.14	1.22
NO_3^-	Autoanalyser	0.5 mgL^{-1} nitrate standard	90.05	2.23	0.24
Plant P	P-XRF	NCS DC73349 'Bush Branches and Leaves'	120	---	---

References

Cherevko, S. and Mayrhofer, K. J. J. (2018). On-line inductively coupled plasma spectrometry in electrochemistry: basic principles and applications. *In: Wandelt, K. (ed.) Encyclopedia of interfacial chemistry: surface science and electrochemistry*, Germany: Elsevier.

Drava, G. and Minganti, V. (2020). Influence of an internal standard in axial ICP-OES analysis of trace elements in plant materials. *Journal of Analytical Atomic Spectrometry*, 35, 301-306.

Homazava, N., Ulrich, A., Trottmann, M., and Krahenbuhl, U. (2007). Micro-capillary system coupled to icp-ms as a novel technique for investigation of micro-corrosion processes. *Journal of Analytical Atomic Spectrometry*, 22, 1122-1130.

Klemm, S. O., Schauer, J. C., Schuhmacher, B., and Hassel, A. W. (2011). A microelectrochemical scanning flow cell with downstream analytics. *Electrochimica Acta*, 56, 4315–4321.

Silva, J. C. J., Baccan, N., and Nobrega, J. A. (2003). Analytical performance of an inductively coupled plasma optical emission spectrometry with dual view configuration. *Journal of the Brazilian Chemical Society*, 14, 310-315.

Thompson, M. (2011). *Handbook of Inductively Coupled Plasma Spectrometry*. New York: Springer-Verlag.